Population balance modeling -an application in particle technology

Sheryl Ehrman

IITB and

University of Maryland

Link to Matlab:

www.glue.umd.edu/~sehrman/popbal.htm

Outline

- Aerosol reactors in industry
- Design problem, sneak peak
- Particle collection using cyclones
- Aerosol topics
  - size distributions
  - aggregates and fractals
  - coagulation/breakup
- Population balance equations
- Discrete and sectional approach
- Design problem, revisited

Acknowledgments

- Population balance lectures and design problems developed in collaboration with Dr. R. Bertrum Diemer, Principal Consultant, Chemical Reaction Engineering, DuPont, Wilmington DE, USA
- Matlab code: Brendan Hoffman, Kelly Tipton, Yechun Wang, Matt McHale, Spring 2003 students
- Support from US National Science Foundation & DuPont

- Purpose
  - increase interest in field of particle technology
  - show practical application of population balance modeling approach

Important aerosol products

- Silica
- Titania
- Carbon black
- Specialty materials
  - Nano zinc oxide used today in sunscreen
  - High surface area catalyst supports (alumina, zirconia, etc..)
  - Chemical mechanical polishing agents (ceria, silica, etc…)

General Aerosol Process Schematic

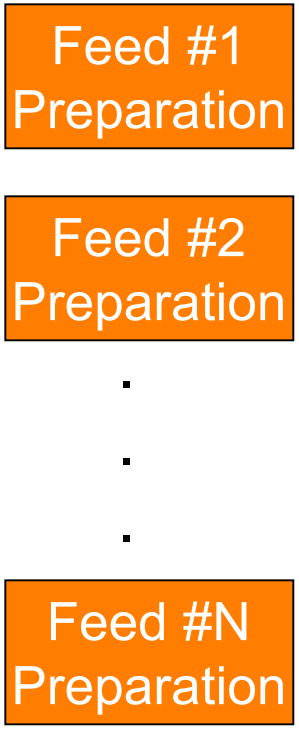

- Vaporization
- Pumping/Compression
- Addition of additives
- Preheating

General Aerosol Process Schematic

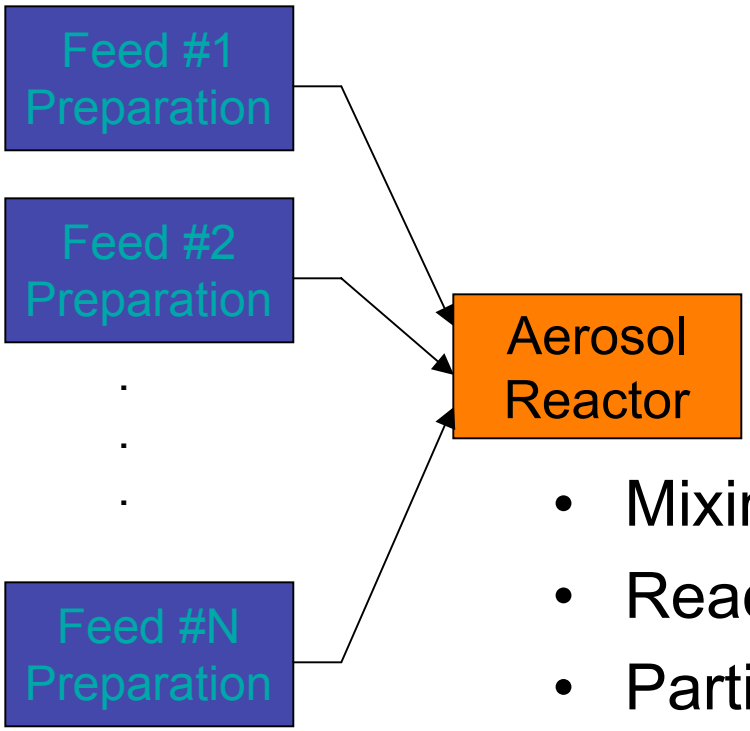

- Mixing
- Reaction Residence Time
- Particle Formation/Growth Control
- Agglomeration Control
- Cooling/Heating
- Wall Scale Removal

General Aerosol Process Schematic

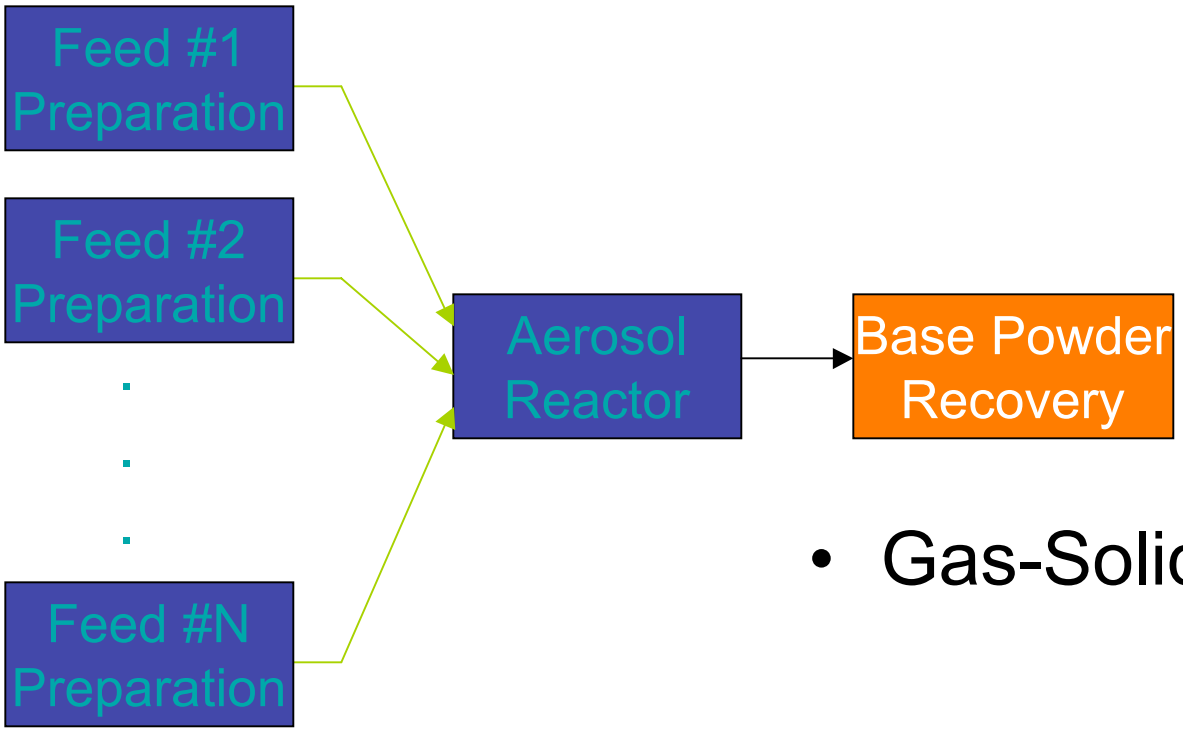

- Gas-Solid Separation

General Aerosol Process Schematic

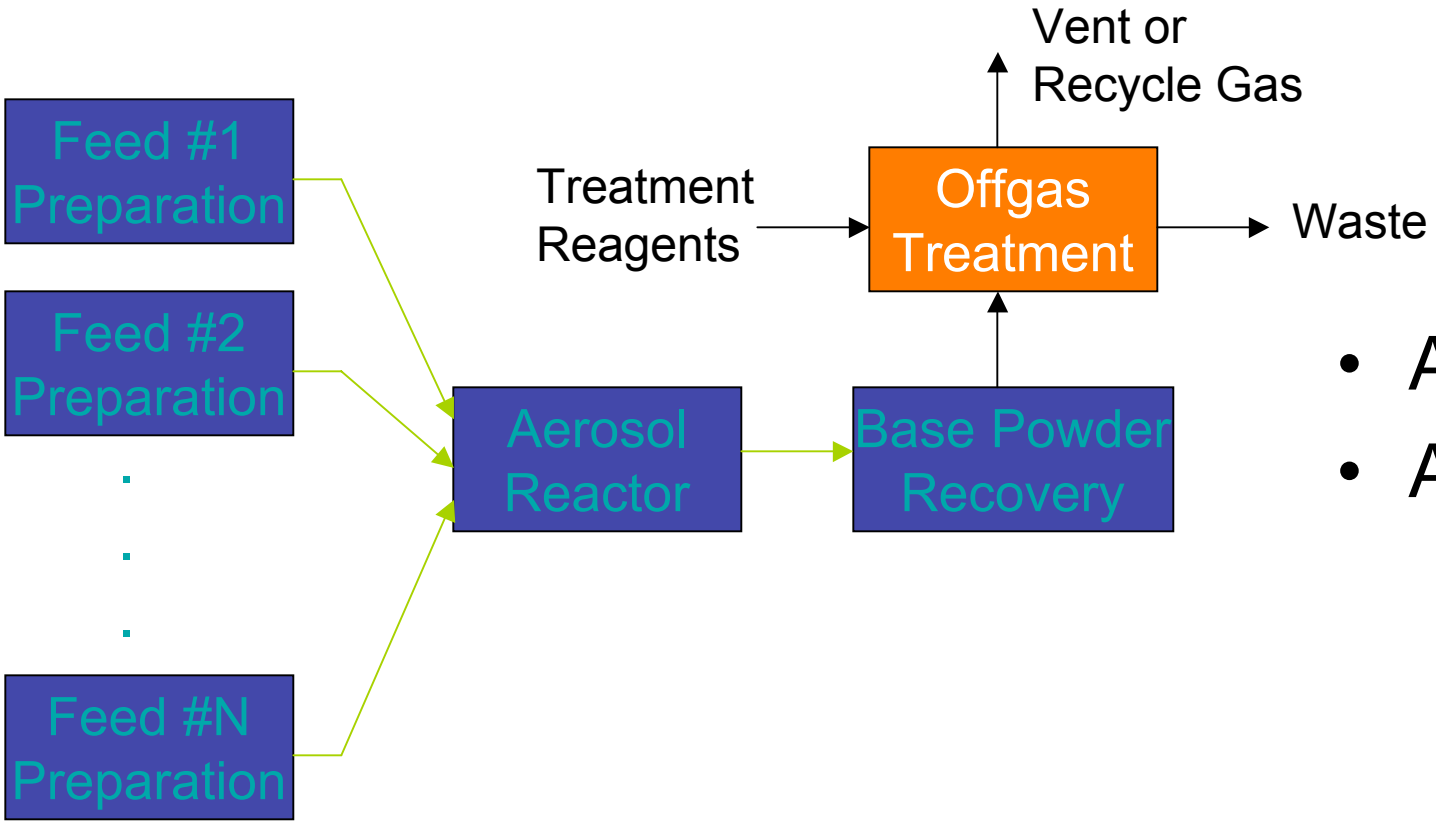

- Absorption
- Adsorption

General Aerosol Process Schematic

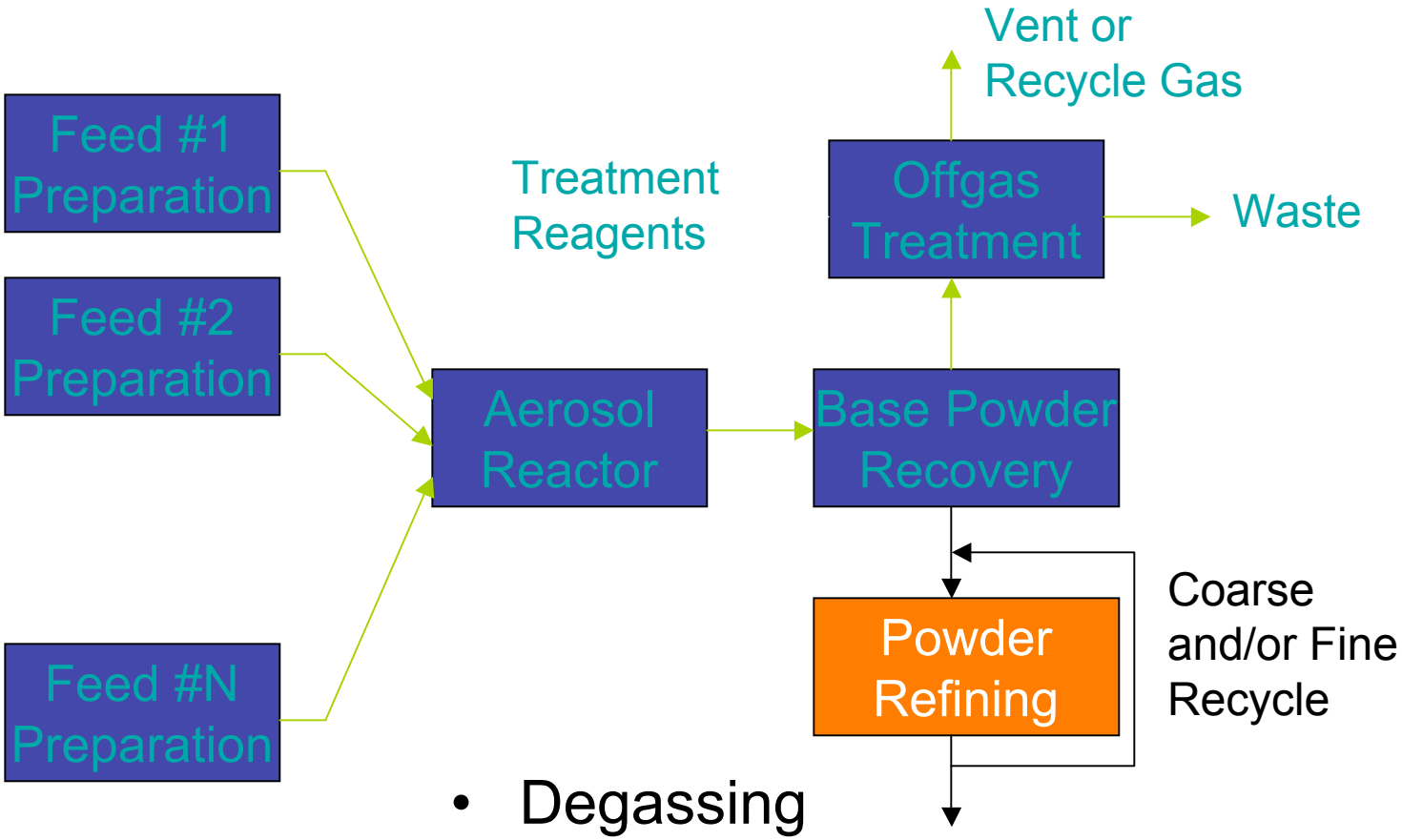

- Degassing
- Desorption
- Conveying
- Size Modification
- Solid Separations

General Aerosol Process Schematic

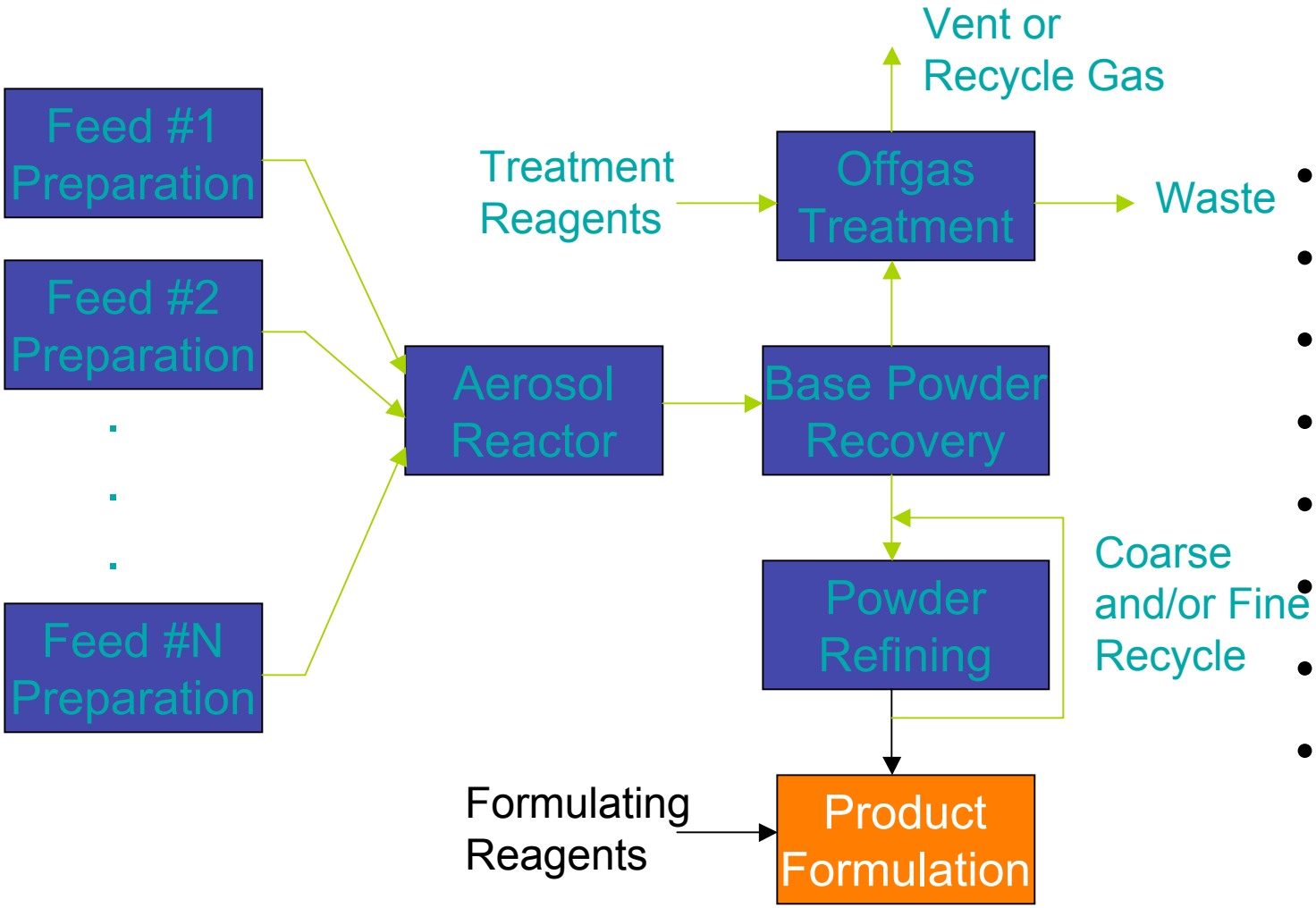

- Coating
- Additives
- Tabletting
- Briquetting
- Granulation
- Slurrying
- Filtration
- Drying

General Aerosol Process Schematic

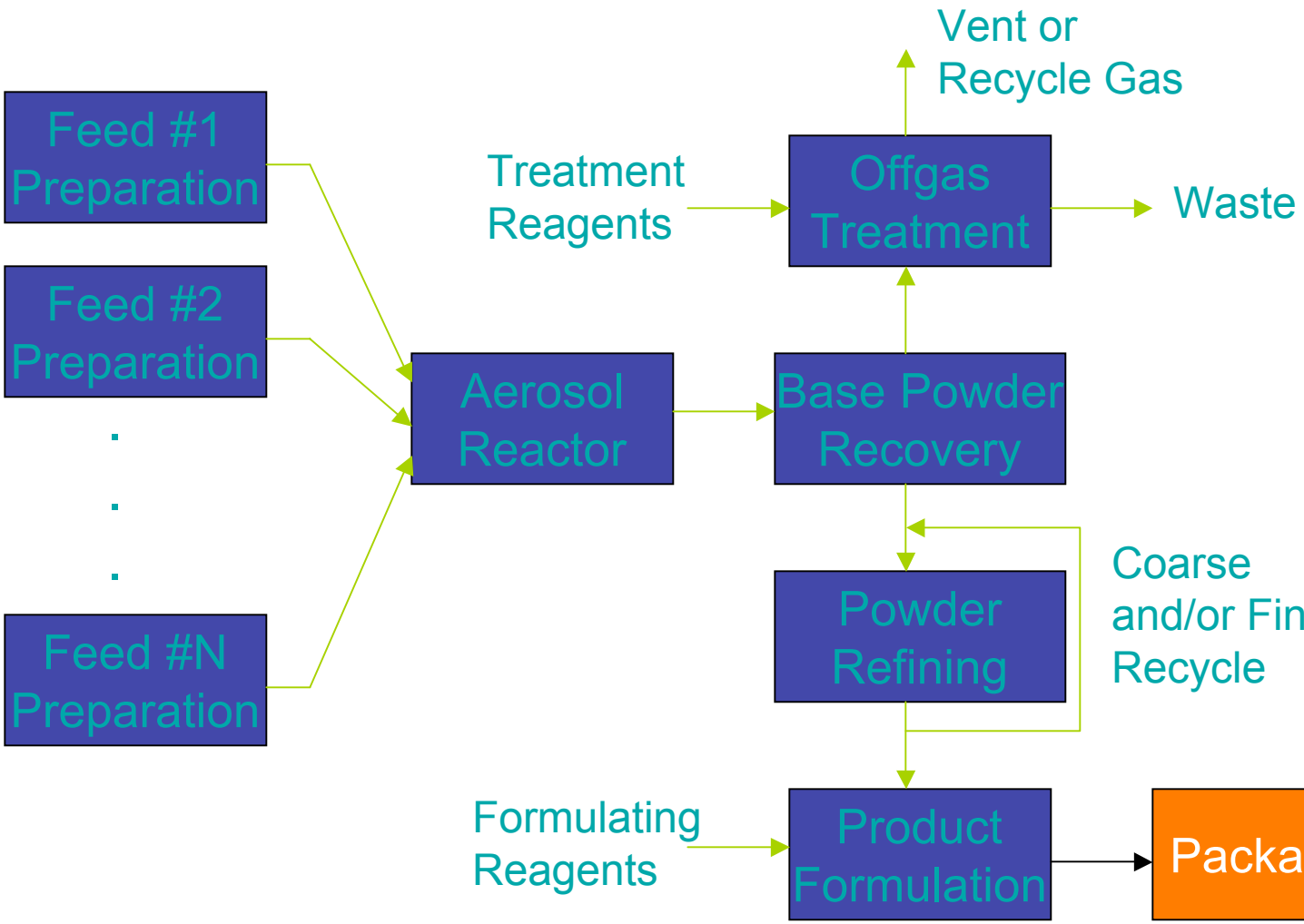

- Bags
- Super Sacks
- Jugs
- Bulk containers
  - trucks
  - tank cars

General Aerosol Process Schematic

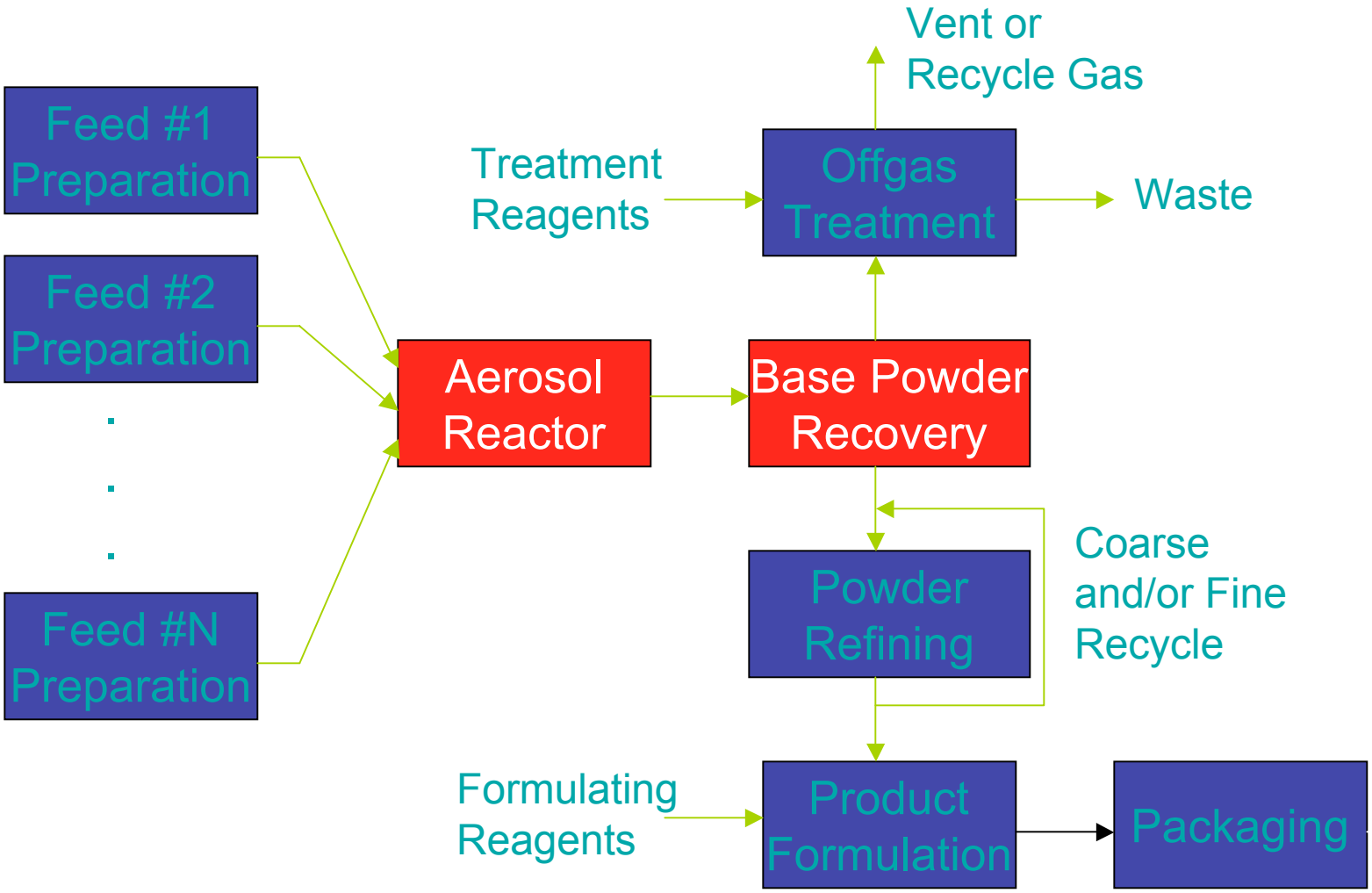

Our focus, reactor and gas solid separation

The Design Problem

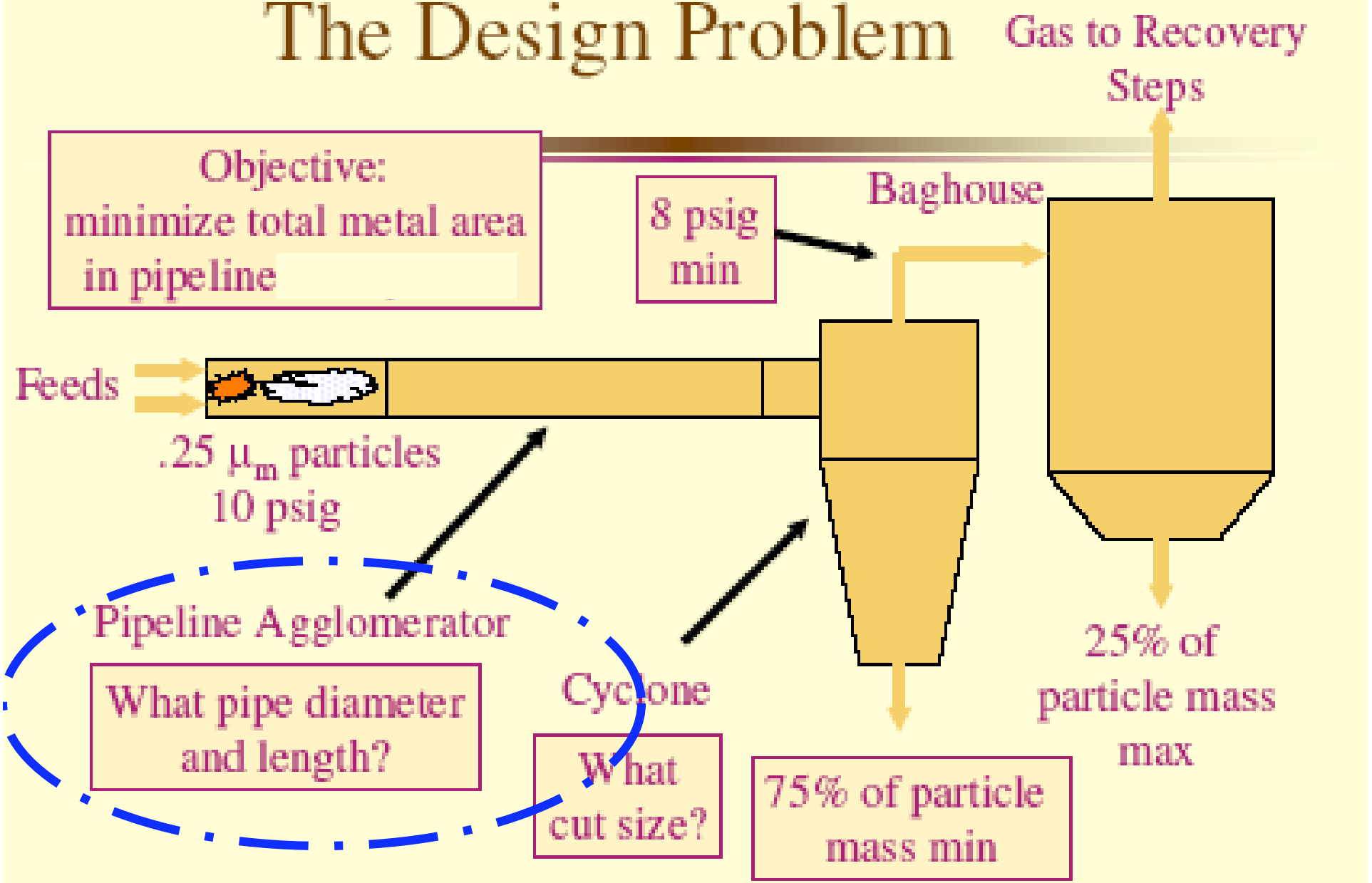

Particle Formation, Growth & Transformation

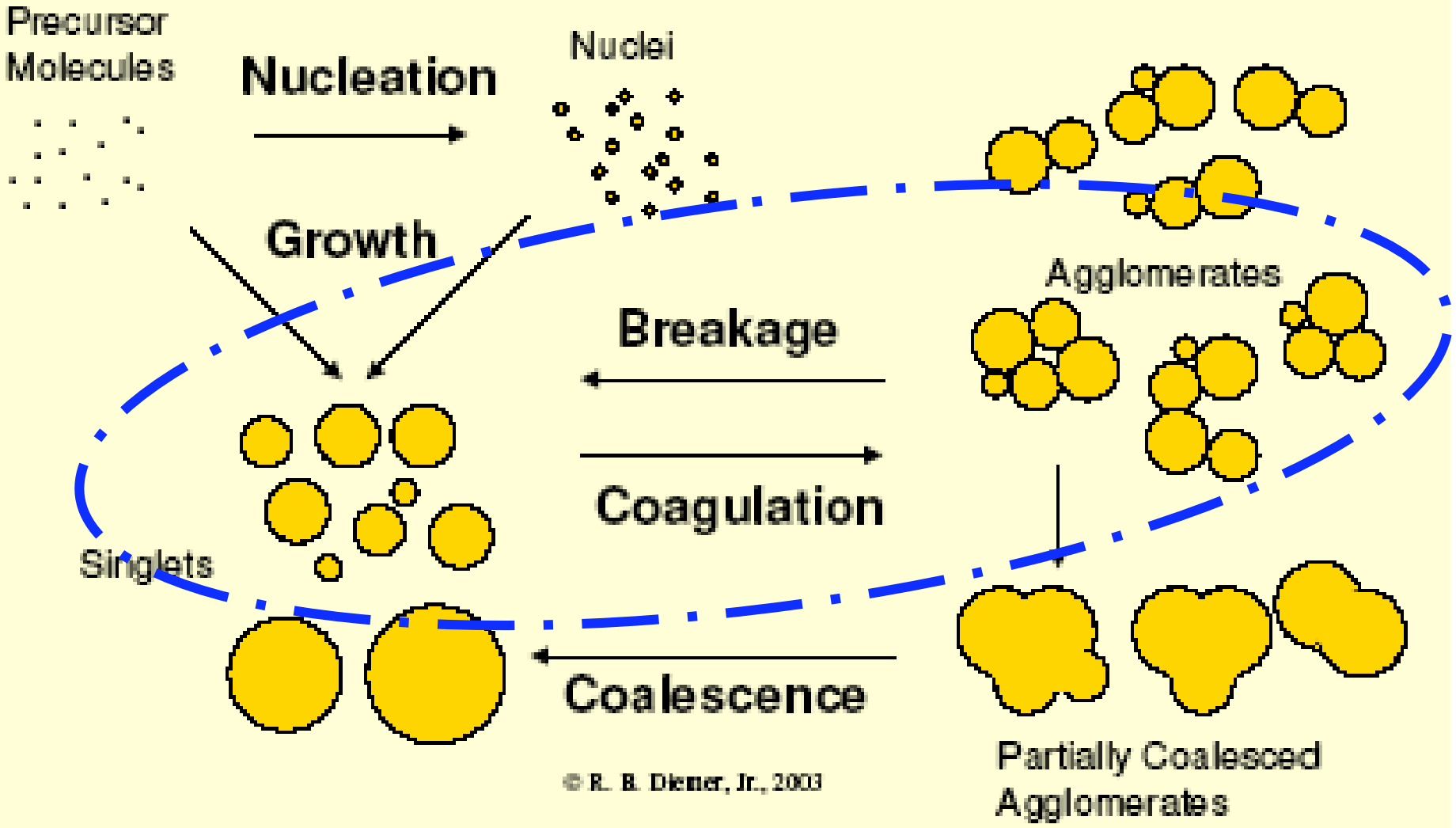

Thermal Carbon Black Process

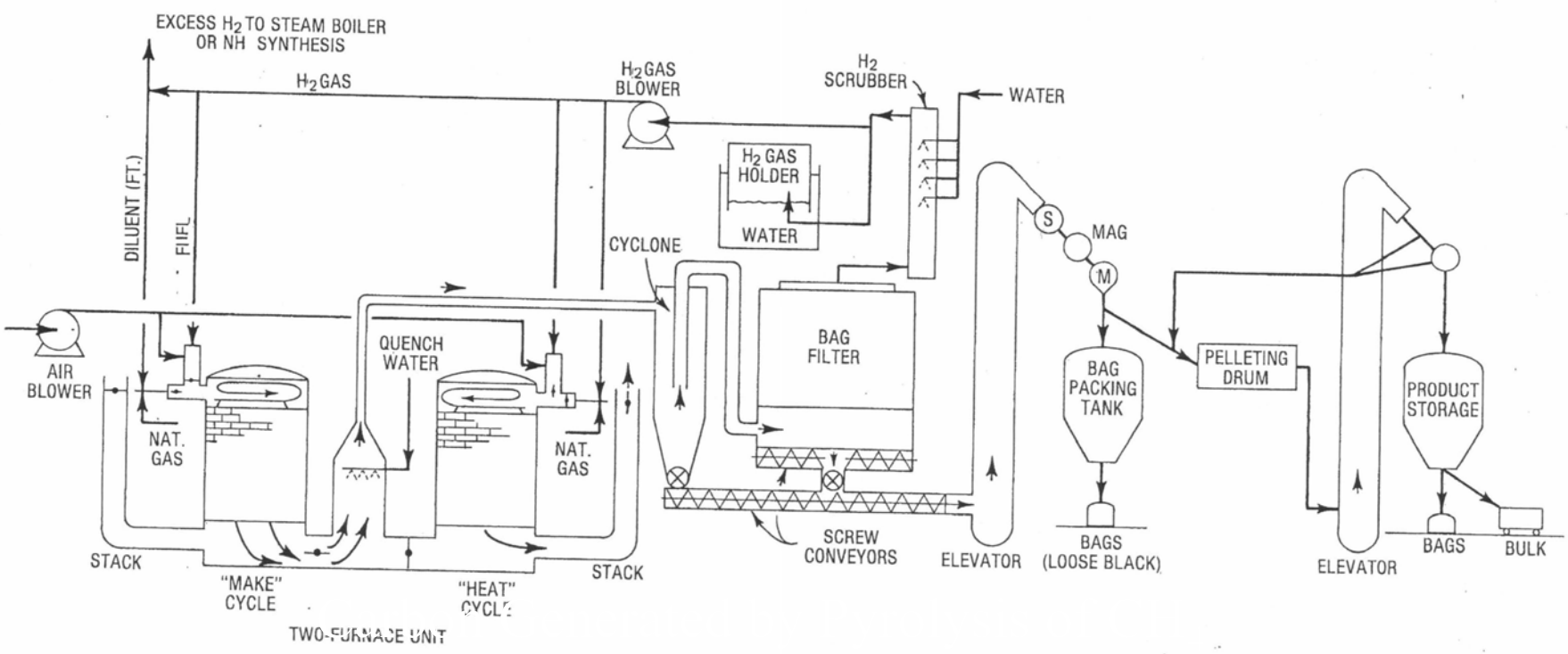

FIG. 26. Thermal process (natural gas feedstock).

Johnson, P. H., and Eberline, C. R., "Carbon Black, Furnace Black", *Encyclopedia of Chemical Processing and Design*, J. J. McKetta, ed., Vol. 6, Marcel Dekker, 1978, pp. 187-257.

Furnace Carbon Black Process

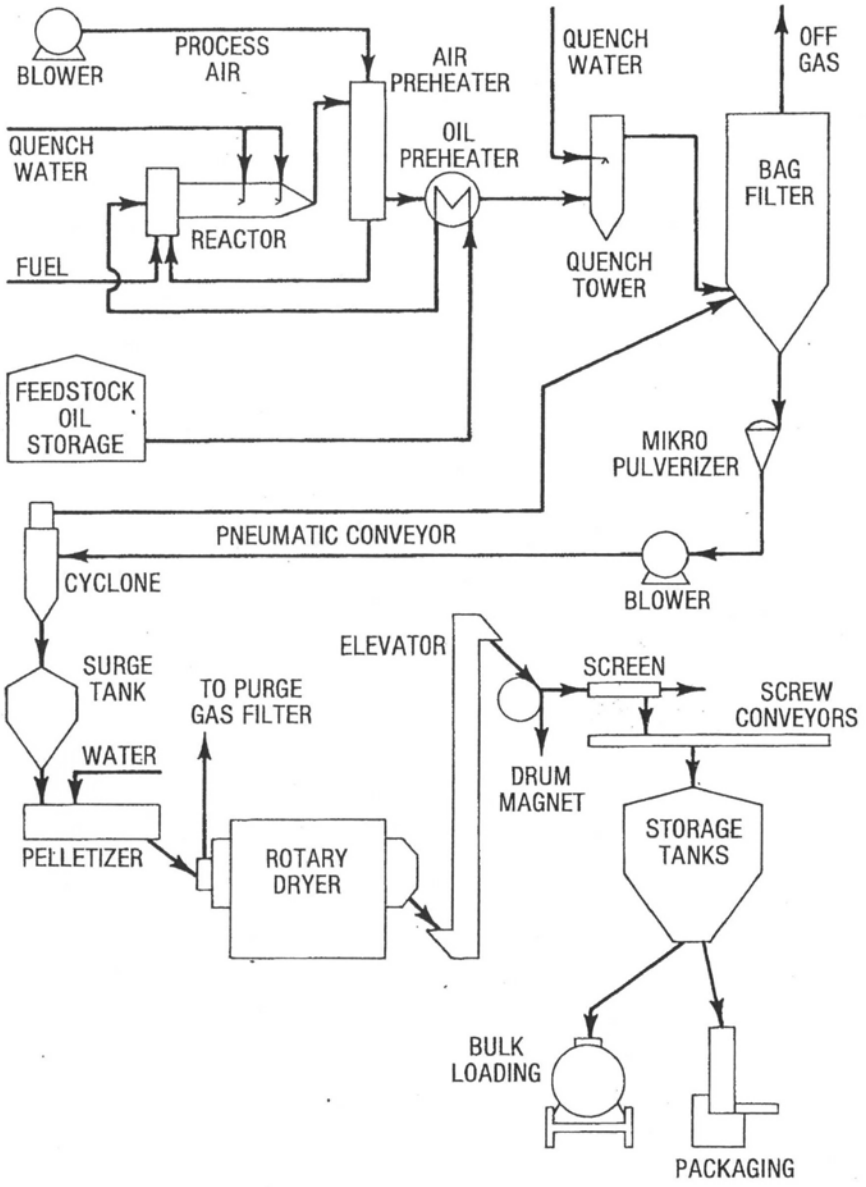

FIG. 18. Oil furnace carbon black process.

Johnson, P. H., and Eberline, C. R., "Carbon Black, Furnace Black", *Encyclopedia of Chemical Processing and Design*, J. J. McKetta, ed., Vol. 6, Marcel Dekker, 1978, pp. 187-257.

Thermal Carbon Black

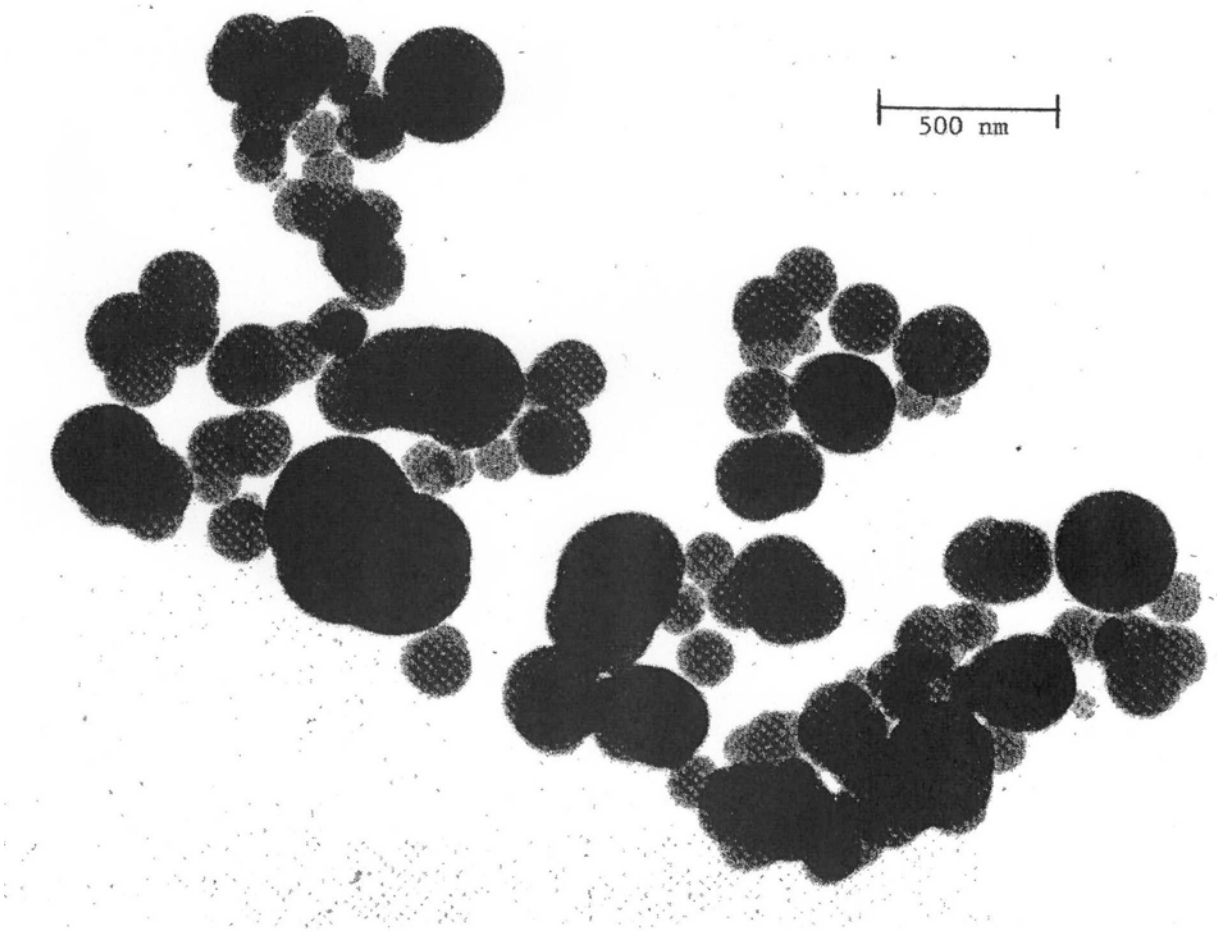

FIG. 7. Thermal black.

- ~200 nm Primary Particles
- 4-6 Primaries/ Agglomerate

Johnson, P. H., and Eberline, C. R., "Carbon Black, Furnace Black", *Encyclopedia of Chemical Processing and Design*, J. J. McKetta, ed., Vol. 6, Marcel Dekker, 1978, pp. 187-257.

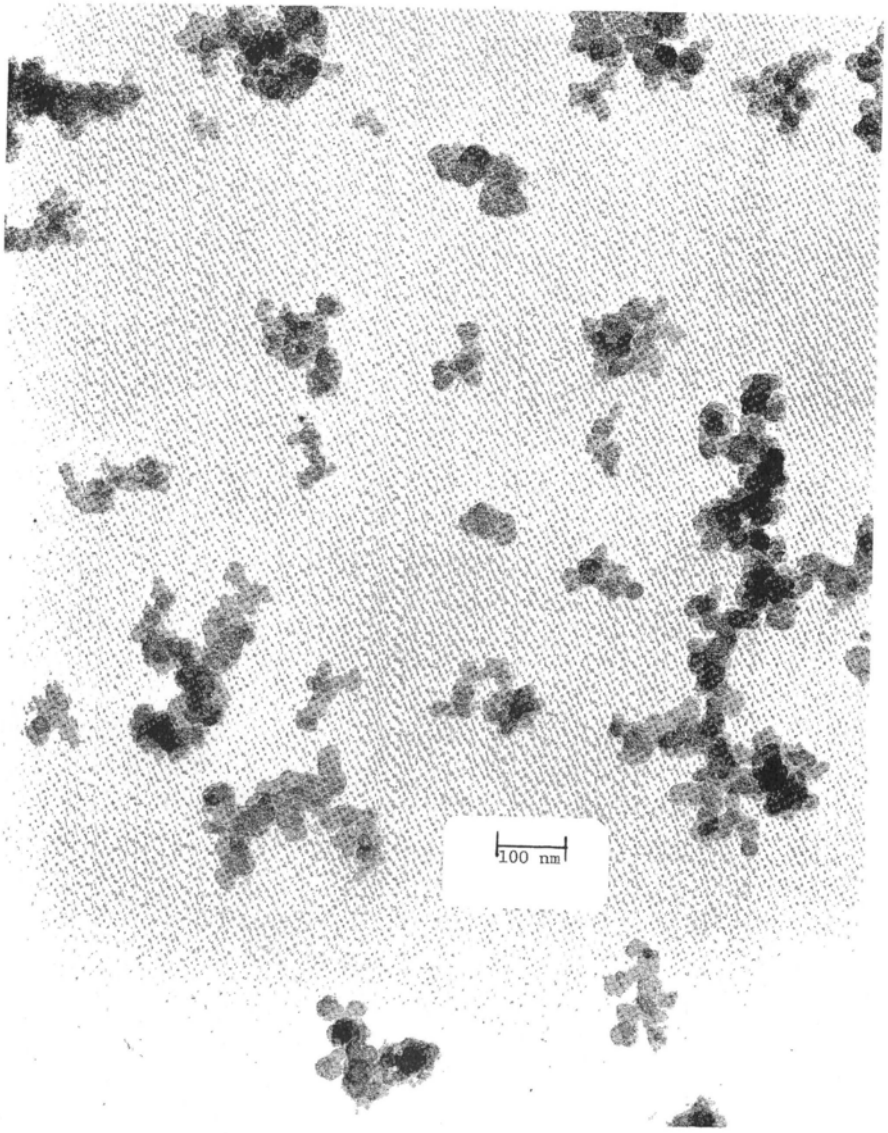

FIG. 8. A structured oil-furnace black.

Oil-Furnace Carbon Black

- ~20 nm Primary Particles
- 10-50 Primaries/ Agglomerate

Johnson, P. H., and Eberline, C. R., "Carbon Black, Furnace Black", *Encyclopedia of Chemical Processing and Design*, J. J. McKetta, ed., Vol. 6, Marcel Dekker, 1978, pp. 187-257.

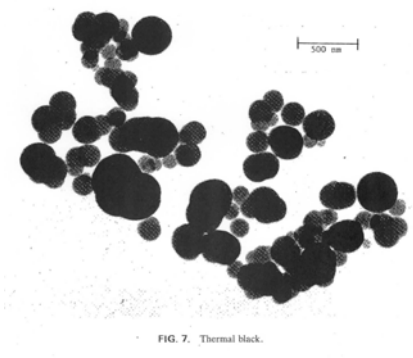

FIG. 7. Thermal black.

What do you see?

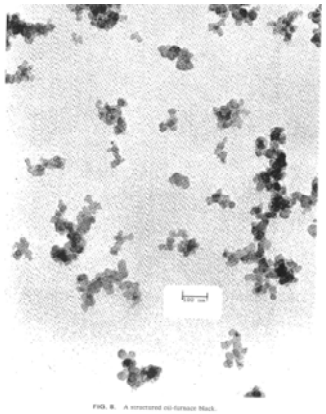

- What do you notice about each sample?

- How do the two images differ?

Particles not all same…

- Diameter
- Volume
- Surface area
- Structure

How to represent size distributions, histogram example:

Size range, microns	number of particles
0 to 10	10
11 to 20	30
21 to 30	80
31 to 40	180
41 to 50	280
51 to 60	169
61 to 70	120
71 to 80	88
81 to 90	40
91 to 100	3

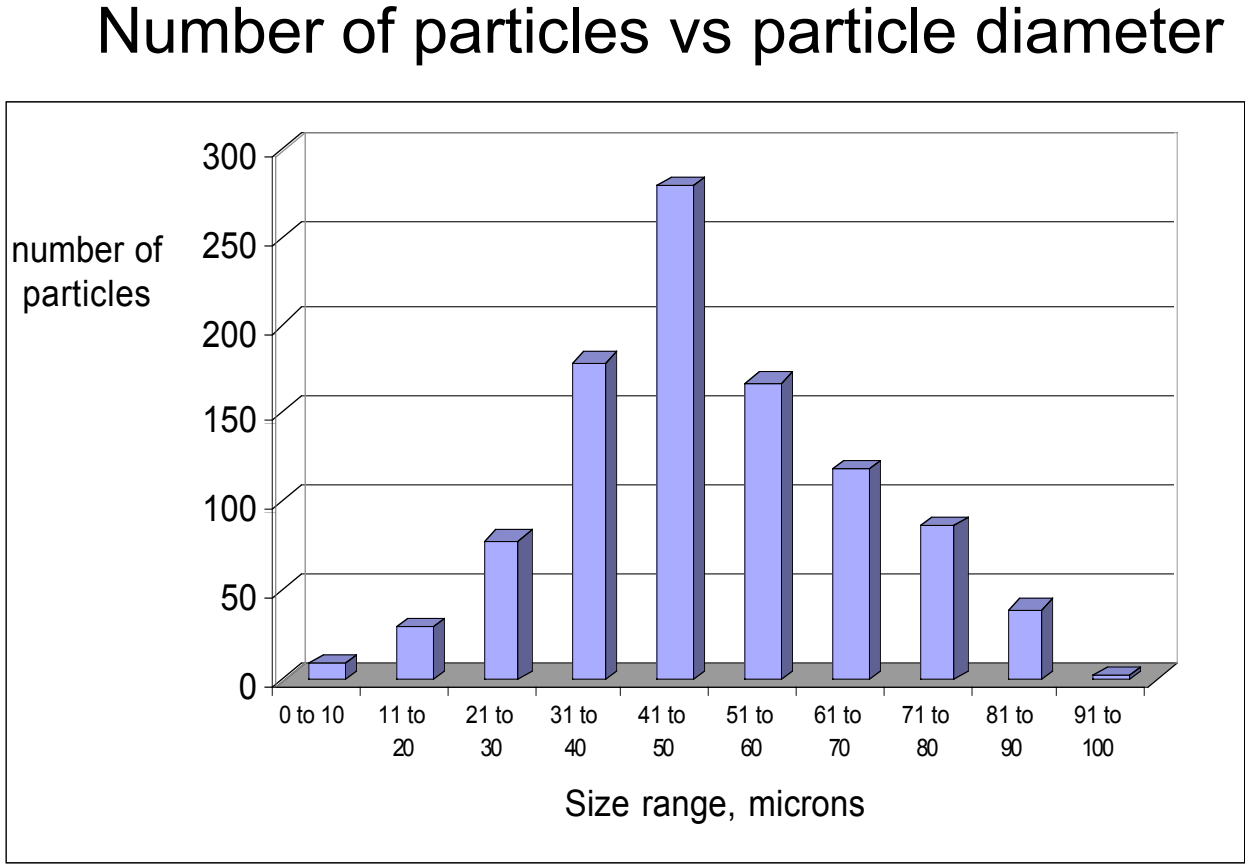

Can create histogram from raw particle size data using Analysis tool pack add-in, with Excel.. After add-in, go to ‘tools’, then ‘data analysis’, then ‘histogram’.

How to represent size distributions, histogram example:

Size range, microns	number of pa	Frequency
0 to 10	10	0.01
11 to 20	30	0.03
21 to 30	80	0.08
31 to 40	180	0.18
41 to 50	280	0.28
51 to 60	169	0.169
61 to 70	120	0.12
71 to 80	88	0.088
81 to 90	40	0.04
91 to 100	3	0.003
total number	1000	

Number frequency vs particle diameter

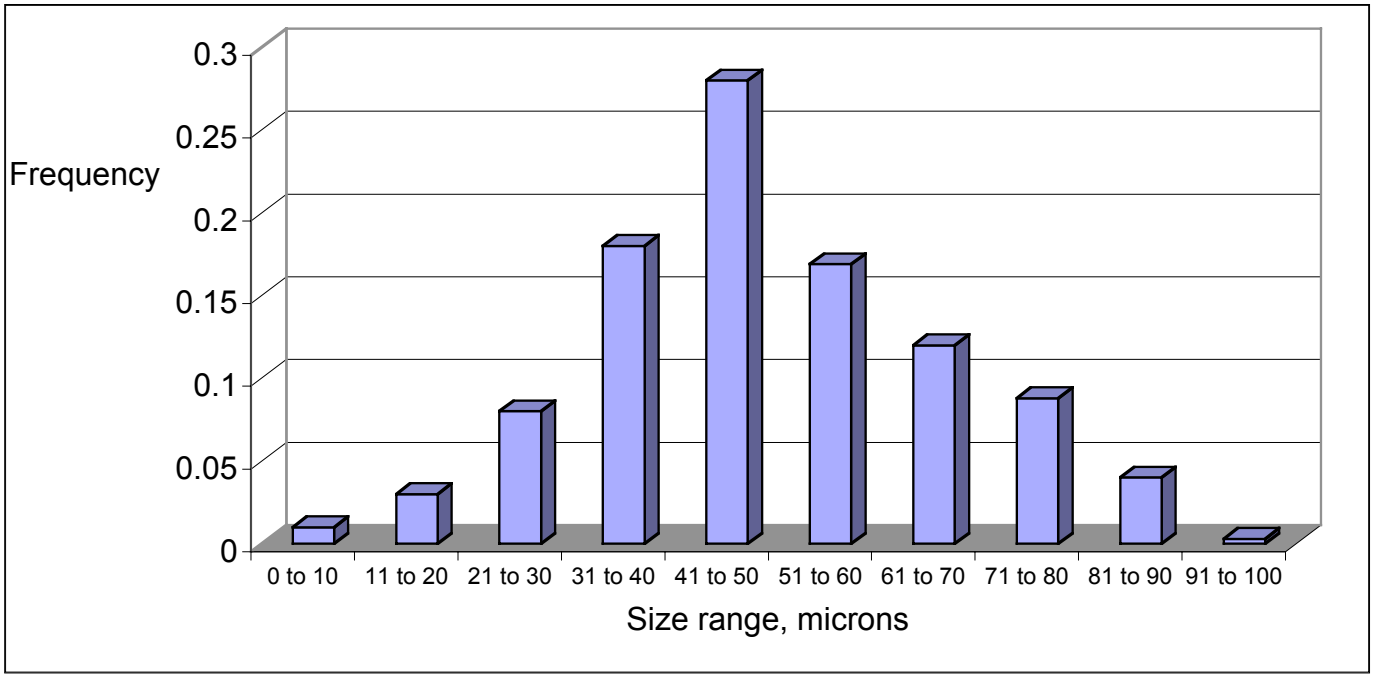

Test yourself…

- If you change the frequency distribution so that is based on the MASS of particles in each size range versus the NUMBER, will the shape of the frequency distribution change?

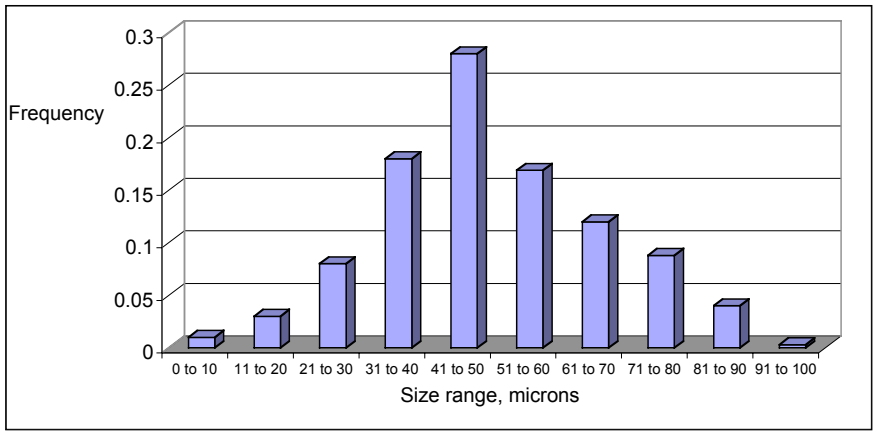

More spreadsheet manipulations

Size range, microns	number of particles	Frequency	assume diameter	mass of particles in each bin, g	Mass frequency
0 to 10	10	0.01	5	6.54E-10	0.00
11 to 20	30	0.03	15	5.30E-08	0.00
21 to 30	80	0.08	25	6.54E-07	0.01
31 to 40	180	0.18	35	4.04E-06	0.05
41 to 50	280	0.28	45	1.34E-05	0.16
51 to 60	169	0.169	55	1.47E-05	0.18
61 to 70	120	0.12	65	1.72E-05	0.21
71 to 80	88	0.088	75	1.94E-05	0.23
81 to 90	40	0.04	85	1.29E-05	0.15
91 to 100	3	0.003	95	1.35E-06	0.02
total number	1000				
total mass assuming 1g/cc density				8.37E-05	

Number vs mass distribution

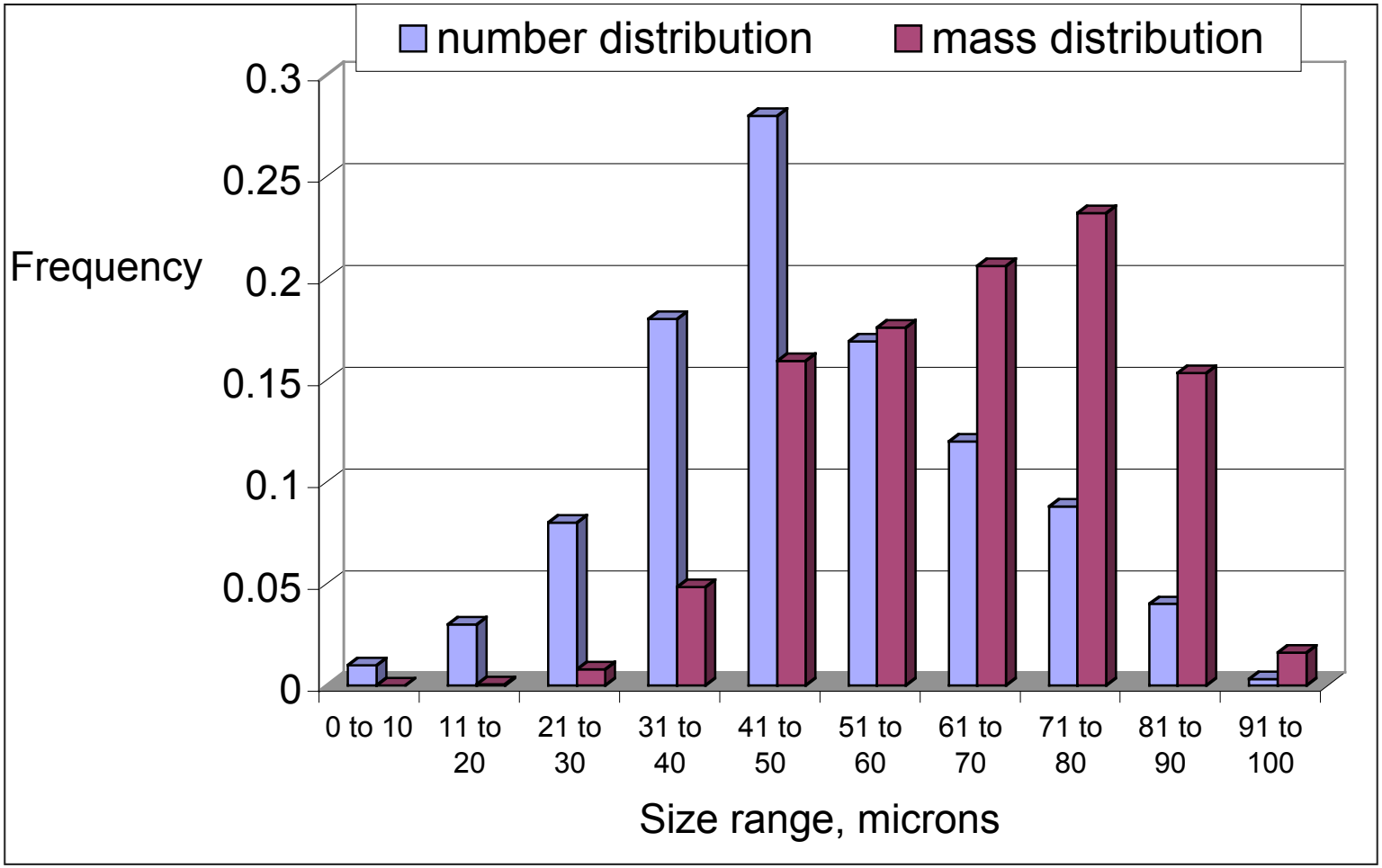

Continuous distributions

Also useful: continuous distributions, where some function, n_d, describes the number of particles of some diameter d_p at a given point, at a given time.

In terms of number concentration:

Let dN = number of particles per unit volume of gas at a given position in space (represented by position vector **r**), at a given time (t), in the particle range d_p to $d_p + d(d_p)$. N = total number of particles per unit volume of gas at a given position in space at a given time. Size distribution function is defined as:

$$n_d(d_p, \mathbf{r}, t) = \frac{dN}{d(d_p)}$$

Can also have size distribution function, n, with particle volume v as size parameter: $n(v, \mathbf{r}, t) = \frac{dN}{dv}$

Aggregates of hard spheres

- When primary particles collide and stick, but do not coalesce, irregular structures are formed

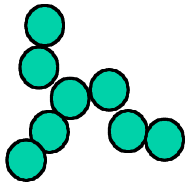

agglomerate

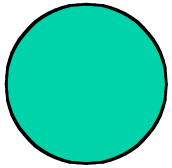

spherical equivalent

how should these structures be characterized?

- Radius gives space taken up, but no information about mass/actual volume. Using only actual volume doesn't indicate how much space it takes up.
- Real flame generated aerosol:

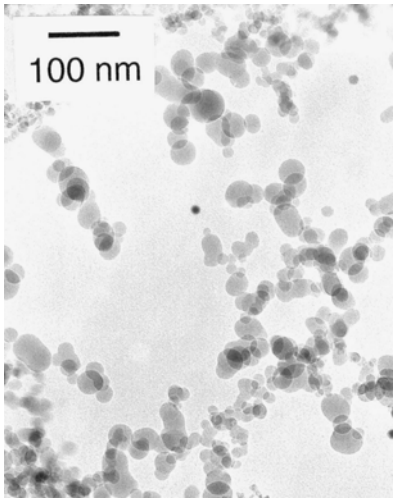

Concept of fractal dimension

- Aerosol particles which consist of agglomerates of ‘primary particles’, (often, combustion generated) may be described using the concept of fractals.
- Fractals - The relationship between diameter of aerosol agglomerates, and the volume of primary particles in the agglomerate can be written:

$$\frac{v}{v_o} = \left(\frac{d}{d_0}\right)^{D_f} \quad \text{where } v_o = \frac{\pi}{6} d_0^3$$

is the volume of the primary particle of diameter d_o

- d typically based on 2 * radius of gyration

Radius of Gyration

"The Radius of Gyration of an Area about a given axis is a distance k from the axis. At this distance k an equivalent area is thought of as a **Line Area** parallel to the original axis. The moment of inertia of this **Line Area** about the original axis is unchanged."
http://www.efunda.com/math/areas/RadiusOfGyrationDef.cfm

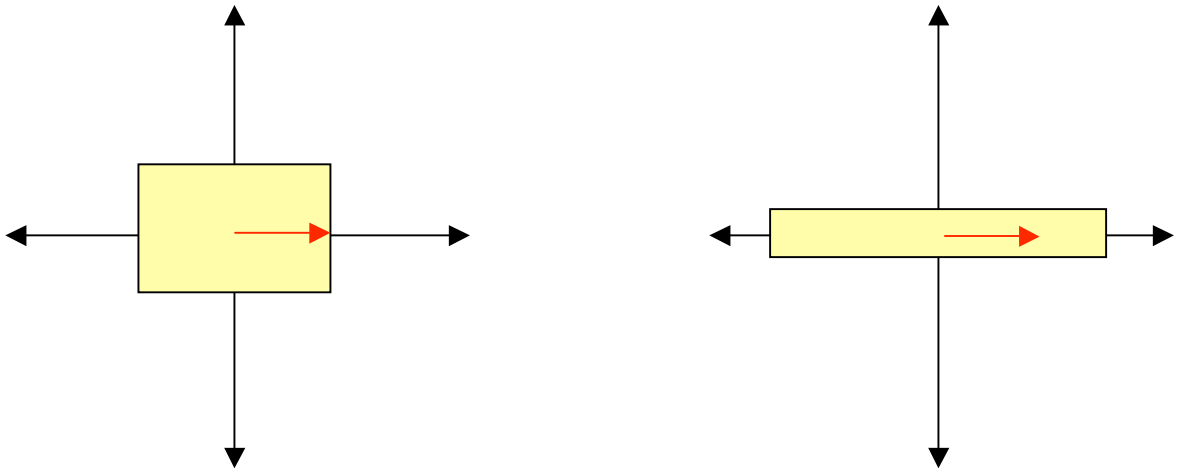

Fractal dimension

- Fractals - $D_f = 2$ = uniform density in a plane, D_f of 3 = uniform density in three dimensions
- Typical values for agglomerates ranges from 1.5 to near 3 depending on mechanism of agglomeration, possible rearrangement, and external field effects
- Small agglomerates (few particles) not really fractal but “fractal-like”
- For hundreds of particles, relationship holds well

Test yourself…

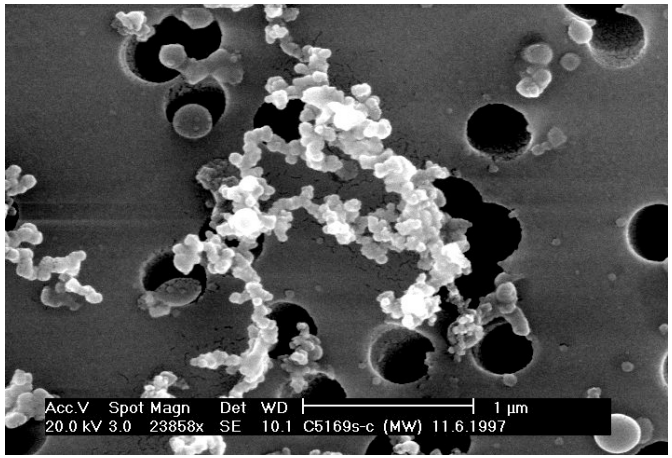

http://www.mpch-mainz.mpg.de/~gth/soot1.jpg

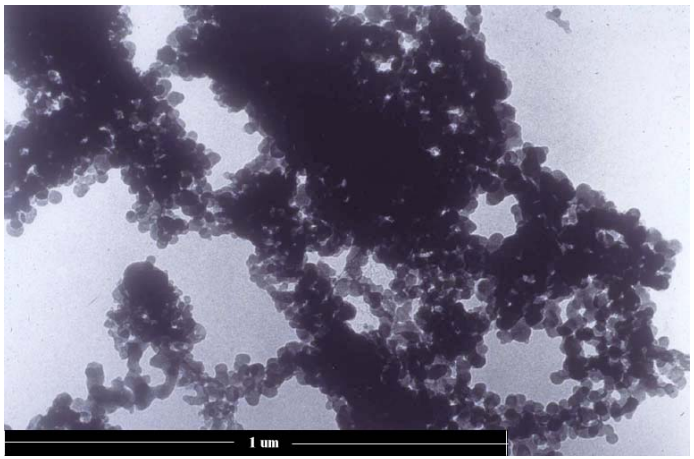

http://faculty.engineering.ucdavis.edu/jenkins/previous/August2002/16_23.jpg

Which picture shows particle agglomerates with a lower fractal dimension?

Working backwards in the problem

- Particle gas separators
- Use different phenomena
  - Gravitational settlers
  - Filters (baghouse)
  - Scrubbers
  - Inertial separators (cyclone)
  - Electrostatic precipitators

Pulse Jet Baghouse

Figure 6.6 Schematic diagram of a pulse-jet baghouse.

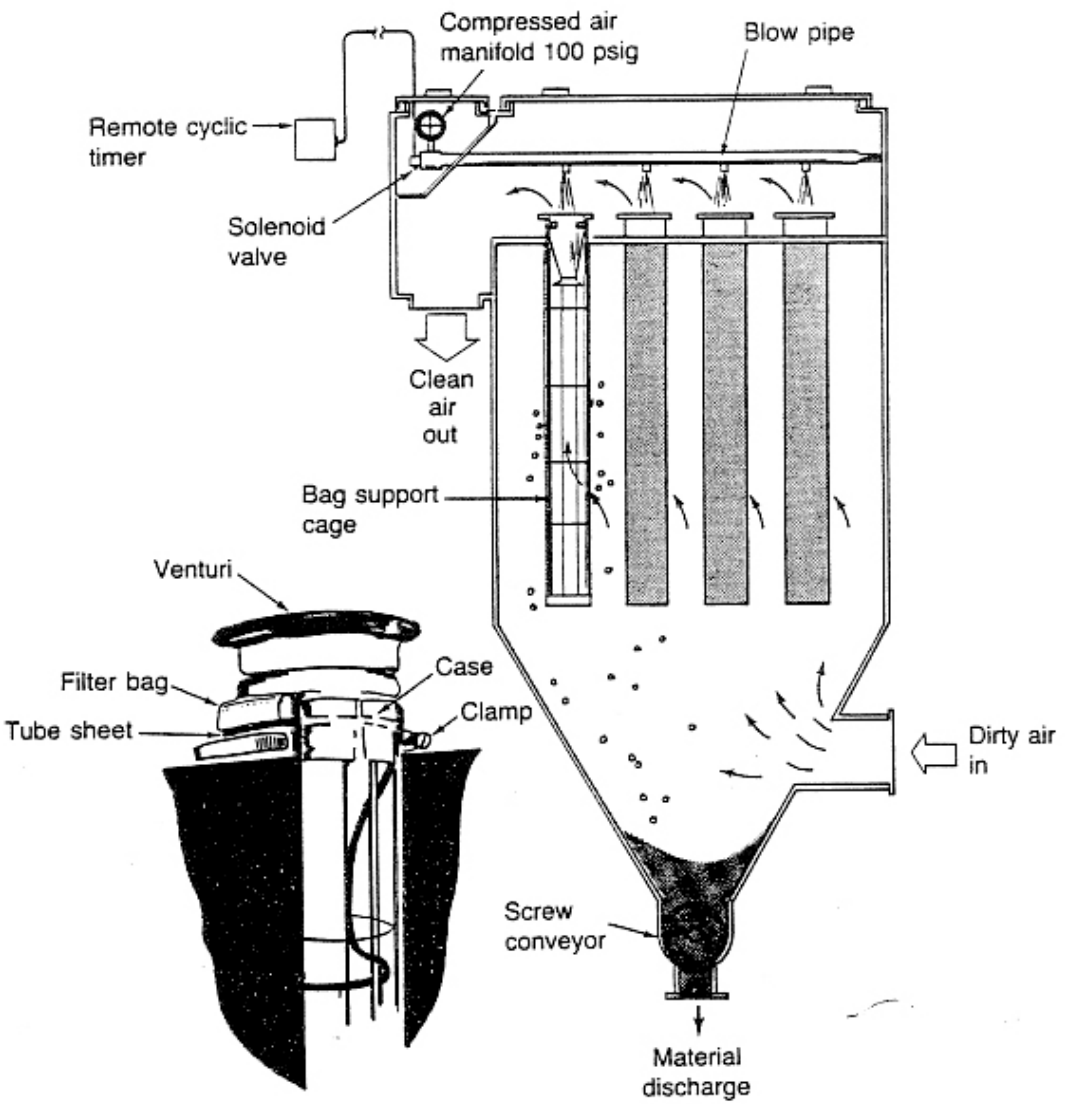

Air Pollution Control: A Design Approach
Cooper & Alley, PWS Eng. Boston 1986

Standard Cyclone

Figure 4.1 Schematic flow diagram of a standard cyclone.

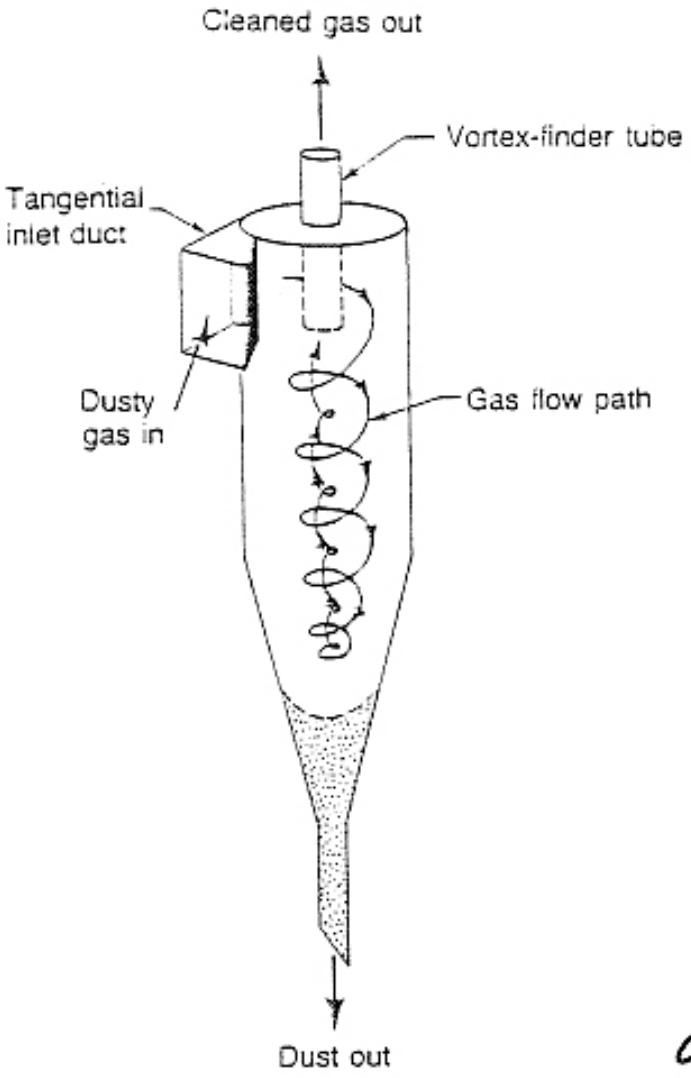

Air Pollution Control
Cooper & Alley (1986)

Force balance on particle in cyclone

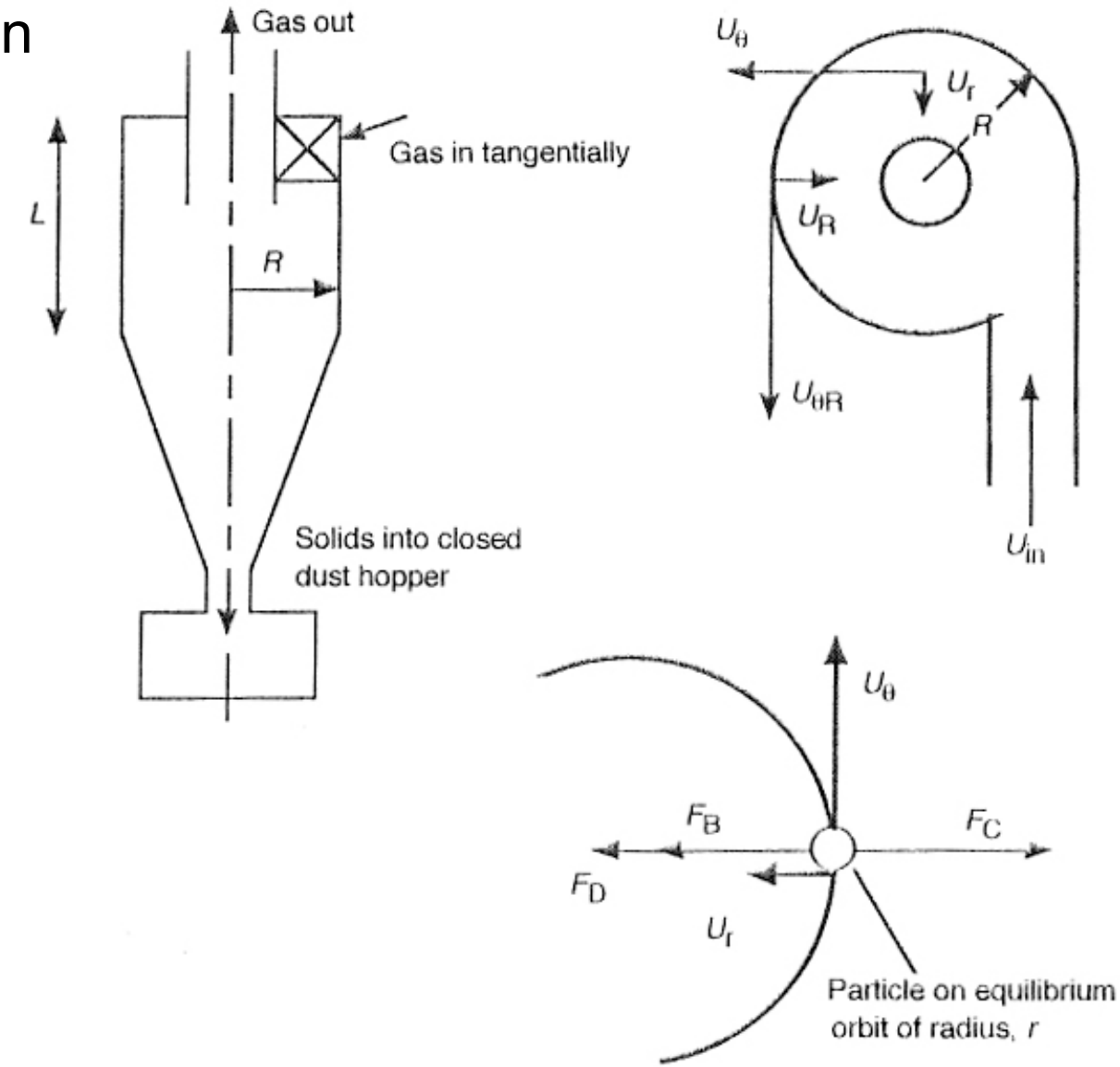

Figure 7.3 Reverse flow cyclone – a simple theory for separation efficiency

Rhodes, Introduction to Particle Technology, Wiley, 1998

Cyclone Efficiency as Function of Particle Diameter

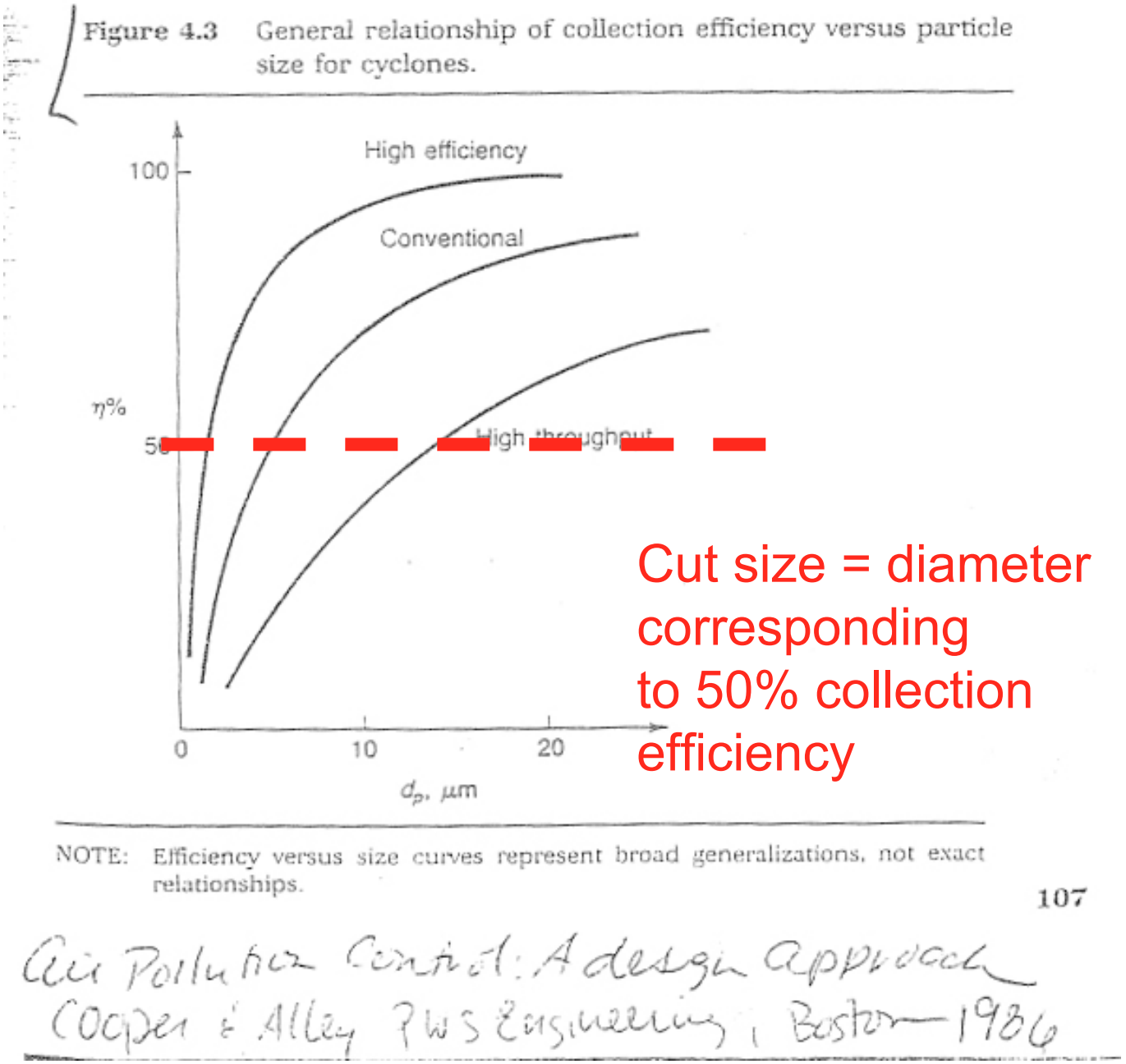

Which type has lowest pressure drop?

Cut size = diameter corresponding to 50% collection efficiency

Cyclones

- Advantages
  - Low pressure drop
  - Cheap to build /maintain (no moving parts)
- Disadvantages
  - Poor efficiency for smaller particles (less than 10 microns)
  - Not suitable for abrasive particles
- Hence, grow particles with agglomerator to increase efficiency

Collection efficiency

- Example curve

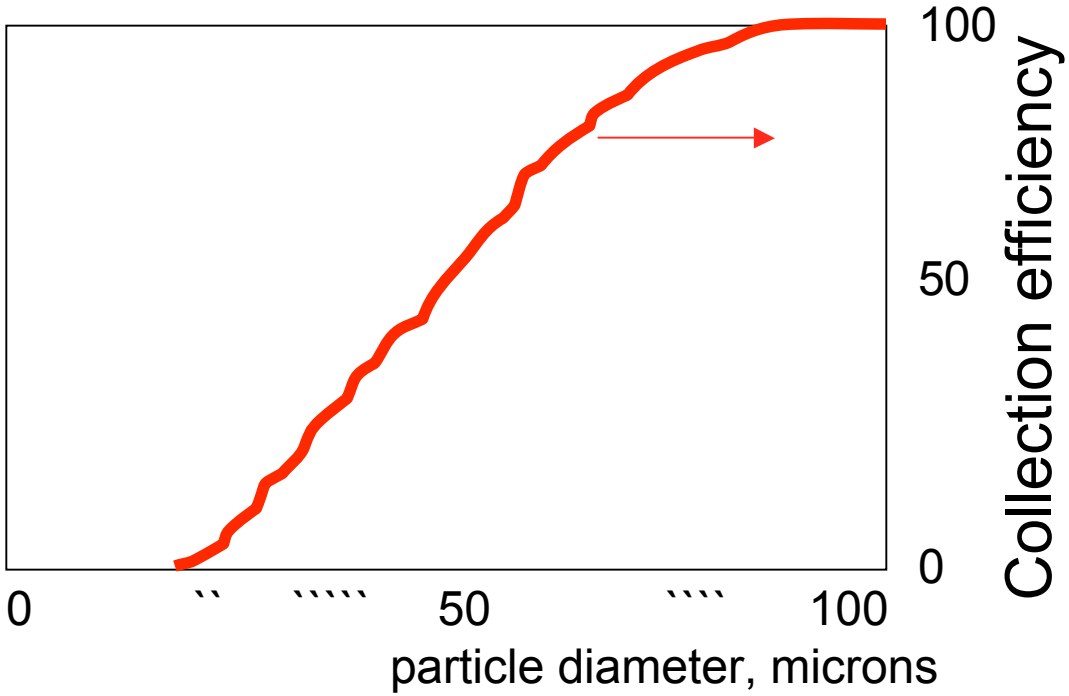

Histogram before cyclone

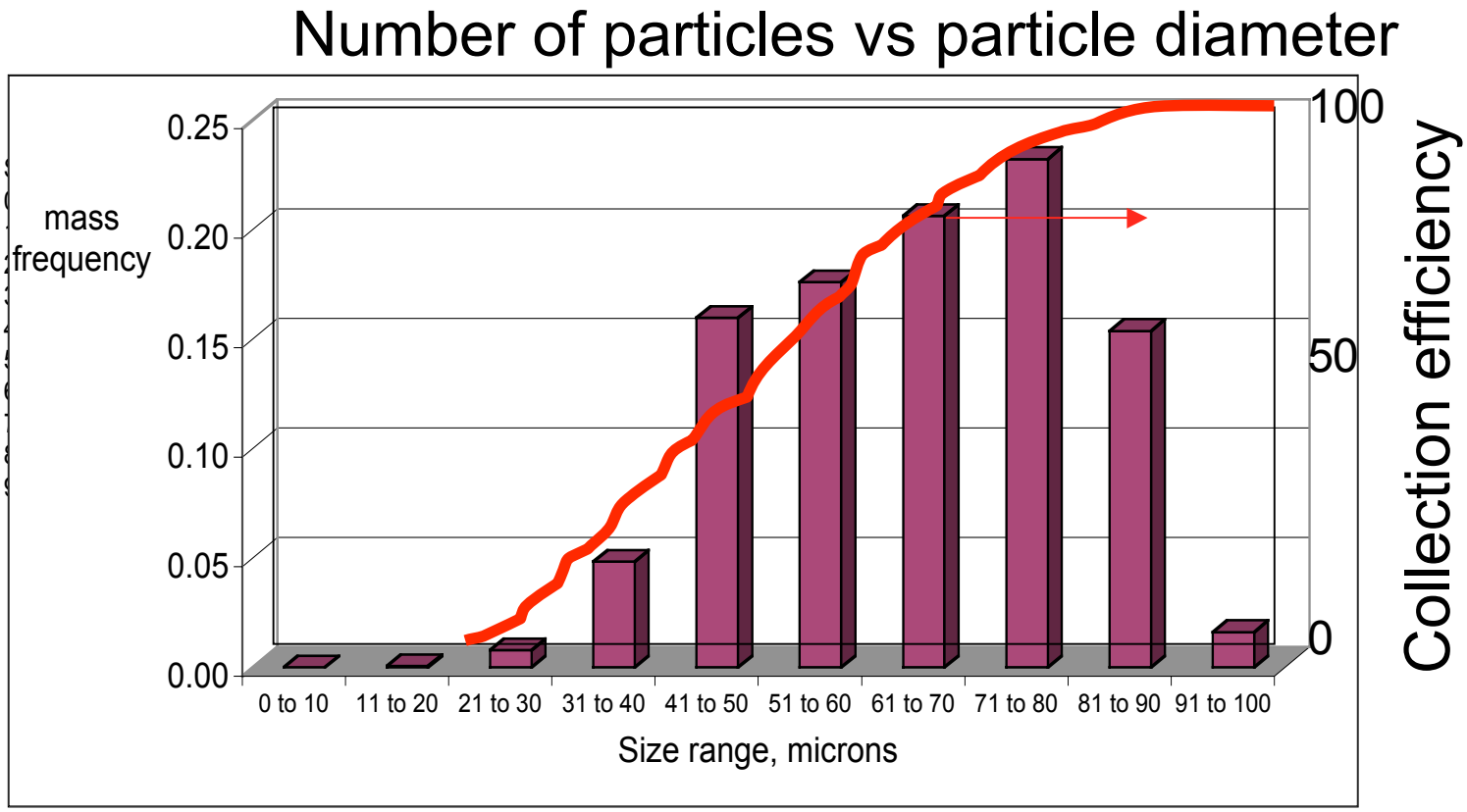

After cyclone

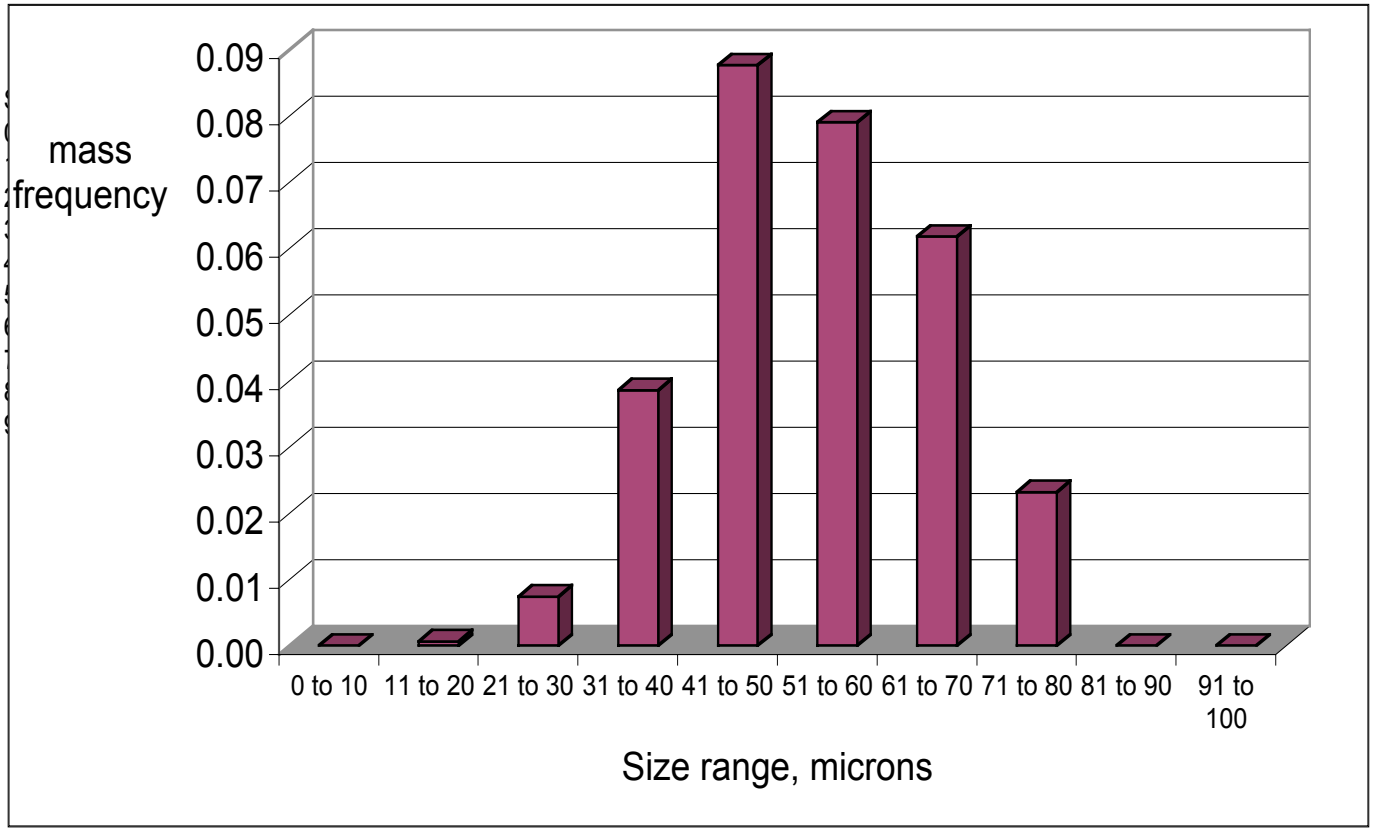

Histogram after cyclone

Number of particles vs particle diameter

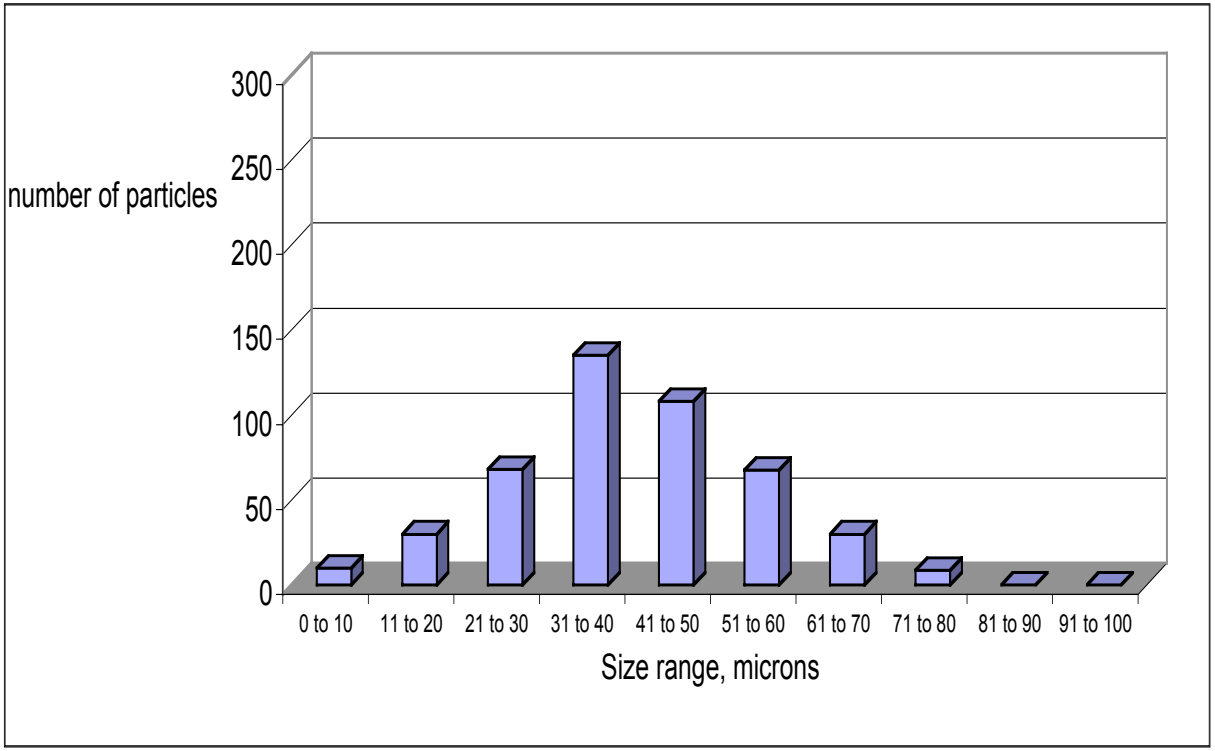

Quick solution?

- Why not make the tube very very long, and just allow a very very long time for coagulation so that the particles become very big?

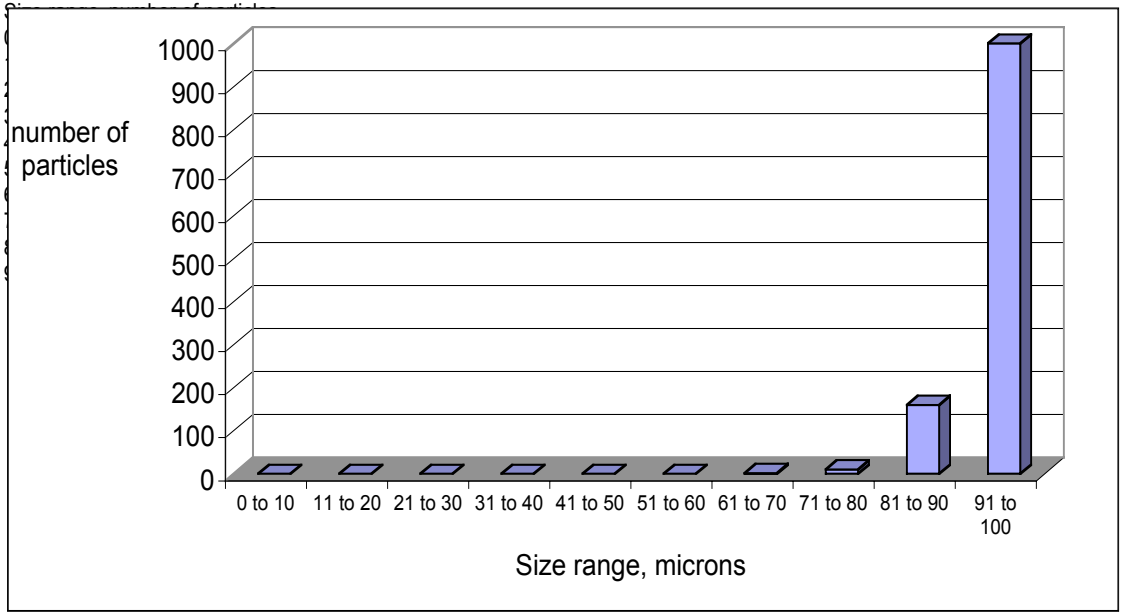

Dynamics of size distributions

- Control volume approach
- Population balance
- Physics of coagulation/breakup

Take a control volume….

J, particle flux vector,
(particles/(area time))
Components- J_x, J_y, J_z

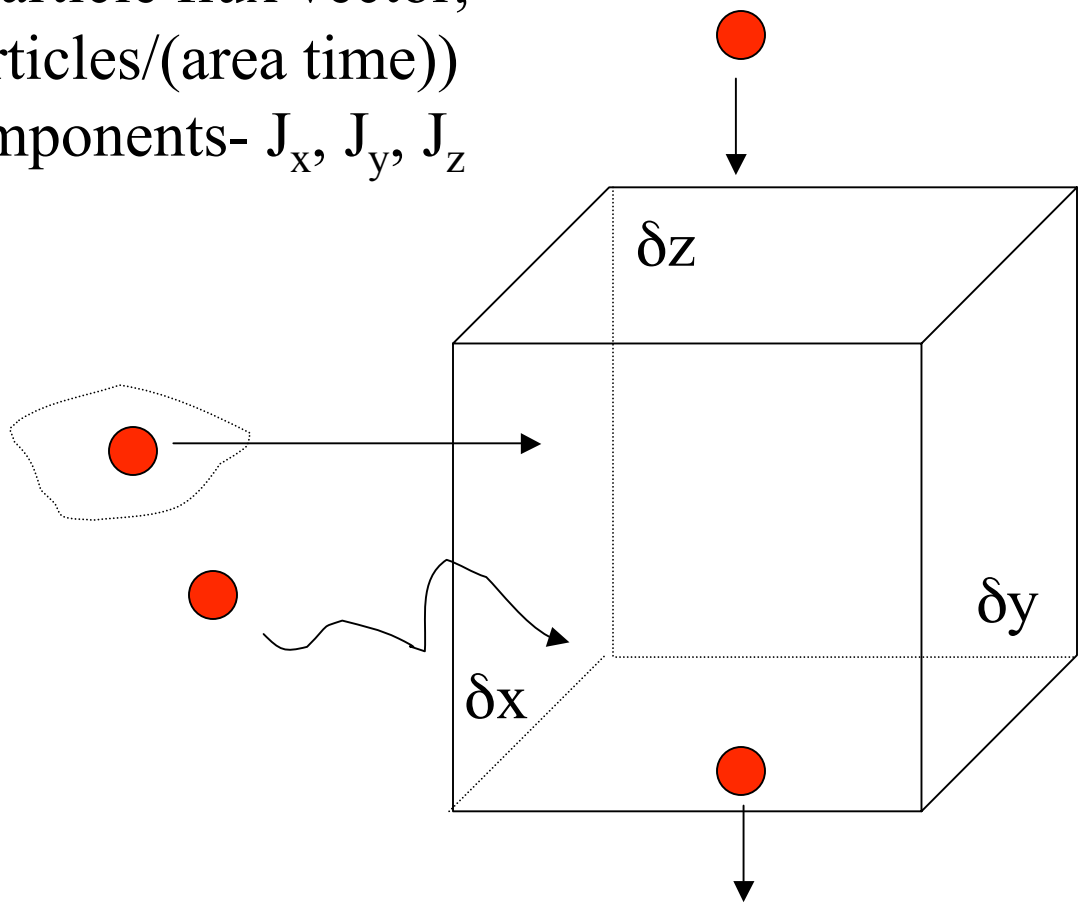

Take a control volume….

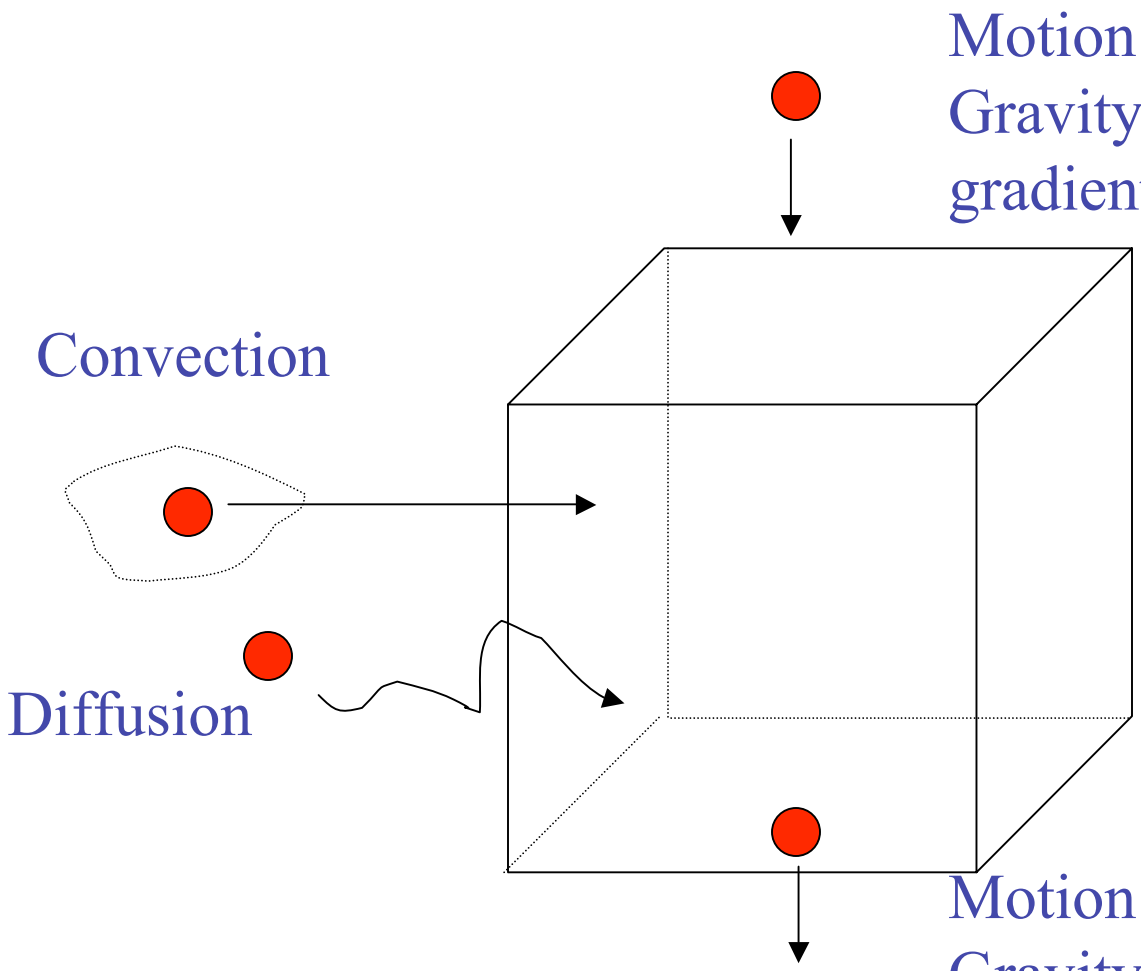

Take a control volume….

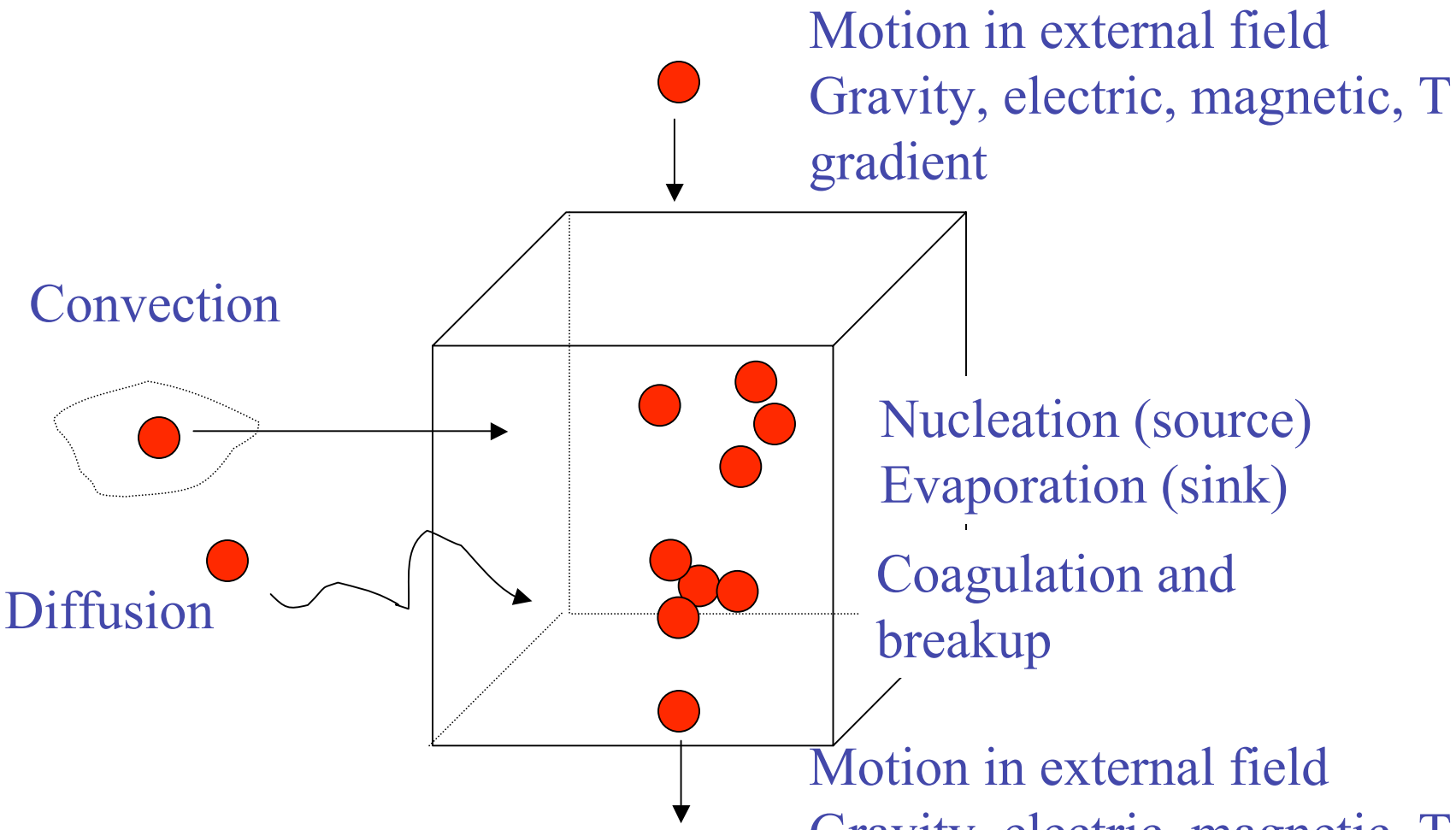

Take a control volume….

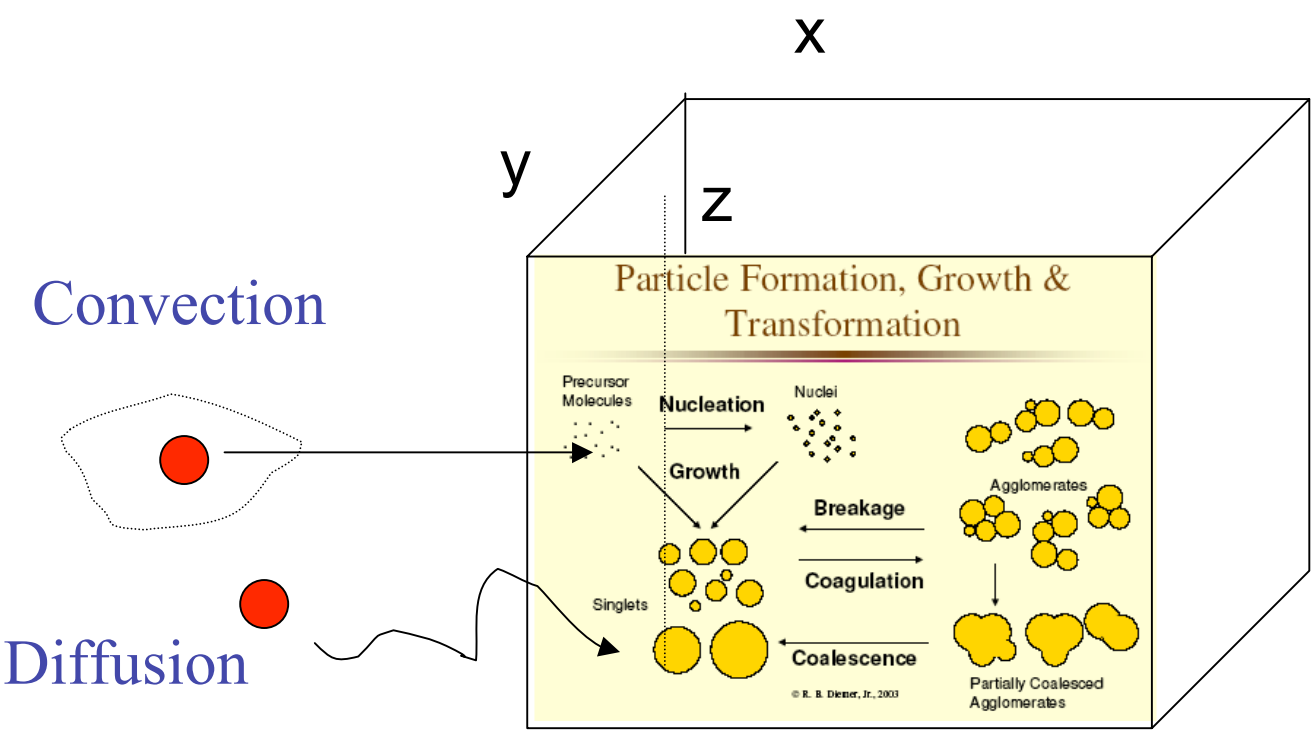

In our problem, no external fields

External coordinates, x,y,z,t

Internal coordinate - particle volume V for 1D population balance

Population balance for dynamics of distributions

- One dimension
  - **Particles, variable diameter**
  - Polymers, variable molecular weight
- 2 dimensions
  - Particles, variable diameter, surface area
  - Polymers, variable molecular weight, number of branch points

Simplifying assumptions, initial conditions

- Assumptions:
  - Steady state, axisymmetric flow, incompressible fluid
  - Plug flow, no slip condition at wall
  - Diffusive transport of particles negligible with respect to convective transport
  - Dynamics of size distribution only varying with axial distance in agglomerator
  - No sources or sinks
- Initial conditions:
  - Particles all same size to start
  - Well mixed

General Differential Form, 1-D Population

$$-\nabla \cdot \left[\mathbf{u}_p(V,\mathbf{x},t)\, n(V,\mathbf{x},t) \right]$$ convection

$$+\nabla \cdot \left[D_p(V,\mathbf{x},t) \nabla n(V,\mathbf{x},t) \right]$$ diffusion

} "In – Out" in external coordinates

$$-\frac{\partial}{\partial V}\left[G(V,\mathbf{x},t)\, n(V,\mathbf{x},t) \right]$$ growth ("In – Out" in internal coordinate)

$$+S(V,\mathbf{x},t)$$ sources & sinks (Net Generation)

$$=$$

$$\frac{\partial n(V,\mathbf{x},t)}{\partial t}$$ accumulation

Note: object's velocity may differ from fluid's velocity owing to either slip or action of external forces

Full 1-D Population Balance
(a partial integrodifferential equation)

$$\frac{\partial n}{\partial t} + \nabla \cdot (\mathbf{u}_p n) - \nabla \cdot (D_p \nabla n) =$$

$$N\,\delta(V - v_o) - \frac{\partial}{\partial V}(G\,n)$$

$$+\frac{1}{2}\int_0^V \beta(v, V - v)\, n(v)\, n(V - v)\, dv - n(V) \int_0^\infty \beta(v, V)\, n(v)\, dv$$

$$+\int_V^\infty \Gamma(\Phi)\, b(V; \Phi)\, n(\Phi)\, d\Phi - \Gamma(V)\, n(V)$$

nucleation term

growth term

coagulation terms

breakage terms

N = nucleation rate
G = accretion rate
β = coagulation rate
Γ = breakage rate
b = daughter distribution
v_0 = nuclei size

Problem Setup

- Steady-state, incompressible, axisymmetric flow
- Plug flow, no slip
- Neglect diffusion
- Population Balance Model:

$$u_z \frac{\partial n}{\partial z} = \int_V^\infty \Gamma(\Phi)\, b(V;\Phi)\, n(\Phi)\, d\Phi - \Gamma(V)\, n(V)$$
$$+ \frac{1}{2}\int_0^V \beta(v, V-v)\, n(v)\, n(V-v)\, dv - n(V)\int_0^\infty \beta(v, V)\, n(v)\, dv$$

Partial List of Techniques

- Discrete Methods
- Sectional Methods

Will discuss

- Similarity Solutions
- LaPlace Transforms
- Orthogonal Polynomial Methods
- Spectral Methods
- Moment Methods
- Monte Carlo Methods

Will not discuss

But first, some particle physics

New dimensionless numbers
Knudsen number = $2\lambda/d_p$
Particle Reynolds number = $\rho_f d_p U/\mu$

Free molecular regime: Kn >>1
Continuum regime: Kn <<1
Transition regime: in between

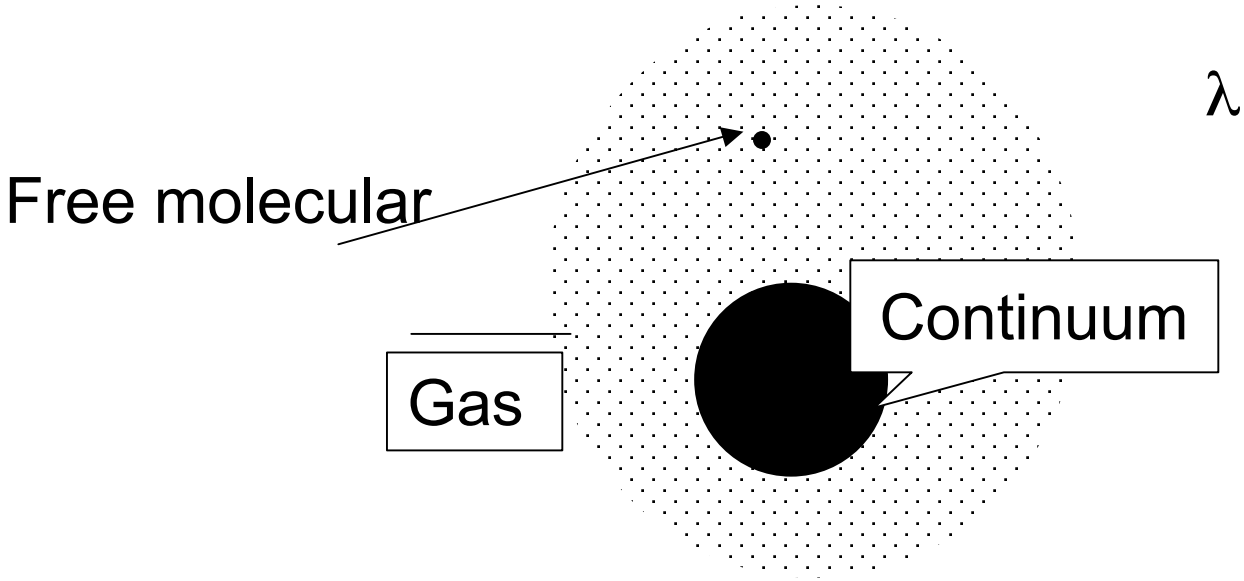

λ -Gas Mean Free Path in air of order 10^{-7} m @STP, U velocity of particle relative to fluid, ρf, fluid density, μ fluid viscosity

Particles in fluid

- So for small particles, collisions with individual gas molecules affect particle motion, growth dynamics

- If size scale of particles --> size scale of eddies in very turbulent flow, turbulence in fluid may affect motion and growth dynamics
  - Levich (1962) agglomeration rate α v_{basic}^9/4
  - Important for particles greater than 1 micron and up

Coagulation - definitions

- Coagulation of solid particles = agglomeration
- When relative motion of particles is Brownian, process = thermal coagulation
- Relative motion from particle- fluid interactions = turbulent coagulation
- Saffman Turner (1956) divided into 2 processes
  - Turbulent shear agglomeration: particles on different streamlines are traveling at different speeds, enhances collisions
  - Turbulent inertial agglomeration: particle trajectories depart from flow streamlines, and lead to collisions

Collision frequency function

Consider the change in number concentration of particles of size i, where $v_i = v_j + v_{i-j}$

collision frequency - # collisions/time between particles of size j and size i-j =

v_i, v_{i-j} are volumes of particles of size j and i- j

$$N_{j,i-j} = \beta\left(v_j, v_{i-j}\right) n_j, n_{i-j}$$

β, also known as a collision kernel, depends on the size of the colliding particles, and properties of system such as temperature

For our problem, we assume all collisions ‘stick’

Test yourself….

- For small particles (free molecular and continuum) will the collision kernel increase or decrease as the system temperature increases?
- For particles in the continuum regime, will the collision kernel increase or decrease as the viscosity of the surrounding gas increases?

Coagulation - discrete distribution bookkeeping

For a discrete size distribution, the rate of formation of particles of size i by collision of particles of size j and i-j, is given by: $\frac{1}{2}\sum_{j=1}^{i-1} N_{j,\,i-j}$ where the factor 1/2 is introduced because each collision is counted twice in summation

Rate of loss of particles of size i by collision with all other particles is given by: $\sum_{j=1}^{\infty} N_{i,j}$

Change in number concentration of particles of size i given by:

$$\frac{dn_i}{dt} = \frac{1}{2}\sum_{j=1}^{i-1} N_{j,i-j} - \sum_{j=1}^{\infty} N_{i,j} = \frac{1}{2}\sum_{j=1}^{i-1} \beta_{j,i-j}(v_j, v_{i-j}) n_j n_{i-j} - n_i \sum_{j=1}^{\infty} \beta_{ij}(v_j, v_i) n_j$$

theory of coagulation for discrete spectrum developed by Smoluchowski (1917) change = formation - loss

Notation change:

Impt for problem statement: Alternate, more general, way to represent two colliding particles, v_j v_{i-j} -->

ϕ, V-ϕ where V is final size of pair after collisions

Coagulation, continuous distributions

continuous nomenclature

n(v) = number of particles per unit volume of size v, a continuous distribution

collision rate:

$$N_{\phi,v-\phi} = \beta(\phi,\ v - \phi)\mathrm{n}(\phi)\mathrm{n}(\mathrm{v} - \phi)\mathrm{d}\phi\mathrm{d}(\mathrm{v} - \phi)$$

where β is the collision frequency function described earlier

The rate of formation of particles of size v by collision of smaller particles of size ϕ and v-ϕ is given by:

$$\textit{formation} \text{ in range } \mathrm{dv} = \frac{1}{2}\left[\int_0^v \beta(\phi, v-\phi)\mathrm{n}(\phi)\mathrm{n}(v-\phi)\mathrm{d}(\mathrm{v} - \phi)\right]\mathrm{d}v$$

$$\textit{loss} \text{ in range } \mathrm{dv} = \left[\int_0^\infty \beta(\phi, v)\mathrm{n}(\phi)\mathrm{n}(v)\mathrm{d}\phi\right]\mathrm{d}v$$

Here, loss is from collisions with all other particles, so must integrate over entire size range

Collision frequency functions

for particles in continuum regime: (Stokes-Einstein relationship valid)

$$\beta(\phi, V-\phi) = \frac{2kT}{3\mu}\left[2 + \left(\frac{\phi}{V-\phi}\right)^{1/3} + \left(\frac{V-\phi}{\phi}\right)^{1/3}\right]$$

for particles in free molecular regime: (derived from kinetic theory of collisions between hard spheres)

$$\beta_{ij} = \left(\frac{3}{4\pi}\right)^{1/6}\left(\frac{6kT}{\rho_p}\right)^{1/2}\left(\frac{1}{\phi} + \frac{1}{v-\phi}\right)^{1/2}\left(\phi^{1/3} + (v-\phi)^{1/3}\right)^2$$

interpolation formulas between regimes given by Fuchs (1964) *The Mechanics of Aerosols*

Collision frequency values:

	$10^{10}\beta$ cm^3/sec		
d_1/d_2	0.01	0.1	1.0
0.01	18		
0.1	240	14.4	
1.0	3200	48	6.8

where particle diameters, d_1 and d_2 are in microns

Test yourself…

- Why are the collision kernel values greater for collisions between smaller and larger particles compared to particles of the same size?

Turbulent coagulation

$$\beta(\phi, V-\phi) = 0.31\sqrt{\frac{\varepsilon}{\nu}}\left[V + 3\phi^{1/3}(V-\phi)^{2/3} + 3\phi^{2/3}(V-\phi)^{1/3}\right]$$

- ν = kinematic viscosity
- ε = energy dissipation rate (rate of conversion of turbulence into heat by molecular viscosity, m^2/s^3)

Comparison… brownian vs. turbulent

- For collisions between 1 micron diameter particles, Brownian kernel ~ 100 x turbulent kernel
- But for collisions between 500 micron diameter particles, turbulent kernel ~ 10 x Brownian kernel

Breakup

- Definitions:
  - Parent: starting agglomerate, size Φ
  - Daughter: resulting fragments, size V
- Different causes of breakup
  - Thermal/Brownian
  - Flow induced
- Simplifying assumption for our problem
- Breakup into equal sized daughter fragments (size V), rate given by:

$$\Gamma(V) = \Gamma_o \left(\frac{\varepsilon}{\nu} \right)^{3/2} V^{1/3}$$

$$b(V;\Phi) = 2\delta\left(V - \frac{\Phi}{2} \right)$$

Discrete Methods

- Size is integer multiple of fundamental size
- Write balance equations for every size
- Gives distribution directly
- Huge number of equations to solve
- Have to decide what the largest size is
- Example for coagulation and breakage:

$$V_i = iV_0; \quad V_0 = \frac{\pi d_0^3}{6}$$

$$u_z \frac{dn_i}{dz} = \frac{1}{2}\sum_{j=1}^{i-1} \beta_{j,i-j} n_j n_{i-j} - n_i \sum_{j=1}^{\infty} \beta_{i,j} n_j + \sum_{j=i+1}^{\infty} \Gamma_j b(i;j) n_j - \Gamma_i n_i$$

Discrete Example Problem Setup

$$\beta_{c,i,j} = \frac{2kT}{3\mu}\left[2+\left(\frac{i}{j}\right)^{1/3}+\left(\frac{j}{i}\right)^{1/3}\right];\quad \beta_{t,i,j} = .31\sqrt{\frac{\varepsilon}{\nu}}V_0\left(i+3i^{2/3}j^{1/3}+3i^{1/3}j^{2/3}+j\right)$$

$$\Gamma_i = \begin{cases} 1\times10^{-8}\,\mathrm{s^2/cm}\left(\dfrac{\varepsilon}{\nu}\right)^{3/2}V_0^{1/3}i^{4/3}, & i>1 \\ 0, & i=1 \end{cases};\quad b(i;j) = \begin{cases} 2, & j=2i \\ 1, & j=2i+1,2i-1 \\ 0, & j<2i-1,\ j>2i+1 \end{cases}$$

$$u_z\frac{dn_i}{dz} = \frac{1}{2}\sum_{j=1}^{i-1}\left(\beta_{c,j,i-j}+\beta_{t,j,i-j}\right)n_j n_{i-j} - n_i\sum_{j=1}^{\infty}\left(\beta_{c,i,j}+\beta_{t,i,j}\right)n_j$$
$$+\Gamma_{2i+1}n_{2i+1}+2\Gamma_{2i}n_{2i}+\Gamma_{2i-1}n_{2i-1}-\Gamma_i n_i$$

Need slightly more than 2×10^6 cells to cover entire mass distribution range!

Sectional Method

- Best rendering due to Litster, Smit and Hounslow
- Collect particles in bins or size classes, with upper/lower size=$2^{1/q}$, “q” optimized for physics

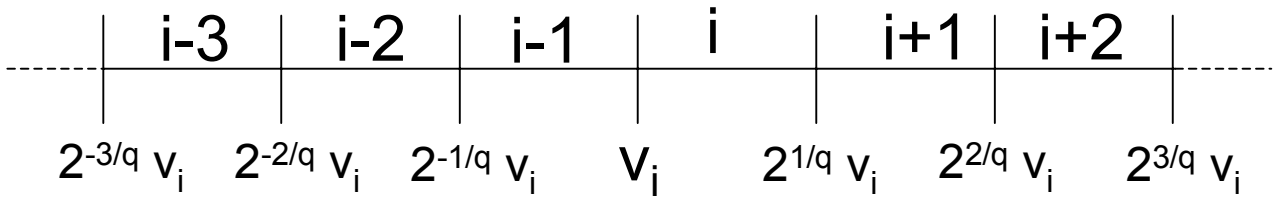

- Balances are written for each size class reducing the number of equations, but too few bins loses resolution
- And… now the equations get more complicated to get the balances right
- Still have problem of growing too large for top class
- Directly computes distribution

Sectional Interaction Types

- Type 1:
  - some particles land in the i^{th} interval and some in a smaller interval
- Type 2:
  - all particles land in the i^{th} interval
- Type 3:
  - some particles land in the i^{th} interval and some in a larger interval
- Type 4:
  - some particles are removed from the i^{th} interval and some from other intervals
- Type 5:
  - particles are removed only from i^{th} interval

Sectionalization Example: q=1

Collision of Particle j with Particle k

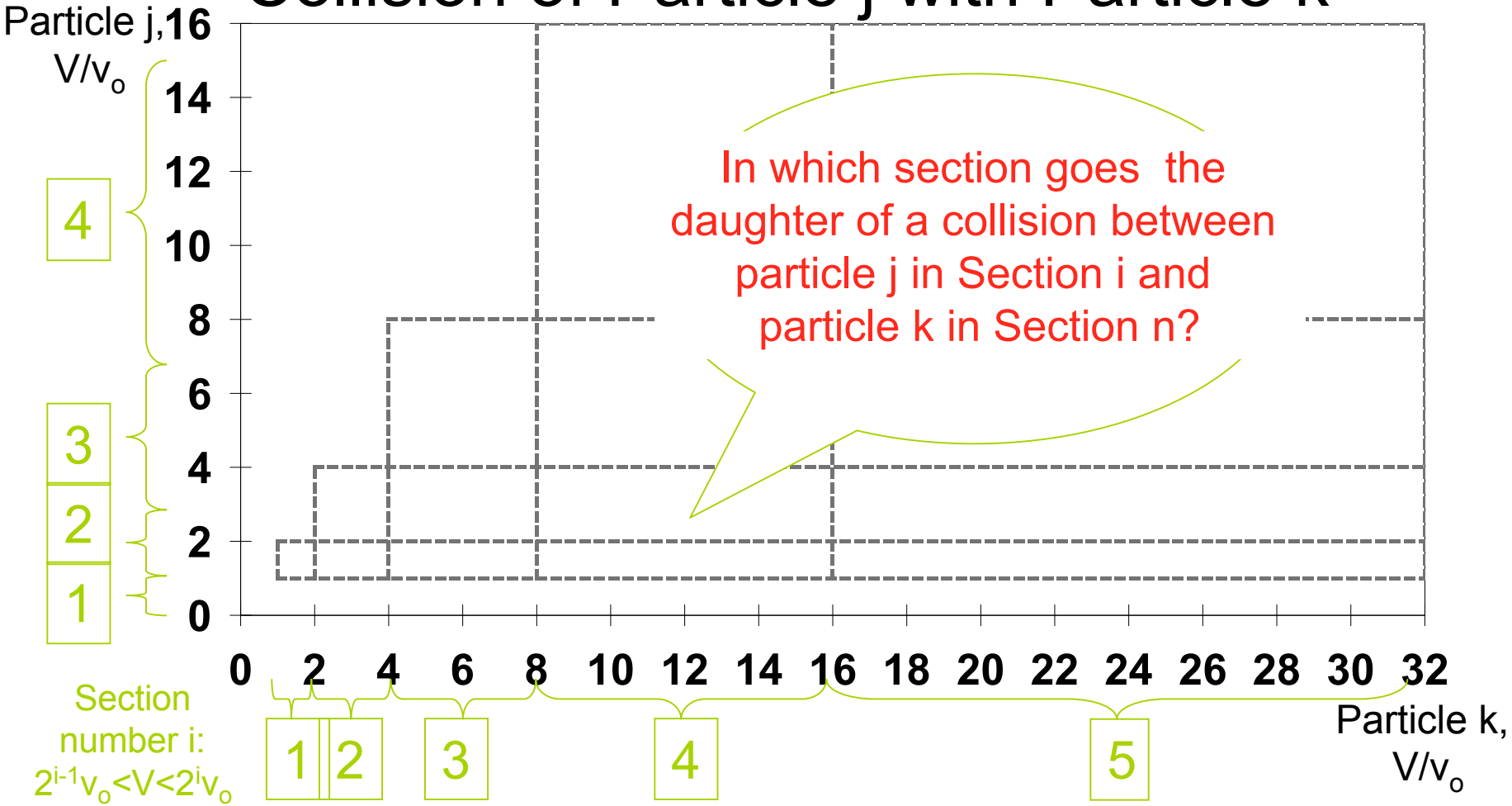

Sectionalization Example: q=1

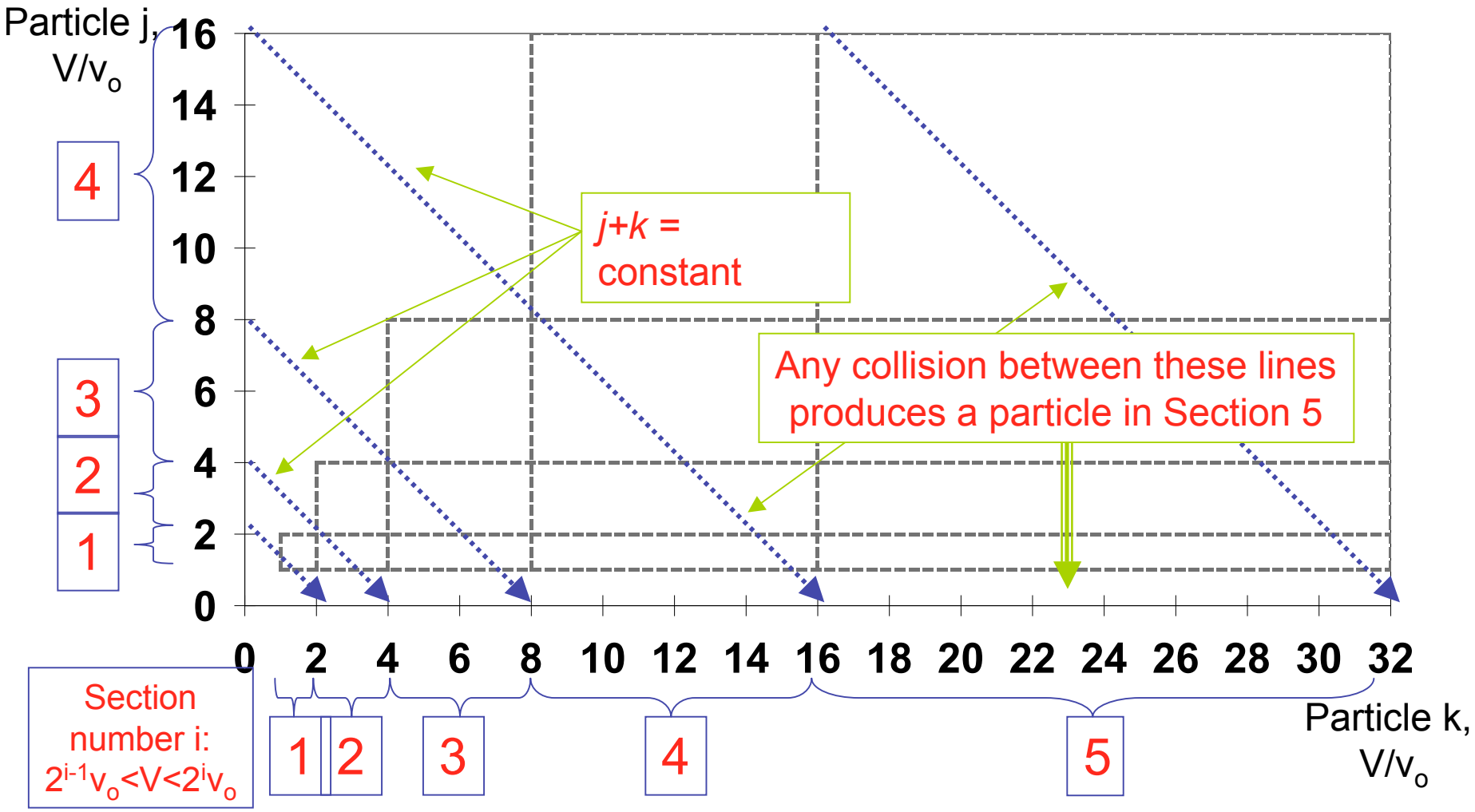

Sectionalization Example: q=1

i,i collisions: map completely into i+1

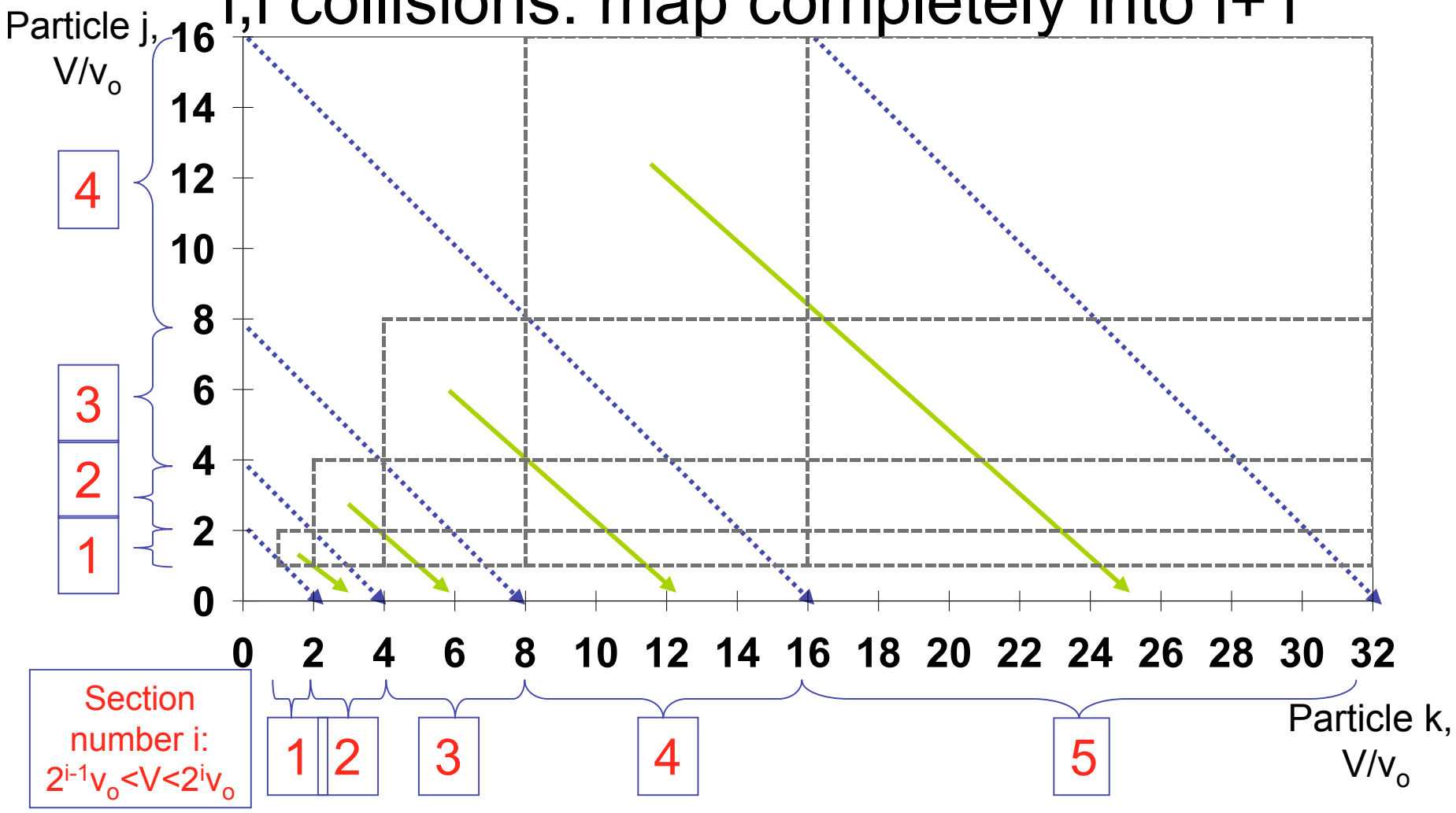

Sectionalization Example: q=1

i,i+1 collisions: 3/4 map into i+2, 1/4 stay in i+1

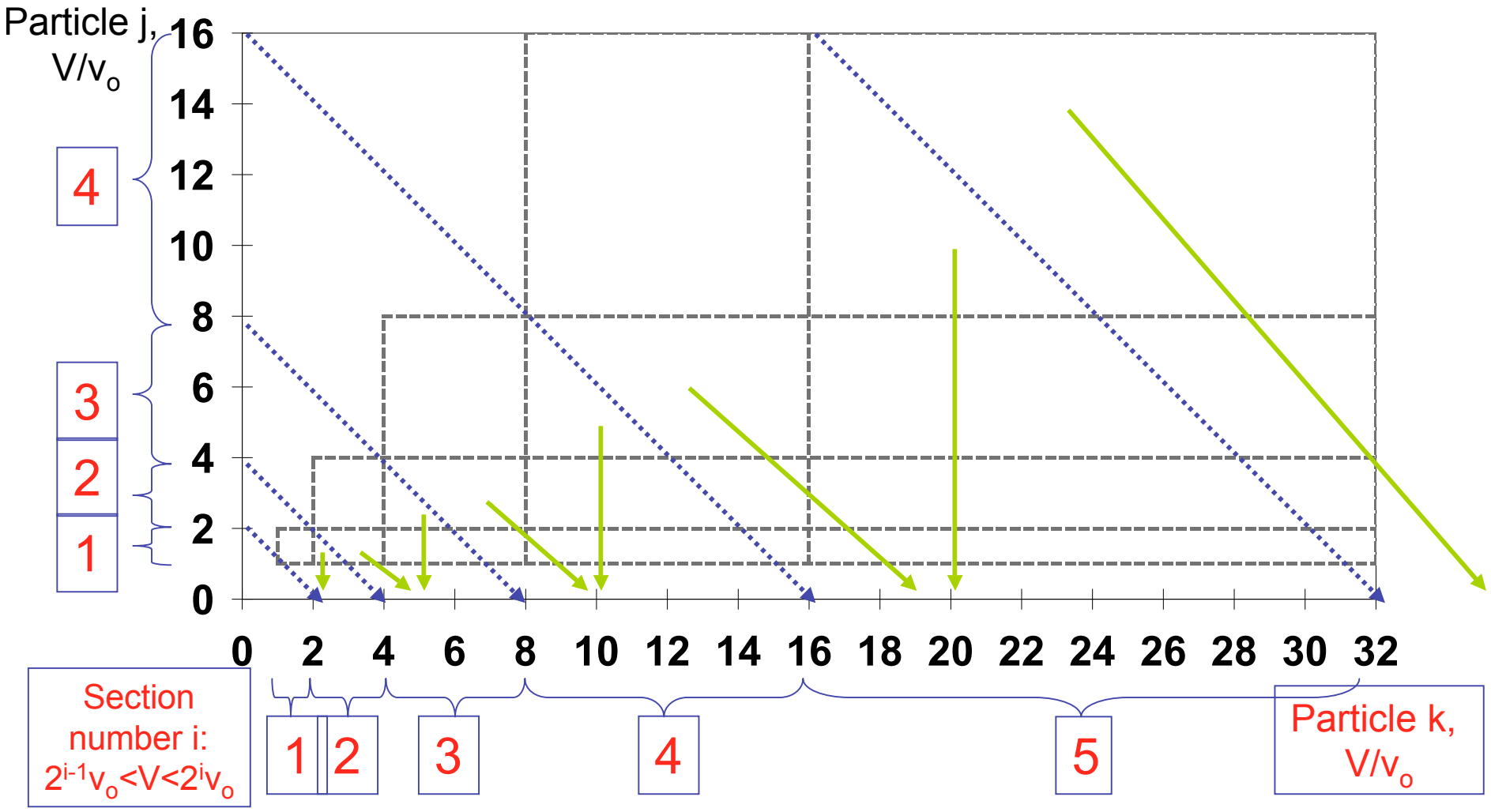

Sectionalization Example: q=1

i,i+2 collisions: 3/8 map into i+3, 5/8 stay in i+2

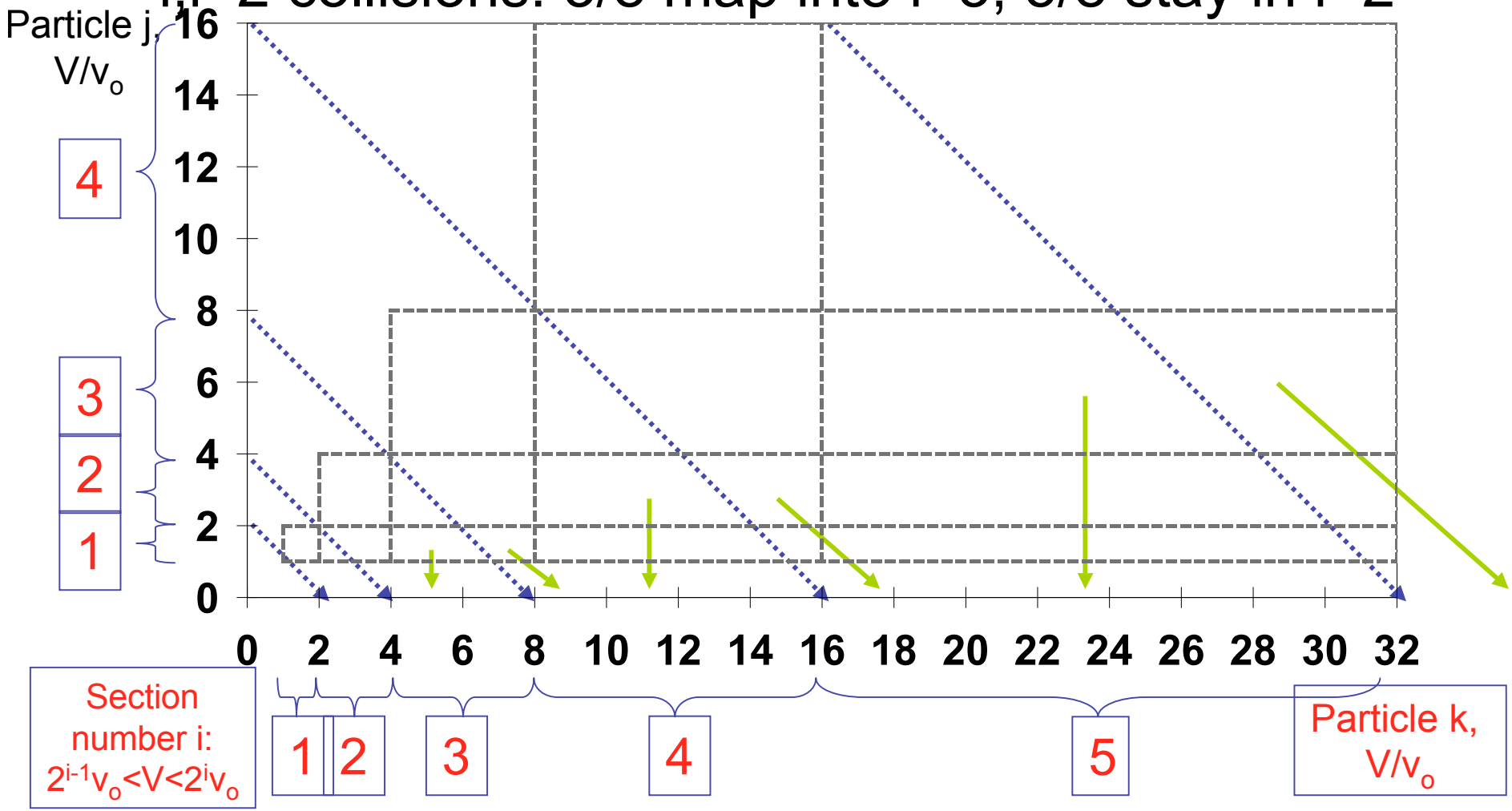

Sectionalization Example: q=1

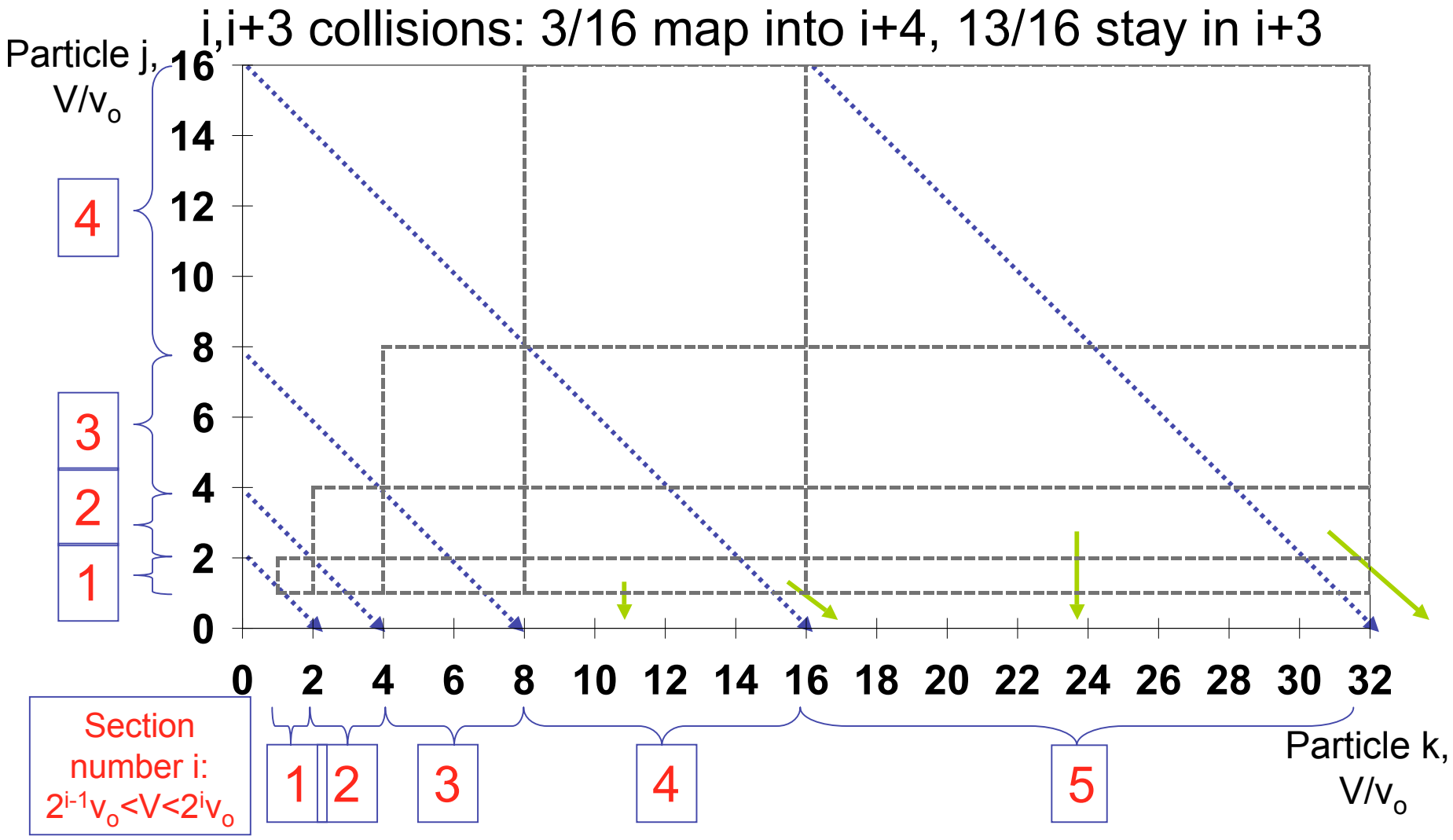

Sectionalization Example: q=1

i,i+4 collisions: 3/32 map into i+5, 29/32 stay in i+4

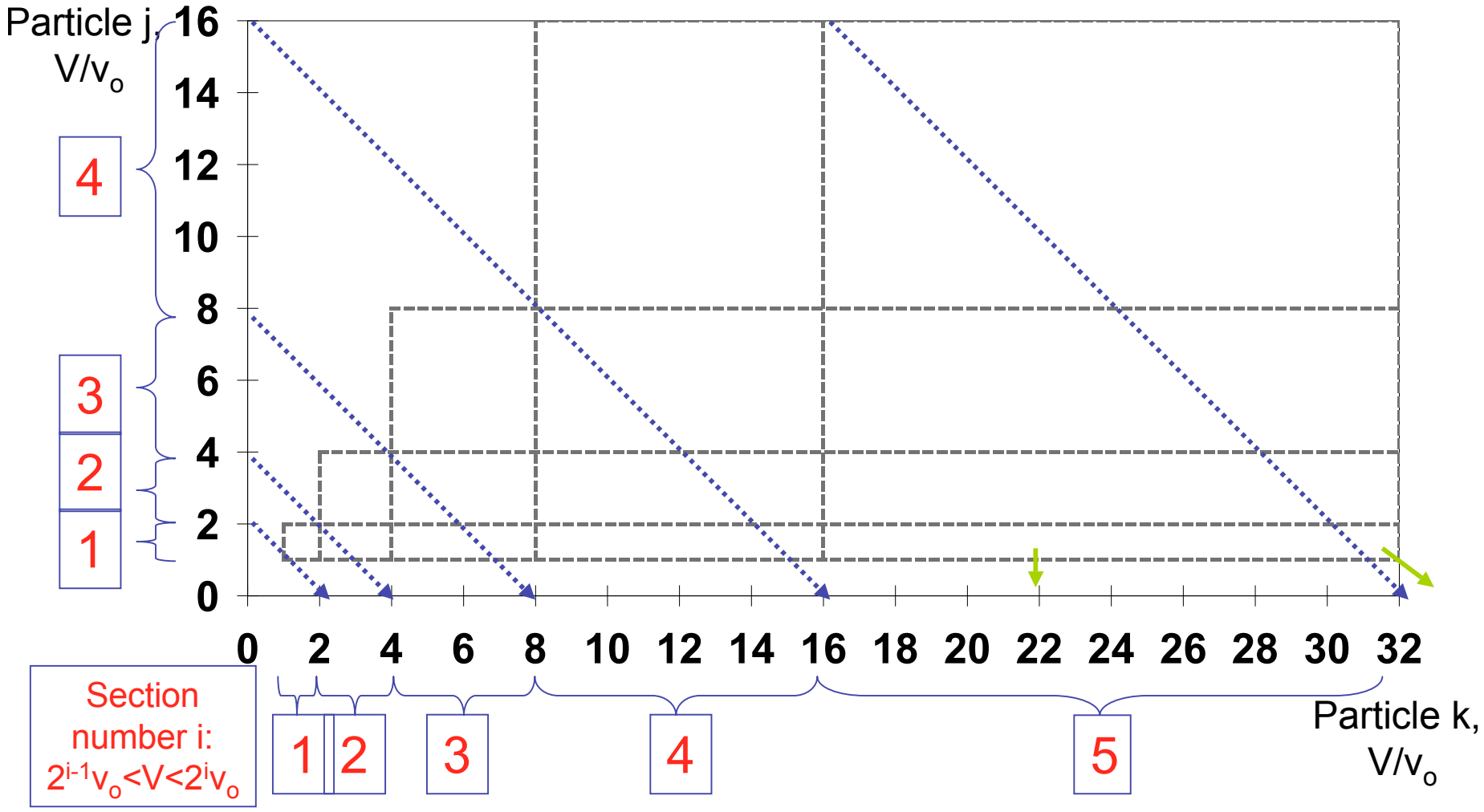

Sectionalization Example: q=1

i,n collisions: $3/2^{n-i+1}$ map into n+1, n>i>0

i,i collisions: all map into i+1

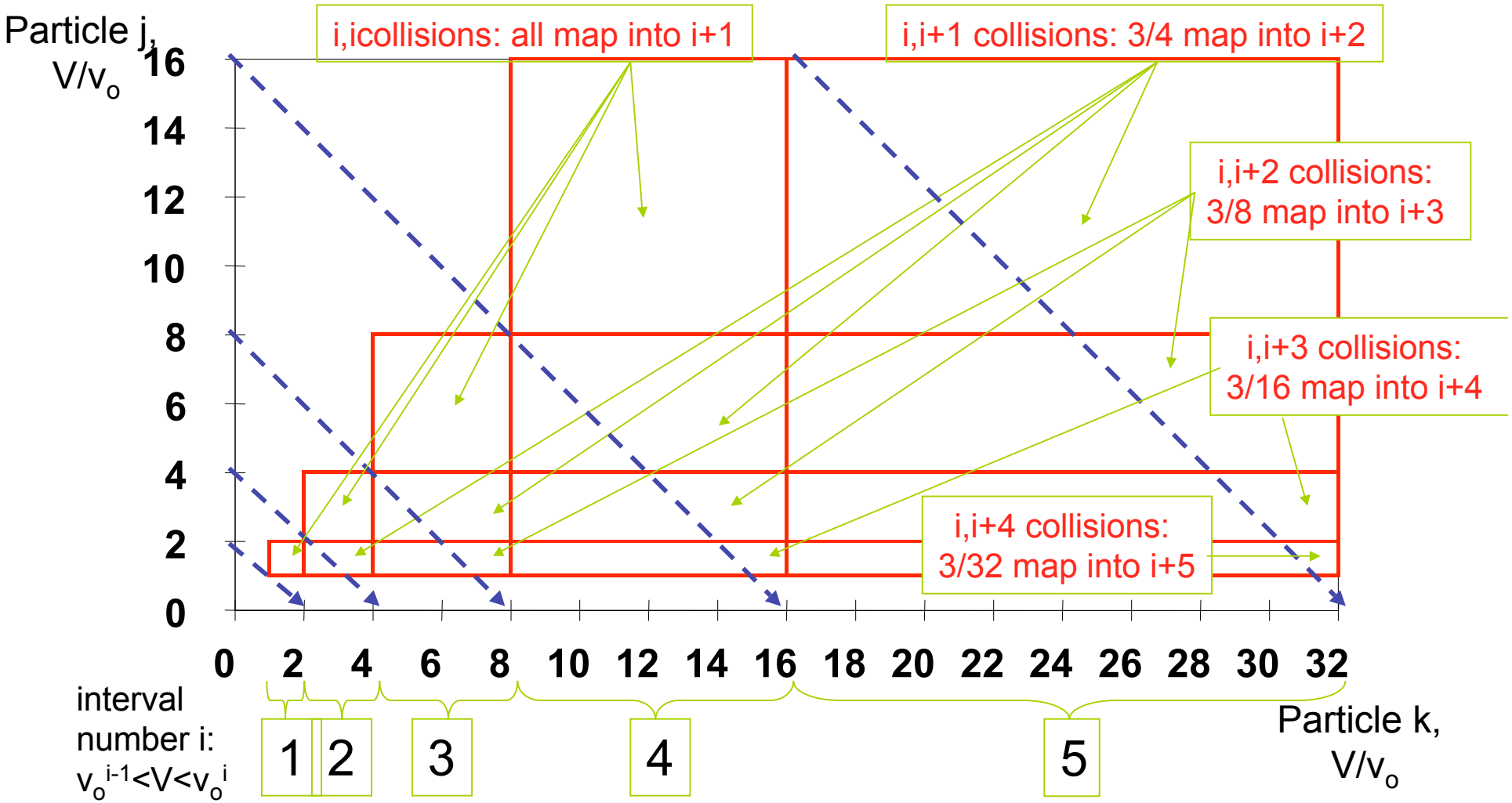

Sectional Coagulation Model, q=1

- Model Equation:

$$u_z \frac{dN_i}{dz} = N_{i-1} \sum_{j=1}^{i-2} \beta_{i-1,j} \theta_{i-1,j} N_j + \frac{1}{2} \beta_{i-1,i-1} N_{i-1}^2 - N_i \left[\sum_{j=1}^{i-1} \beta_{i,j} \theta_{i,j} N_j + \sum_{j=i}^{\infty} \beta_{i,j} N_j \right]$$

- Tentatively:

$$\theta_{i,j} = C \frac{3}{2} 2^{j-i}$$

- Can show (via 0th and 1st moments) that:
  - number balance gives correct general form for arbitrary $\theta_{i,j}$
  - mass balance only closes for C=2/3 when $V_i/V_j = 2^{i-j}$
  - final expression: $\theta_{i,j} = 2^{j-i}$
  - kernels evaluated via:

$$\bar{V}_i = 2^{i-1} \bar{V}_1 \quad \text{with} \quad \bar{V}_1 = \frac{V_0 + 2V_0}{2} = \frac{3V_0}{2} \quad \text{(recovers 3/2 factor)}$$

Gaa!

- At least breakup is easier to visualize
- True equi-sized daughter distributions
- All particles from bin i that breakup will map to lower bin i-1

Sectional Example Problem Setup (for q=1)

$$\beta_{i,j} = \frac{2kT}{3\mu}\left[2 + 2^{(i-j)/3} + 2^{(j-i)/3}\right] + .31\sqrt{\frac{\varepsilon}{\nu}}\left(\frac{3V_0}{2}\right)\left[2^{i-1} + 3\left(2^{(2i+j)/3-1} + 2^{(i+2j)/3-1}\right) + 2^{j-1}\right]$$

$$\Gamma_i = \begin{cases} 1\times10^{-8}\,\mathrm{s^2/cm}\left(\frac{\varepsilon}{\nu}\right)^{3/2}\left(\frac{3V_0}{2}\right)^{1/3} 2^{(i-1)/3}, & i>1 \\ 0, & i=1 \end{cases}; \quad b(i;j) = \begin{cases} 2, & j=i+1 \\ 0, & j\neq i+1 \end{cases}$$

$$u_z\frac{dN_i}{dz} = N_{i-1}\sum_{j=1}^{i-2}\frac{\beta_{i-1,j}}{2^{i-j-1}}N_j + \frac{1}{2}\beta_{i-1,i-1}N_{i-1}^2 - N_i\left[\sum_{j=1}^{i-1}\frac{\beta_{i,j}}{2^{i-j}}N_j + \sum_{j=i}^{\infty}\beta_{i,j}N_j\right]$$
$$+2\Gamma_{i+1}N_{i+1} - \Gamma_i N_i$$

Need about 22 sections to cover entire mass distribution range, suggest using 25-30

General $2^{1/q}$ Sectional Coagulation Model

$$\frac{dN_i}{dt} = N_{i-1}\sum_{j=1}^{i-S(q)-1}\beta_{i-1,j}\theta_{i-1,j}N_j + \frac{1}{2}\beta_{i-q,i-q}N_{i-q}^2 - N_i\left[\sum_{j=1}^{i-S(q)}\beta_{i,j}\theta_{i,j}N_j + \sum_{j=i-S(q)+1}^{\infty}\beta_{i,j}N_j\right]$$

$$\left.\begin{aligned} &+\sum_{k=2}^{q}\sum_{j=i-S(q-k+2)-k+1}^{i-S(q-k+1)-k}\beta_{i-k,j}\left(\theta_{i-1,j}+\psi_k\right)N_{i-k}N_j \\ &-\sum_{k=2}^{q}\sum_{j=i-S(q-k+2)-k+2}^{i-S(q-k+1)-k+1}\beta_{i-k+1,j}\left(\theta_{i,j}+2^{1/q}\psi_{k+1}\right)N_{i-k+1}N_j \end{aligned}\right\}$$ 2 new terms

$$S(q)=\sum_{m=1}^{q}m;\quad \theta_{i,j}=\frac{2^{(j-i)/q}}{2^{1/q}-1};\quad \psi_k=\frac{2^{(1-k)/q}-1}{2^{1/q}-1}$$

Sectional Example Problem Setup (for q=1)
Nondimensionalization

$$\beta_{i,j} = \beta_c^o \Psi_{c\,i,j} + \beta_t^o \left(\frac{3V_0}{2}\right) \Psi_{t\,i,j}; \quad \Gamma_i = \Gamma^o \left(\frac{3V_0}{2}\right)^{1/3} 2^{(i-4)/3}$$

$$\beta_c^o = \frac{2kT}{3\mu}; \quad \Psi_{c,i,j} = 2 + 2^{(i-j)/3} + 2^{(j-i)/3}; \quad \Gamma^o = 1\times 10^{-8}\,\mathrm{s^2/cm}\left(\frac{\varepsilon}{\nu}\right)^{3/2}$$

$$\beta_t^o = .31\sqrt{\frac{\varepsilon}{\nu}}; \quad \Psi_{t\,i,j} = 2^{i-1} + 3\left(2^{(2i+j)/3-1} + 2^{(i+2j)/3-1}\right) + 2^{j-1}$$

$$\Theta = \frac{\tau}{\tau_c} = \frac{\beta_c^o M_0^o z}{u_z}; \quad \Theta_t = \frac{\tau_t}{\tau_c} = \frac{2\beta_c^o}{3\beta_t^o V_0}; \quad \Theta_b = \frac{\tau_b}{\tau_c} = \frac{\beta_c^o M_0^o}{\Gamma^o}\left(\frac{2}{3V_0}\right)^{1/3}$$

$$\Psi_{i,j} = \Psi_{c\,i,j} + \frac{\Psi_{t\,i,j}}{\Theta_t}; \quad n_i = \frac{N_i}{M_0^o}; \quad M_0^o = \frac{2M_1}{3V_0} = \frac{4M_1}{\pi d_0^3}$$

$$\frac{dn_i}{d\Theta} = n_{i-1}\sum_{j=1}^{i-2}\frac{\Psi_{i-1,j}}{2^{i-j-1}}n_j + \frac{1}{2}\Psi_{i-1,i-1}n_{i-1}^2 - n_i\left[\sum_{j=1}^{i-1}\frac{\Psi_{i,j}}{2^{i-j}}n_j + \sum_{j=i}^{\infty}\Psi_{i,j}n_j\right] + \frac{2^{(i-4)/3}}{\Theta_b}\left(2^{4/3}n_{i-1} - n_i\right)$$

Solution tools:

- YOU need to figure out, and modify
  - Change # sections
  - change pipe dimensions
- popbal.m
  - Main, runs functions, checks efficiency, adjusts pipe length till 75% efficiency in cyclone met, checks mass closure
- numdist.m
  - Function, solves ODEs
- gamma.m
  - Function, calculates breakup kernels
- beta.m
  - Function, calculates coagulation kernels

References

1. Nelson, R. D.; Davies, R.; Jacob, K., Teach -em particle technology. *Chemical Engineering Education* **1995,** 29, (1), 12-15.
2. Litster, J. D.; Smit, D. J.; Hounslow, M. J., Adjustable discretized population balance for growth and aggregation. *AIChE Journal* **1995,** 41, (3), 591-603.
3. Diemer, R. B.; Ehrman, S. H., Pipeline agglomerator design as a model test case. *Powder Technology* **2005,** 156, 129-145.

Embedded spreadsheet for histogram

Size range, microns	number of particles	Frequency	assume diameter	mass of particles in each bin, g	Mass frequency
0 to 10	10	0.01	5	6.54E-10	0.00
11 to 20	30	0.03	15	5.30E-08	0.00
21 to 30	80	0.08	25	6.54E-07	0.01
31 to 40	180	0.18	35	4.04E-06	0.05
41 to 50	280	0.28	45	1.34E-05	0.16
51 to 60	169	0.169	55	1.47E-05	0.18
61 to 70	120	0.12	65	1.72E-05	0.21
71 to 80	88	0.088	75	1.94E-05	0.23
81 to 90	40	0.04	85	1.29E-05	0.15
91 to 100	3	0.003	95	1.35E-06	0.02
total number	1000				
total mass assuming 1g/cc density				8.6E-05	

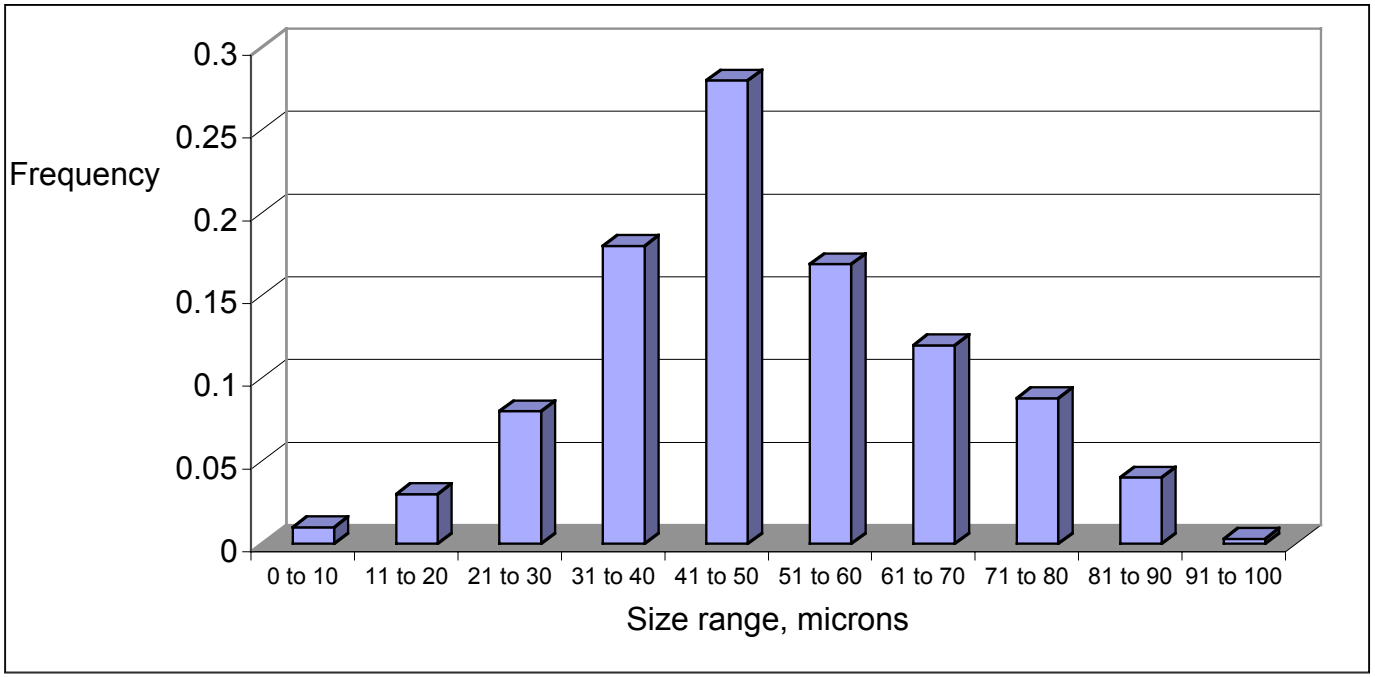

WIKIPEDIA

Population balance equation

Population balance equations (PBEs) have been introduced in several branches of modern science, mainly in Chemical Engineering, to describe the evolution of a population of particles. This includes topics like crystallization, liquid-liquid extraction, gas-liquid dispersions, liquid-liquid reactions, comminution, aerosol engineering, biology (where the separate entities are cells), polymerization, etc. Population balance equations can be said to be derived as an extension of the Smoluchowski coagulation equation which describes only the coalescence of particles. PBEs, more generally, define how populations of separate entities develop in specific properties over time. They are a set of Integro-partial differential equations which gives the mean-field behavior of a population of particles from the analysis of behavior of single particle in local conditions.[1] Particulate systems are characterized by the birth and death of particles. For example, consider precipitation process (formation of solid from liquid solution) which has the subprocesses nucleation, agglomeration, breakage, etc., that result in the increase or decrease of the number of particles of a particular radius (assuming formation of spherical particles). Population balance is nothing but a *balance on the number of particles of a particular state* (in this example, *size*).

Formulation of PBE

Consider the average number of particles with particle properties denoted by a particle state vector (**x**,**r**) (where **x** corresponds to particle properties like size, density, etc. also known as internal coordinates and, **r** corresponds to spatial position or external coordinates) dispersed in a continuous phase defined by a phase vector Y(**r**,t) (which again is a function of all such vectors which denote the phase properties at various locations) is denoted by f(**x**,**r**,t). Hence it gives the particle characteristics in property and space domains. Let h(**x**,**r**,**Y**,t) denote the birth rate of particles per unit volume of particle state space, so the number conservation can be written as[1]

$$\frac{d}{dt}\int_{\Omega_x(t)} dV_x \int_{\Omega_r(t)} dV_r\, f(\mathbf{x},\mathbf{r},t) = \int_{\Omega_x(t)} dV_x \int_{\Omega_r(t)} dV_r\, h(\mathbf{x},\mathbf{r},\mathbf{Y},t)$$

This is a generalized form of PBE.[1]

Solution to PBE

Monte Carlo methods [2] ,[3] discretization methods and moment methods [2][3][4][5][6] are mainly used to solve these equations. The choice depends on the application and computing infrastructure.

References

1. Ramkrishna, D.: *Population Balances: Theory and Applications to Particulate Systems in Engineering*, Academic Press, 2000
2. Hashemian, N.; Armaou, A. (2016). "Simulation, model-reduction and state estimation of a two-component coagulation process" (http://onlinelibrary.wiley.com/doi/10.1002/aic.15146/pdf). *AIChE Journal*. **62**: 1557–1567. doi:10.1002/aic.15146 (https://doi.org/10.1002%2Faic.15146).

3. Hashemian, N.; Ghanaatpishe, M.; Armaou, A. (2016). "Development of a reduced order model for bi-component granulation processes via laguerre polynomials" (http://ieeexplore.ieee.org/xpl/login.jsp?tp=&arnumber=7525483&url=http%3A%2F%2Fieeexplore.ieee.org%2Fxpls%2Fabs_all.jsp%3Farnumber%3D7525483). *Proceedings of the American Control Conference*: 3668–3673. doi:10.1109/ACC.2016.7525483 (https://doi.org/10.1109%2FACC.2016.7525483).
4. Description of Aerosol Dynamics by the Quadrature Method of Moments, Robert McGrawa, Aerosol Science and Technology, Volume 27, Issue 2, 1997, pages 255-265
5. Yu, M., Lin, J., and Chan, T. (2008). A New Moment Method for Solving the Coagulation Equation for Particles in Brownian Motion. Aerosol Sci. Technol., 42(9):705–713.
6. Marchisio, D. L., and Fox, R. O. (2005). Solution of Population Balance Equa- tions Using the Direct Quadrature Method of Moments. J. Aerosol Sci., 36(1):43–73.

12

Population Balance Models

Keywords: Models, Population Balance

All the previous models discussed in last lectures have been based on the basic mass, momentum and energy balances. The equations that involve dispersion are most representative of a process when the mixing is on a relatively small scale. For mixing in stirred tanks (in turbulence), dispersion models are not effective. Certain categories of models which cannot successfully be treated within the framework of the models based on transport phenomena can be treated by the population balance concept.

The application of population -balance principles to the modelling of flow and mixing characteristics in vessels was formally organized by Danckwert's. He defined certain distribution functions for the residence time of the fluid elements in a process vessel.RTD functions give information about the fraction of the fluid that spends a certain time in a process vessel. RTD models do not give point- to – point variation of the dependent variables. Danckwert's description was based on macroscopic lumped-population-balance. Population balance models represents macro-mixing that are sufficient ti give adequate estimates of the behavior of the process.

Description of Flow Pattern's in Process Vessel's

There are two types of ideal flow patterns in our process vessels;

1. Plug flow pattern – Piston Flow
2. Bochmix Flow Pattern – Perfectly mixed

Plug flow occurs when the fluid velocity is uniform over the entire cross-section of the vessel.

Perfect mixing assumes that the vessel contents are completely homogenous down to a molecular scale.

Between these two extreme's lie flow patterns in actual process.

In channeling (known as by-passing) some elements of fluid slip on pass through the vessel considerably faster than others do. Channeling may be found in flow through purely packed

vessels, through vessels of small length-to-diameter ratios or through heat exchanger's with proper baffling.

Stagnant packets (dead space) may occur in header's, at the base of pressure gauges, or in the odd-shaped corner's, represents regions with extremely pure contacting.

AGE DISTRIBUTION FUNCTIONS

The residence time of a fluid element is the time that elapses from the time the element enters the vessel to the time it leaves it. The age of a fluid element at a given instant of time is the time that elapses between the element's entrance into the vessel and the given instant , and is of course , less than or equal to the residence time. The age is equal to the residence time for those molecules that are just leaving the vessel.

INTERNAL AGE DISTRIBUTION OF A FLUID IN A CLOSED VESSEL

The functional notation I(t) will be used for the internal age distribution frequency of fluid elements in a vessel. I(t) have the unit- fraction of ages per unit time.

$$\int_0^\infty I(t)\,dt = 1 \qquad \ldots 12.1$$

The time t=0 refers to an arbitrary initial time and not the start of the flow of fluid into the vessel. In physical terms, eq. (12.1) states that all fluid has an age between 0 and ∞.

As a consequence of the above, the fraction of vessel contents younger than a specified age t is,

$$\int_0^t I(t')\,dt' = 1 \qquad \ldots 12.2$$

While the fraction older than t is ,

$$\int_t^\infty I(t')\,dt' = 1 - \int_0^t I(t')\,dt' \qquad \ldots 12.3$$

Age Distribution of the Exit Stream; The Residence Distribution of fluid in a closed vessel, E(t)

The function E(t) is the age distribution frequency of the fluid elements leaving the vessel and has the units of fraction of ages per unit time. The fraction of exit ages itself is E(t)Δt. The function is normalized to;

$$\int_0^\infty E(t)\,dt = 1 \qquad \ldots 12.4$$

The fraction of fluid in the exit stream younger than age t is

$$\int_0^t E(t')\,dt' = 1 \qquad \ldots 12.5$$

while the fraction of material older than t is

$$\int_t^\infty E(t')\,dt' = 1 - \int_0^t E(t')\,dt' = 1 \qquad \ldots 12.6$$

The mean RTD is found from the first moment

$$\bar{t} = \int_0^\infty tE(t)\,dt = \frac{V}{Q} \qquad \ldots 12.7$$

$$\frac{V}{Q} = \bar{t} = \boldsymbol{\tau}$$

In a similar fashion the mean age of fluid elements inside the vessel is,

$$\bar{t_1} = \int_0^\infty tI(t)\,dt \qquad \ldots 12.8$$

Intensity Function, Λ(t)

It is defined as fraction of fluid in the vessel of age t that will leave at time between t and t+Δt. The intensity function is useful in detecting the existence of dead space and by passing.

Relations between Age Distribution Functions:

The three age distribution frequency functions described above are related through the unsteady state macroscopic age population balance. The balance is made in the units of time. The input age distribution is zero. The general macroscopic population balances can be used to relate E(t) and I(t), but a simpler alternate method is used here.

Consider a constant volume vessel, V, with constant flow rate Q and call all fluid entering the vessel at t>0 new fluid. The existing contents at t=0 are the old fluid. At some time t, eq. 12.2 gives the function of new fluid.

Amount of new fluid in vessel = $V\int_0^t I(t')\,dt'$

Eq. 12.6 gives the fraction of out flowing fluid at any instant of time, that has an age greater than t; the amount of old fluid that has left the vessel during all times from 0 to t is

Amount of old fluid gone from the vessel = $\int_0^t Q\,dt' \int_{t'}^{\infty} E(t'')\,dt''$

Then by a simple balance, the old fluid left must have been replaced by the new fluid,

$$V\int_0^t I(t')\,dt' = \int_0^t Q\,dt' \int_{t'}^{\infty} E(t'')\,dt'' \qquad \ldots 12.9$$

Differentiation of both sides of eq. 12.9 with respect to time with the introduction of eq.12.7 gives,

$$\bar{t}I(t) = \int_t^{\infty} E(t')\,dt' = 1 - \int_0^t E(t')\,dt' \qquad \ldots 12.10$$

Differentiating once more,

$$E(t) = -\bar{t}\frac{dI(t)}{dt} \qquad \ldots 12.11$$

The intensity function can also be related to the E(t) and I(t) functions from

{ Amount of fluid leaving between t and t+Δt } = { Amount not leaving before time t } [Fraction of age t that will leave between times t, t+Δt]

$$QE(t)dt = [VI(t)][\Lambda(t)dt] \qquad \ldots 12.12$$

$$\Lambda(t) = \frac{1}{\bar{t}}\frac{E(t)}{I(t)} = -\frac{d[ln\bar{t}I(t)]}{dt} \quad \ldots 12.13$$

Each of the age distribution functions can be expressed in dimensionless form.

$$\theta = \frac{t}{\bar{t}} \quad \ldots 12.14$$

Thus, $E(\theta)d\theta = E(t)dt, I(\theta)d\theta = I(t)dt$

$$E(\theta) = \bar{t}E(t) \quad \ldots 12.15$$

$$I(\theta) = \bar{t}I(t) \quad \ldots 12.16$$

$$\Lambda(\theta) = \bar{t}\Lambda(t) \quad \ldots 12.17$$

$$E(\theta) = -\frac{d\,I(\theta)}{d\theta}\,I(\theta) \quad \ldots 12.18$$

$$\Lambda(\theta) = \frac{E(\theta)}{I(\theta)} = -\frac{\ln(\theta)}{d\theta} \quad \ldots 12.19$$

Population Balances in Engineering

- Crystallization, Precipitation
- Coagulation, Agglomeration and Flocculation
- Particle Breakage, Particle Attrition
- Dissolution/Leaching
- Cell Growth
  - Fermentation
  - Tissue Engineering

Constant Stirred Tank Crystallizer (MSMPR)

- On-line Analysis
  - Feed Flow Rate Controlled
  - Product Flow Rate Controlled
  - Liquid Level Controlled
  - Reactor
    - pH - √
    - Ionic Strength - √
    - Temperature - √
    - Stirrer RPM - √
    - Stirrer Torque - √
    - Heat Balance - √
  - Particle Size
    - Movie/Stills of Particles
- Off-line Analysis
    - Beckman-Coulter LS230
    - AA + ICP of feed and output
    - Yield

$CaCl_2$-NaCl-KCl

- 45% $CaCl_2$
  - NaCl+KCl
- Baffled Stirred Tank
  - Cooling
  - Impurity Removal

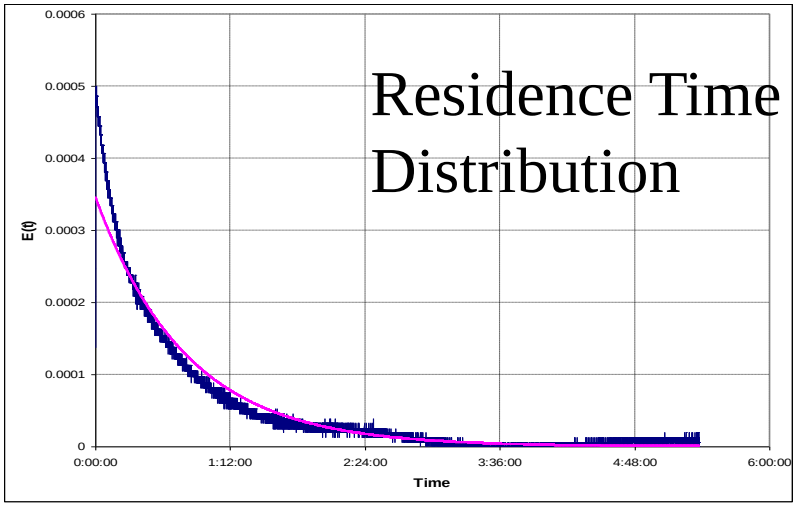

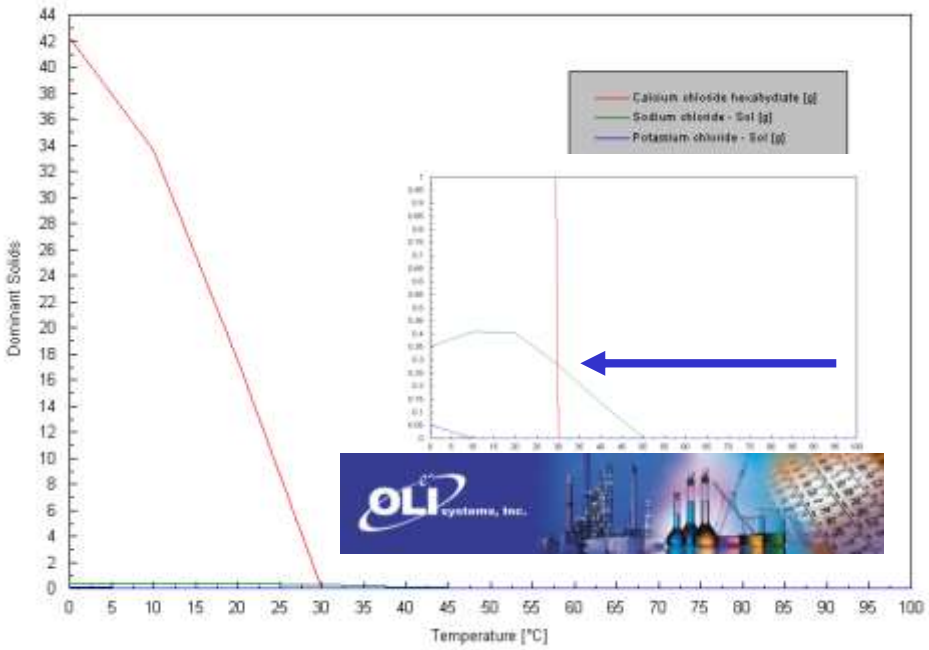

$CaCl_2$ Results - Sample #10-01

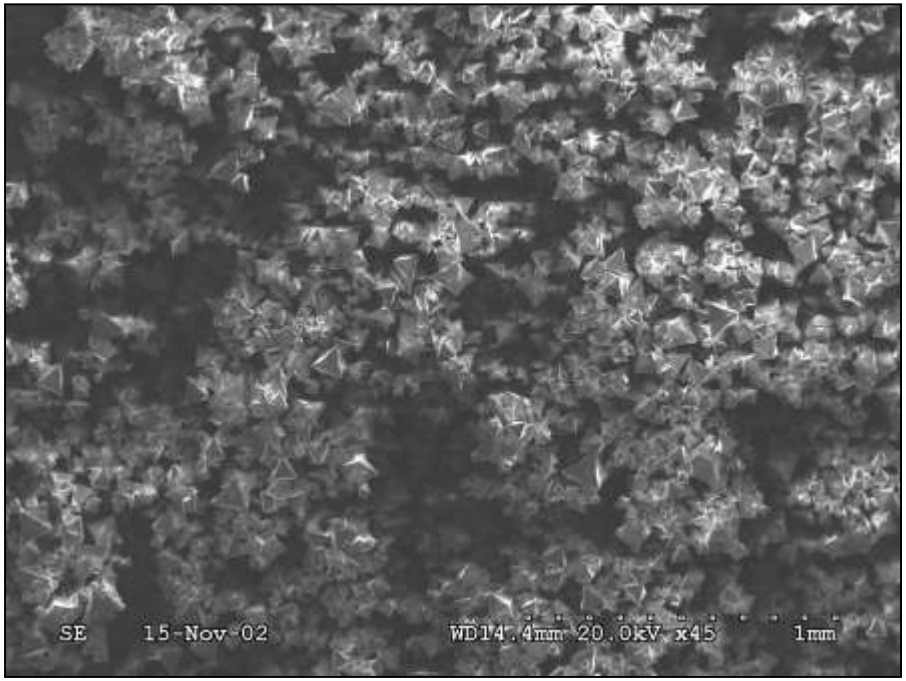

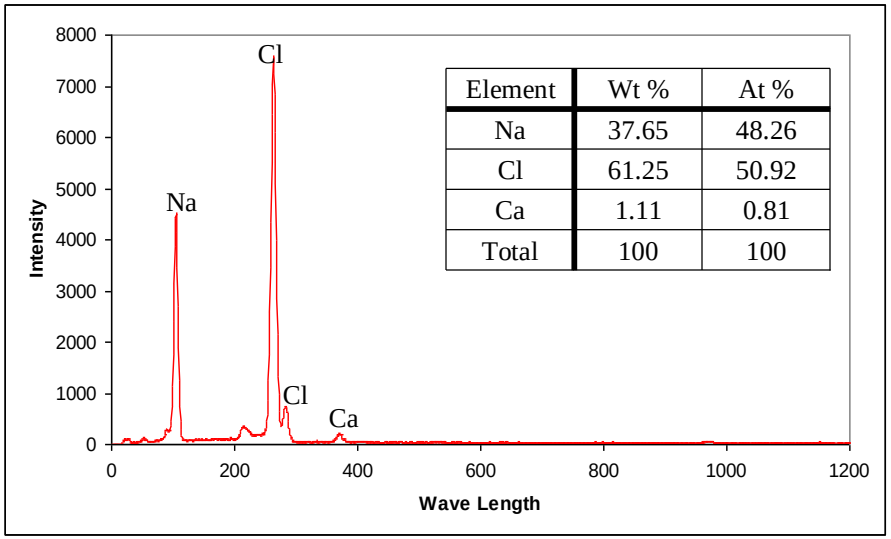

Element	Wt %	At %
Na	37.65	48.26
Cl	61.25	50.92
Ca	1.11	0.81
Total	100	100

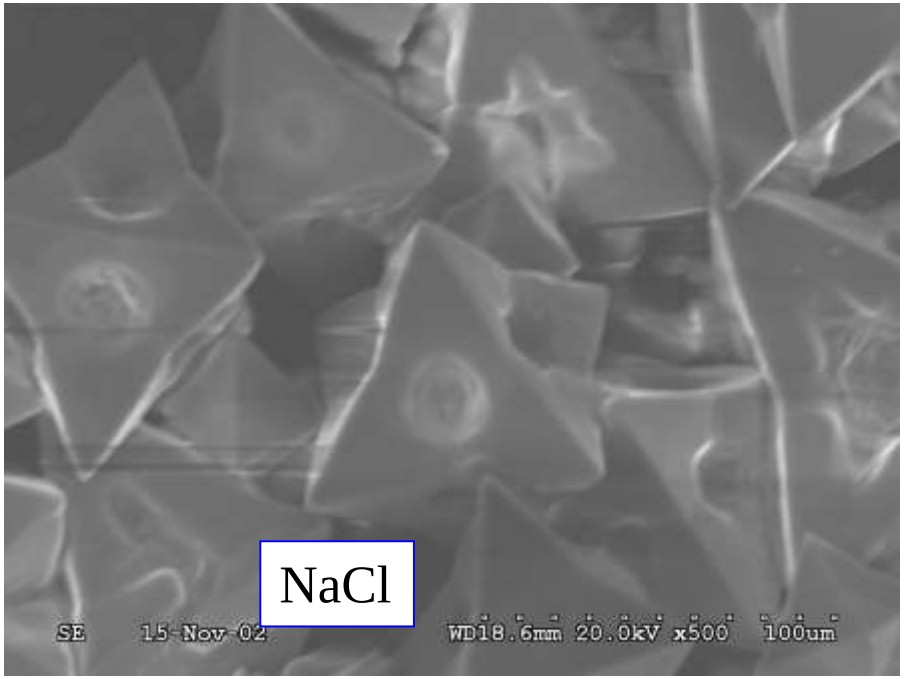

Particle Size Analysis with Beckman Coulter LS230

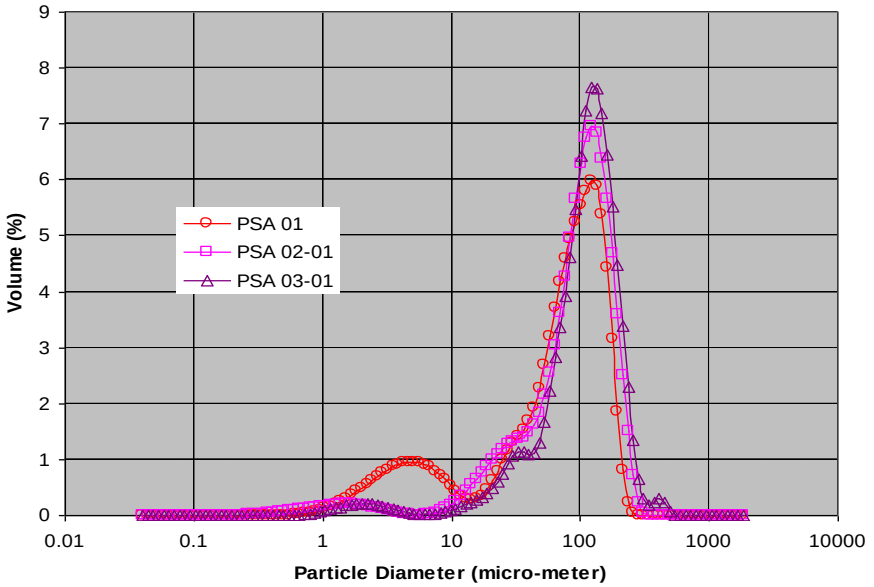

Sample #11-02

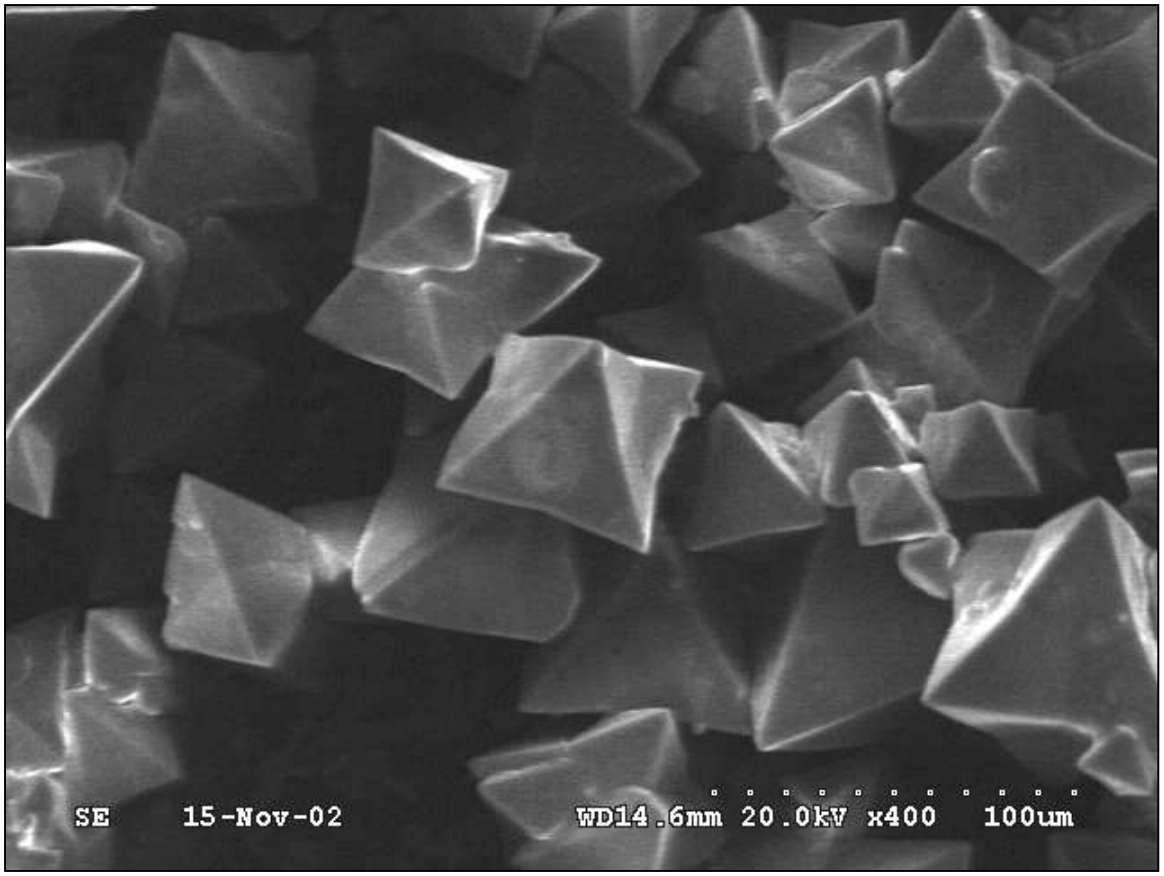

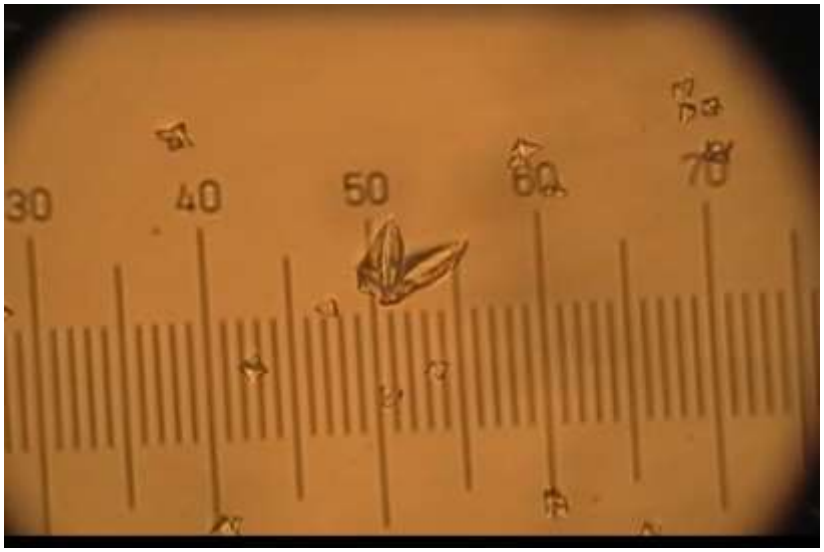

30 min.

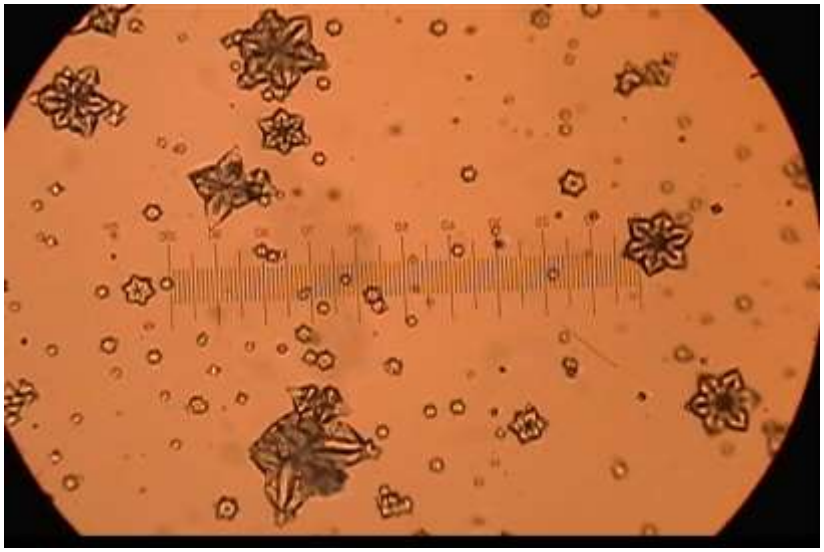

90 min.

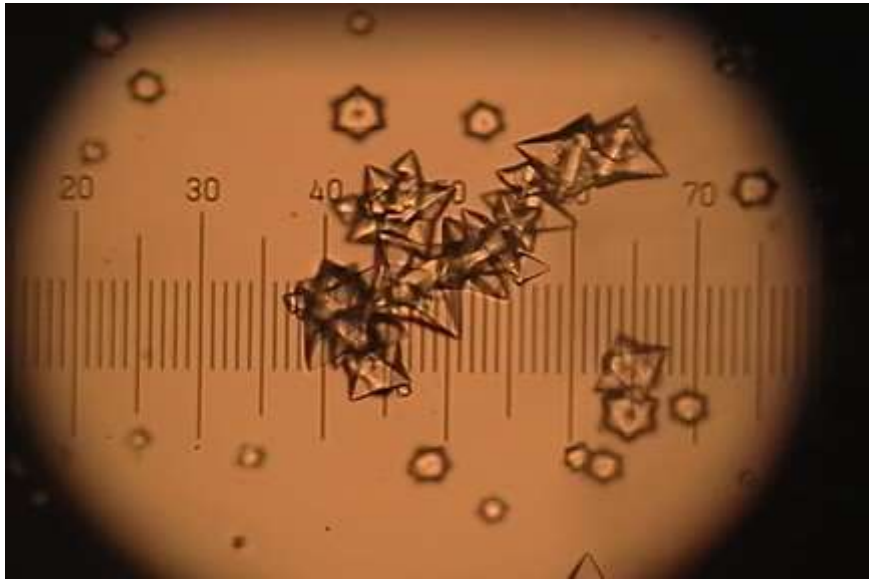

6 hr.

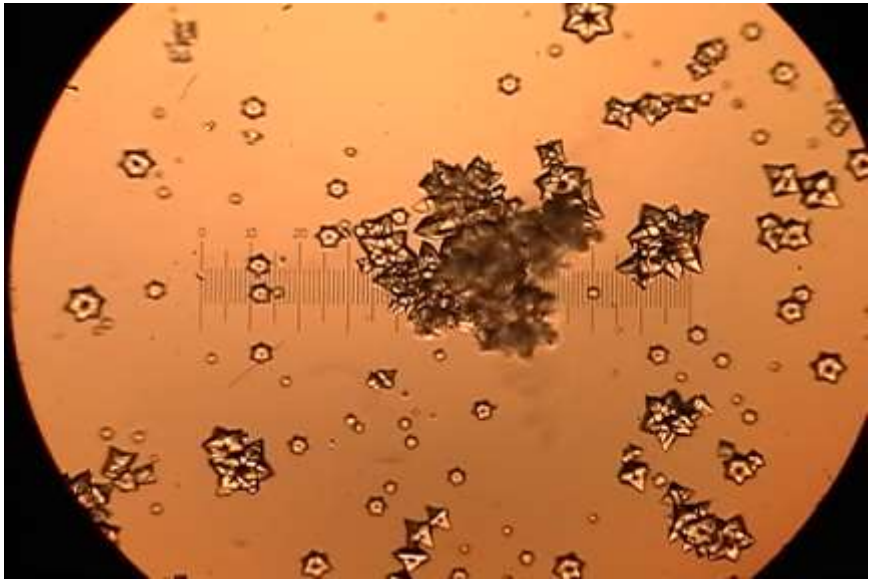

6 hr.

07/25/03 Reaction Temp: 30.1°C, Flow Rate: 45 ml/min, Mixing Power: 287.7 rpm, Reactor Volume: 1400 ml

Particle Size Distribution with Time

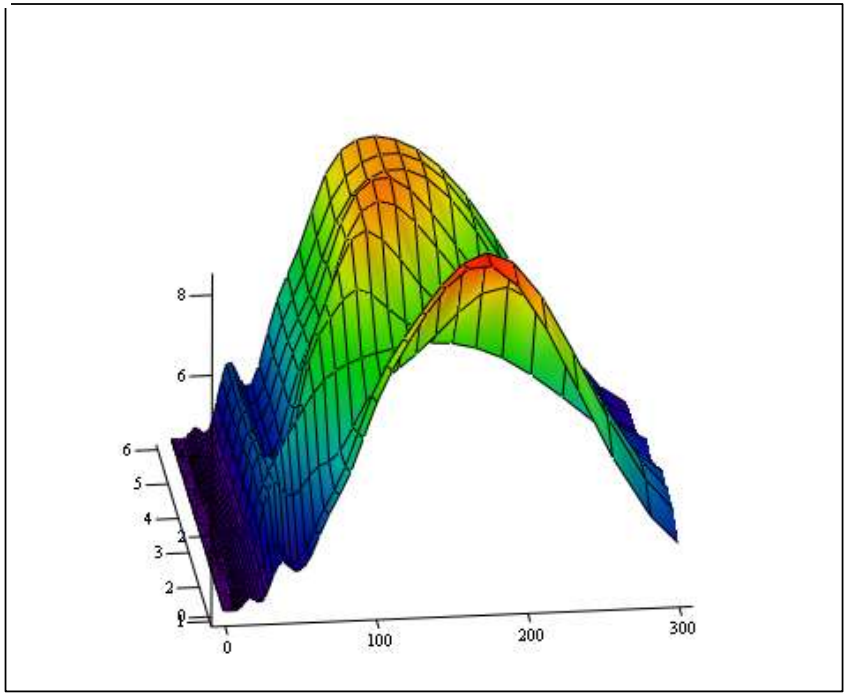

(x, y, z)

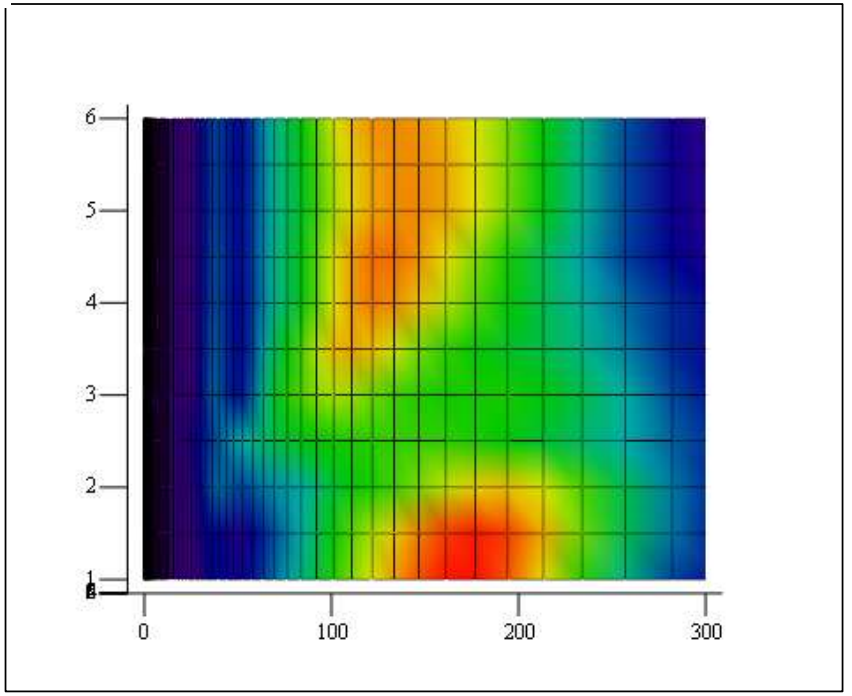

(x, y, z)

07/25/03

Reaction Temp: 30.1ºC, Flow Rate: 45 ml/min, Mixing Power: 287.7 rpm, Reactor Volume: 1400 ml

Particulate Mechanisms

- Nucleation
  - Heterogeneous
  - Secondary
    - (crystal impact with impeller creates nuclei)
- Particle Growth
  - Diffusion Limit
  - Other mechanisms
- Particle Breakage/Attrition
- Particle Aggregation

Traditional Population Balance – differential number

$$\frac{\partial f_N(x,t)}{\partial t} + \frac{\partial [G(x,t)\, f_N(x,t)]}{\partial x} = Birth - Death =$$

$$+ \int_x^\infty \varsigma(x')\, b(x')\, p(x|x')\, f_N(x',t)\,dx' - b(x)\, f_N(x,t) \quad Breakage$$

$$+ \frac{1}{2}\int_0^x a(x-x')\, f_N(x-x',t)\, f_N(x',t)\,dx' - f_N(x,t)\int_0^\infty a(x,x')\, f_N(x',t)\,dx' \quad Aggregation$$

with boundary conditions

$$f_N(x,t) = 0 \quad as \quad x \Rightarrow \infty$$

$$\left.\frac{\partial [G(x,t)\, f_N(x,t)]}{\partial x}\right|_{x=x_o} = \frac{\partial f_N(x = x_o, t)}{\partial t} \quad \text{Nucleation Rate } \textit{at size } x_o$$

and initial condition

$$f_N(x,t) = f_{N,o}(x) \quad at \quad t = 0.$$

Nucleation

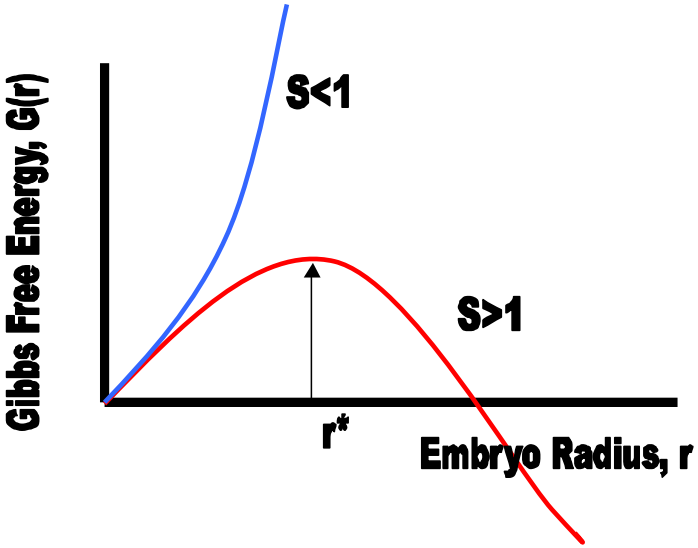

- primary homogeneous
  - Classical Nucleation
    - $J(\#/m^3sec)=J_{max}\ exp(-G(r^*)/RT)$
- primary heterogeneous
  - Classical Nucleation + new surface energy
    - $J(\#/m^3sec)=J_{max}\ exp(-G_{het}(r^*)/RT)$
- secondary
    - $J\ (\#/m^3sec) = f(rpm, S, Solids\ Mass\ Fraction)$

Crystal Growth Rate Mechanisms

$$dR/dt = K^{*}f(S)^{*}g(R)$$

Growth Mechanism	C	f(S)	g(R)	Ref
Diffusion Bulk	$\hat{V}DC_{eq}$	S-1	1/R	1
Mono Surface Nucleation	$\beta_A D\, d^{-3}$	$\exp[\Delta G^{*}_{s}/k_B T]$§	R^2	2
Poly Surface Nucleation	$\frac{(Dd/3)}{(N_A C_{eq})^{2/3}}$	$(S-1)^{2/3}\exp[\Delta G^{*}_{s}/k_B T]$§	1	3
Screw Dislocation	$D_s n_{se}\beta/(y_o^2 \rho)$	$S^2/S_1 \tanh(S_1/S)$§§	1	4
Heat Conduction	$\hat{V}k_H R T^2/\Delta H_f$	lnS §§§	1/R	-
Chemical Reaction	$\eta\hat{V}DC_{eq}$	S-1	1/R	-

§ $\Delta G_s^{*} = \beta_L^2 \gamma_e^2 d^2/(1\beta_A k_B T \ln S)$

§§ $S_1 = (y_o/y_s)S$

§§§ $\ln S = {}_T\int^T \Delta H_f/(RT^2)\, dT$

Particle Collision Rate due to Turbulence

Regime	size $a_i + a_j$	Collision Velocity $\Delta u(a_i, a_j)$	Collision Frequency Factor $\beta(a_i, a_j, r,t)$
Brownian Diffusion	$0 > a_i + a_j > \eta$		$(\frac{2}{3})(a_i + a_j)(\frac{k_B T}{\mu})(\frac{1}{a_i} + \frac{1}{a_j})$
Turbulent subrange			
Viscous	$\eta > a_i + a_j > 6\eta$	$0.257\left(\frac{\varepsilon}{\nu}\right)^{1/2}(a_i + a_j)$	$1.29\ (\langle\varepsilon^{1/2}\rangle/\nu^{1/2})\ (a_i + a_j)^3$ Equivalent to $(4/3)\ \gamma\ (a_i + a_j)^3$
Transition	$6\eta \le a_i + a_j < 25\eta$	$0.471\frac{\varepsilon^{5/12}}{\nu^{1/4}}(a_i + a_j)^{2/3}$	$2.36\ \langle\varepsilon^{5/12}\rangle\nu^{-1/4}(a_i + a_j)^{8/3}$
Inertial	$25\eta \le a_i + a_j < L/2$	$1.37(\varepsilon)^{1/3}(a_i + a_j)^{1/3}$	$6.87\ \langle\varepsilon^{1/3}\rangle(a_i + a_j)^{7/3}$
Macro	$L/2 > a_i + a_j \sim L$	$\sqrt{2}(\varepsilon L)^{1/3}$	$7.09\ \langle\varepsilon^{1/}3\rangle L^{1/3}(a_i + a_j)^2$

Kusters, K.A. "The Influence of Turbulence on Aggregation of Small Particles in Agitated Vessels," Technical University Eindhoven, The Netherlands, 1991.

Breakage Kinetics

- Breakage Rate =

Collision Frequency * Target Efficiency * Breakage Probability

Collisions — Collision Efficiency

Particle-wall

Particle-impeller

Particle-baffle

Particle-Particle due to either diffusion or turbulence

Crystallizers are Complicated

- Size Increases by
  - Aggregation
  - Growth
- Size Decreases by
  - Breakage
  - Dissolution
- Number of Particles Increases by
  - Nucleation
  - Breakage
  - Less Aggregation

HOW TO DECOUPLE?

Do not try to solve all at once!

Decomposition of the Problem

- Using standard operating conditions for tank,
  - Study aggregation separately
  - Study breakage separately
- Focus on aggregation and breakage under batch conditions after crystallization has been run to steady state

Traditional Population Balance – differential number

$$\frac{\partial f_N(x,t)}{\partial t} + \frac{\partial [G(x,t) f_N(x,t)]}{\partial x} = Birth - Death =$$

$$+ \int_x^\infty \varsigma(x') b(x') p(x|x') f_N(x',t) dx' - b(x) f_N(x,t) \quad Breakage$$

$$+ \frac{1}{2} \int_0^x a(x-x') f_N(x-x',t) f_N(x',t) dx' - f_N(x,t) \int_0^\infty a(x,x') f_N(x',t) dx' \quad Aggregation$$

with boundary conditions

$$f_N(x,t) = 0 \quad as \quad x \Rightarrow \infty$$

$$\left. \frac{\partial [G(x,t) f_N(x,t)]}{\partial x} \right|_{x=x_o} = \frac{\partial f_N(x = x_o, t)}{\partial t} \quad \text{Nucleation Rate } \textit{at size } x_o$$

and initial condition

$$f_N(x,t) = f_{N,o}(x) \quad at \quad t = 0.$$

Stieltjes Formulation[1] – Cumulative Mass

Ramkrishna, D., "Population Balances,"
Academic Press, 2000, p.56 and private communications.

$$\frac{\partial F_m(x,t)}{\partial t} + \int_0^x x' \frac{\partial}{\partial x'}\left[\frac{g_M(x',t)}{x'}\frac{\partial F_m(x,t)}{\partial x'}\right]dx' = \hat{B} - \hat{D} =$$

$$\frac{\partial F_m(x,t)}{\partial t} + g_M(x',t)\frac{\partial F_m(x,t)}{\partial x'} - \int_0^x \frac{g_M(x',t)}{x'}\partial_x F_m(x',t) = \hat{B} - \hat{D} =$$

$$\int_x^\infty b(x')P_m(x|x')\partial_x F(x',t) \quad \textit{Breakage}$$

$$-\mu_1(t)\int_{s=0}^{x}\int_{u=x-s}^{\infty}\frac{a(s,u)}{u}\partial_x F(u,t)\,\partial_x F(s,t) \quad \textit{Agglomeration}$$

with boundary conditions

$$\left.\frac{\partial F_m(x,t)}{\partial t}\right|_{x=x_o} \quad \text{Mass Nucleation Rate at size, } x_o$$

$$F_m(x,t) = 0 \quad at \quad x = 0, \quad F_m(x,t) = 1 \quad at \quad x = \infty$$

and initial condition

$$F_m(x,t) = F_{m,o}(x) \quad at \quad t = 0$$

Sinc Approximation

$$F_m(x,t) \approx \sum_{j=-N}^{N} \sum_{k=-M}^{M} \operatorname{sinc}\left(\frac{\varphi(x)}{h_x} - j\right) \operatorname{sinc}\left(\frac{\phi(t)}{h_t} - k\right) F_m(x_j, t_k)$$

$$\varphi(x) = \ln(x)$$

$$x_j = \varphi^{-1}(jh_x) = \exp(jh_x)$$

$$h_x = \frac{c_1}{\sqrt{N}}$$

$$\phi(t) = \ln[t/(T-t)]$$

$$t_k = \phi^{-1}(kh_t) = \frac{T\exp(kh_t)}{1+\exp(kh_t)}$$

$$h_t = \frac{c_2}{\sqrt{M}}$$

$$\operatorname{sinc}(z) = \frac{\sin(\pi z)}{\pi z}$$

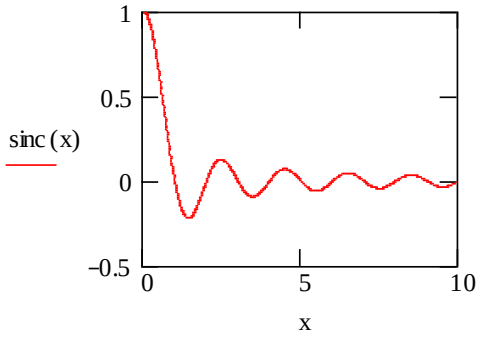

Final Formulation

$$F_m(x,t) = F_{m,o}(x,t=0) +$$

$$-\int_0^t g_M(x',t')\frac{\partial F_m(x',t')}{\partial x'}dt' + \int_0^t\int_0^x \frac{g_M(x',t')}{x'}\partial_x F_m(x',t')dt' \quad \textit{growth}$$

$$+\int_0^t\int_x^\infty b(x')P_m(x|x')\partial_x F(x',t')dt' \quad \textit{Breakage}$$

$$-\int_0^t \mu_1(t')\int_{s=0}^x\int_{u=x-s}^\infty \frac{a(s,u)}{u}\,\partial_x F(u,t')\,\partial_x F(s,t')dt' \quad \textit{Agglomeration}$$

$$\overline{\overline{F_m}} = \overline{\overline{F_{m,o}}} +$$

$$-\overline{\overline{At_{I+}}}\bullet[\overline{\overline{g_M}}]\bullet[\overline{\overline{Ax_D}}\bullet\overline{\overline{F_m}}] + \overline{\overline{At_{I+}}}\bullet\overline{\overline{Ax_{I+}}}\bullet[\overline{\overline{\frac{g_M}{\bar{x}}}}]\bullet[\overline{\overline{Ax_D}}\bullet\overline{\overline{F_m}}] \quad \textit{Growth}$$

$$+\overline{\overline{At_{I+}}}\bullet\overline{\overline{Ax_{I+}}}\bullet\left\{\overline{\overline{[bP_m]}}\bullet[\overline{\overline{Ax_D}}\bullet\overline{\overline{F_m}}]\right\} \quad \textit{Breakage}$$

$$-\overline{\overline{At_{I+}}}\bullet\left[diag[\mu_1(\bar{t})]\,\overline{\overline{X}}\,\tilde{P}\right] \quad \textit{Agglomeration}$$

Sinc Results – Batch

- Power Law Breakage
  - $S(x)=x^{1.2}$
  - Kt=0.1

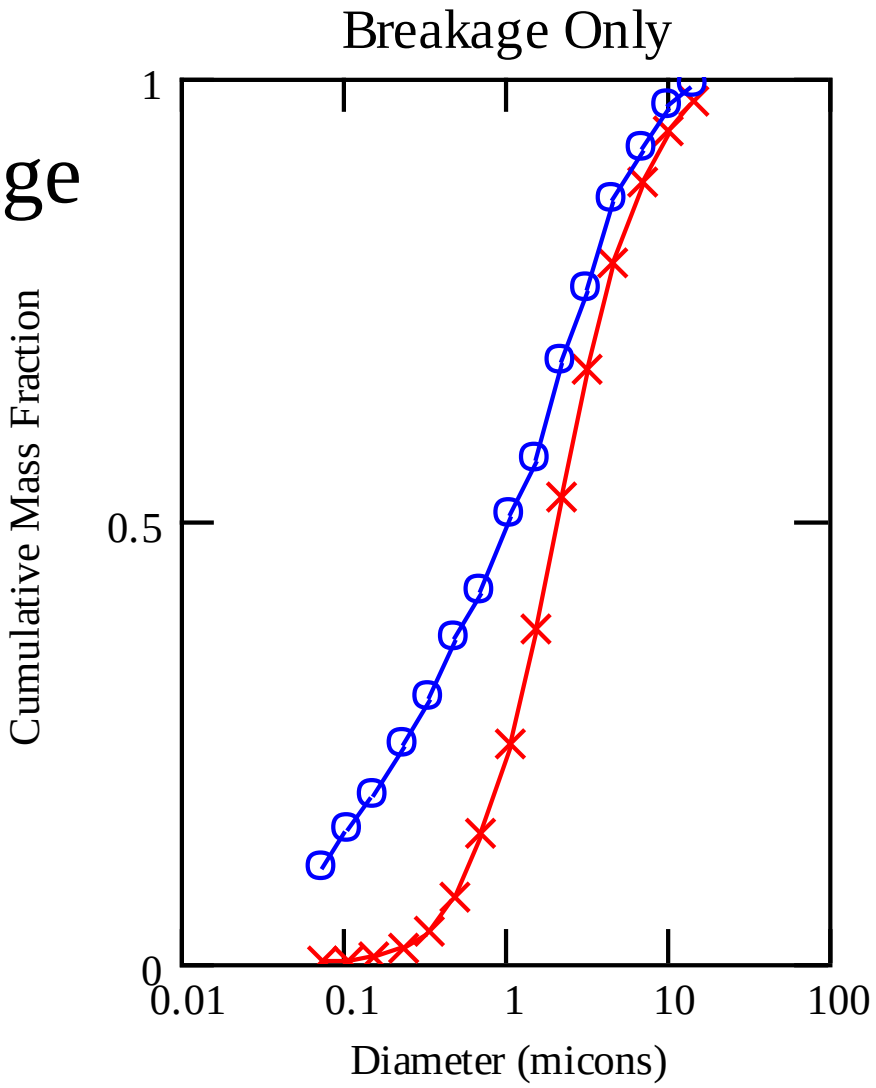

Sinc Result -Batch

- Aggregation Only
  - Sum Kernal
  - Kt=0.5
  - $\mu = 0.1$

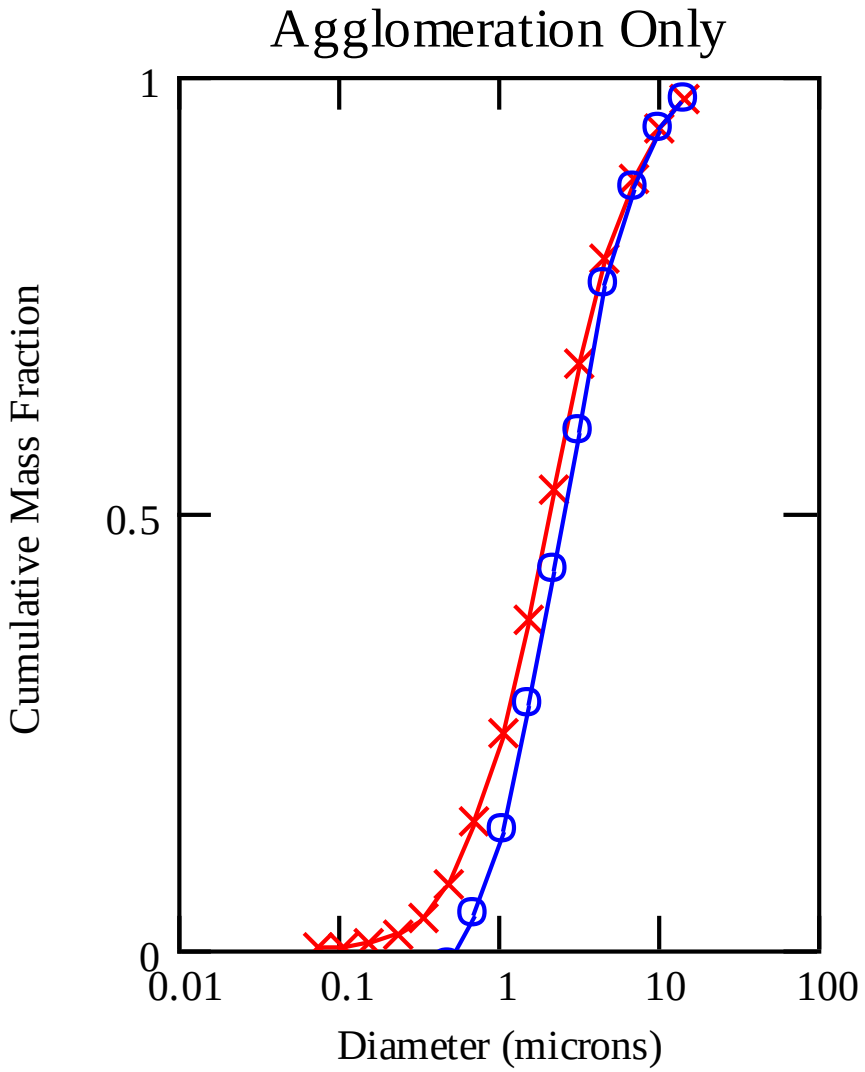

Sinc Result- Batch

- Aggregation & Breakage
  - Compensating Effects

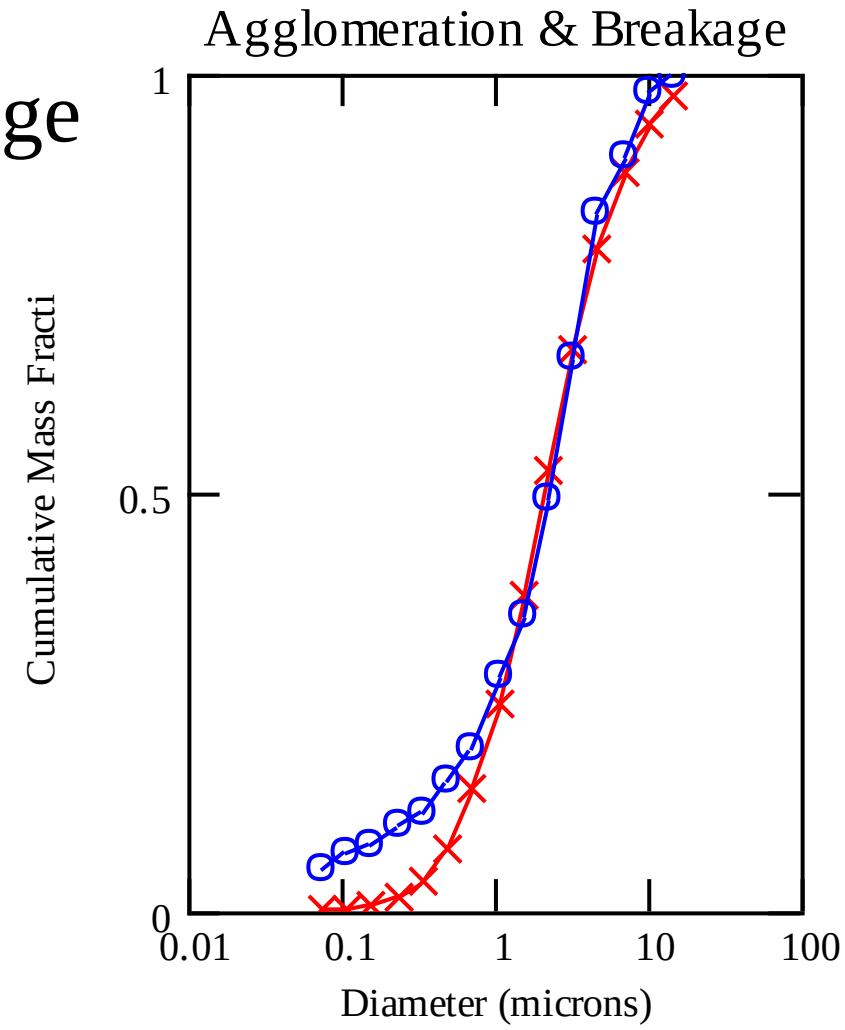

Need to Know

- Aggregation Rate Constant
- Breakage Rate Constant
- Breakage Selectivity
- Breakage Daughter Distribution

- Where are we going to get these?

Focused Experimentation

- Using standard operating conditions for tank,
  - Study aggregation separately
  - Study breakage separately
- Forced Fitting of the Data

Diatomite Breakage

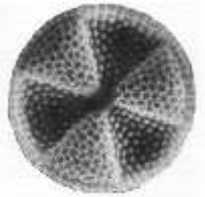

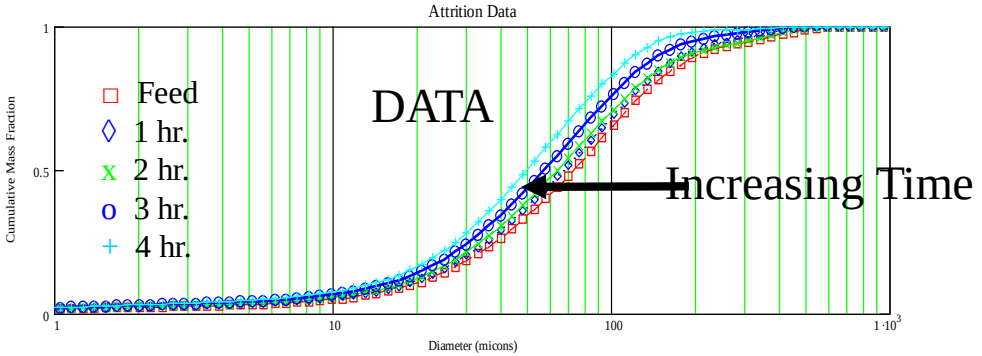

- Batch Experiment for Breakage
  - 10% wt. Commercial Diatomite
- 1.4 L baffled batch stirred tank
  - 300 rpm
  - Sampling every hr.
- Progeny Function
- Rate Function

$$P_m(x|x') = \frac{1-\exp(-x/x')}{1-\exp(-1)}$$

$$b(x) := \left(\frac{x}{2\cdot x_0}\right)^{1.4} \cdot \Phi\left(x - 2\cdot x_0\right)$$

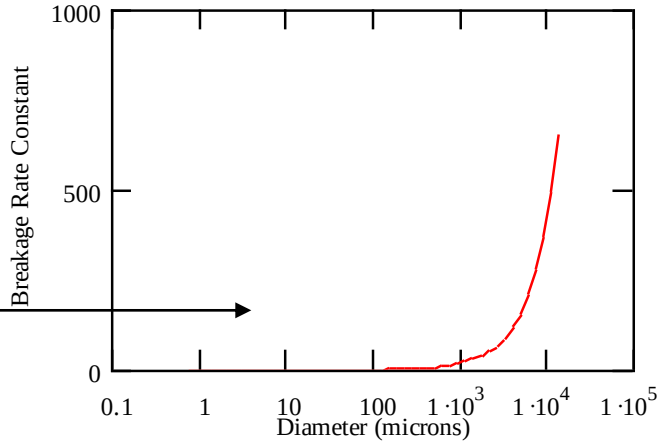

Diatomite Attrition

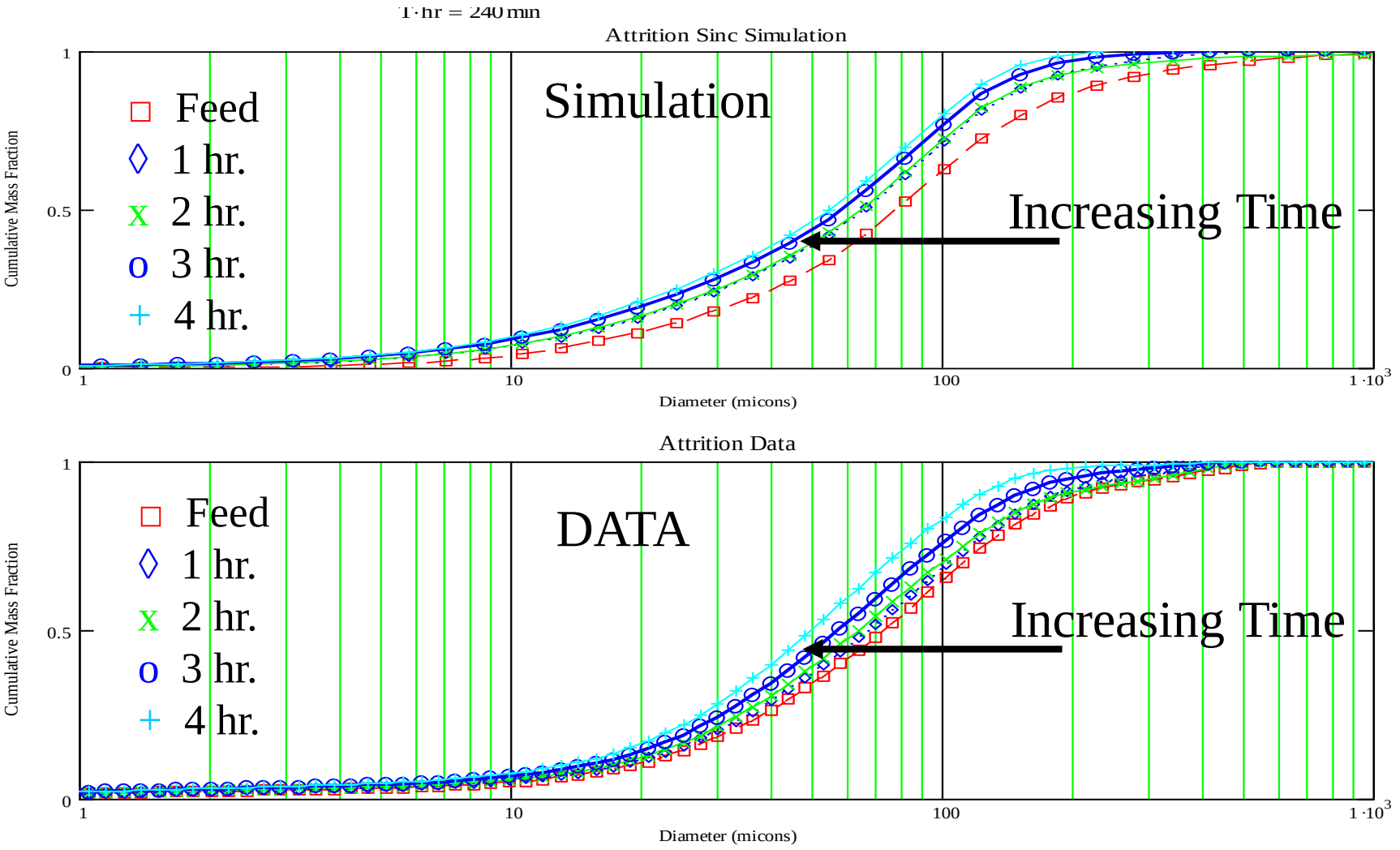

Polystyrene Latex Aggregation

- Batch Experiment for Aggregation
  - 1% wt. Commercial Polystyrene Latex (1 micron) in 10^{-3} M NaCl
- 1.4 L baffled batch stirred tank
  - 100 rpm
  - Sampling every 10 min.
- Dynamic Balance
  - Breakage (diatomite expt.)
  - Aggregation
    - a(x,y) = x + y

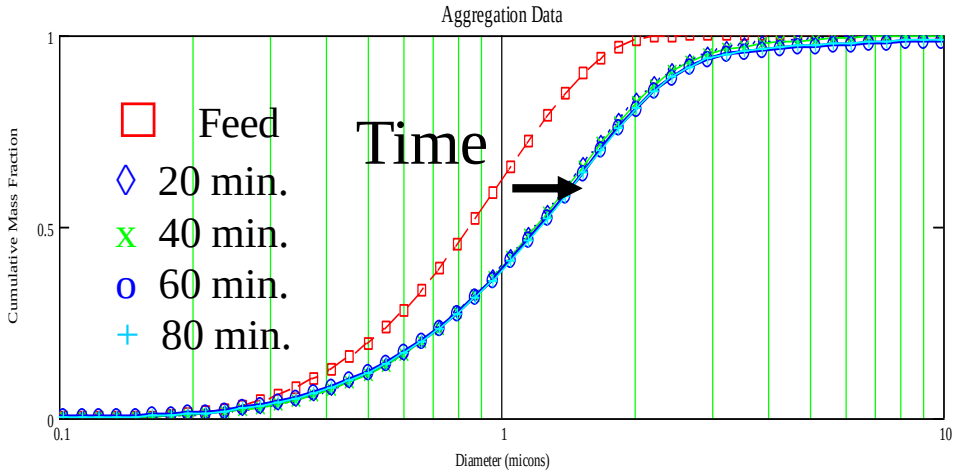

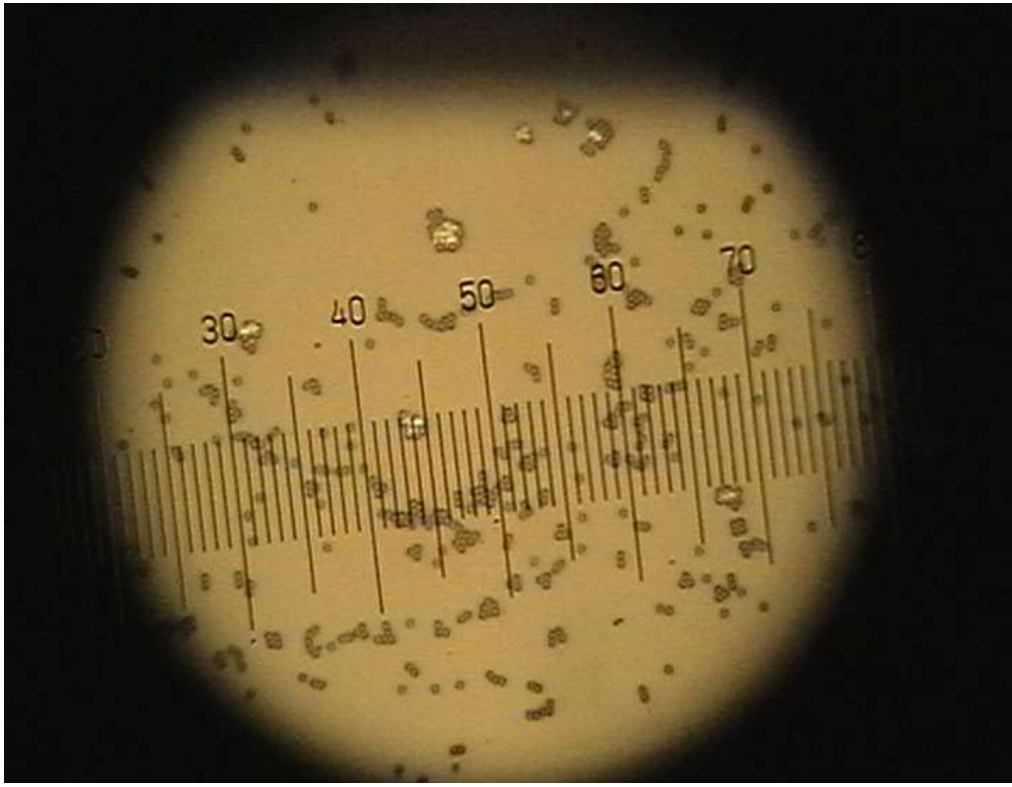

Dynamic Balance for Polystyrene Latex

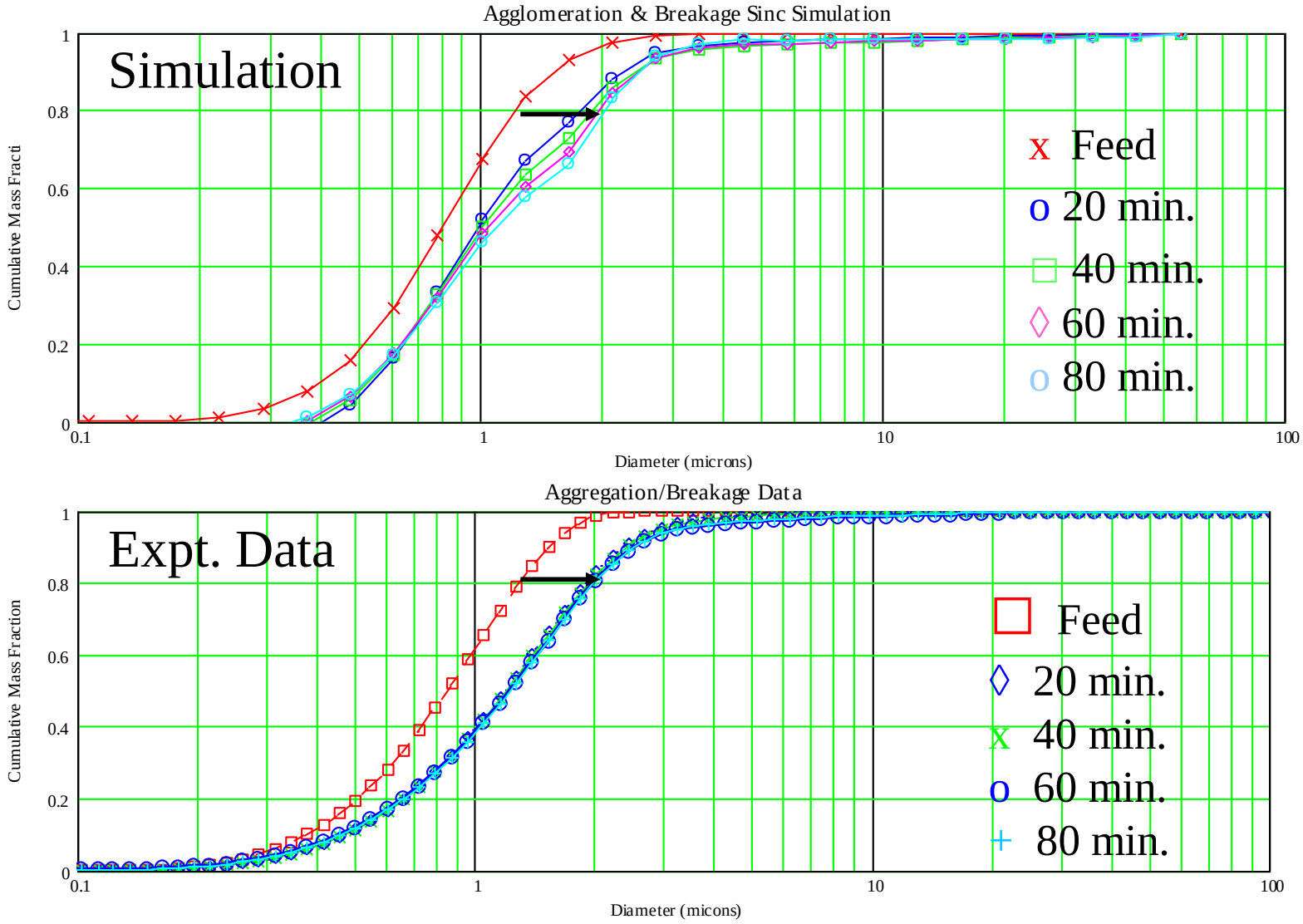

Polystyrene Latex Aggregation

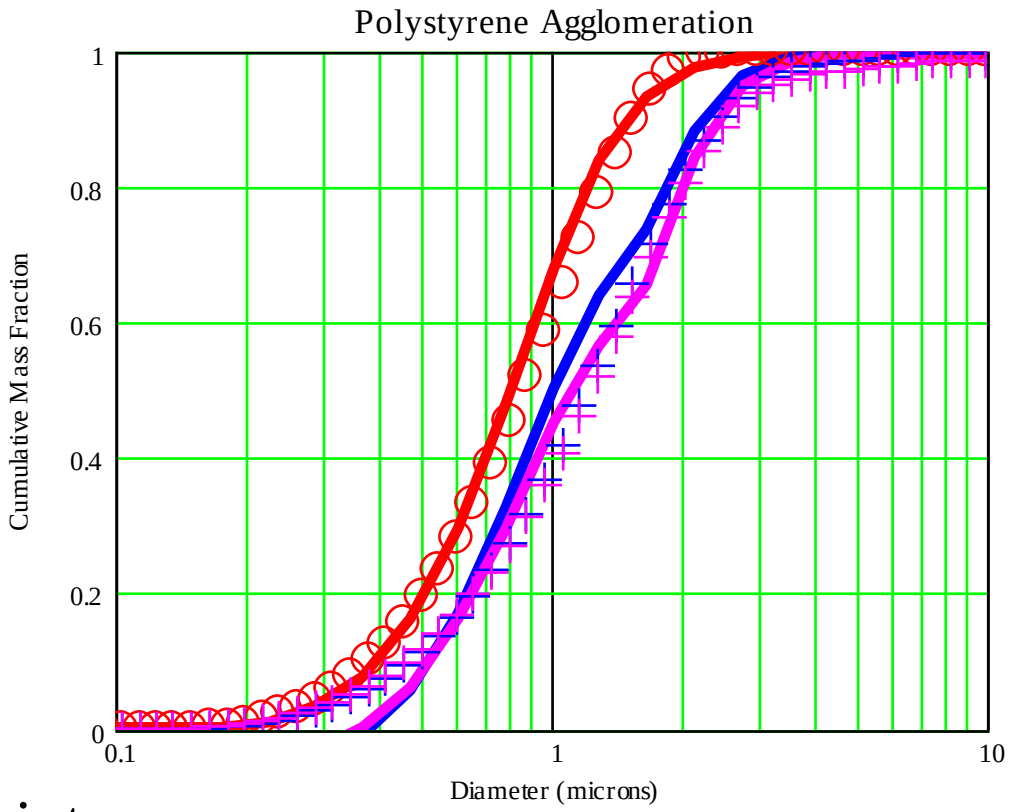

Data = Points

Sinc Simulation = Lines

Focus on Aggregation and Breakage after Crystallization

- Stop Feed – Batch Tank
  - Constant RPM, Constant Temperature
    - Supersaturation is Constant
      - No nucleation
      - No particle growth
  - Measure Changes in Particle Size Distribution

NaCl Aggregation

- 1.4 L Batch, Baffled Stirred Tank
  - 287 rpm
- Charge from Crystallization
  - 2% NaCl particles in 47% $CaCl_2$ solution
  - Aggregation/Attrition over 3 hrs.

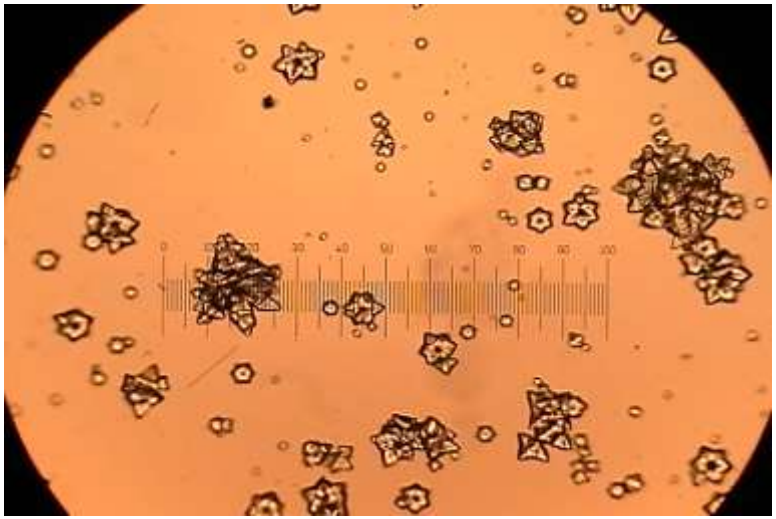

Aggregation/Breakage Data

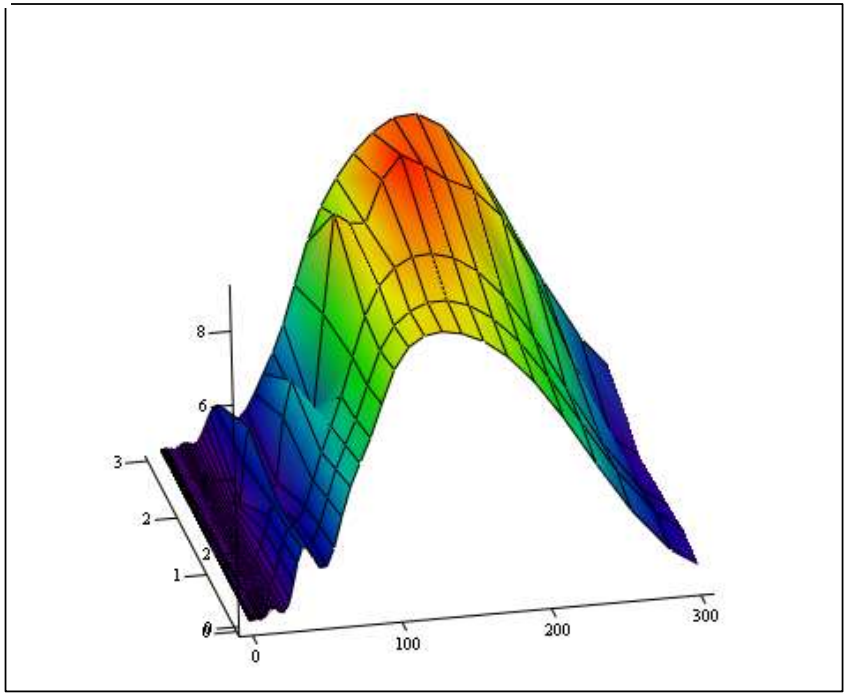

(x, y, z)

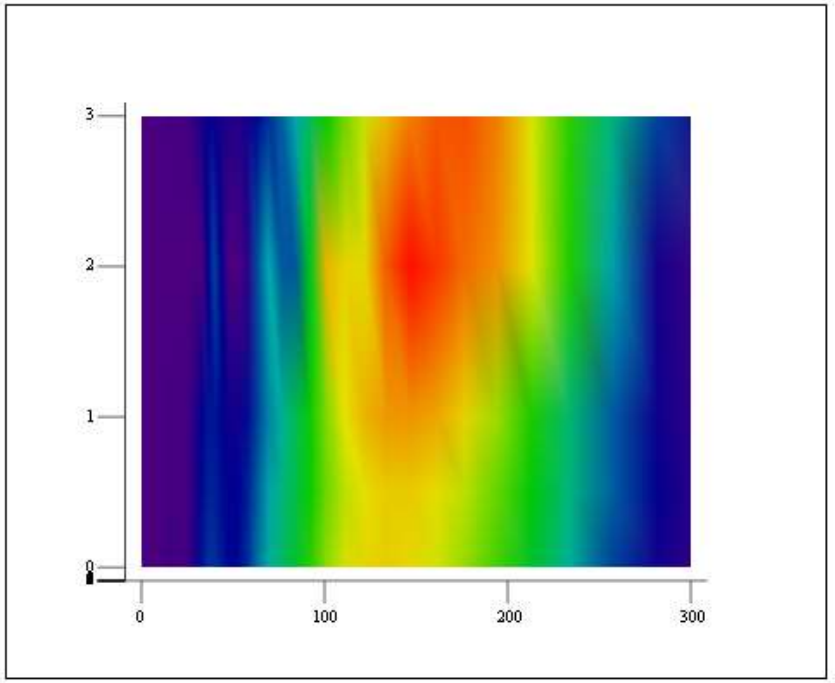

(x, y, z)

07/25/03
Reaction Temp: 30.1°C, Flow Rate: 45 ml/min, Mixing Power: 287.7 rpm, Reactor Volume: 1400 ml

Aggregation/Breakage

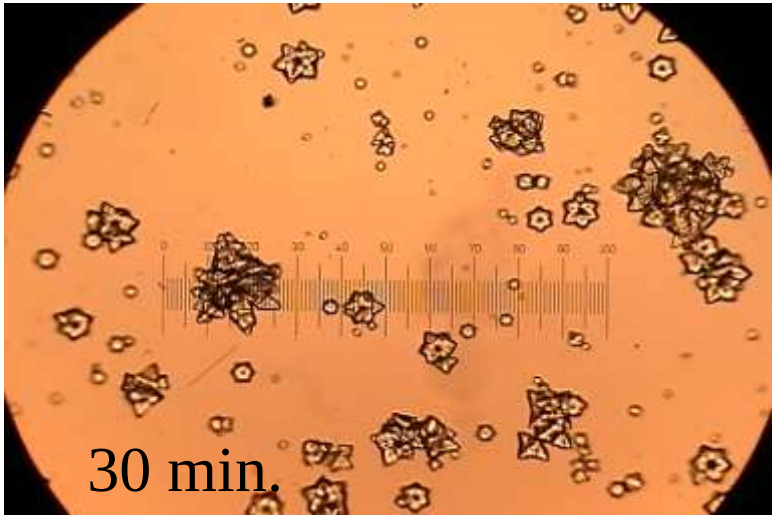

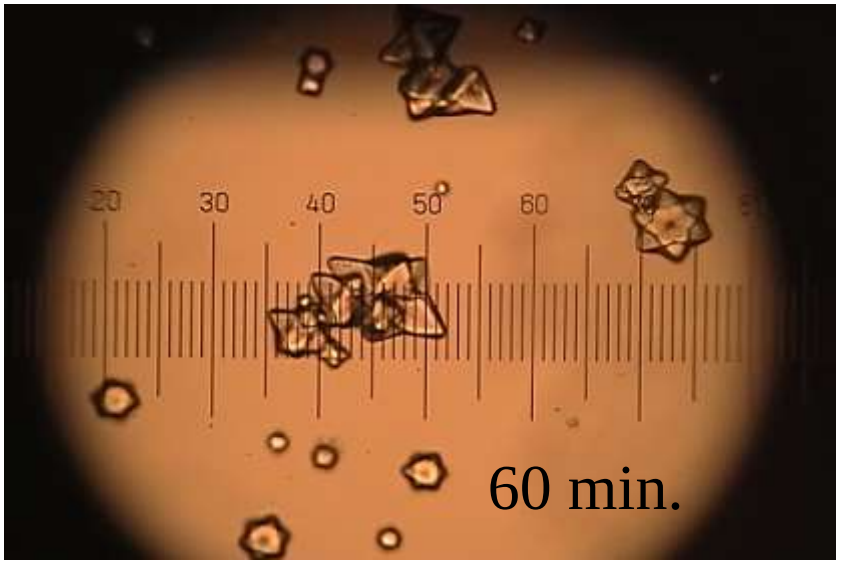

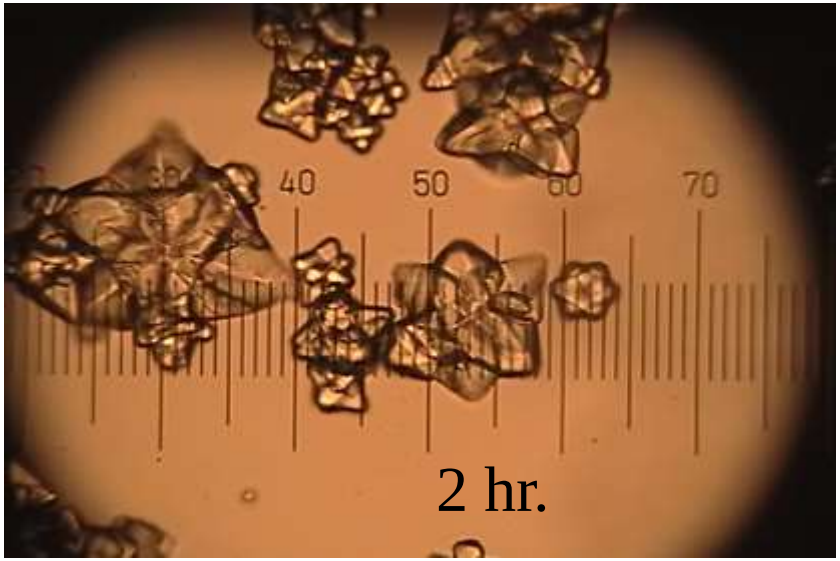

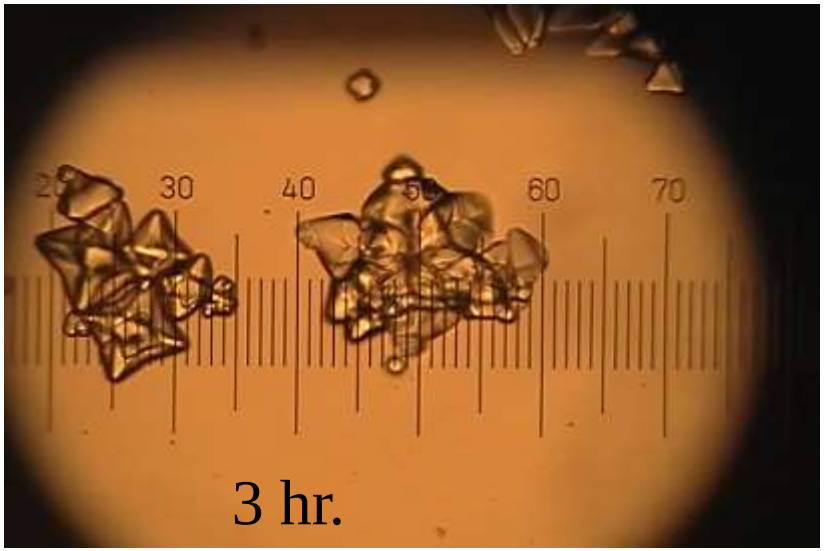

07/25/03 Reaction Temp: 30.1°C, Flow Rate: 45 ml/min, Mixing Power: 287.7 rpm, Reactor Volume: 1400 ml

Traditional Population Balance – differential number

$$\frac{\partial f_N(x,t)}{\partial t} + \frac{\partial [g(x,t) f_N(x,t)]}{\partial x} = Birth - Death =$$

$$+ \int_x^\infty \varsigma(x') b(x') p(x|x') f_N(x',t) dx' - b(x) f_N(x,t) \quad Breakage$$

$$+ \frac{1}{2} \int_0^x a(x-x') f_N(x-x',t) f_N(x',t) dx' - f_N(x,t) \int_0^\infty a(x,x') f_N(x',t) dx' \quad Aggregation$$

with boundary conditions

$$f_N(x,t) = 0 \quad as \quad x \Rightarrow \infty$$

$$\left. \frac{\partial [g(x,t) f_N(x,t)]}{\partial x} \right|_{x=x_o} = \frac{\partial f_N(x = x_o, t)}{\partial t} \quad \text{Nucleation Rate } \textit{at size } x_o$$

and initial condition

$$f_N(x,t) = f_{N,o}(x) \quad at \quad t = 0.$$

Particle Collision Rate due to Turbulence

Regime	**size $a_i + a_j$**	**Collision Velocity $\Delta u(a_i , a_j)$**	**Collision Frequency Factor $\beta(a_i, a_j, r,t)$**
Brownian Diffusion	**$0 > a_i + a_j > \eta$**		$(\frac{2}{3})(a_i + a_j)(\frac{k_B T}{\mu})(\frac{1}{a_i} + \frac{1}{a_j})$
Turbulent subrange			
Viscous	**$\eta > a_i + a_j > 6\eta$**	$0.257\left(\frac{\varepsilon}{\nu}\right)^{1/2}(a_i + a_j)$	**$1.29 (\langle\varepsilon^{1/2}\rangle/\nu^{1/2}) (a_i + a_j)^3$** **Equivalent to** **$(4/3)\ \gamma\ (a_i + a_j)^3$**
Transition	**$6\eta \le a_i + a_j < 25\eta$**	$0.471\frac{\varepsilon^{5/12}}{\nu^{1/4}}(a_i + a_j)^{2/3}$	**$2.36 \langle\varepsilon^{5/12}\rangle\nu^{-1/4}(a_i + a_j)^{8/3}$**
Inertial	**$25\eta \le a_i + a_j < L/2$**	$1.37(\varepsilon)^{1/3}(a_i + a_j)^{1/3}$	**$6.87 \langle\varepsilon^{1/3}\rangle(a_i + a_j)^{7/3}$**
Macro	**$L/2 > a_i + a_j \sim L$**	$\sqrt{2}(\varepsilon L)^{1/3}$	**$7.09 \langle\varepsilon^{1/}3\rangle L^{1/3}(a_i + a_j)^2$**

Kusters, K.A. "The Influence of Turbulence on Aggregation of Small Particles in Agitated Vessels," Technical University Eindhoven, The Netherlands, 1991.

Energy Dissipation Rate [w/kg] (ε) Profile

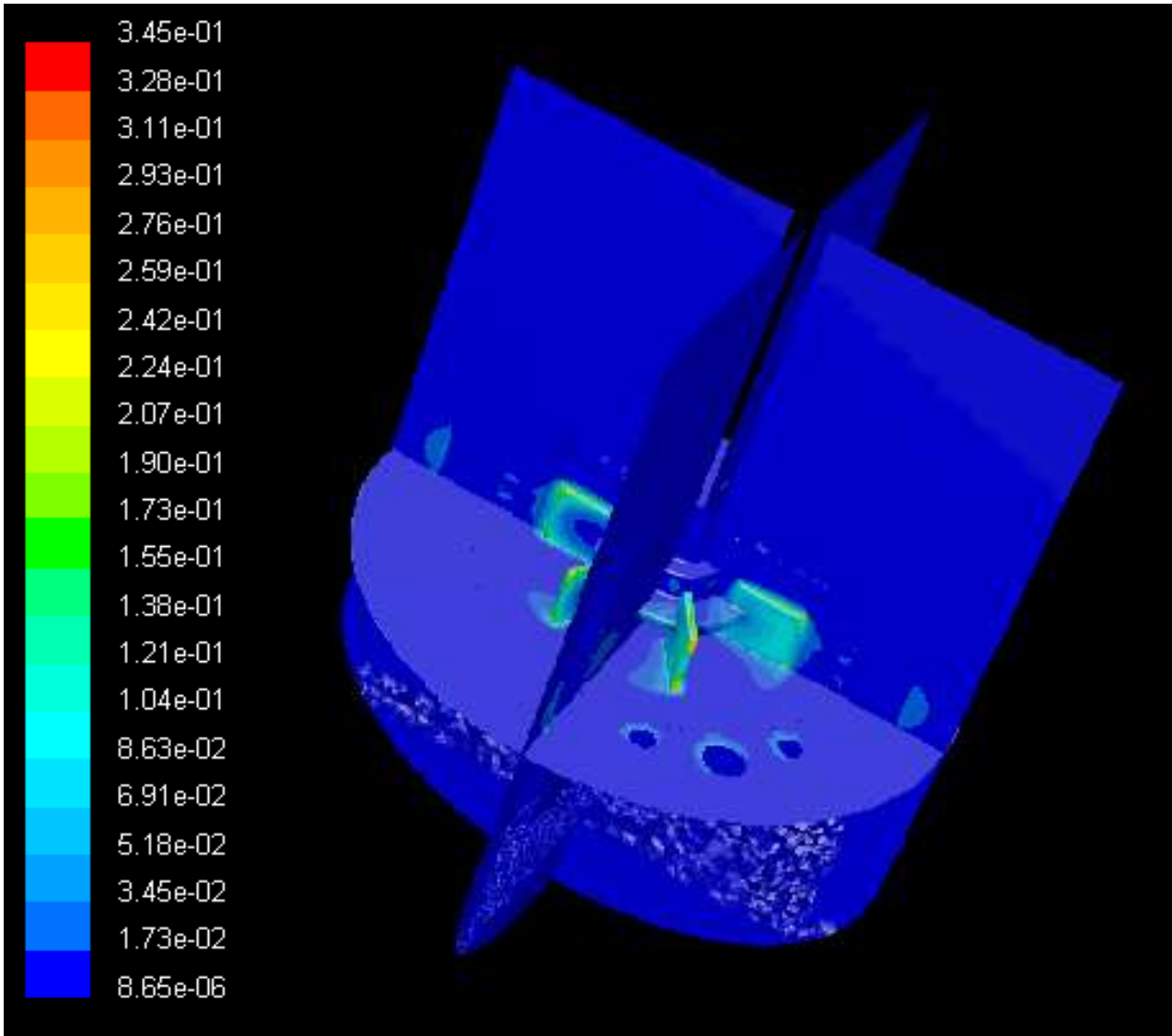

FLUENT

Energy Dissipation Rate on Individual Particle Track

- High ε when passes through impeller zone
- Effectively
  - ε =0 elsewhere

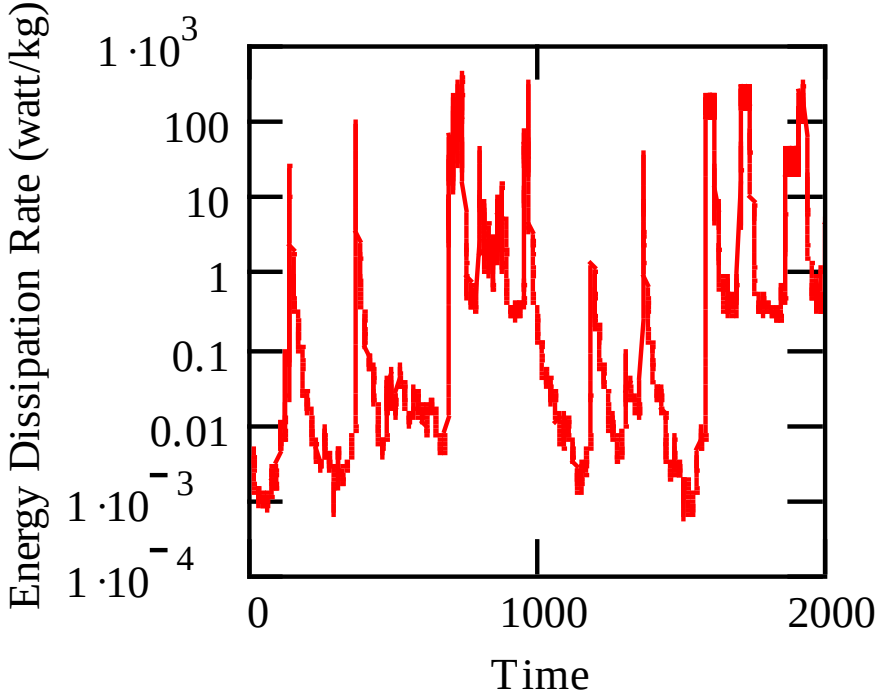

Energy Dissipation Rate Statistics

- ε_{max} = 429 w/kg
- Multimode Distribution
- Probability α $\varepsilon^{-3/2}$
  - Decay of Isotropic Turbulence
- V= 1.4 L, Q=40 ml/min., 80 rpm

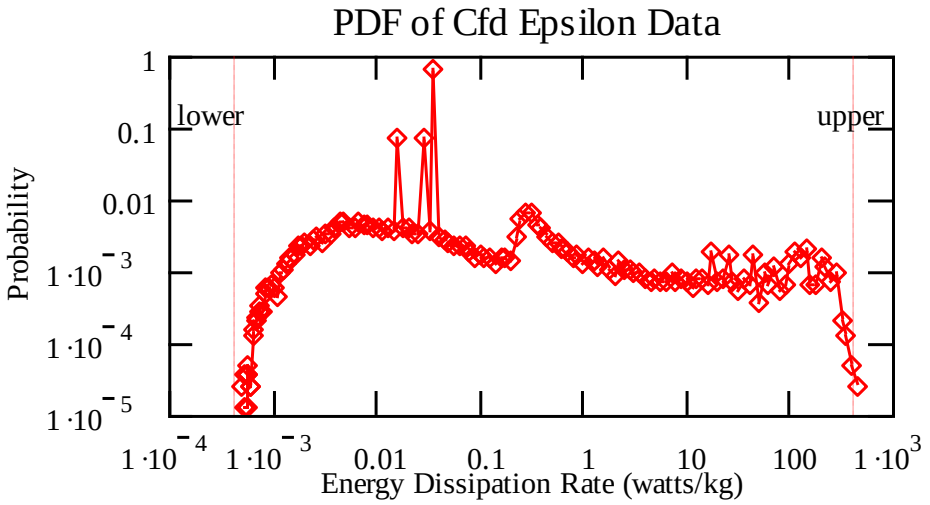

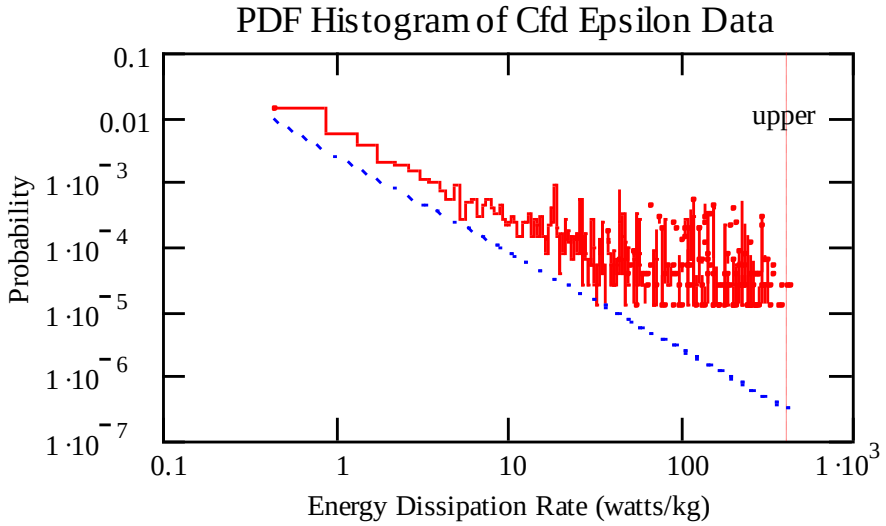

Aggregation Rate

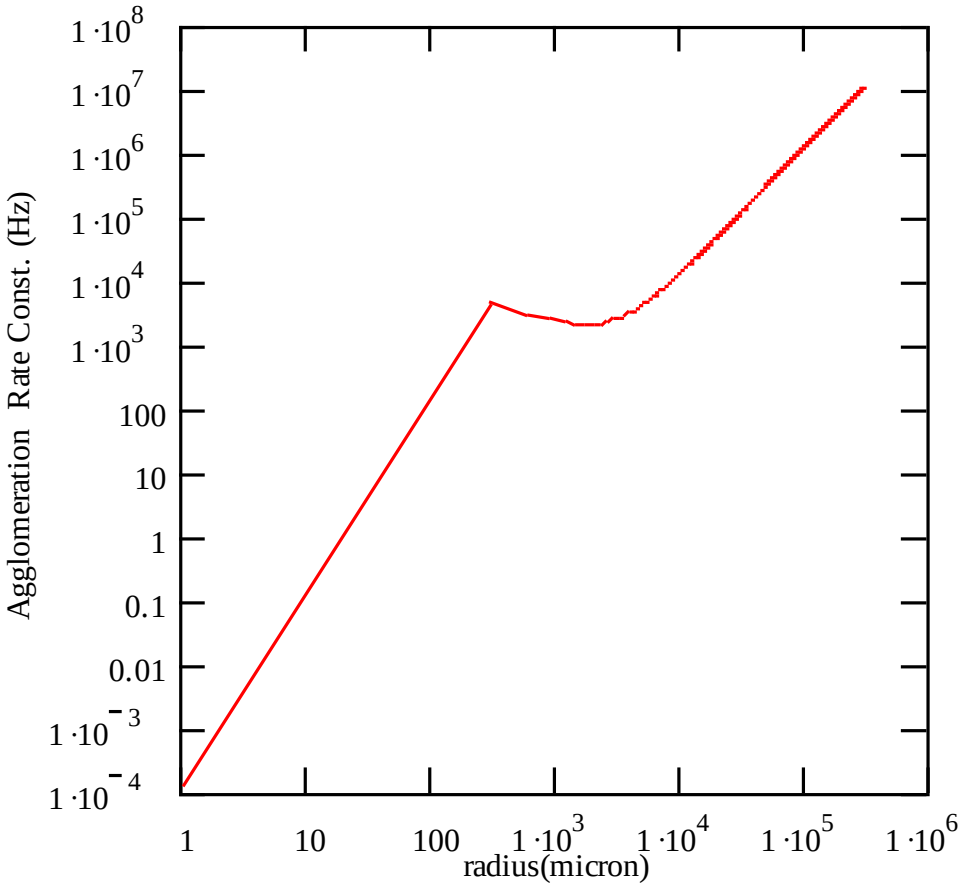

07/25/03

Reaction Temp: 30.1ºC, Flow Rate: 45 ml/min, Mixing Power: 287.7 rpm, Reactor Volume: 1400 ml

Breakage Kinetics

- Breakage Rate =

Collision Frequency * Target Efficiency * Breakage Probability

Collisions — Collision Efficiency

Particle-wall

Particle-impeller

Particle-baffle

Particle-Particle due to either diffusion or turbulence

Use Fluid Dynamics with Sinc Methods

- Particle Breakage
  - Particle Collisions with
    - Particles (same equations as aggregation)
      - depend upon turbulent energy dissipation rate
    - Baffles/walls – impaction efficiency
    - Impeller – collision frequency
  - Sufficient Energy of Collision to Break Particle

$$\eta_{target} = \left(\frac{N_{St}}{0.32 + N_{St}} \right)^{2.1}$$

$$W_{p,\min} = 64 \frac{G_2^{\,3} \Gamma_2^{\,3}}{H_2^{\,5} K_r^{\,3}}$$

$$p(x) = \frac{2.25\, x^{-3.25}}{x_{\min}^{-2.25} - x_{\max}^{-2.25}}$$

Gahn, C. and Mersmann, A., Chem. Eng. Sci. 54,1274-82(1999).

Particle Breakage Efficiency

- Baffle
- Wall
- Impeller
- Other Particles

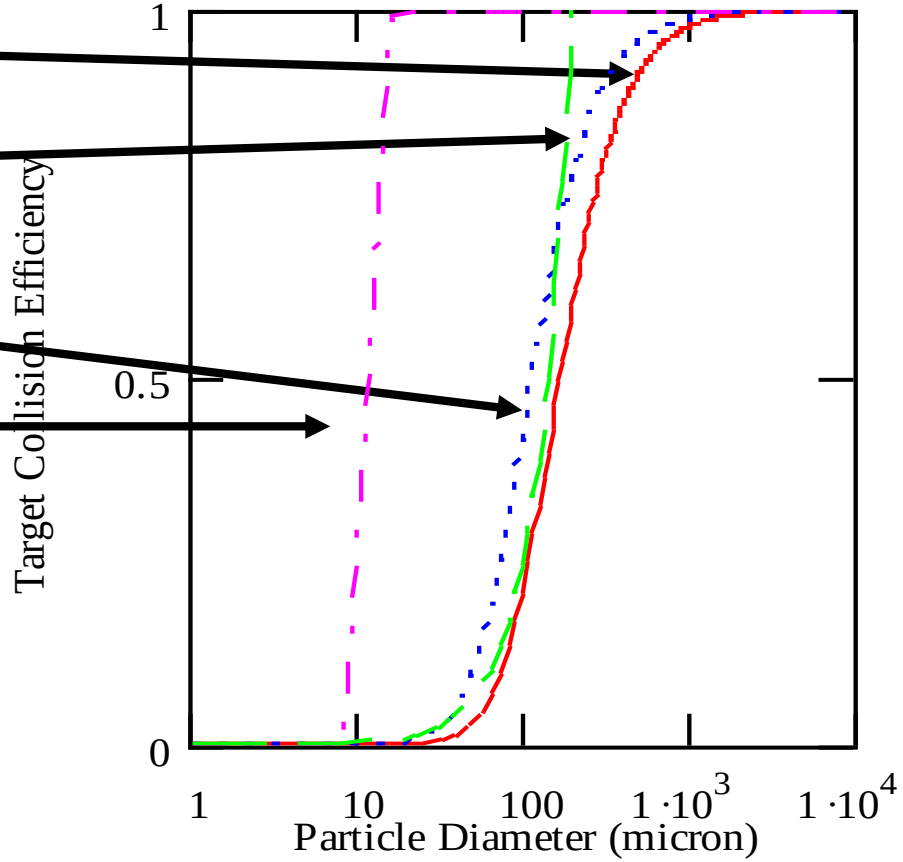

07/25/03

Reaction Temp: 30.1°C, Flow Rate: 45 ml/min, Mixing Power: 287.7 rpm, Reactor Volume: 1400 ml

Breakage Rate

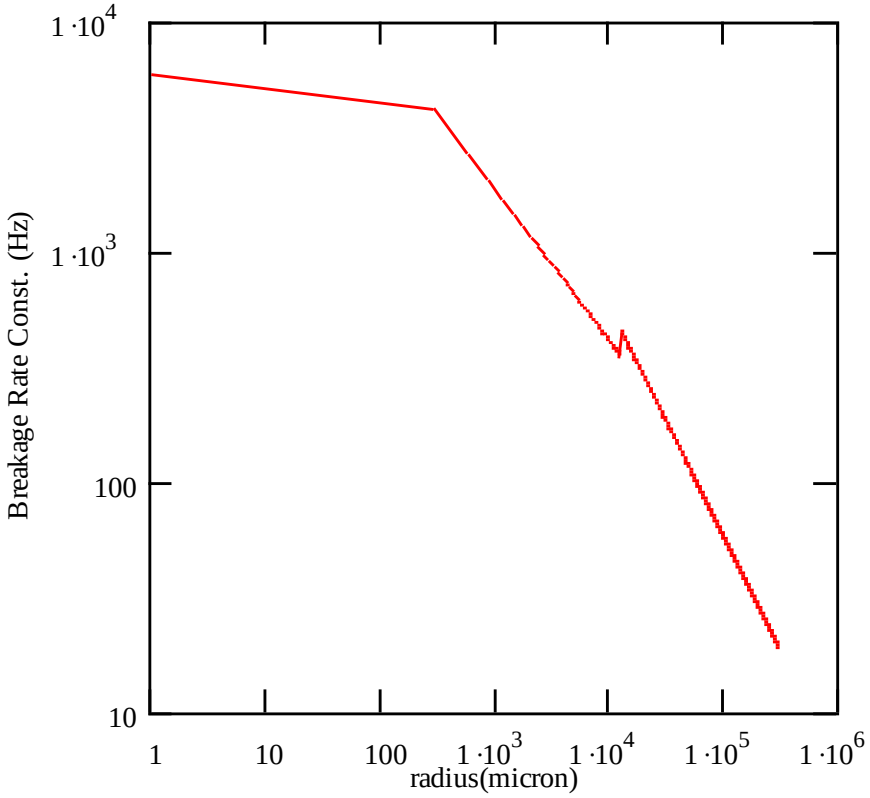

07/25/03

Reaction Temp: 30.1°C, Flow Rate: 45 ml/min, Mixing Power: 287.7 rpm, Reactor Volume: 1400 ml

Model Results – Aggregation/Breakage

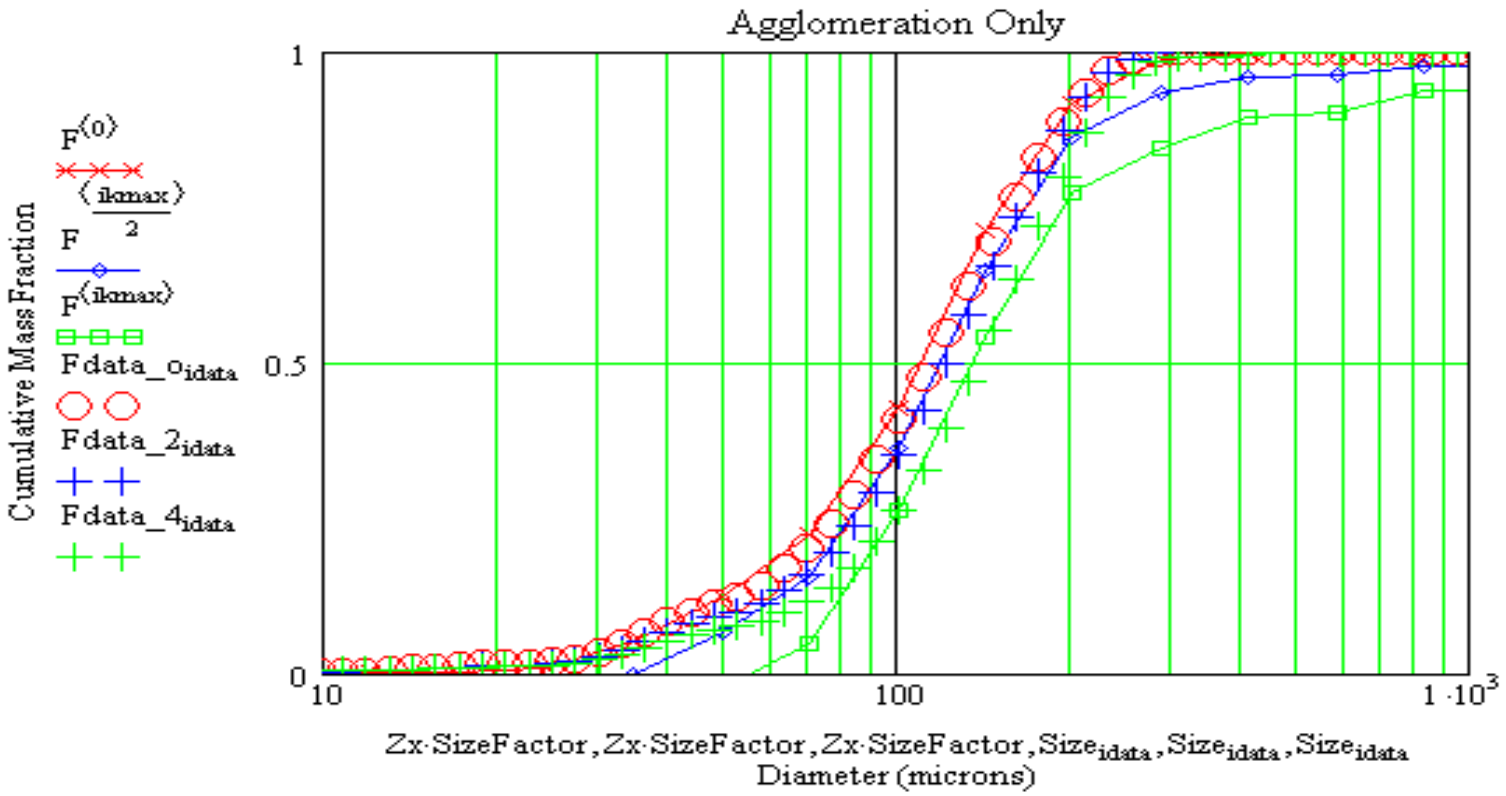

A_Factor=400, a colloid stability parameter

Conclusions

- Getting Crystallization Parameters from Experimental Data
  - Requires
    - Decomposition of the multiplicity of phenomenon
    - Knowledge of fundamental particle mechanisms
    - Simple calculation tool for stirred tank

Introduction to Population Balance Modeling

Topics

- Modeling Philosophies
  - Where Population Balance Models (PBMs) fit in
- Important Characteristics
- Framework
- Uses
  - Cancer Examples
- Parameter Identification
- Potential Applications

Variations of Scale

- Tumor scale properties
  - Physical characteristics
  - Disease class
- Cellular level
  - Growth and death rates
  - Mutation rates
- Subcellular characteristi
  - Genetic profile
  - Reaction networks (meta
  - CD markers

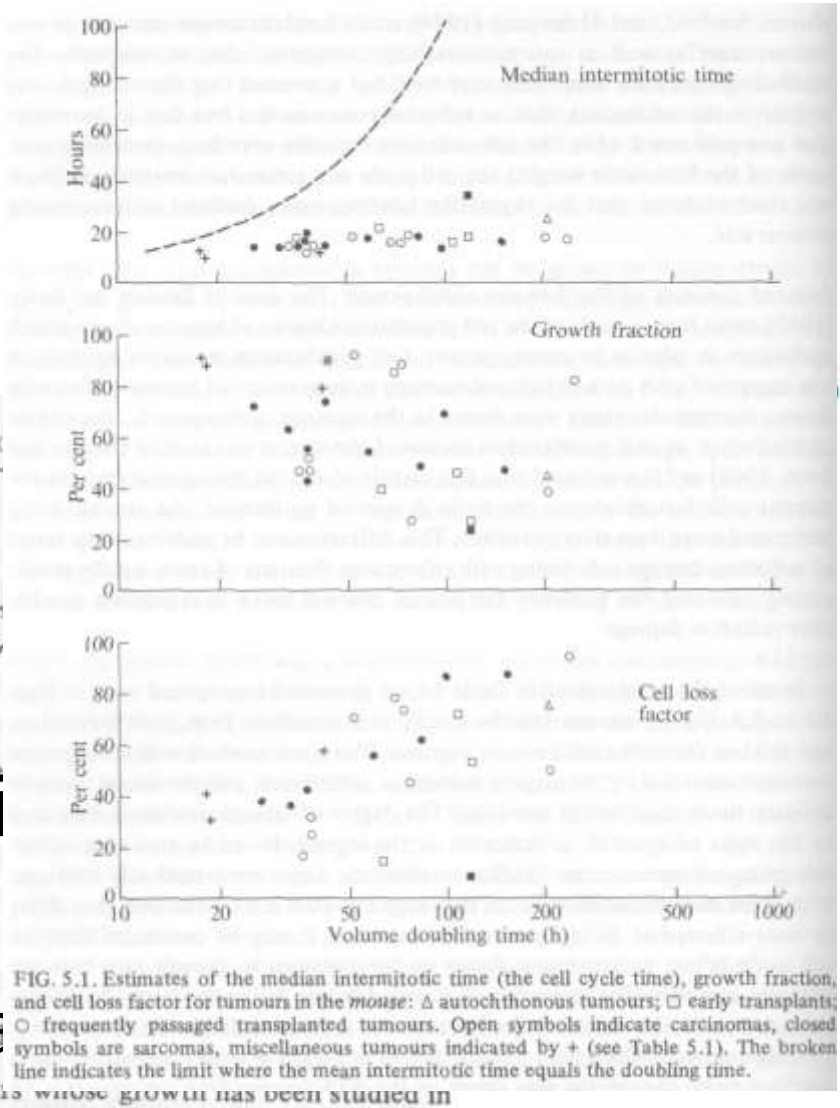

FIG. 5.1. Estimates of the median intermitotic time (the cell cycle time), growth fraction, and cell loss factor for tumours in the *mouse*: △ autochthonous tumours; □ early transplants; ○ frequently passaged transplanted tumours. Open symbols indicate carcinomas, closed symbols are sarcomas, miscellaneous tumours indicated by + (see Table 5.1). The broken line indicates the limit where the mean intermitotic time equals the doubling time.

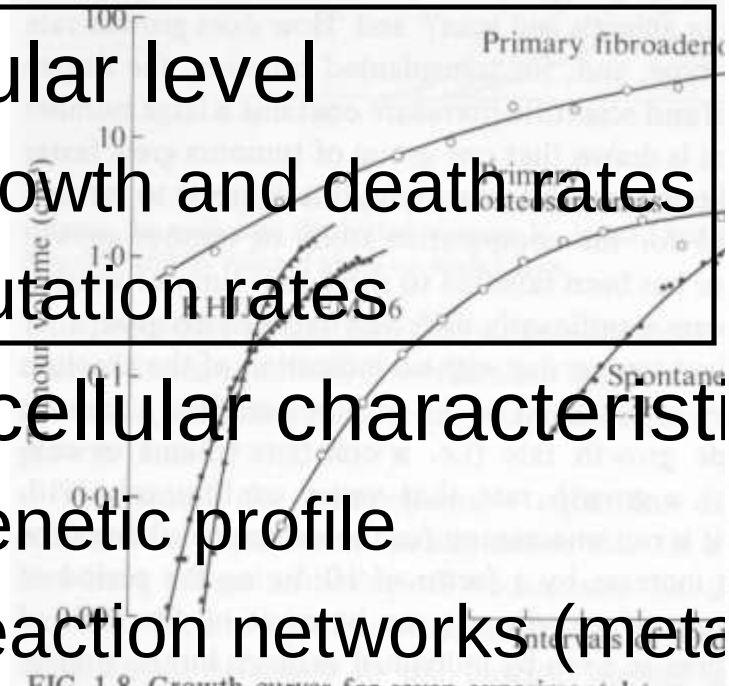

FIG. 1.8. Growth curves for seven experimental tumours whose growth has been studied in detail. In each case the data have been fitted by a Gompertz equation and the corresponding parameters are listed in Table 1.1, together with the relevant sources.

Steel 1977

Level of Model Detail – Population Growth

- Empirical Models
  - Course structure
  - Averaged cell behavior
  - Gompertz growth
- Mechanistic Models
  - Fine structure
  - Cdc/Cdk interactions

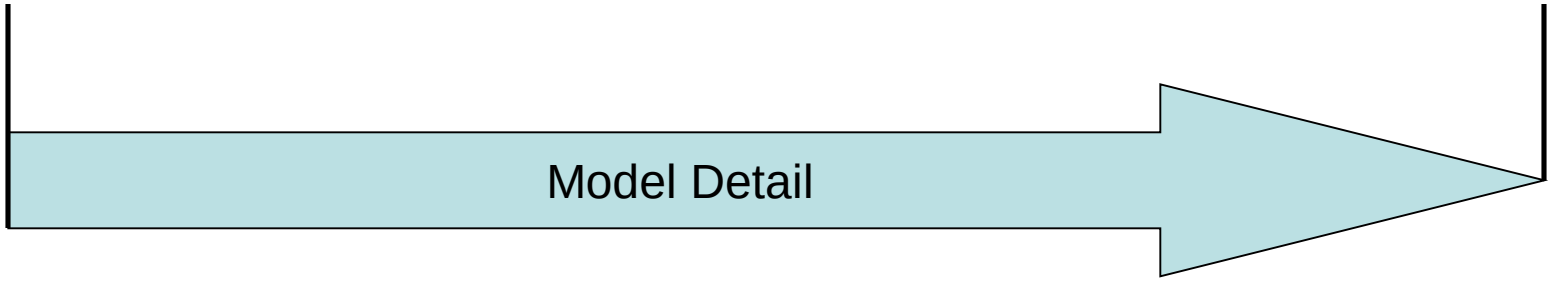

- Population Balance Models
  - “key” parameters (i.e. DNA, volume, age)
  - Details are lumped and averaged
  - Heterogeneous behavior

State vector

- Completely averaged
  - X = [ ]
- Few state variables
  - X = [size spatial_location internal_drug_level]
- More mechanistic
  - X = [Cdk1 CycA CycE…]

- Population Balance
  - Expected distribution among cells

Population Balance Model Requirements

- Transition rates (e.g. division rate)

$$\Gamma_{i,j}(x_1, x_2, x_3)$$

- Rates of change – growth rates

$$\dot{\mathbf{X}}(x_1, x_2, x_3, \mathbf{y})$$

- Constitutive model or experiments

- Advantages
  - Simplified description of system
  - Flexible framework

- Disadvantages
  - Proper identification of system (Burundi not the same as Denmark)
  - Identification of rates

Modeling Philosophies

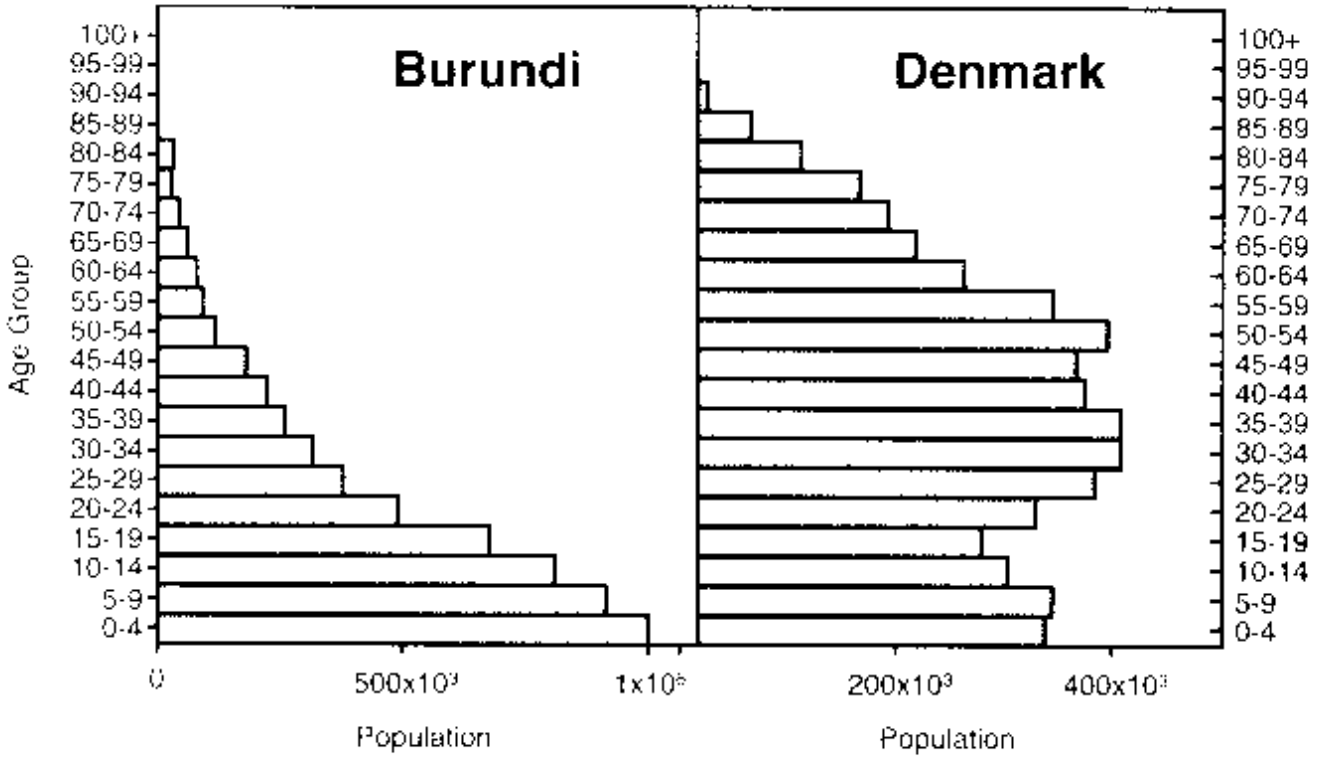

Figure 1.1 Population pyramids for Burundi and Denmark, 2000. (*Source: U.S. Census Bureau.*)

Hjortsø 2005

- Birth and death rates
  - Empirical
  - PBM – vary with age and country
  - Mechanistic – need to know the causes behind age-dependence

Expected Number Density

- Distribution of cell states

2 discrete states (i.e. Denmark)

1 continuous variable (i.e. age)

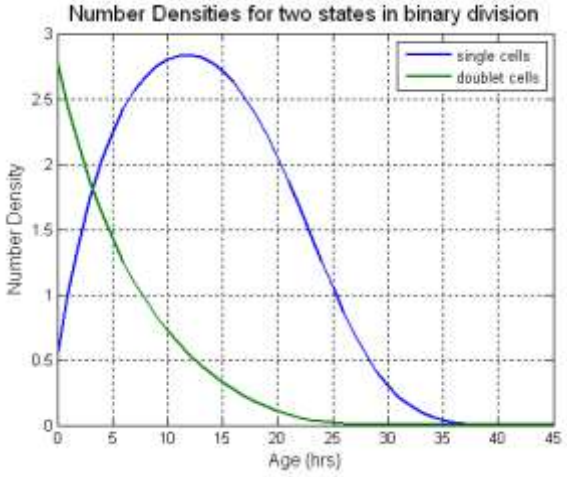

2 continuous variables

(i.e. age and weight)

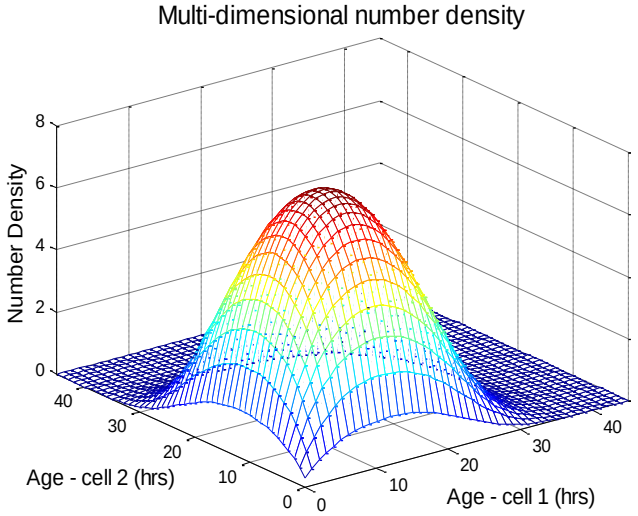

- Total number density

$$E\left[N(a,b;t)\right] = N_1(a,b;t) = \int_a^b n_1(x,t)dx$$

$$E\left[N(a,b;c,d;t)\right] = N_1(a,b;c,d;t) = \int_c^d \int_a^b n_1(x,t)dxdx'$$

Population Description

- Continuous variables
- Time
- Cell
  - Mass
  - Volume
  - Age
  - DNA or RNA
  - Protein
- Patient
  - Age

- Discrete indices
- Cell
  - Cell cycle phase
  - Genetic mutations
  - Differentiation state
- Patient
  - M / F
  - Race / ethnicity

Example – Cell Cycle Specific Behaviors

- Cell cycle specific drug
  - Discrete – cell cycle phase, p
  - Continuous – age, τ, (time since last transition)
- $n_1(p, \tau, t)$

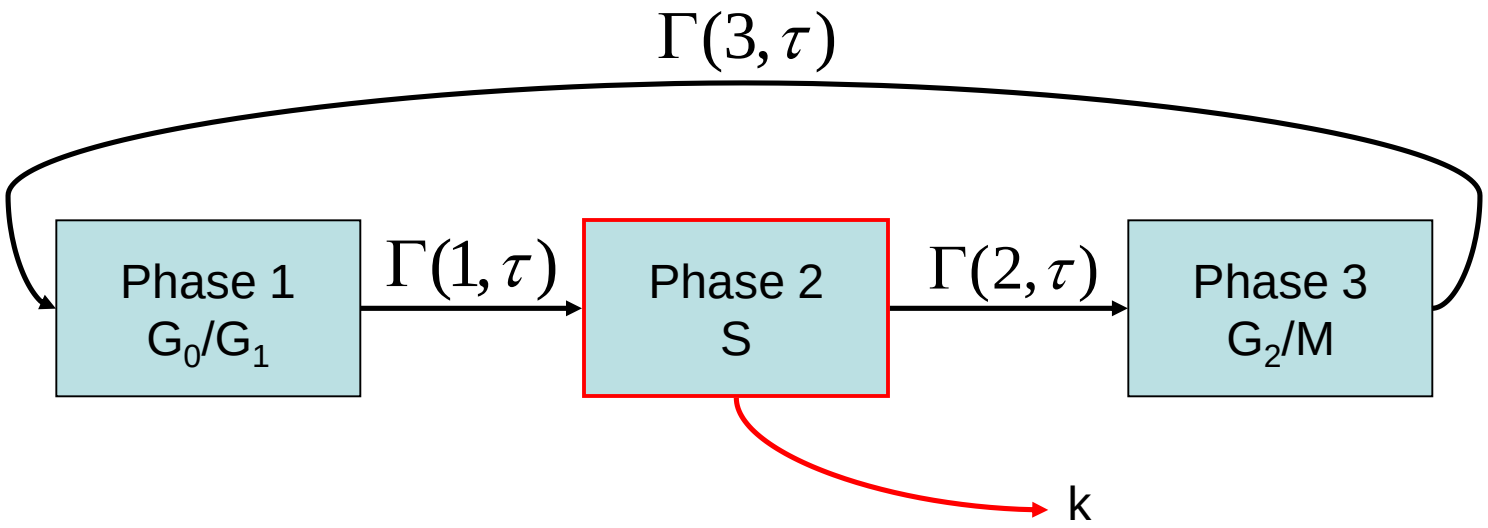

Cell Cycle Control (Tyson and Novak 2004)

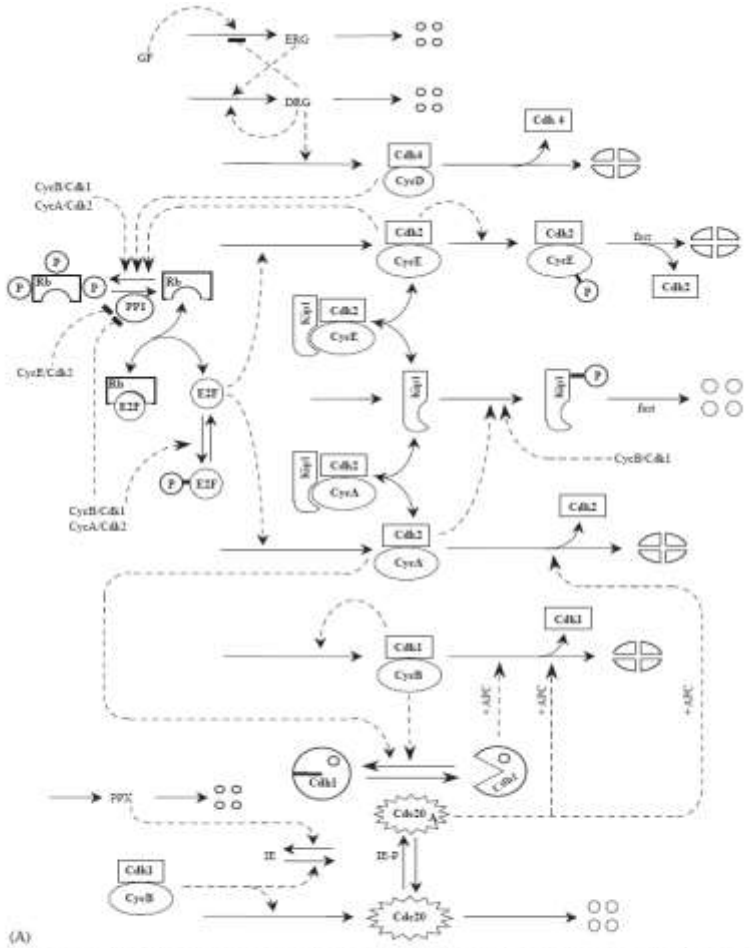

(A)

Fig. 1. Molecular network regulating the progression of mammalian cells through the cell cycle. (A) In the center of the diagram we propose a ye like cell-cycle "engine" composed of Cdk2/CycE, Cdk2/CycA, Cdk1/CycB, and some ancillary proteins (Kip1, Cdh1 and Cdc20). This part of diagram should be compared to Chen et al. (2000). To the engine we attach three components characteristic of mammalian cell-cycle controls: (i) retinoblastoma protein, Rb, which binds to and inhibits E2F, a transcription factor for production of CycA and CycE, (ii) the cyclin-depen kinase, Cdk4/CycD, which phosphorylates and inactivates Rb, and (iii) the signal-transduction pathway, GF–ERG–DRG, which controls C synthesis in response to GF stimulation. Although not indicated on the wiring diagram, the model includes the fact that Kip1 binds to CycD/C but does not inhibit its activity. (B) A more detailed representation of the binding and phosphorylation reactions that govern Rb–E2F interacti In deriving the model equations (Table 3), we assume that binding and release reactions are fast compared to phosphorylation dephosphorylation reactions.

Table 3
Mathematical model of mammalian cell-cycle controls

$$\frac{d[ERG]}{dt} = v\frac{k_{15}}{1+([DRG]/J_{15})^2} - k_{16}[ERG] \quad (1)$$

$$\frac{d[DRG]}{dt} = v\left(k'_{15}[ERG] + \frac{k_{15}([DRG]/J_{15})^2}{1+([DRG]/J_{15})^2}\right) - k_{16}[DRG] \quad (2)$$

$$\frac{d[cycD]}{dt} = vk_3[DRG] + V_3[CycD:Kip1] + k_{26}[CycD:Kip1] - k_{24}[cycD][Kip1] - k_{34}[CycD] \quad (3)$$

$$\frac{d[cycD:Kip1]}{dt} = k_{24}[CycD][Kip1] - k_{244}[CycD:Kip1] - V_3[CycD:Kip1] - k_{36}[CycD:Kip1] \quad (4)$$

$$\frac{d[cycE]}{dt} = v(k'_7 + k_7[E2F_A]) - V_4[cycE] - k_{25}[CycE][Kip1] + k_{254}[CycE:Kip1] + V_6[CycE:Kip1] \quad (5)$$

$$\frac{d[cycE:Kip1]}{dt} = k_{25}[CycE][Kip1] - k_{254}[CycE:Kip1] - V_6[CycE:Kip1] - V_5[CycE:Kip1] \quad (6)$$

$$\frac{d[cycA]}{dt} = vk_{20}[E2FA][mass] - k_{36}[Cdc20][cycA] - k_{23}[CycA][Kip1] + k_{25}[CycA:Kip1] + V_6[CycA:Kip1] \quad (7)$$

$$\frac{d[cycA:Kip1]}{dt} = k_{23}[CycA][Kip1] - k_{234}[CycA:Kip1] - V_6[CycA:Kip1] - k_{36}[Cdc20][CycA:Kip1] \quad (8)$$

$$\frac{d[Kip1]}{dt} = vk_9 - V_9[Kip1] - k_{24}[CycD][Kip1] + k_{244}[CycD:Kip1] + k_{34}[CycD:Kip1] - k_{23}[Kip1][CycE]+[CycA]) + k_{234}([CycE:Kip1]+[CycA:Kip1]) + V_5[CycE:Kip1] + k_{36}[Cdc20][CycA:Kip1] \quad (9)$$

$$\frac{d[E2F]}{dt} = k_{22}([E2F^T] - [E2F]) - (k'_{27} + k_{27}([CycA]+[CycB]))[E2F] \quad (10)$$

$$\frac{d[cycB]}{dt} = v\left(k'_4 + \frac{k_4([CycB]/J_4)^2}{1+([CycB]/J_4)^2}\right) - V_4[CycB] \quad (11)$$

$$\frac{d[Cdh1]}{dt} = (k'_9 + k_9[Cdh20])\frac{1-[Cdh1]}{J_9+1-[Cdh1]} - V_9\frac{[Cdh1]}{J_9+[Cdh1]} \quad (12)$$

$$\frac{d[Cdc20_T]}{dt} = v(k'_{11} + k_{11}[CycB]) - k_{12}[Cdc20_T] \quad (13)$$

$$\frac{d[Cdc20]}{dt} = k_{13}[IEP]\frac{[Cdc20_T]-[Cdc20]}{J_{13}+[Cdc20_T]-[Cdc20]} - k_{14}\frac{[Cdc20]}{J_{14}+[Cdc20]} - k_{12}[Cdc20] \quad (14)$$

$$\frac{d[PPX]}{dt} = vk_{18} - k_{19}[PPX] \quad (15)$$

$$\frac{d[IEP]}{dt} = k_{18}[CycB]\frac{1-[IEP]}{J_{18}+1-[IEP]} - k_{19}[PPX]\frac{[IEP]}{J_{19}+[IEP]} \quad (16)$$

$$\frac{d[GM]}{dt} = k_{21}[mass]H\left(\frac{[Rb_{hyper}]}{[Rb_T]}\right) - k_{26}[GM] \quad (17)$$

$$\frac{d[mass]}{dt} = v_8[GM] \quad (18)$$

Steady-state relations

$$[PP1_A] = \frac{[PP1_T]}{1+K_{21}(\phi_E[CycE]+[CycA])+\phi_B[CycB]} \quad (19)$$

$$[Rb_{hyper}] = \frac{[Rb_T]}{1+\frac{k_{20}/J_{20}}{k'_{19}([PP1_T]-[PP1_A])+k_{19}[PP1_A]}\left(\frac{[Rb_T]}{1+K_{21}(\phi_E[CycE]+[CycA])+\phi_B[CycB]}\right)} \quad (20)$$

$$[E2F_A] = \frac{([E2F_T]-[E2F:Rb])[E2F]}{[E2F_T]} \quad (21)$$

Cell cycle arrest (Tao et al. 2003)

Table 1. Genes involved in cell-cycle regulation and apoptosis whose expression is upregulated or downregulated in etoposide-treated human CD34+ cord blood cells compared to control as analyzed by cDNA array

Gene Name	Accession No.	Description	Relative* Expression	Fold Change*
Cell Cycle Regulator				
MDM2	NM_002392	p53-associated gene.	0.17	*21.3* (up)
P21	U03106	Wild-type p53 activated fragment-1 (WAF1).	0.23	6.6 (up)
Cyclin A2	NM_001237	Cyclin A.	0.78	−2.8 (down)
CDC2	NM_001786	Cell cycle control gene CDC2.	0.20	−1.3 (down)
c-myc	V00568	C-myc oncogene.	1.28	−5.9 (down)
TNF Superfamily				
Fas	M67454	Fas antigen (fas).	0.06	*10.0* (up)
TRAIL R1	NM_003844	Cytotoxic ligand TRAIL receptor.	0.04	8.6 (up)
TRAIL R2	AF012535	Death receptor 5 (DR5).	0.32	3.2 (up)
TRAIL R4	NM_003840	Decoy receptor 2 (DcR2).	0.02	13.2 (up)
4-1BBL	U03398	Receptor 4-1BB ligand.	0.91	1.7 (up)
THANK	AF116456	B-cell activating factor (BAFF).	0.12	−4.9 (down)
TNF RI	M63121	Tumor necrosis factor receptor.	0.29	−1.4 (down)
Apoptosis-Related and *bcl-2*–Related				
Cox-2	M90100	Cyclooxygenase-2 (Cox-2).	0.11	1.8 (up)
FLIPL	AF015452	Usurpin-γ	0.31	1.7 (up)
GALECTIN-3	AB006780	Lectin, galactoside-binding, soluble, 3 (galectin-3)	0.10	2.2 (up)
IAP-1	U45878	Inhibitor of apoptosis protein 1.	0.15	1.9 (up)
nNOS	U17327	Neuronal nitric oxide synthase (NOS1).	0.19	2.8 (up)
SARP-1	AF017986	Secreted apoptosis-related protein 1 (SARP1).	0.64	1.9 (up)
AIF	NM_004208	Apoptosis-inducing factor (AIF), nuclear gene encoding mitochondrial protein.	0.66	−1.3 (down)
DAD-1	NM_001344	Defender against cell death 1 (DAD1).	0.74	−1.6 (down)
DAXX	NM_005453	mRNA for death-associated protein, Daxx.	0.54	−1.3 (down)
GAPDH	M33197	Glyceraldehyde-3-phosphate dehydrogenase (GAPDH).	19.52	−1.5 (down)
Bax-α	L22473	Baxα	0.34	2.4 (up)
bcl-w	NM_004050	*bcl-w* (*bcl-w*).	0.58	1.6 (up)
Mcl-1	L08246	Myeloid cell differentiation protein (MCL1).	0.63	1.7 (up)
bcl-2	NM_000633	B-cell CLL/lymphoma 2 (BCL-2).	0.24	−1.3 (down)

*The numbers denote that expression of a gene relative to the expression of gene encoding transferrin receptor in control CD34+ cord blood cells. Relative expression is calculated as a ratio of detected mRNA of a gene and that of the transferrin receptor gene.

†A positive number indicates that expression of a gene is upregulated while a negative value indicates downregulation of a gene in etoposide-treated CD34+ cord blood cells.

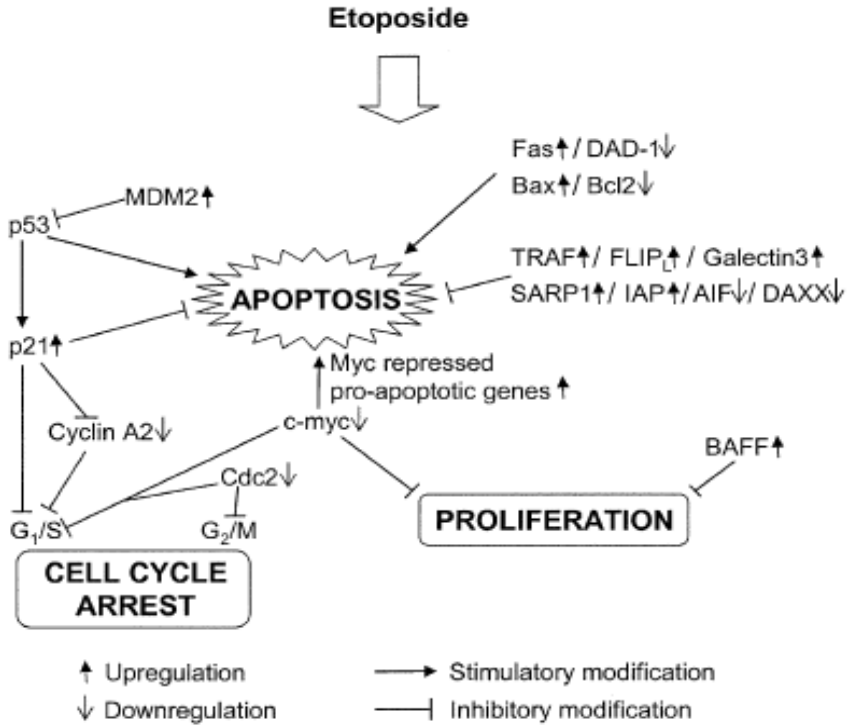

Figure 6. Schematic representation of basic molecular components existing in and putative pathways utilized by human CD34+ cells in their response to etoposide treatment based on cDNA array and quantitative real-time RT-PCR data. Myc and p53 are main pathways elicited by human CD34+ cells in their response to etoposide treatment. Multiple known pro-survival and pro-apoptotic pathways were simultaneously activated.

PBMs in biological settings

- Cell cycle-specific chemo
- Budding yeast dynamics
- Rate of monoclonal antibody production in hybridoma cells
- Bioreactor productivity under changing substrate conditions
- Ecological models
  - Predator-prey

Topics

- Modeling Philosophies
  - Where Population Balance Models (PBMs) fit in
- Important Characteristics
- Framework
- Uses
  - Cancer Examples
- Parameter Identification
- Potential Applications

Variations of Scale

- Tumor scale properties
  - Physical characteristics
  - Disease class
- Cellular level
  - Growth and death rates
  - Mutation rates
- Subcellular characteristics
  - Genetic profile
  - Reaction networks (metabol- and prote-omics)
  - CD markers

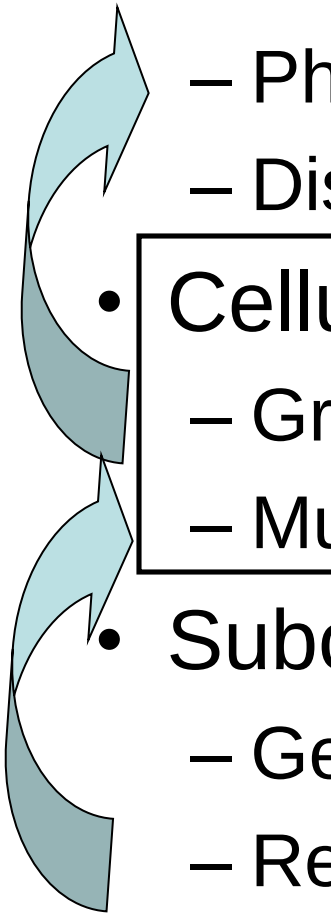

Modeling Philosophies

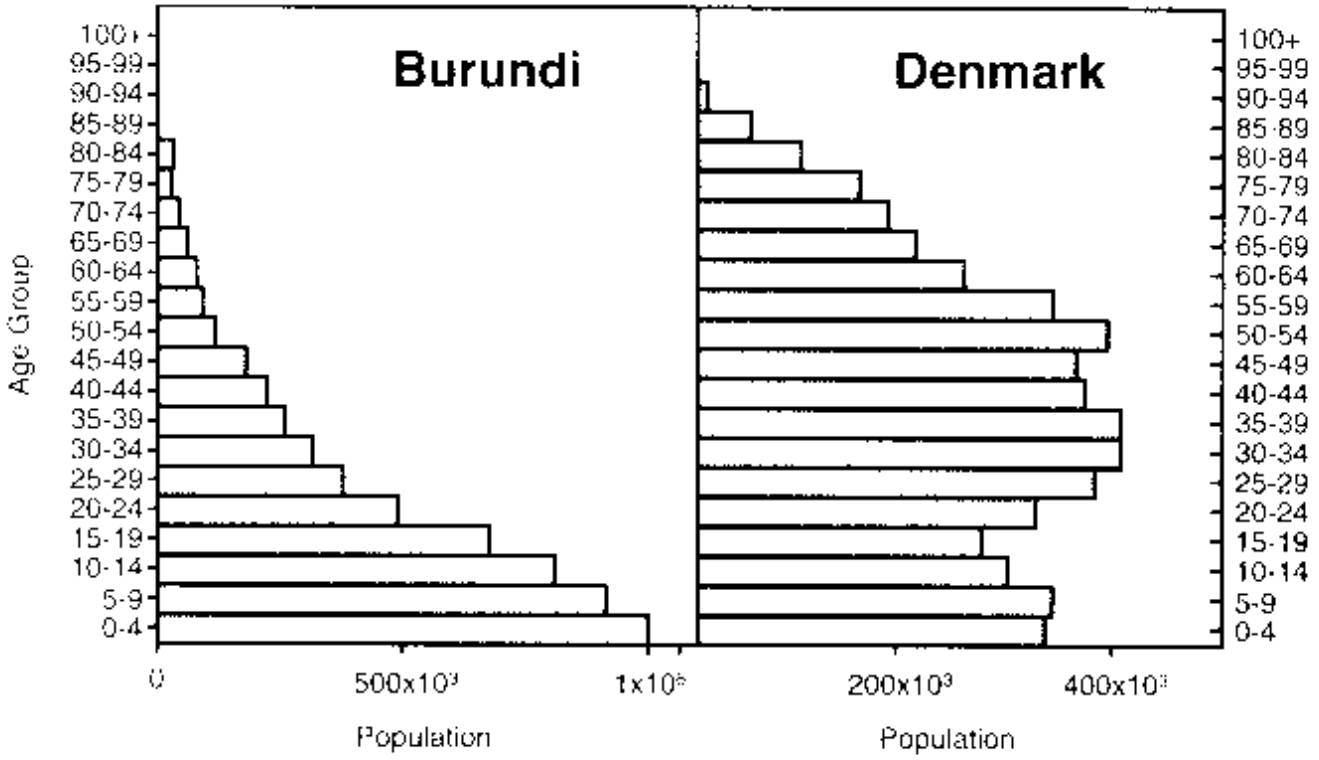

Figure 1.1 Population pyramids for Burundi and Denmark, 2000. (*Source: U.S. Census Bureau.*)

Hjortsø 2005

- Birth and death rates
  - Empirical
  - PBM – vary with age and country (STATE VECTOR)
  - Mechanistic – need to know the causes behind age-dependence

Population Balance Model Requirements

- Transition rates (e.g. division and rates)

$$\Gamma_{i,j}(x_1, x_2, x_3)$$

- Rates of change – growth rates

$$\dot{\mathbf{X}}(x_1, x_2, x_3, \mathbf{y})$$

- Constitutive model or experiments

- Advantages
  - Simplified description of system
  - Flexible framework

- Disadvantages
  - Proper identification of system (Burundi not the same as Denmark)
  - Identification of rates

Cell Cycle Control (Tyson and Novak 2004)

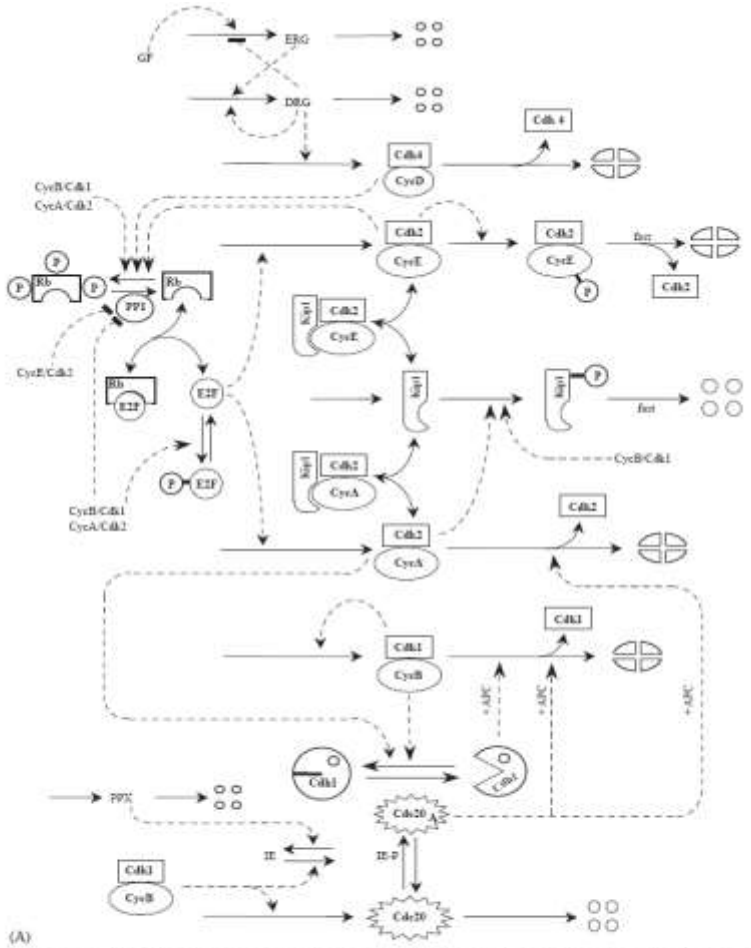

(A)

Fig. 1. Molecular network regulating the progression of mammalian cells through the cell cycle. (A) In the center of the diagram we propose a ye like cell-cycle "engine" composed of Cdk2/CycE, Cdk2/CycA, Cdk1/CycB, and some ancillary proteins (Kip1, Cdh1 and Cdc20). This part of diagram should be compared to Chen et al. (2000). To the engine we attach three components characteristic of mammalian cell-cycle controls: (i) retinoblastoma protein, Rb, which binds to and inhibits E2F, a transcription factor for production of CycA and CycE, (ii) the cyclin-depen kinase, Cdk4/CycD, which phosphorylates and inactivates Rb, and (iii) the signal-transduction pathway, GF–ERG–DRG, which controls C synthesis in response to GF stimulation. Although not indicated on the wiring diagram, the model includes the fact that Kip1 binds to CycD/C but does not inhibit its activity. (B) A more detailed representation of the binding and phosphorylation reactions that govern Rb–E2F interacti In deriving the model equations (Table 3), we assume that binding and release reactions are fast compared to phosphorylation dephosphorylation reactions.

Table 3
Mathematical model of mammalian cell-cycle controls

$$\frac{d[ERG]}{dt} = v\frac{k_{15}}{1+([DRG]/J_{15})^2} - k_{16}[ERG] \quad (1)$$

$$\frac{d[DRG]}{dt} = v\left(k'_{15}[ERG] + \frac{k_{15}([DRG]/J_{15})^2}{1+([DRG]/J_{15})^2}\right) - k_{16}[DRG] \quad (2)$$

$$\frac{d[cycD]}{dt} = vk_3[DRG] + V_3[CycD:Kip1] + k_{26}[CycD:Kip1] - k_{24}[cycD][Kip1] - k_{34}[CycD] \quad (3)$$

$$\frac{d[cycD:Kip1]}{dt} = k_{24}[CycD][Kip1] - k_{244}[CycD:Kip1] - V_3[CycD:Kip1] - k_{36}[CycD:Kip1] \quad (4)$$

$$\frac{d[cycE]}{dt} = v(k'_7 + k_7[E2F_A]) - V_4[cycE] - k_{25}[CycE][Kip1] + k_{254}[CycE:Kip1] + V_6[CycE:Kip1] \quad (5)$$

$$\frac{d[cycE:Kip1]}{dt} = k_{25}[CycE][Kip1] - k_{254}[CycE:Kip1] - V_6[CycE:Kip1] - V_5[CycE:Kip1] \quad (6)$$

$$\frac{d[cycA]}{dt} = vk_{20}[E2FA][mass] - k_{36}[Cdc20][cycA] - k_{23}[CycA][Kip1] + k_{25}[CycA:Kip1] + V_6[CycA:Kip1] \quad (7)$$

$$\frac{d[cycA:Kip1]}{dt} = k_{23}[CycA][Kip1] - k_{234}[CycA:Kip1] - V_6[CycA:Kip1] - k_{36}[Cdc20][CycA:Kip1] \quad (8)$$

$$\frac{d[Kip1]}{dt} = vk_9 - V_9[Kip1] - k_{24}[CycD][Kip1] + k_{244}[CycD:Kip1] + k_{34}[CycD:Kip1] - k_{23}[Kip1][CycE]+[CycA]) + k_{234}([CycE:Kip1]+[CycA:Kip1]) + V_5[CycE:Kip1] + k_{36}[Cdc20][CycA:Kip1] \quad (9)$$

$$\frac{d[E2F]}{dt} = k_{22}([E2F^T] - [E2F]) - (k'_{27} + k_{27}([CycA]+[CycB]))[E2F] \quad (10)$$

$$\frac{d[cycB]}{dt} = v\left(k'_4 + \frac{k_4([CycB]/J_4)^2}{1+([CycB]/J_4)^2}\right) - V_4[CycB] \quad (11)$$

$$\frac{d[Cdh1]}{dt} = (k'_9 + k_9[Cdh20])\frac{1-[Cdh1]}{J_9+1-[Cdh1]} - V_9\frac{[Cdh1]}{J_9+[Cdh1]} \quad (12)$$

$$\frac{d[Cdc20_T]}{dt} = v(k'_{11} + k_{11}[CycB]) - k_{12}[Cdc20_T] \quad (13)$$

$$\frac{d[Cdc20]}{dt} = k_{13}[IEP]\frac{[Cdc20_T]-[Cdc20]}{J_{13}+[Cdc20_T]-[Cdc20]} - k_{14}\frac{[Cdc20]}{J_{14}+[Cdc20]} - k_{12}[Cdc20] \quad (14)$$

$$\frac{d[PPX]}{dt} = vk_{18} - k_{19}[PPX] \quad (15)$$

$$\frac{d[IEP]}{dt} = k_{18}[CycB]\frac{1-[IEP]}{J_{18}+1-[IEP]} - k_{19}[PPX]\frac{[IEP]}{J_{19}+[IEP]} \quad (16)$$

$$\frac{d[GM]}{dt} = k_{21}[mass]H\left(\frac{[Rb_{hyper}]}{[Rb_T]}\right) - k_{26}[GM] \quad (17)$$

$$\frac{d[mass]}{dt} = v_8[GM] \quad (18)$$

Steady-state relations

$$[PP1_A] = \frac{[PP1_T]}{1+K_{21}(\phi_E[CycE]+[CycA])+\phi_B[CycB]} \quad (19)$$

$$[Rb_{hyper}] = \frac{[Rb_T]}{1+\frac{k_{20}/J_{20}}{k'_{19}([PP1_T]-[PP1_A])+k_{19}[PP1_A]}\left(\frac{[Rb_T]}{1+K_{21}(\phi_E[CycE]+[CycA])+\phi_B[CycB]}\right)} \quad (20)$$

$$[E2F_A] = \frac{([E2F_T]-[E2F:Rb])[E2F]}{[E2F_T]} \quad (21)$$

Changes Number Density

- Changes in cell states

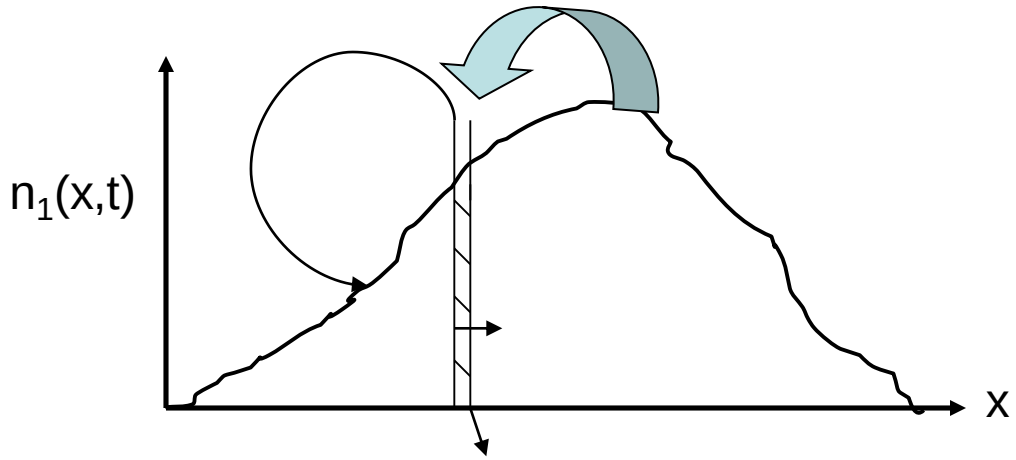

- Cell behavior (growth, division and death, and phase transitions) are functions of a cell's state

Population Balance – pure growth

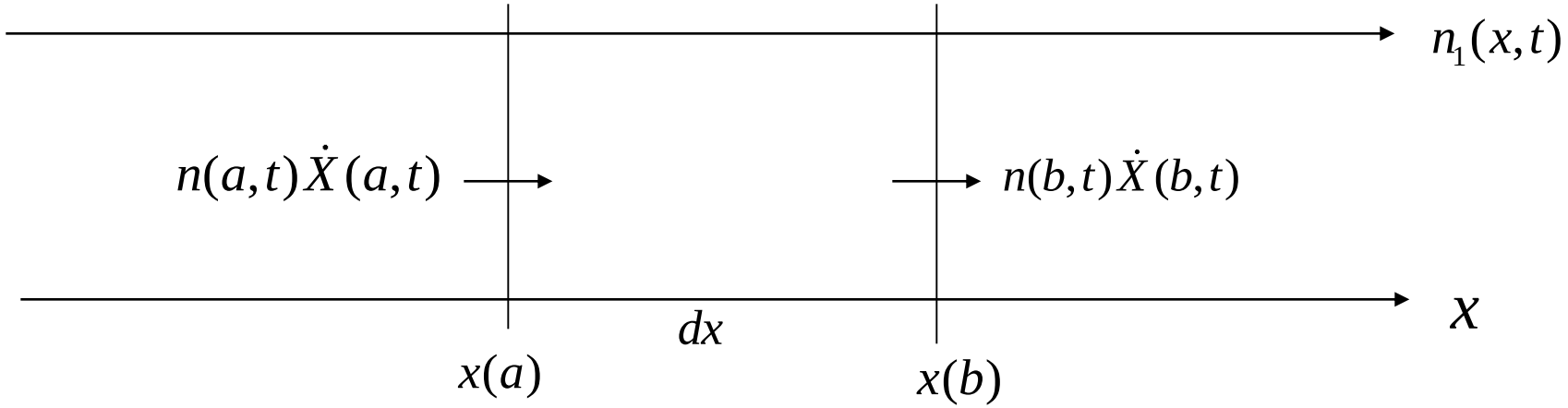

$$\frac{d}{dt}\int_a^b n_1(x,t)dx = n_1(a,t)\dot{X}(a,t) - n_1(b,t)\dot{X}(b,t)$$

$$\int_a^b \frac{\partial}{\partial t} n_1(x,t)dx = -\int_a^b \frac{\partial}{\partial x}\left(\dot{X}(x,t)n_1(x,t)\right)dx$$

$$\frac{\partial n_1(x,t)}{\partial t} + \frac{\partial}{\partial x}\left(\dot{X}(x,t)n_1(x,t)\right) = 0$$

Growth rate

Transitions between discrete states

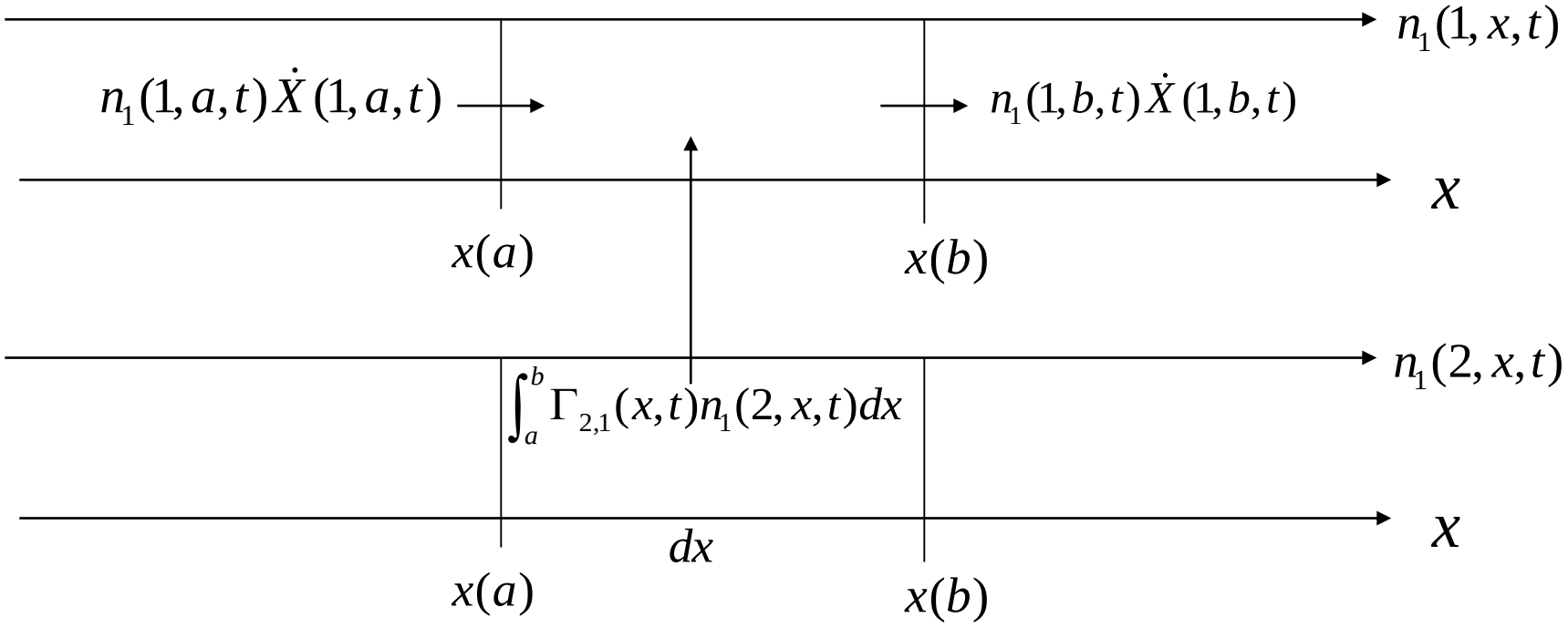

$$\frac{\partial n_1(1,x,t)}{\partial t} + \frac{\partial}{\partial x}\left(\dot{X}(1,x,t)n_1(1,x,t)\right) = \sum_{i,1}\Gamma_{i,1}(i,x,t)n_1(i,x,t) - \sum_{i,1}\Gamma_{1,i}(x,t)n_1(1,x,t)$$

Growth rate

Transition rates

Cell division and death

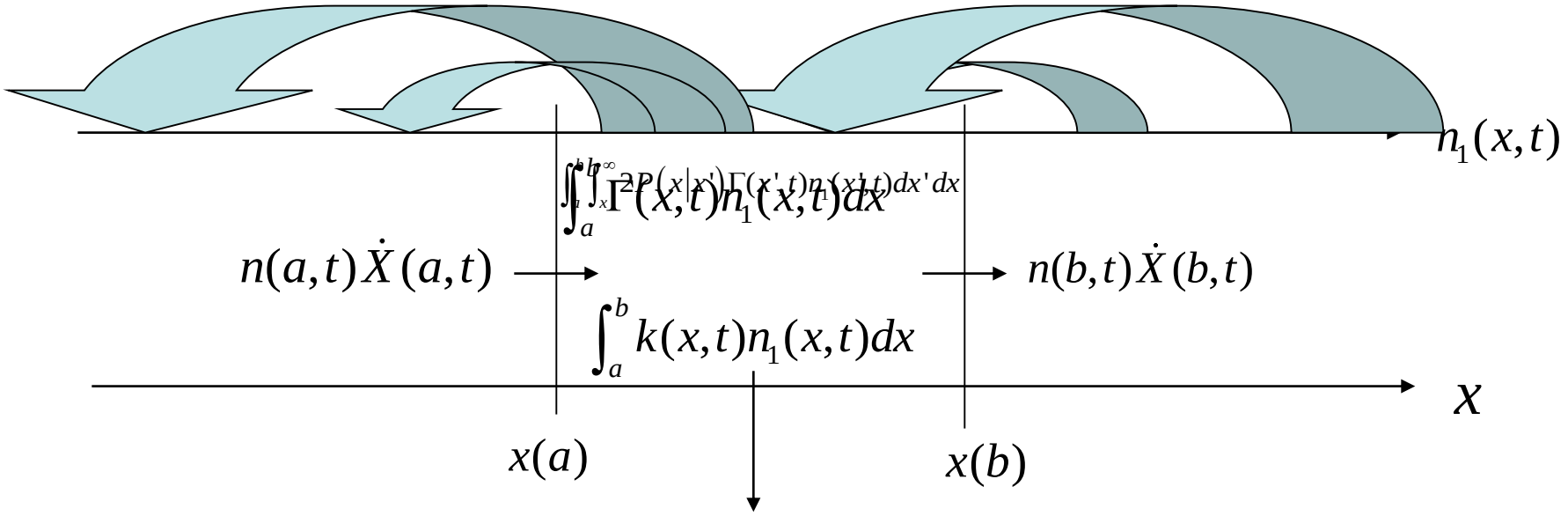

$$\frac{\partial n_1(x,t)}{\partial t} + \frac{\partial}{\partial x}\left(\dot{X}(x,t)n_1(x,t)\right) = \int_x^\infty 2P\left(x\middle|x'\right)\Gamma(x',t)n_1(x',t)dx' - \left(\Gamma(x,t)+k(x,t)\right)n_1(x,t)$$

Growth rate

Division rate

Death rate

Mathematical Model
Cellular -> Macroscopic

- Tumor size and character
  - Simulate cells and observe bulk behavior
- Cell behavior
  - Mutations
  - Spatial effects
  - Cell cycle phase
  - Quiescence
  - Pharmacodynamics
- Mostly theoretical work
  - Occasionally some parameters available

- Optimization of chemo
  - Dosage
  - Frequency
  - Drug combinations
- Solid tumor
  - Size limitations due to nutrients and inhibitors
- Leukemia
  - Quiescent and proliferating populations
  - Cell cycle-specific chemotherapy
- Mutations
  - Branching process

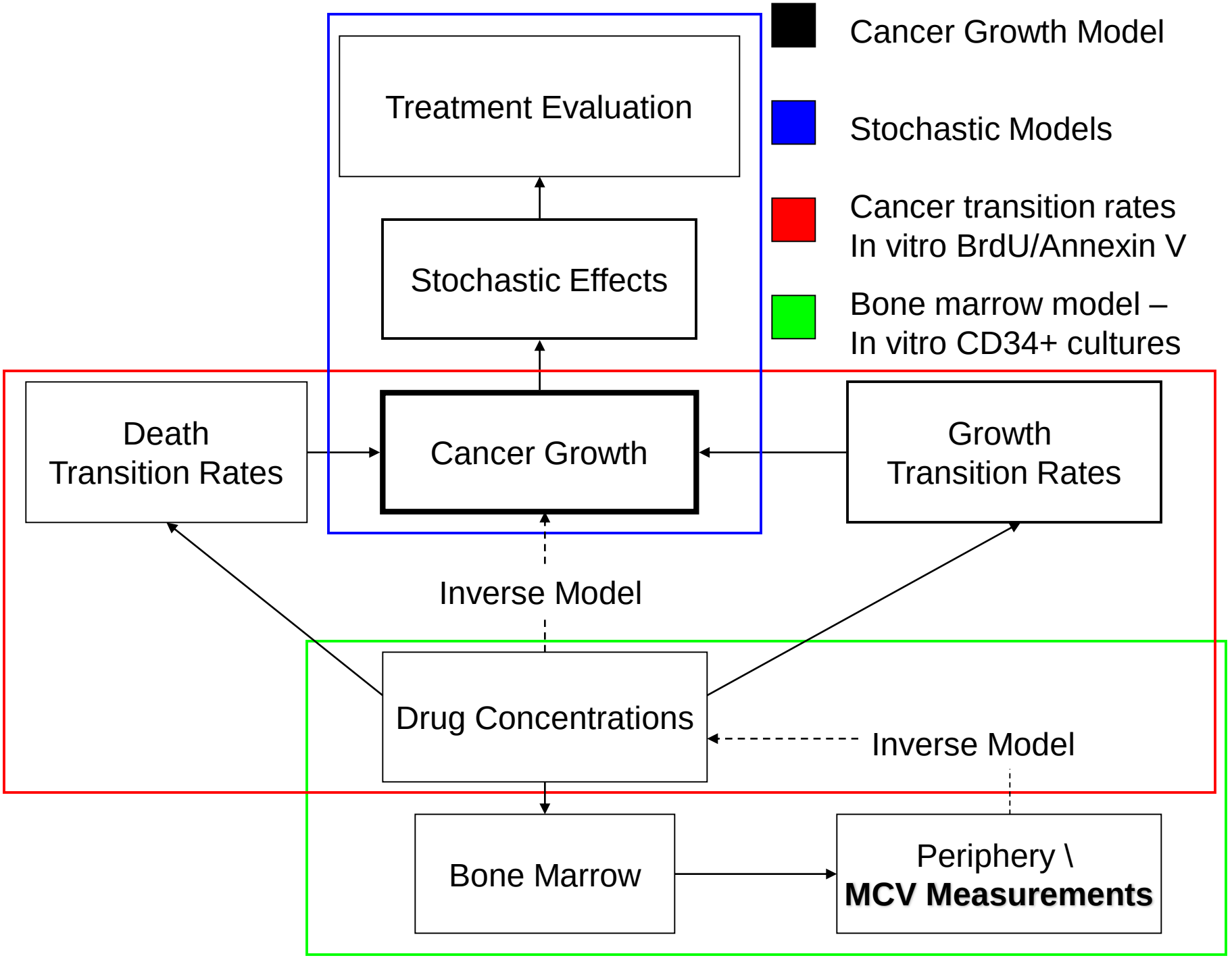
Cancer Growth Model
Stochastic Models
Cancer transition rates
In vitro BrdU/Annexin V
Bone marrow model –
In vitro CD34+ cultures
Treatment Evaluation
Stochastic Effects
Death
Transition Rates
Cancer Growth
Growth
Transition Rates
Inverse Model
Drug Concentrations
Inverse Model
Bone Marrow
Periphery \
MCV Measurements

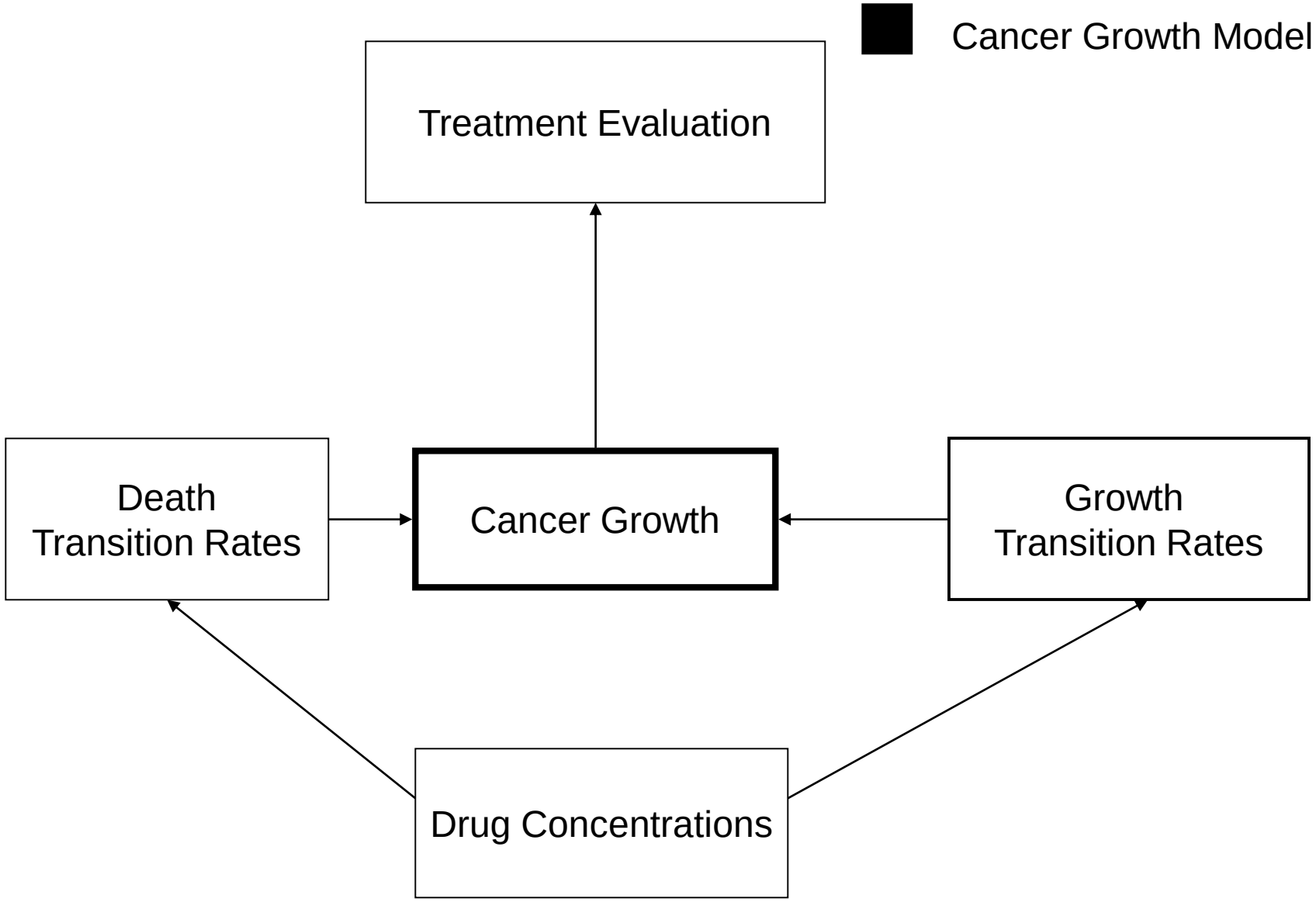
Cancer Growth Model
Treatment Evaluation
Death
Transition Rates
Cancer Growth
Growth
Transition Rates
Drug Concentrations

Example – Cell Cycle Specific Behaviors

- Cell cycle specific drug
  - Discrete – cell cycle phase, p
  - Continuous – age, τ, (time since last transition)
- $n_1(p, \tau, t)$

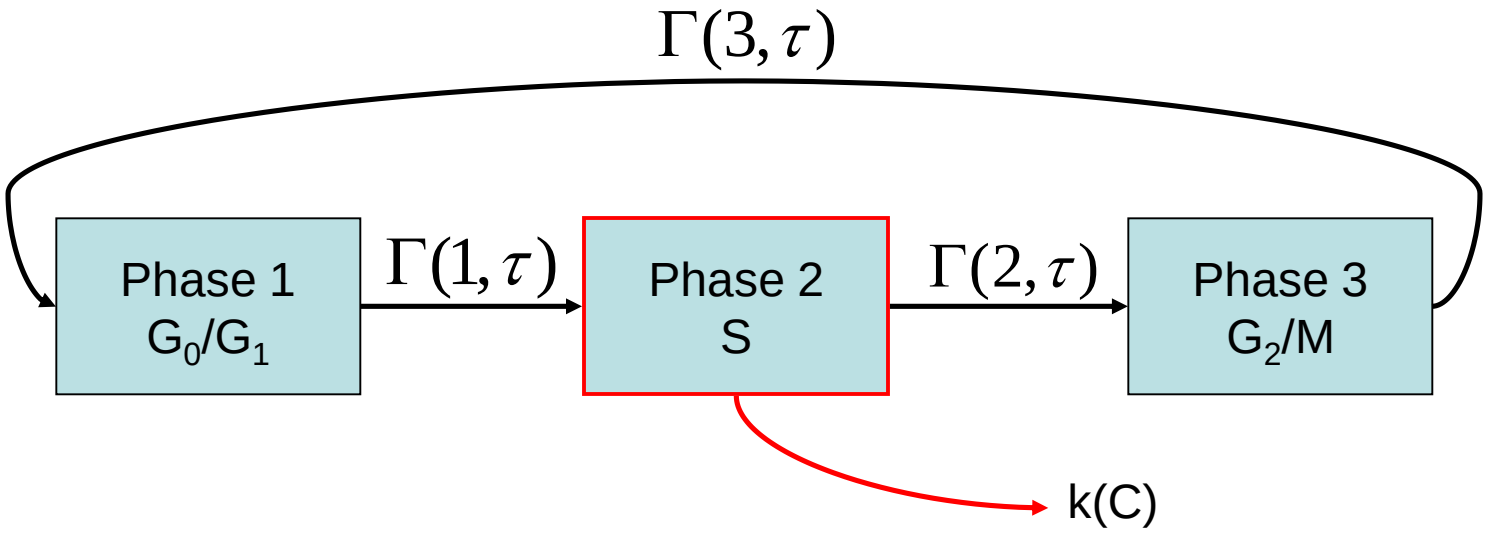

In vitro verification

- Total population dynamics
- Phase oscillations
  - Period
  - Amplitude
  - Dampening
- Co-culture of Jurkat and HL60 performed for selective treatment

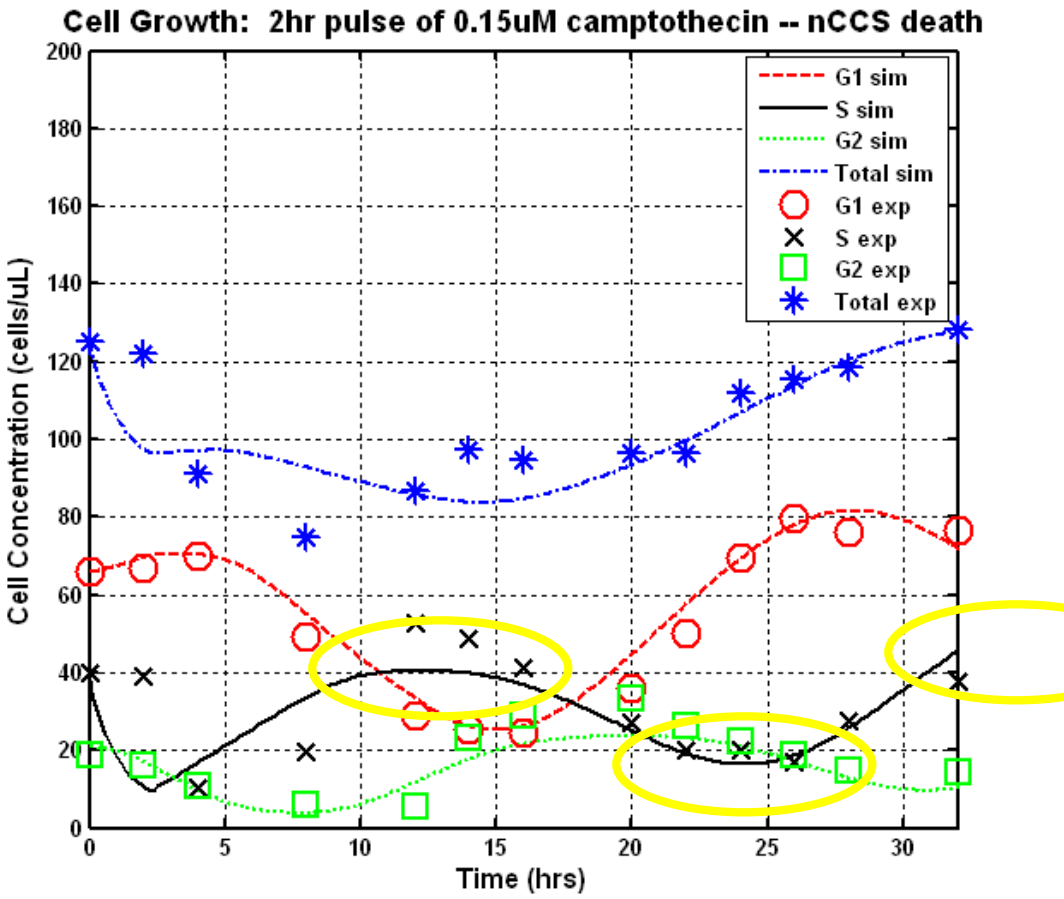

Sherer et al. 2006

Use in Treatment Designs

Timing effects

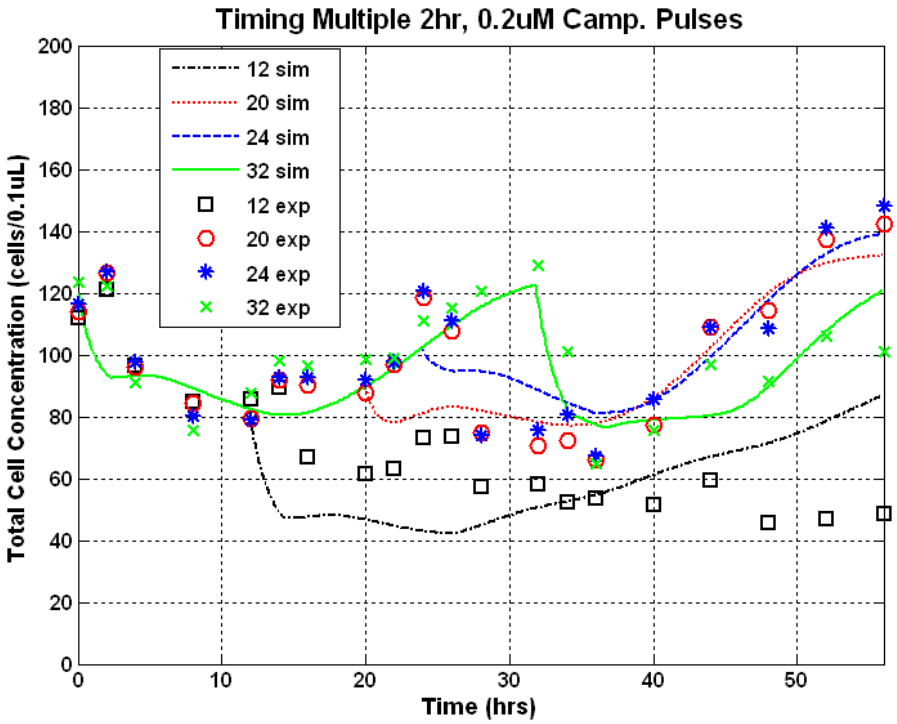

Treatment Optimization

Heathy cells vs. cancerous

Drug Dosage

Administration Timings

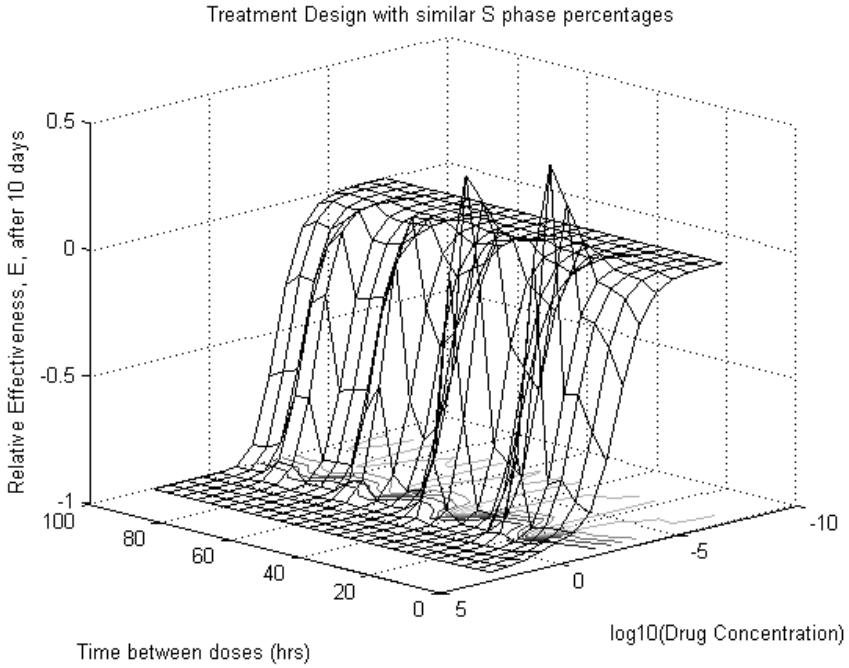

Model Extrapolation
In vivo factors

Drug half-life

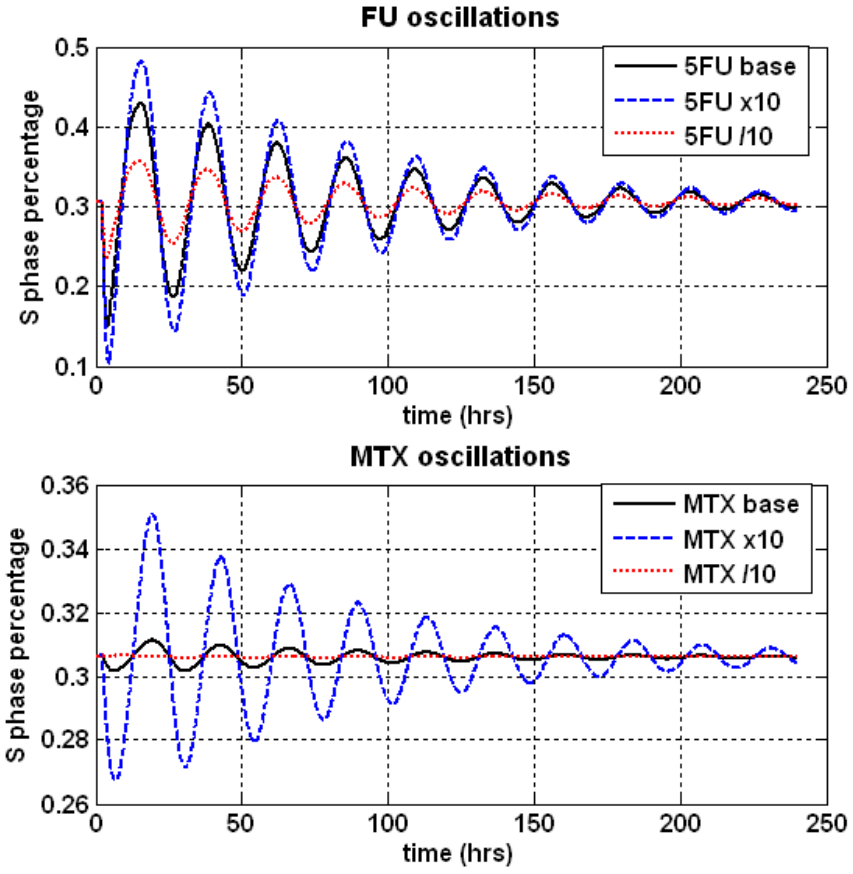

Activation of quiescent population in bone marrow

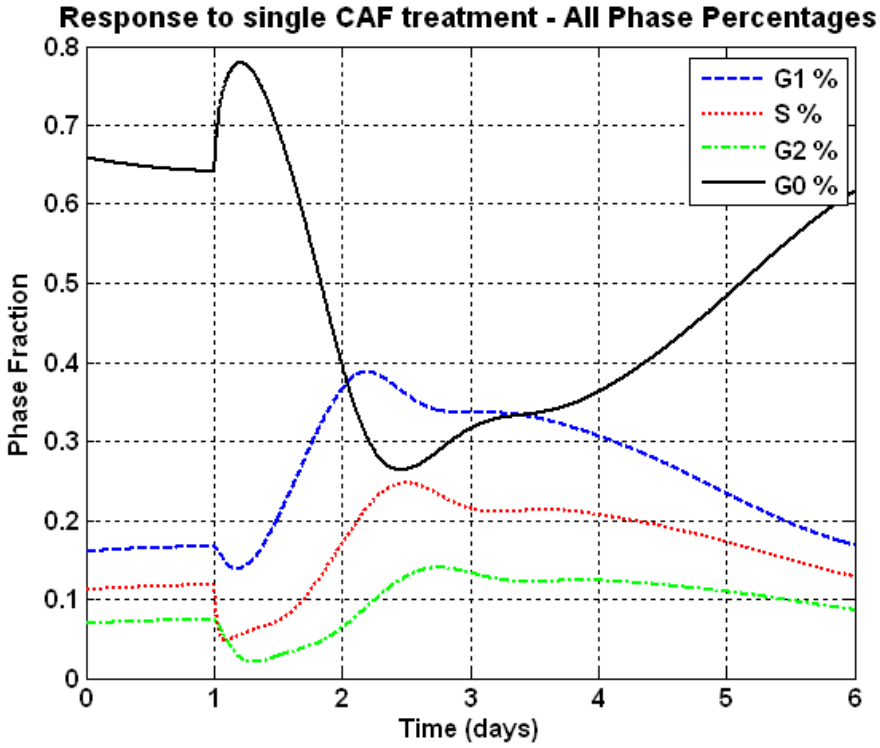

Age-averaged PBM

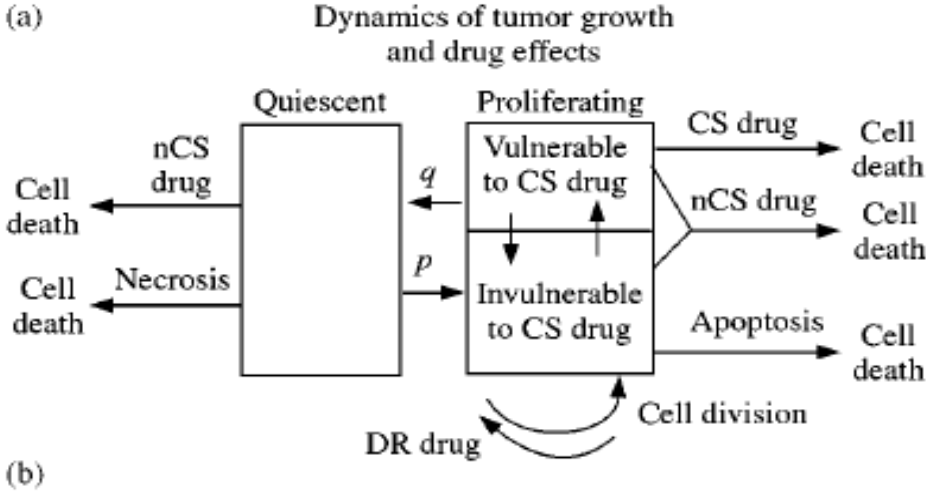

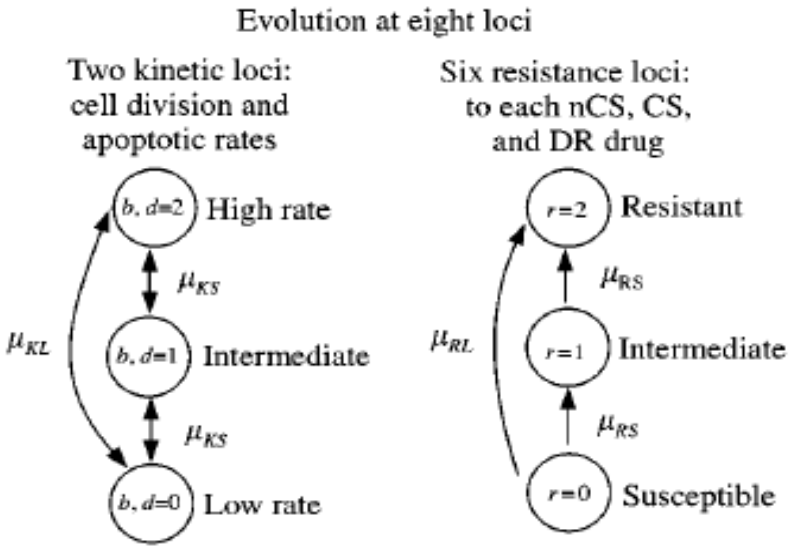

FIG. 1. (a) Diagram of the cellular dynamics of the model. Cells in the proliferating state may divide, die via apoptosis, or enter the quiescent state. Cells in the resting state may die via necrosis or transfer back to the proliferating state. nCS drugs kill cells in both the resting and the proliferating states, while CS drugs kill only a fraction of proliferating cells in a particular phase of the cell cycle. DR drugs slow the progression of cells through cell division. (b) Diagram of mutations in the model that generate intra-tumor heterogeneity. Mutations may occur at loci affecting the cell division and apoptotic rates, as well as at six loci each controlling drug resistance to a particular drug. Mutations of large effect occur with probability $\mu_{RL} = \mu_{KL} = 10^{-6}$, and those of small effect with probability $\mu_{RS} = \mu_{KS} = 10^{-4}$.

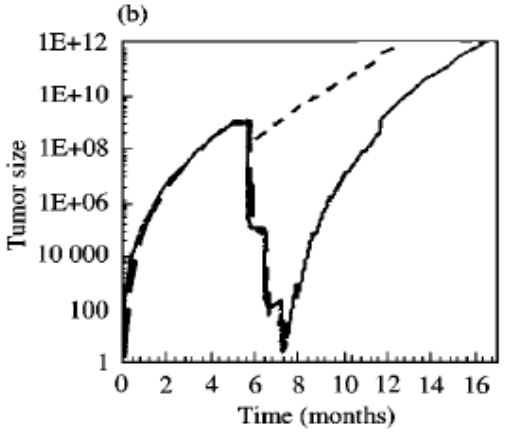

Gardner SN. "Modelling multi-drug chemotherapy: tailoring treatment to individuals." Journal of Theoretical Biology, 214: 181-207, 2002.

Prognosis Tree

a < 0.01

If a<0.01 if a>0.01

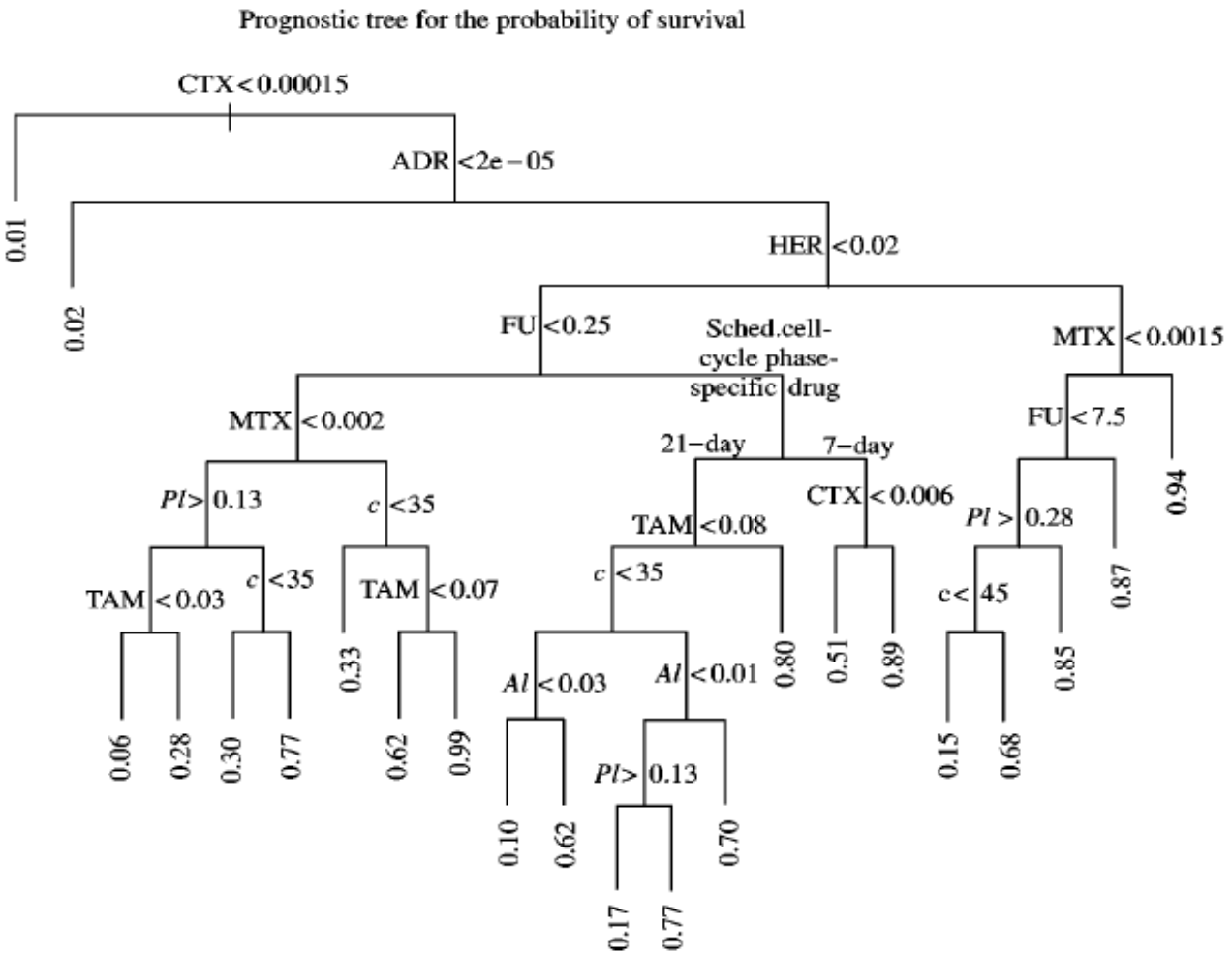

FIG. 6. Decision tree constructed from the simulation of 26 896 tumors. The physician-controlled factors of drug dose and schedule are illustrated in bold, and the tumor-specific factors of *AI*, *PI*, and *c* are in italics. (a) Probability of survival. (b) Duration in months from tumor detection to patient death.

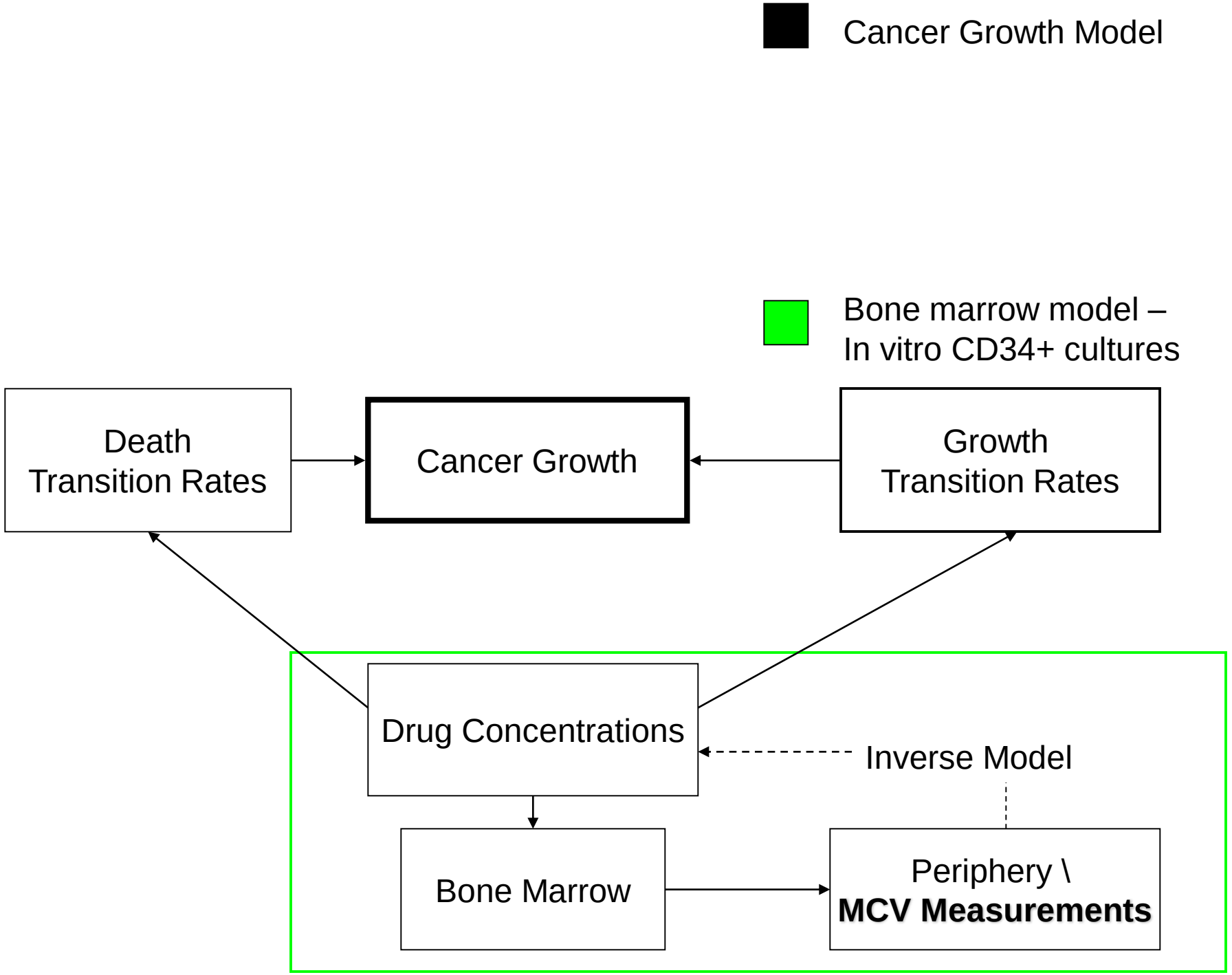
Cancer Growth Model
Bone marrow model –
In vitro CD34+ cultures
Death
Transition Rates
Cancer Growth
Growth
Transition Rates
Drug Concentrations
Inverse Model
Bone Marrow
Periphery \
MCV Measurements

Modeling a surrogate marker for the drug 6MP

- Bone marrow
  - 6MP inhibits DNA synthesis
- Blood stream
  - Red blood cells (RBCs) become larger
  - RBC size correlates with steady-state 6MP level

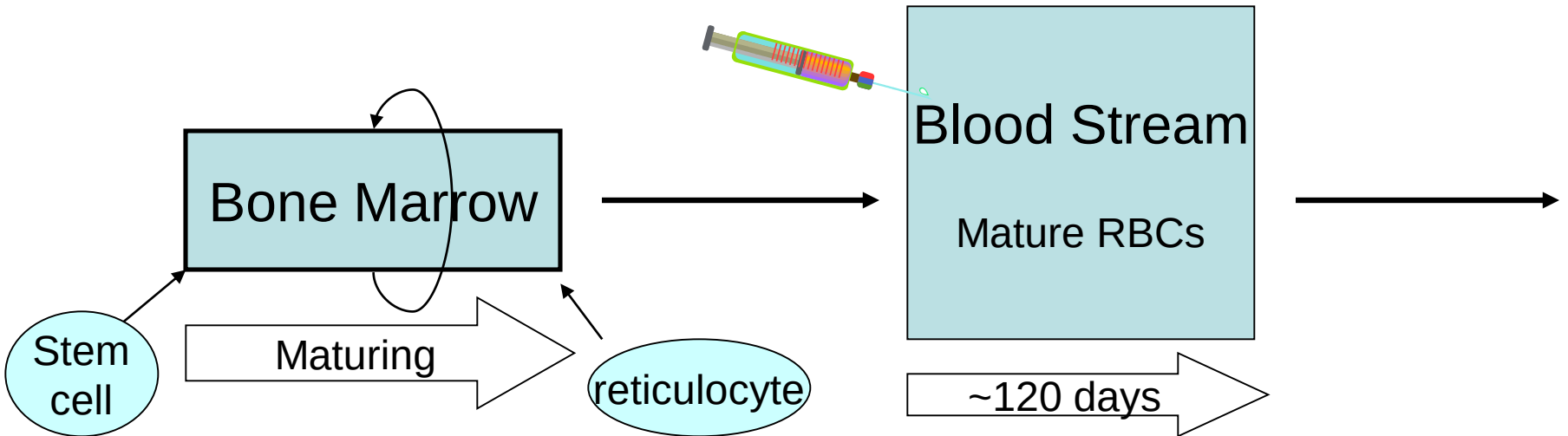

RBC Maturation

- Cell volume
- DNA inhibition
  - Time since division
  - *DNA synthesis rate*
- Maturation
  - Discrete state
    - Transferrin and glycophorin A
  - *Continuous*
    - Time spent in state

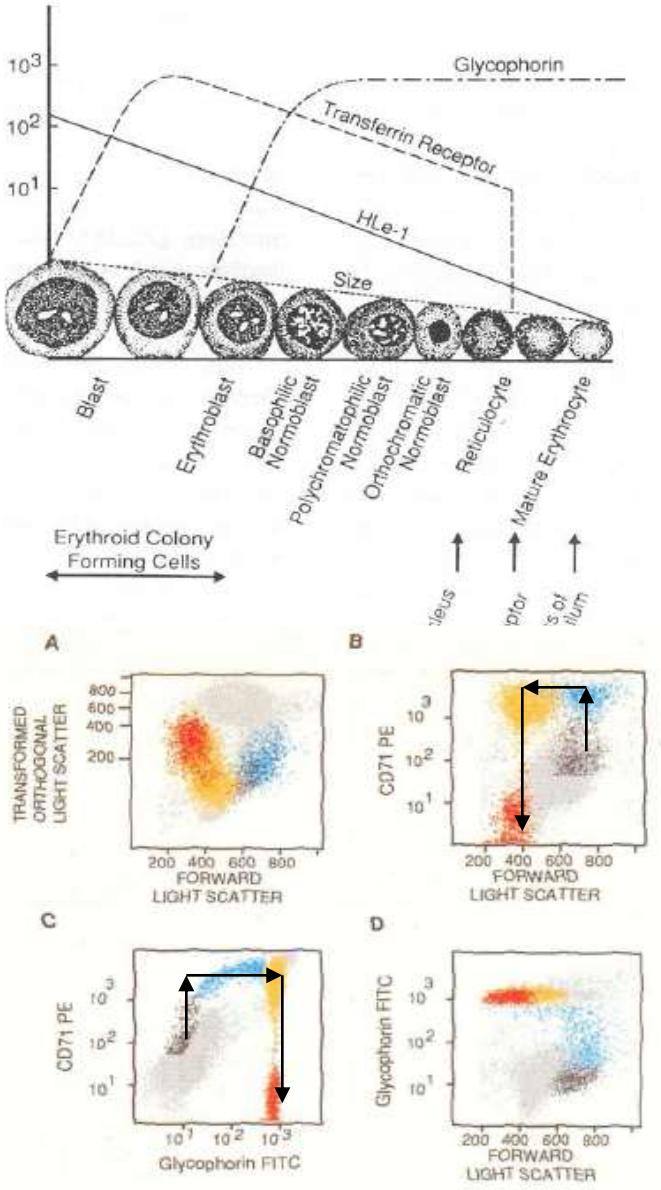

Hillman and Finch 1996

Forward Model (hypothetical)

- Days: 6TGN reaches steady-state (SS)
- Weeks: Marrow maturation in new SS
- Months: Periphery in new SS

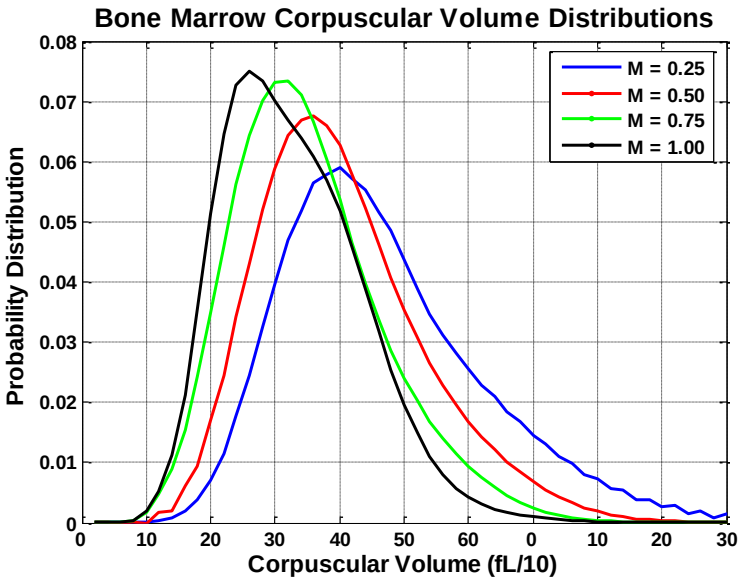

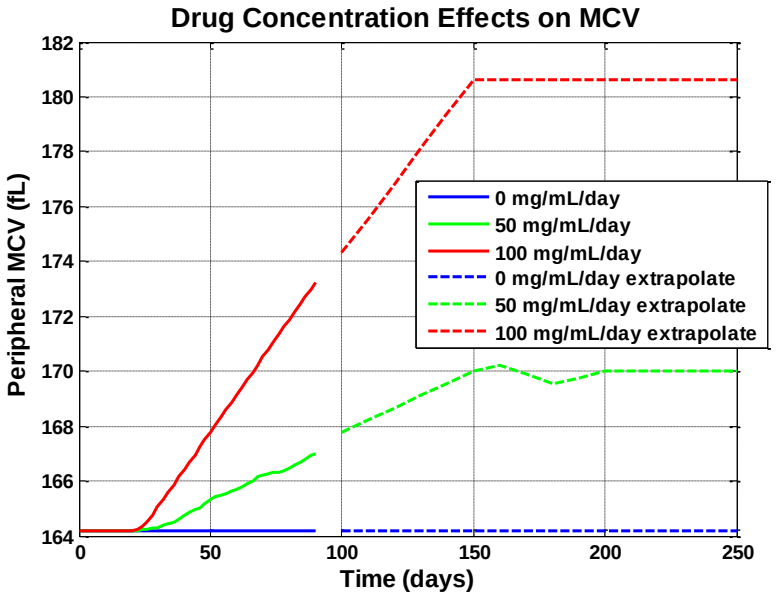

MCV => Drug level

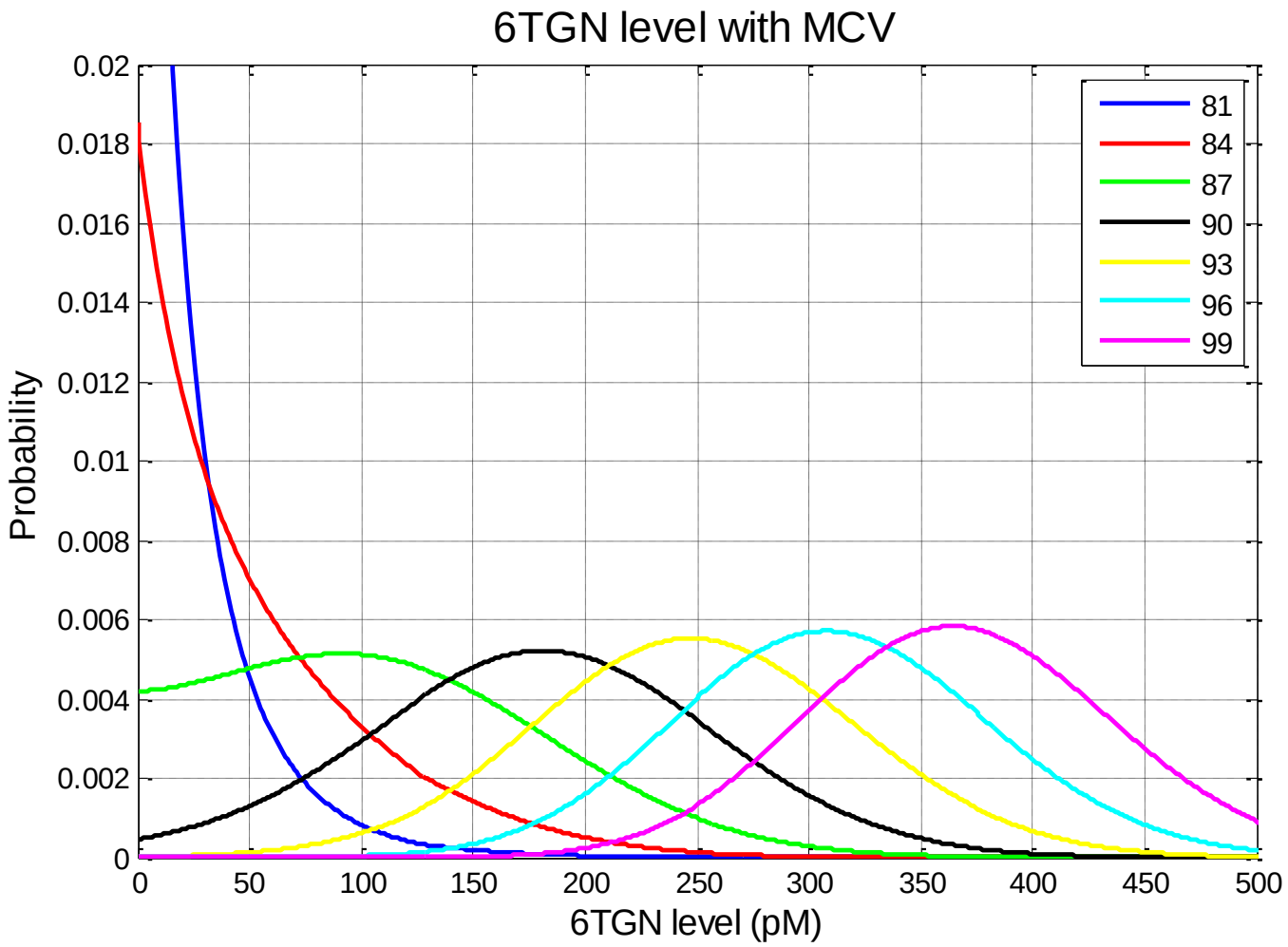

Topics

- Modeling Philosophies
  - Where Population Balance Models (PBMs) fit in
- Important Characteristics
- Framework
- Uses
  - Cancer Examples
- Parameter Identification
- Potential Applications

Example – Cell Cycle Specific Behaviors

- Cell cycle specific drug
  - Discrete – cell cycle phase, p
  - Continuous – age, τ, (time since last transition)
- $n_1(p, \tau, t)$

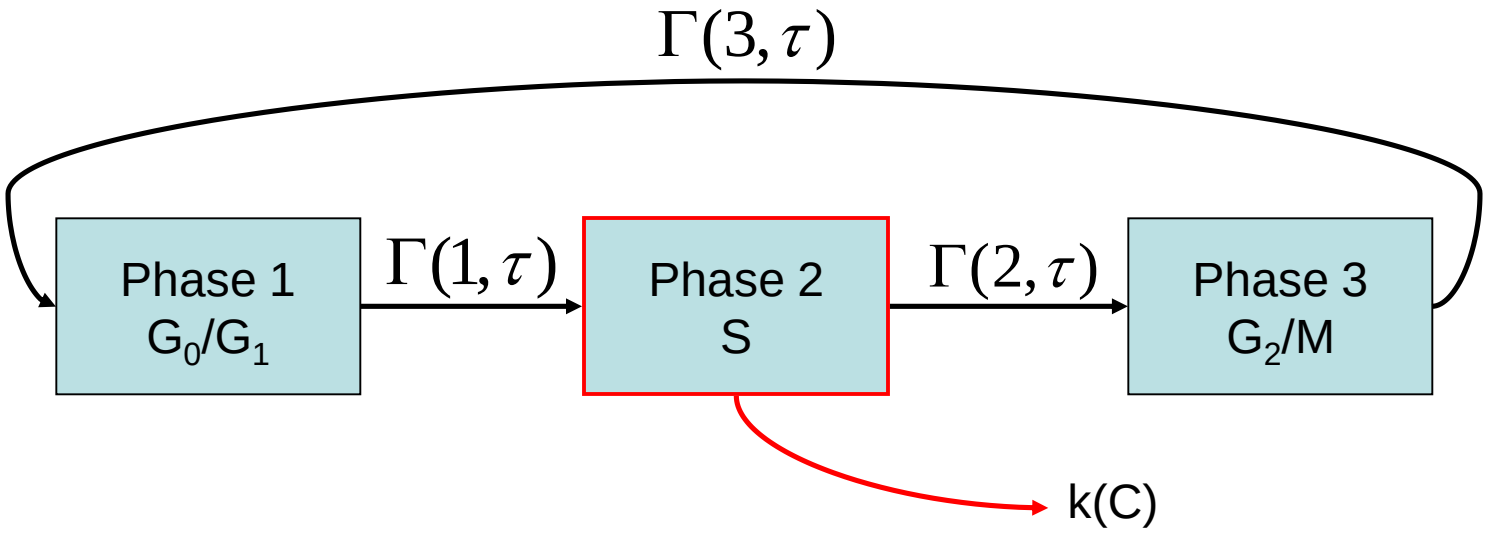

In vitro verification

- Total population dynamics
- Phase oscillations
  - Period
  - Amplitude
  - Dampening
- Co-culture of Jurkat and HL60 performed for selective treatment

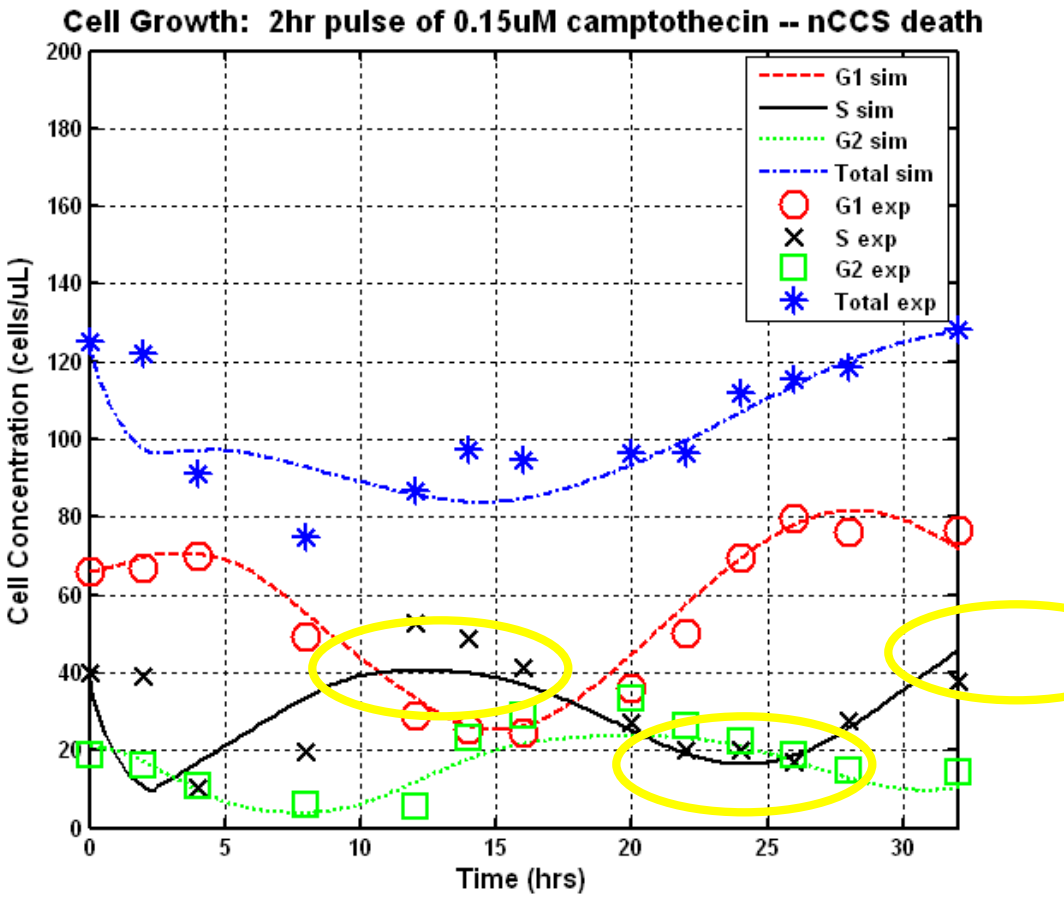

Age-averaged PBM

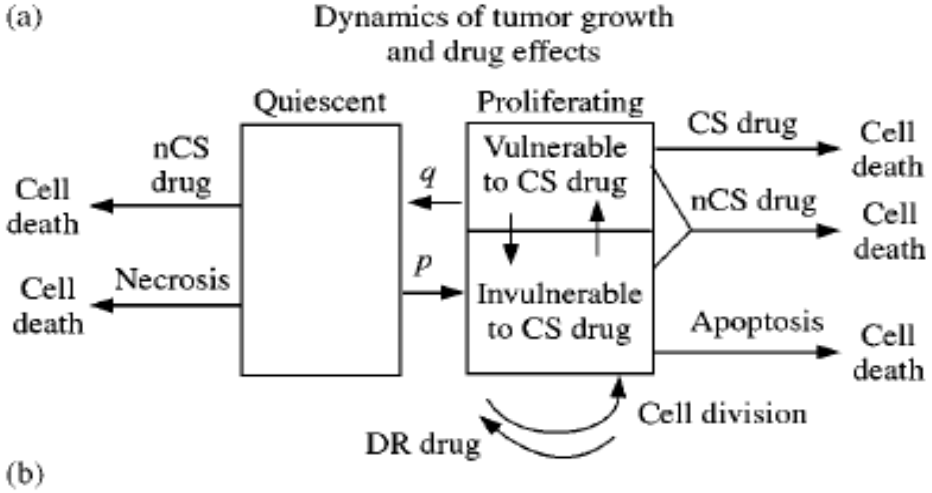

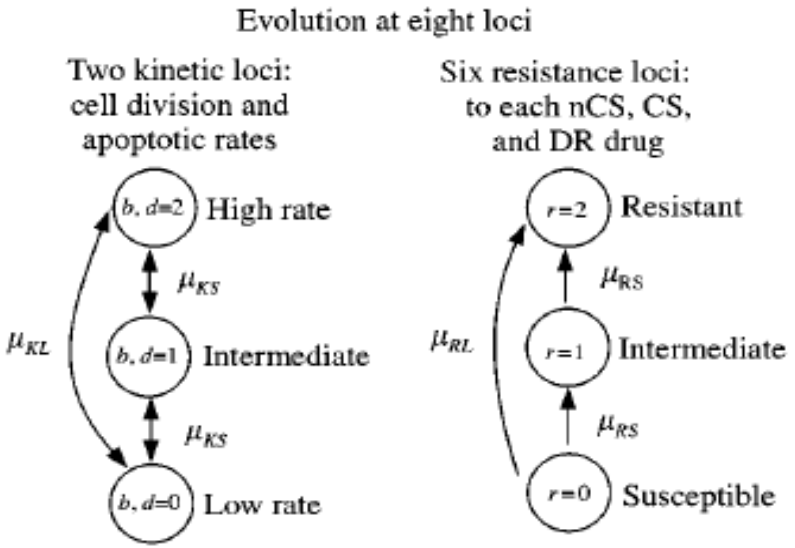

FIG. 1. (a) Diagram of the cellular dynamics of the model. Cells in the proliferating state may divide, die via apoptosis, or enter the quiescent state. Cells in the resting state may die via necrosis or transfer back to the proliferating state. nCS drugs kill cells in both the resting and the proliferating states, while CS drugs kill only a fraction of proliferating cells in a particular phase of the cell cycle. DR drugs slow the progression of cells through cell division. (b) Diagram of mutations in the model that generate intra-tumor heterogeneity. Mutations may occur at loci affecting the cell division and apoptotic rates, as well as at six loci each controlling drug resistance to a particular drug. Mutations of large effect occur with probability $\mu_{RL} = \mu_{KL} = 10^{-6}$, and those of small effect with probability $\mu_{RS} = \mu_{KS} = 10^{-4}$.

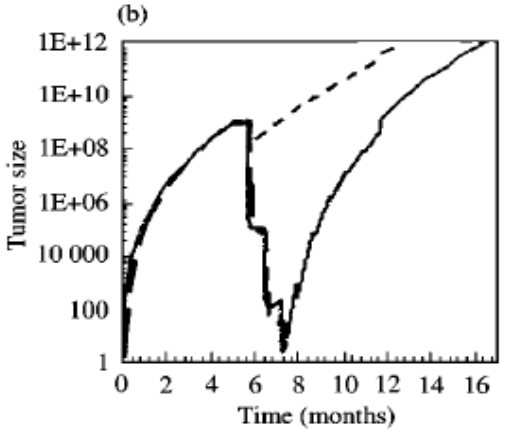

Gardner SN. "Modelling multi-drug chemotherapy: tailoring treatment to individuals." Journal of Theoretical Biology, 214: 181-207, 2002.

Prognosis Tree

a < 0.01

If a<0.01 if a>0.01

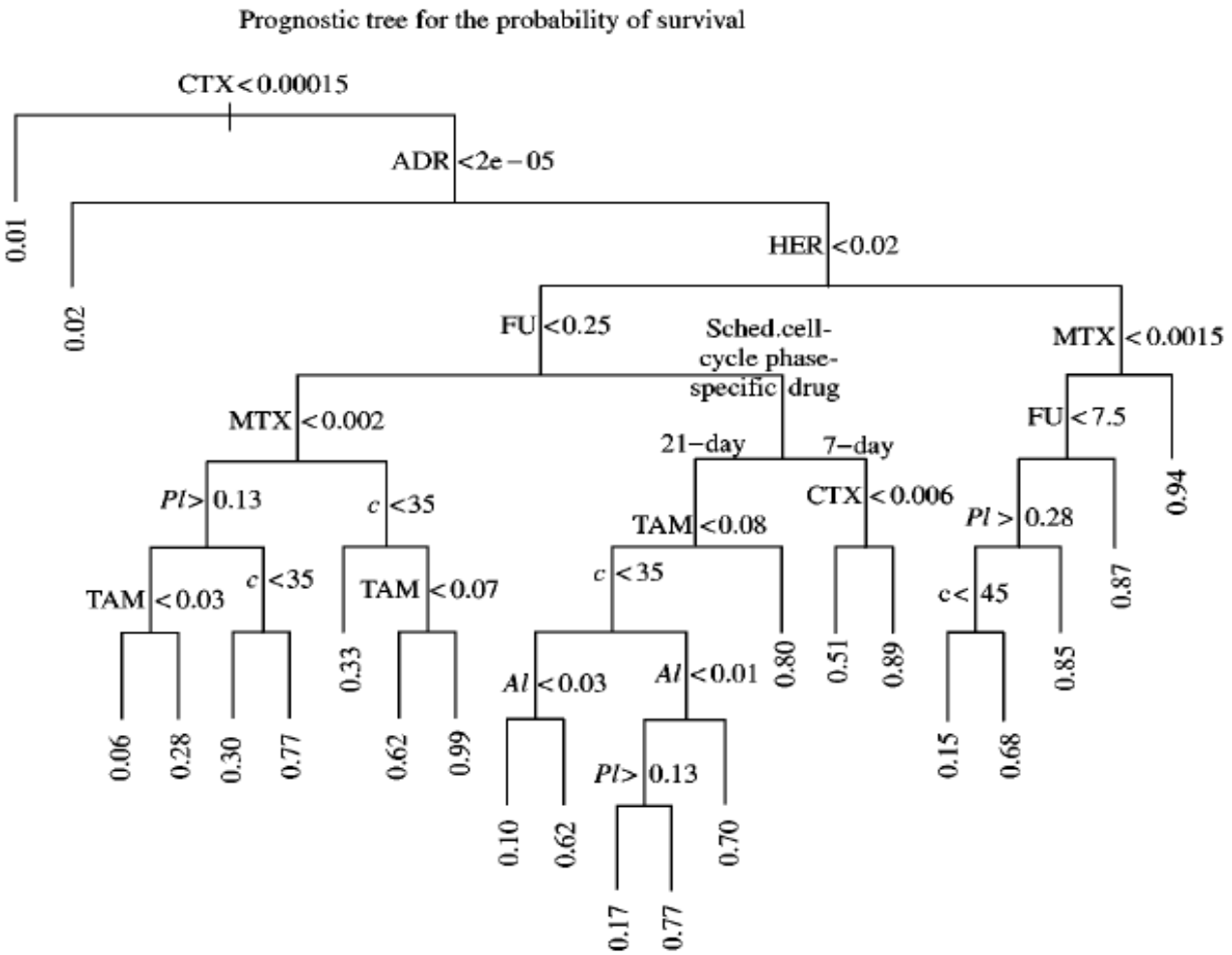

FIG. 6. Decision tree constructed from the simulation of 26 896 tumors. The physician-controlled factors of drug dose and schedule are illustrated in bold, and the tumor-specific factors of *AI*, *PI*, and *c* are in italics. (a) Probability of survival. (b) Duration in months from tumor detection to patient death.

Ramkrishna's resonance chemotherapy model

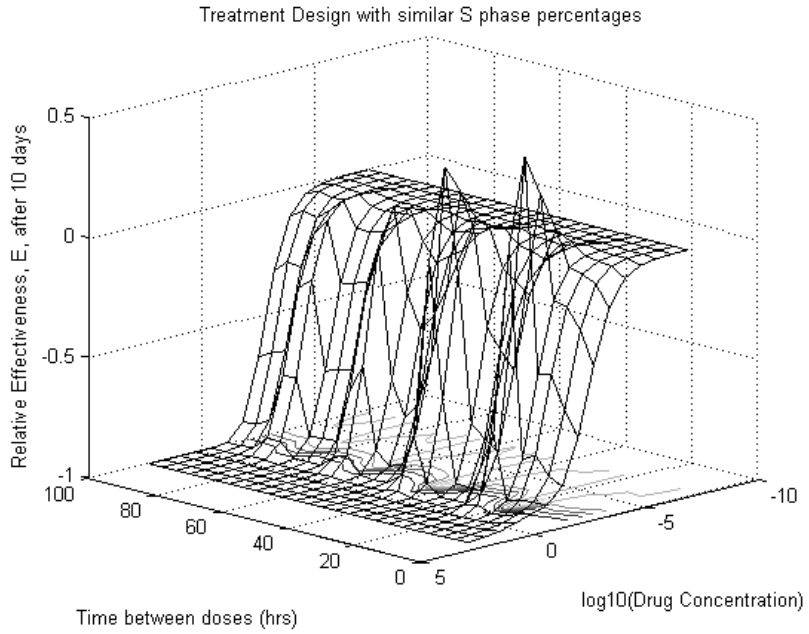

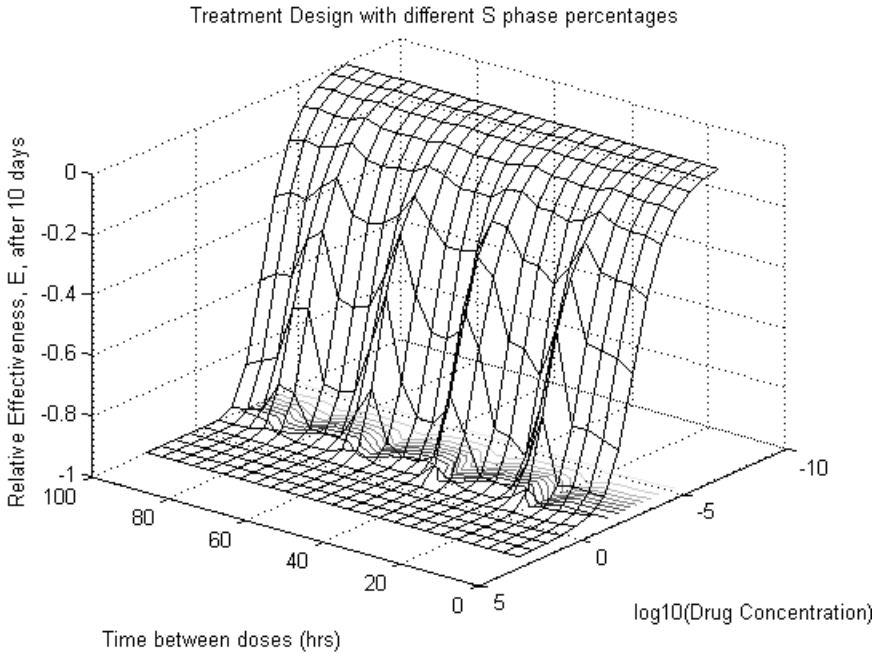

- Hypothesis testing (potential protocols)
- Patient specific treatments
- Treatment strength necessary or desired

Cell Cycle Transitions $\Gamma(1,\tau)$

- Cannot measure ages
- Balanced growth
  - Γ => age distributions
  - Predict dynamics
- BrdU
  - Labels S subpopulation
  - Phase transient amidst balanced growth
- Match transition rates

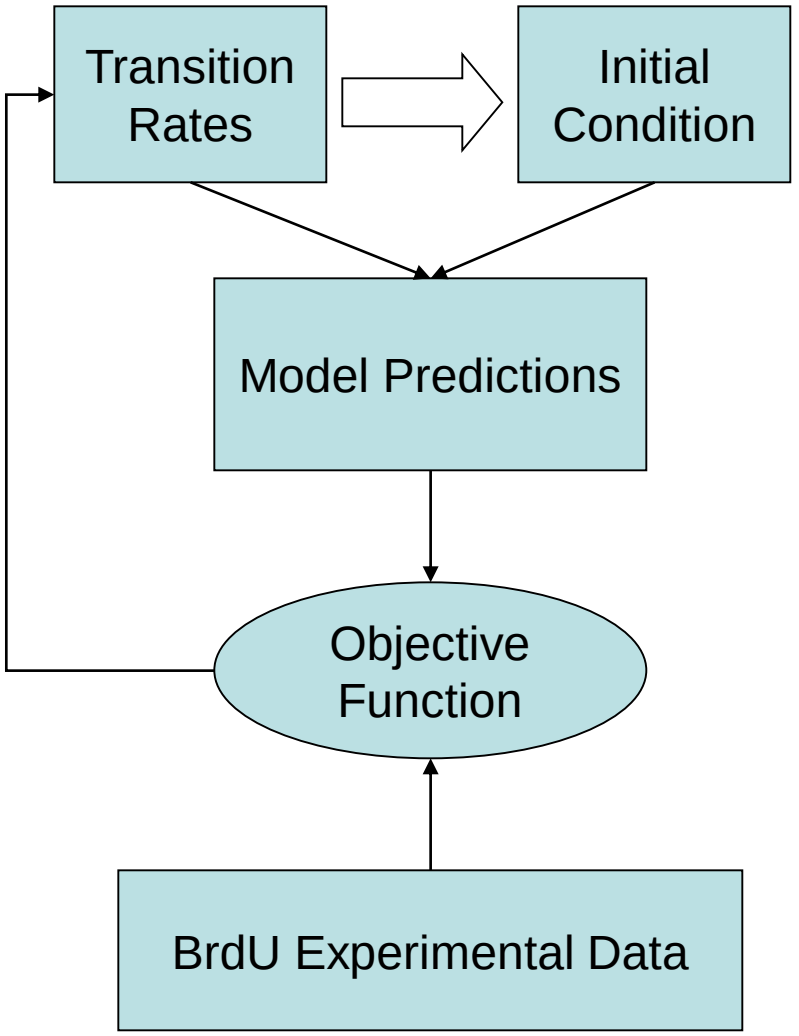

Initial Condition

- Balanced growth

$$n_i(\tau,t) = N_i(t)\, f_i(\tau) \quad \text{where} \quad \int_0^\infty f_i(\tau) = 1$$

- Population increase

$$\frac{d\mathbf{N}(t)}{dt} = \mathbf{D}\mathbf{N}(t)$$

$$D_{ij} = \int_0^\infty \left[D_{ij}^{in}(\tau) - D_{ij}^{out}(\tau) \right] f_j(\tau)\, d\tau$$

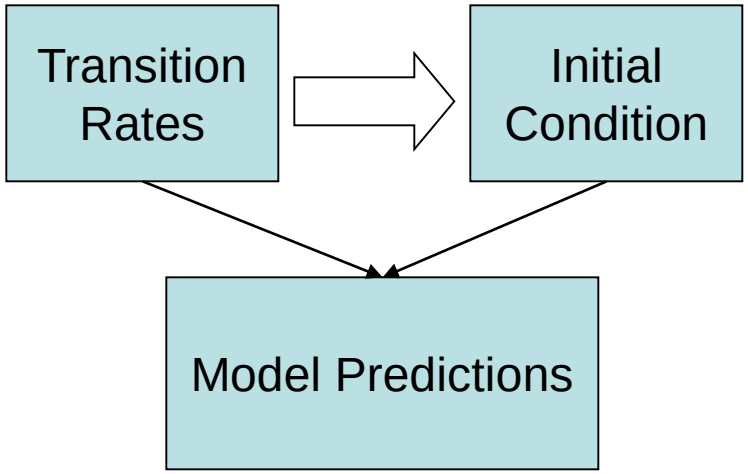

- Eigen analysis
  - Balanced growth age-distribution

$$f_i(\tau) = \left\{ \int_0^\infty \exp\left[-\int_0^{\tau'} \left(D_{ii}^{out}(\tau'') + \mu \right) d\tau'' \right] d\tau' \right\}^{-1} \exp\left[-\int_0^{\tau} \left(D_{ii}^{out}(\tau') + \mu \right) d\tau' \right]$$

Unbalanced subpopulation growth amidst total population balance growth

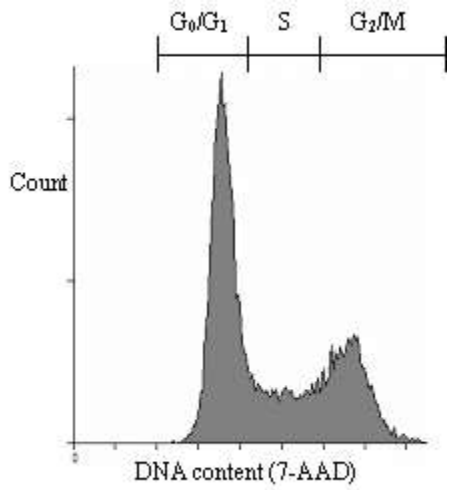

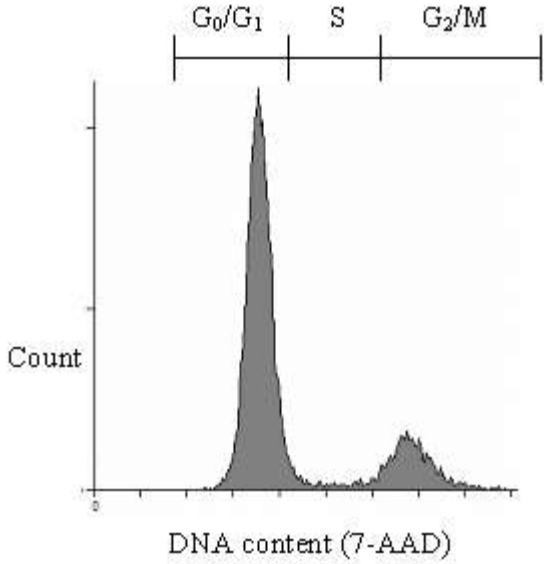

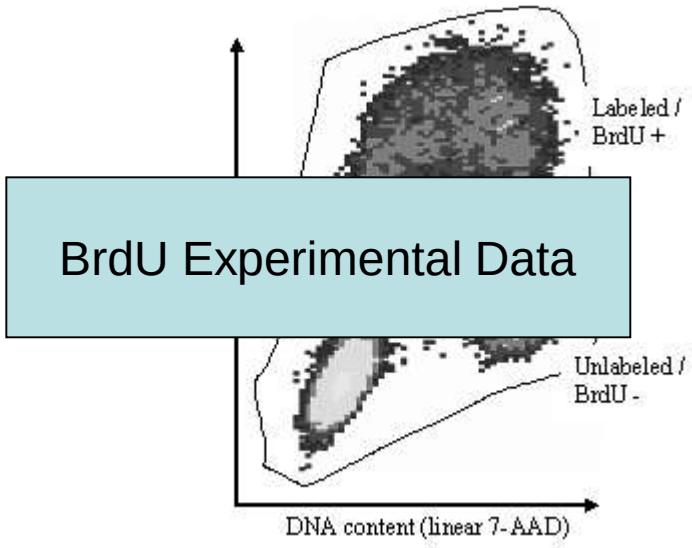

BrdU Experimental Data

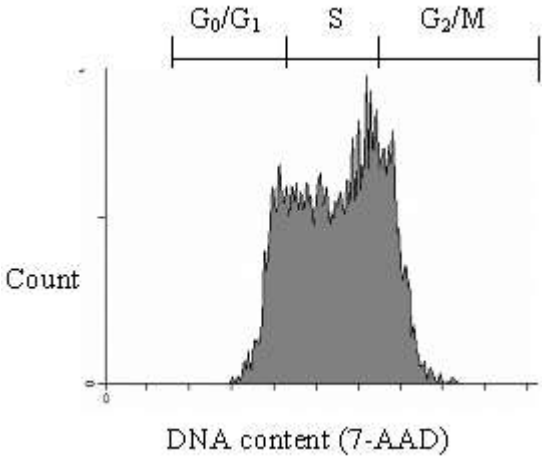

Cell Cycle Transition Rates

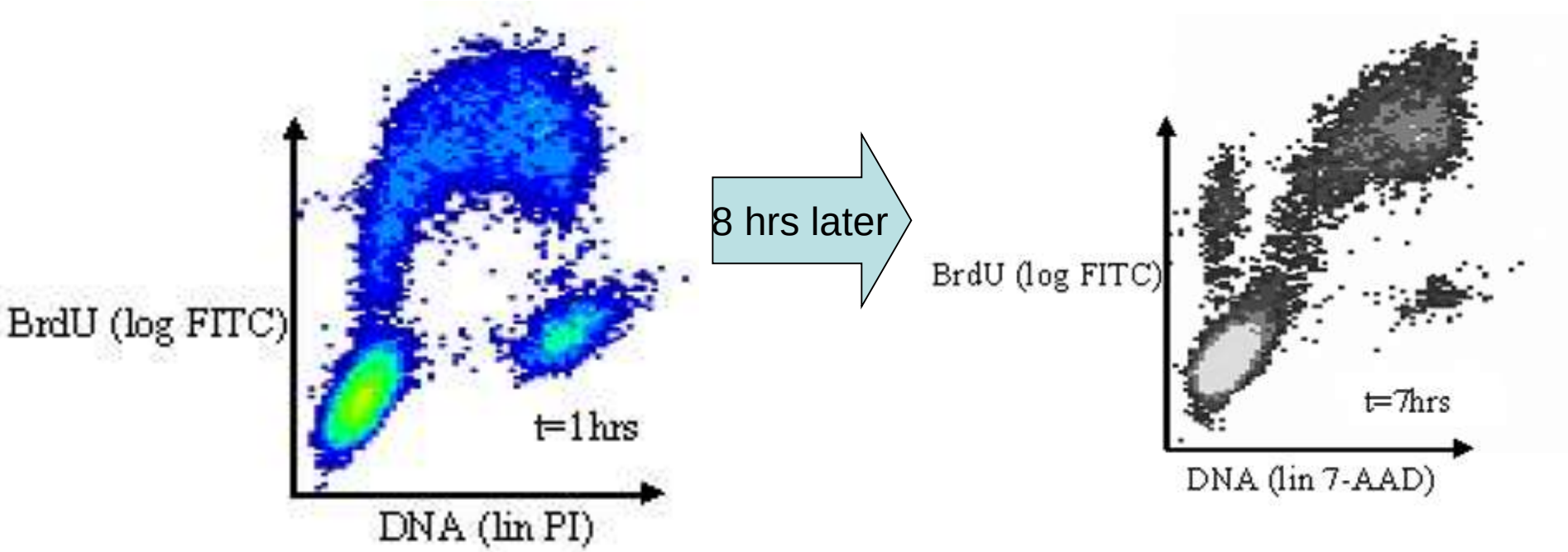

BrdU Labeling (cell cycle)

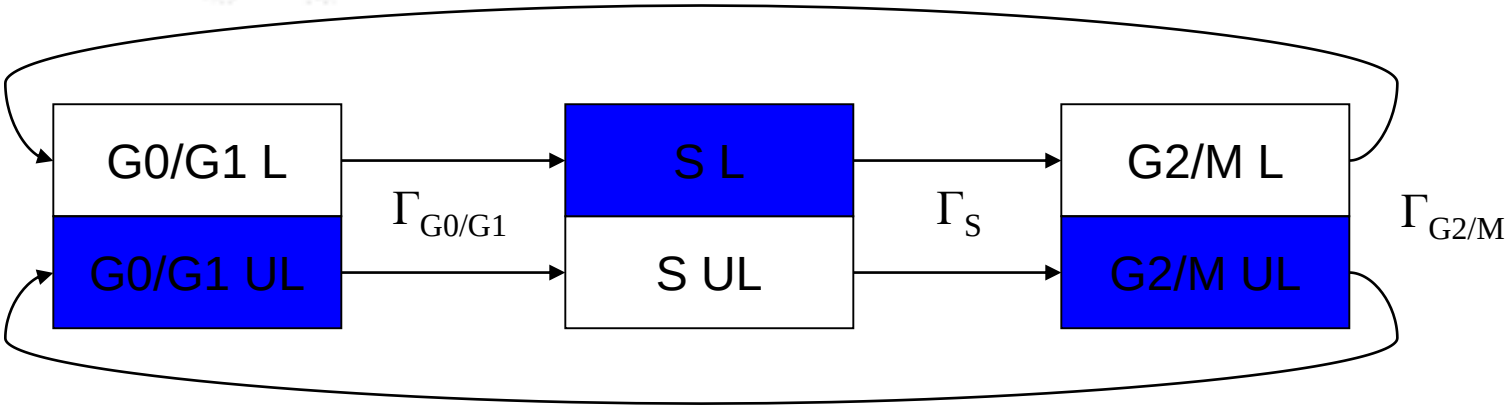

Transition Rates ⇔ Residence Time Distribution

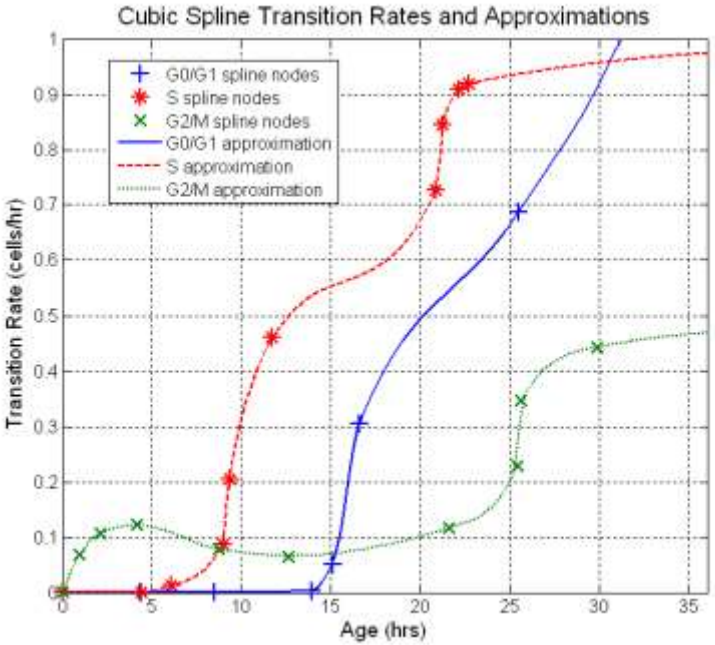

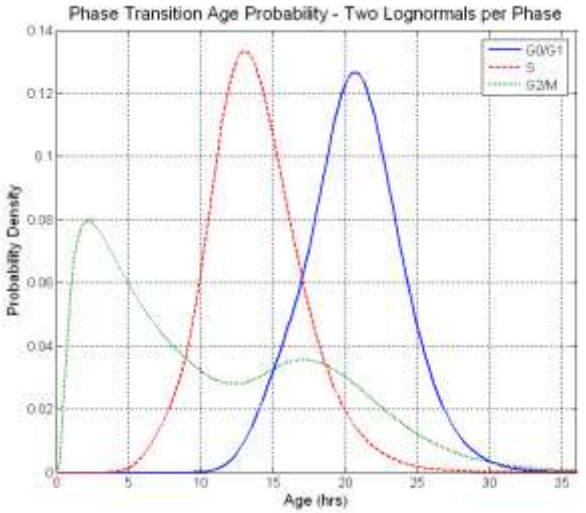

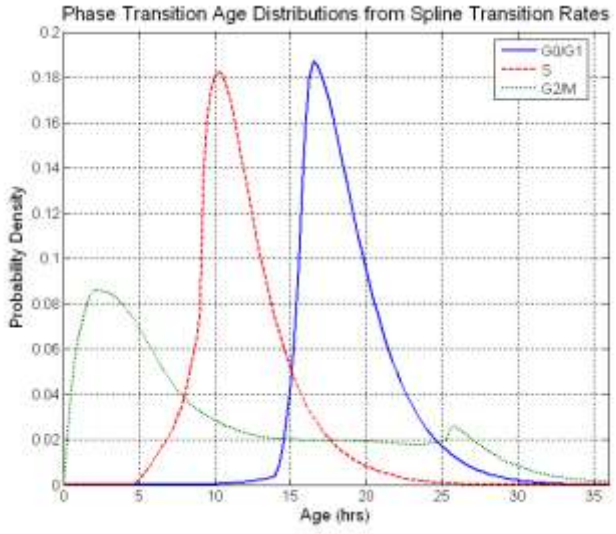

Sherer et al. 2007

Example – protein (p) structured cell cycle rates

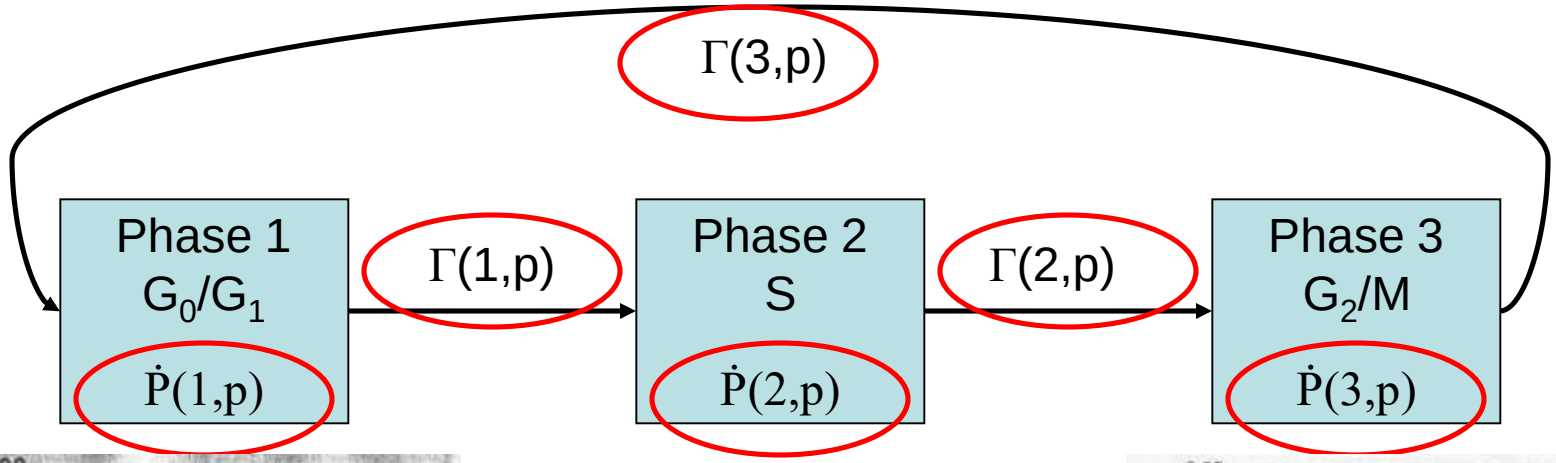

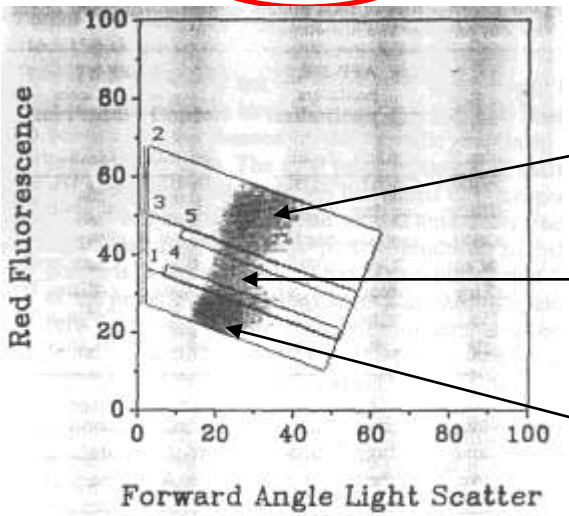

G_2/M phase

S phase

G_0/G_1 phase

Figure 8. Cytogram of red fluorescence intensity vs. forward-angle light scattering intensity for AFP-27E cells which were stained with propidium iodide and FITC after receiving the described treatment. Labeled regions represent gates that were used to generate protein content distributions on the condition that cell properties fell within the indicated region. This cytogram was constructed with data acquired for 5×10^4 cells.

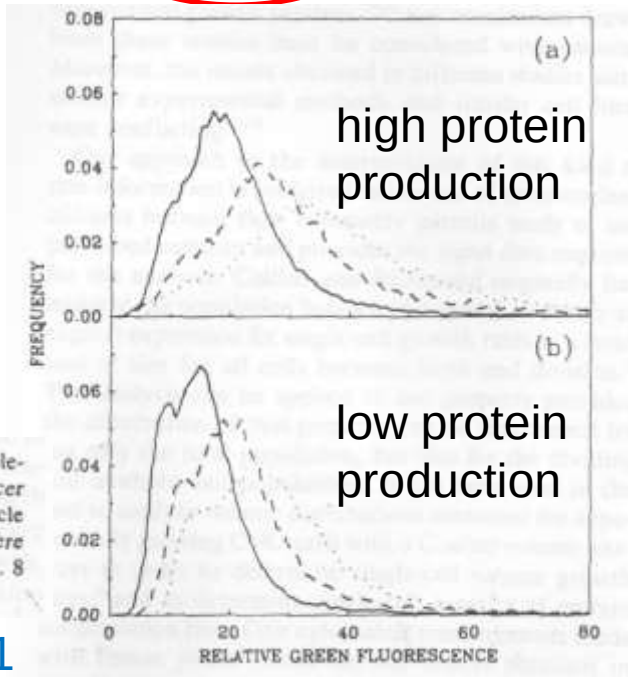

Figure 9. Distributions of green fluorescence intensity for double-stained (a) AFP-27E producer cells and (b) AFP-NP nonproducer cells from the G_1 (——), S (– – – –), and $G_2 + M$ (· · · ·) cell cycle phases. These distributions are frequency functions which were obtained according to the described gating procedure (see Fig. 8 and text).

Kromenaker and Srienc 1991

Rate Identification Procedure

- Assume balanced growth
  - Specific growth rate
- Measure
  - Stable cell cycle phase protein distributions
  - Protein distributions at transition
- Inverse model
  - Phase transition rates
  - Protein synthesis rates

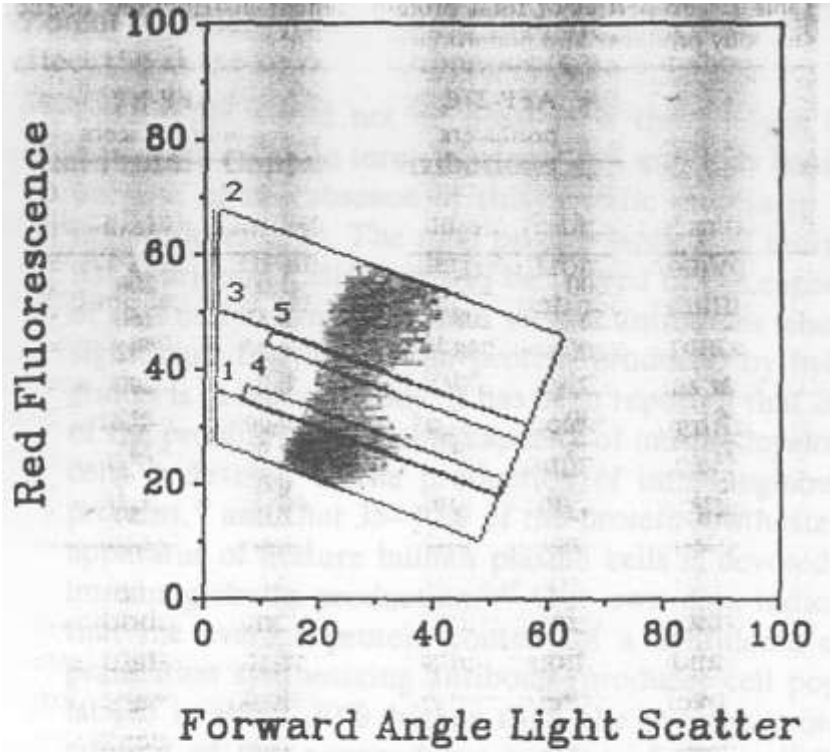

Figure 8. Cytogram of red fluorescence intensity vs. forward-angle light scattering intensity for AFP-27E cells which were stained with propidium iodide and FITC after receiving the described treatment. Labeled regions represent gates that were used to generate protein content distributions on the condition that cell properties fell within the indicated region. This cytogram was constructed with data acquired for 5×10^4 cells.

Modeling a surrogate marker for the drug 6MP

- Bone marrow
  - 6MP inhibits DNA synthesis
- Blood stream
  - Red blood cells (RBCs) become larger
  - RBC size correlates with steady-state 6MP level

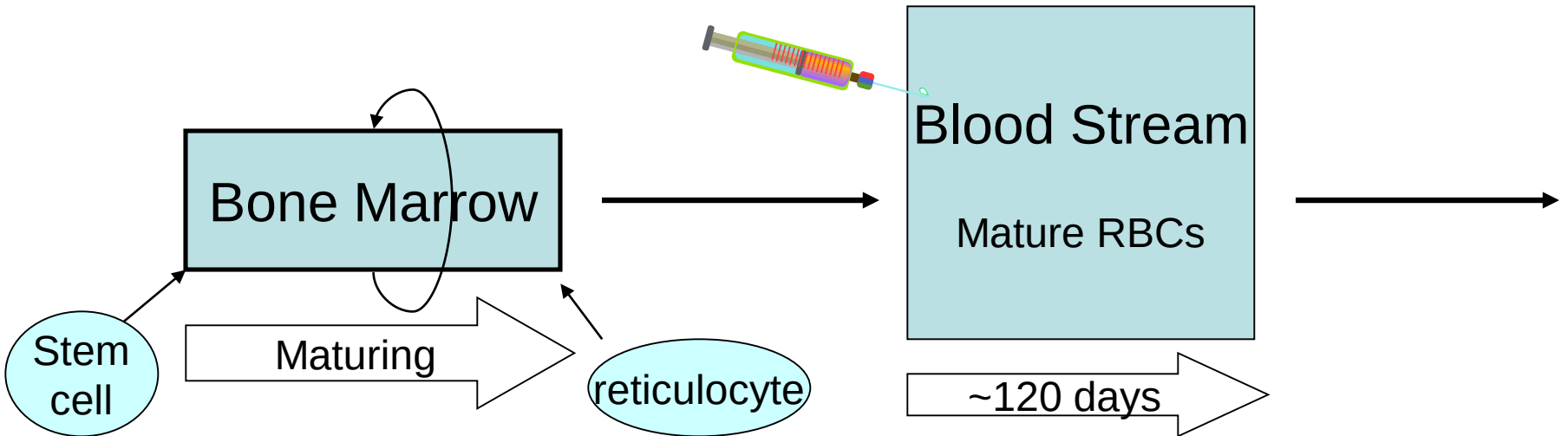

RBC Maturation

- Cell volume
- DNA inhibition
  - Time since division
  - *DNA synthesis rate*
- Maturation
  - Discrete state
    - Transferrin and glycophorin A
  - *Continuous*
    - Time spent in state

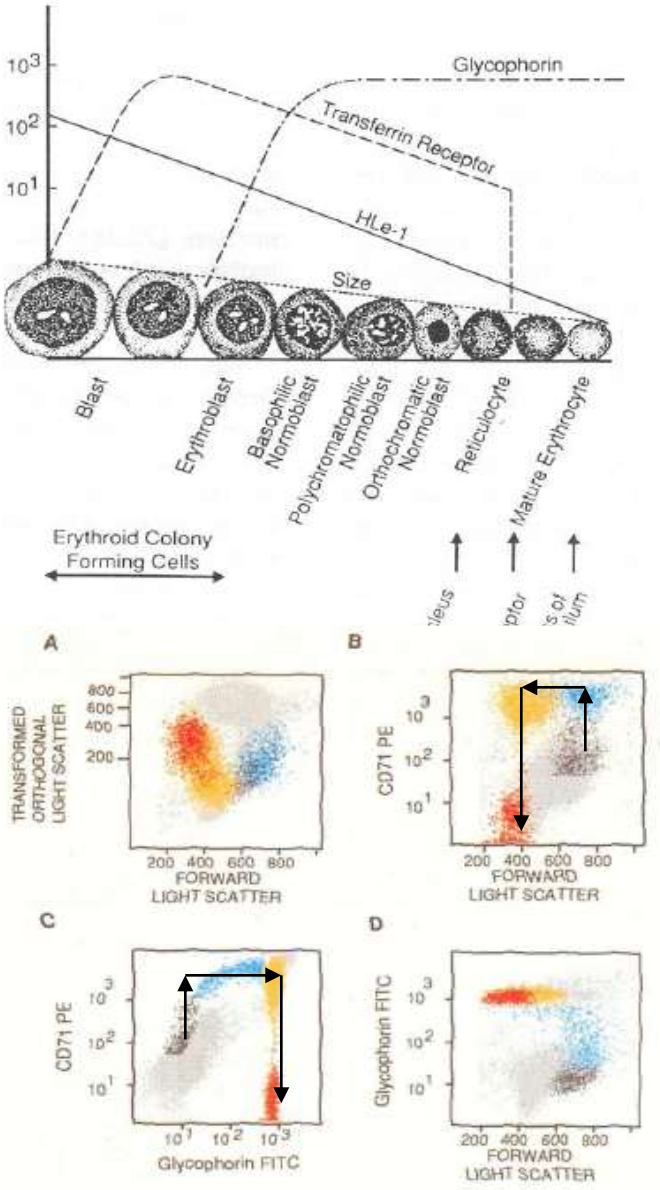

Maturation + division + growth rates

- Maturation
  - Tag cells in 1st stage with pkh26
  - Track movement
- Division
  - Cell generations
- Growth
  - Satisfy volume distributions

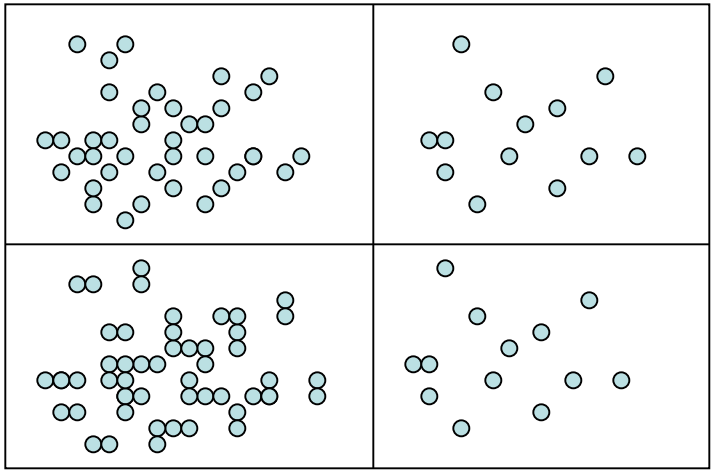

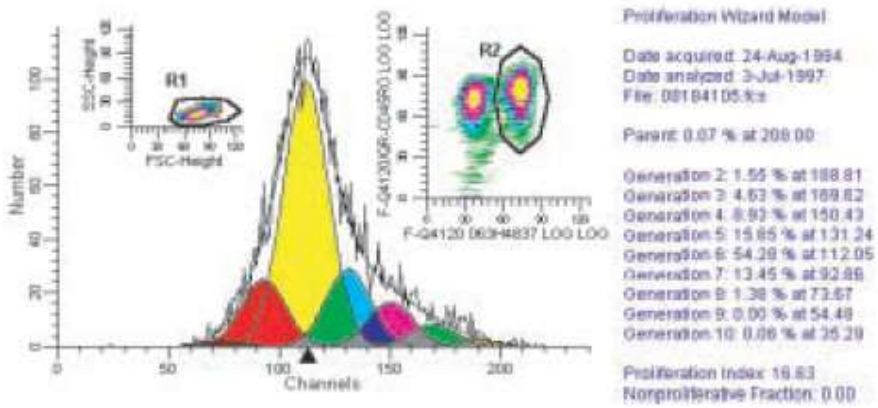

Figure 4. Deconvoluted histogram of CD4+/CD45RO+ subset in PKH26-labeled PBL activated with 2.5 μg/ml PHA for 6 days. Inset shows gates set by light scatter and immunophenotype.

MCV => Drug level

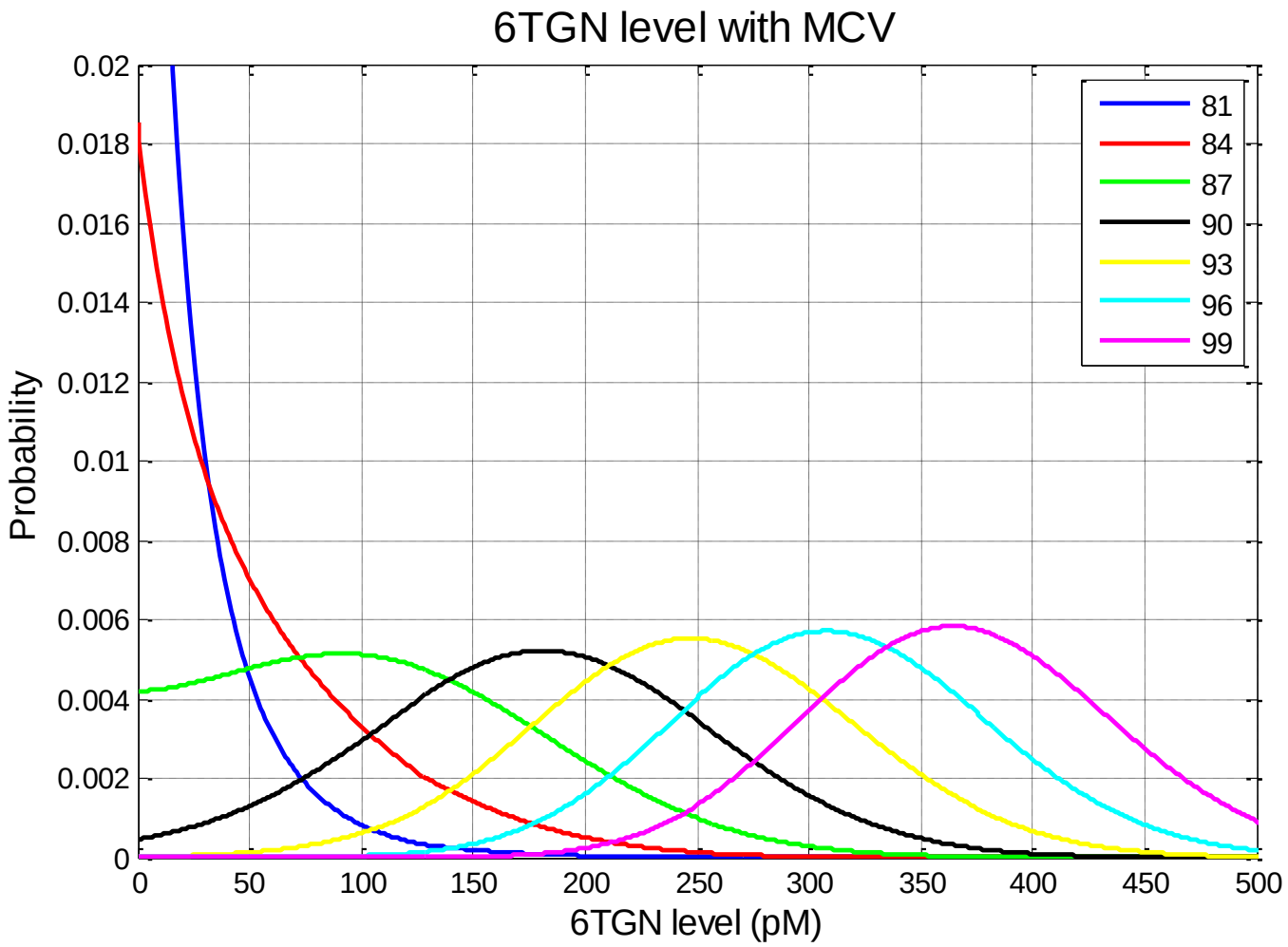

Treatment Evaluation

- Actual cell behavior may be unobservable
  - Remission
  - Predictive models
- Model parameters known
- Treatment constantly adjusted
  - Immune system (Neutrophil count)
  - Toxic side effects
- Objective
  - Increase cure “rate”
  - Increase quality of life
- Quantitative comparison
  - Expected population
  - Likelihood of cure

Small number of cells

- Uncertainty in timing of events
  - Extrinsically stochastic
  - Average out if large number of cells
  - Greater variations if small number of cells
- Master probability density
  - Monte Carlo simulations
  - Cell number probability distribution
- Seminal cancerous cells
- Nearing “cure”
- Dependent upon transition rate functions

Cell number probability distribution & likelihood of cure

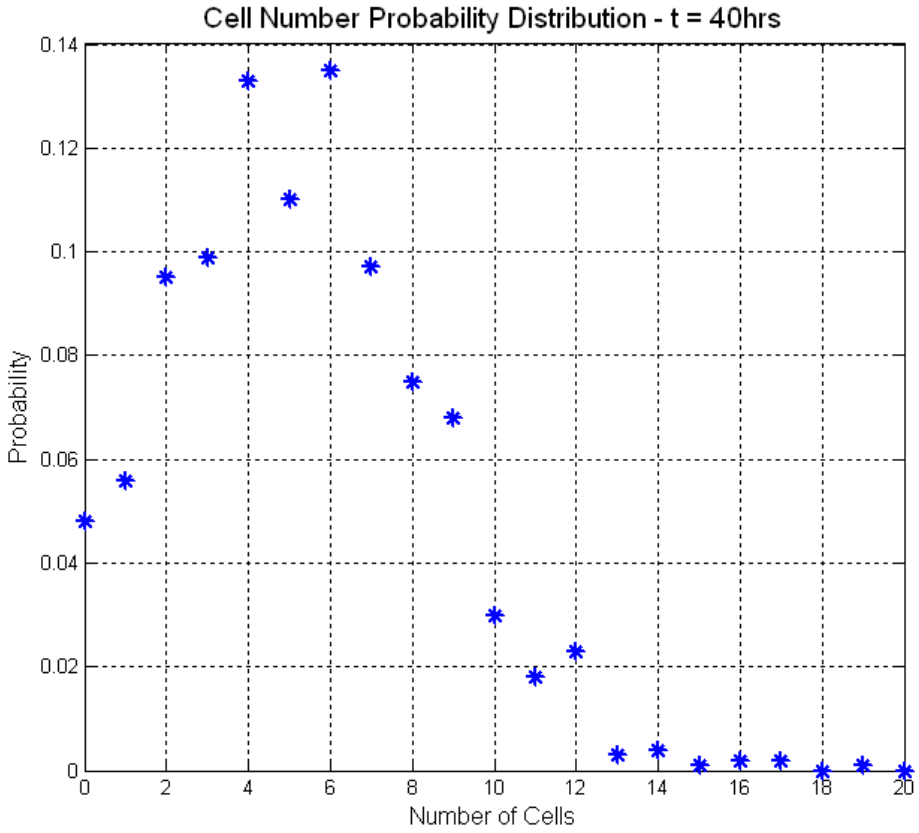

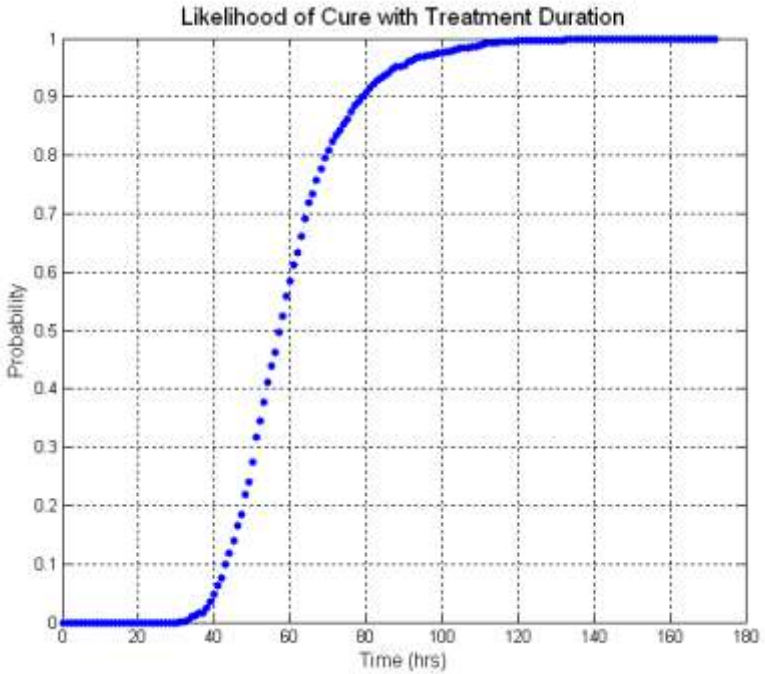

Sherer et al. 2007

Approximate treatment necessary to nearly ensure cure

- Small expected population
  - Small population mean
- Be certain that the population is small
  - Small standard deviation in number of cells

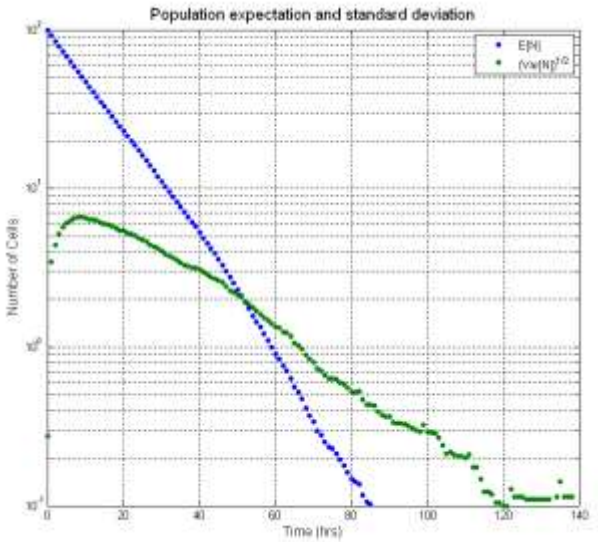

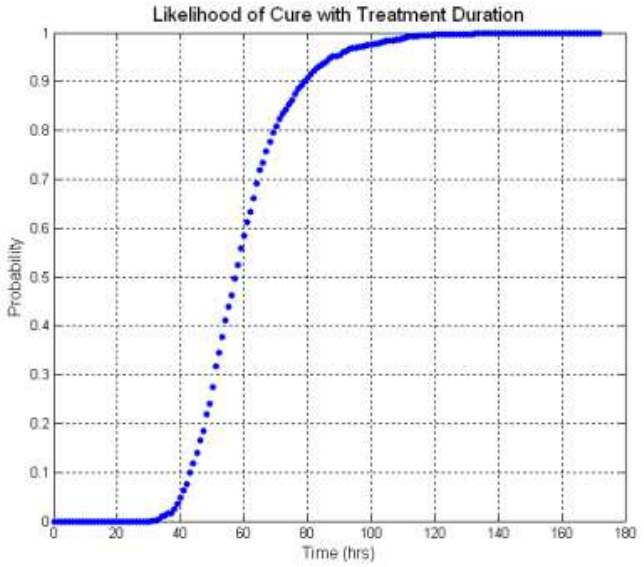

Patient Variability

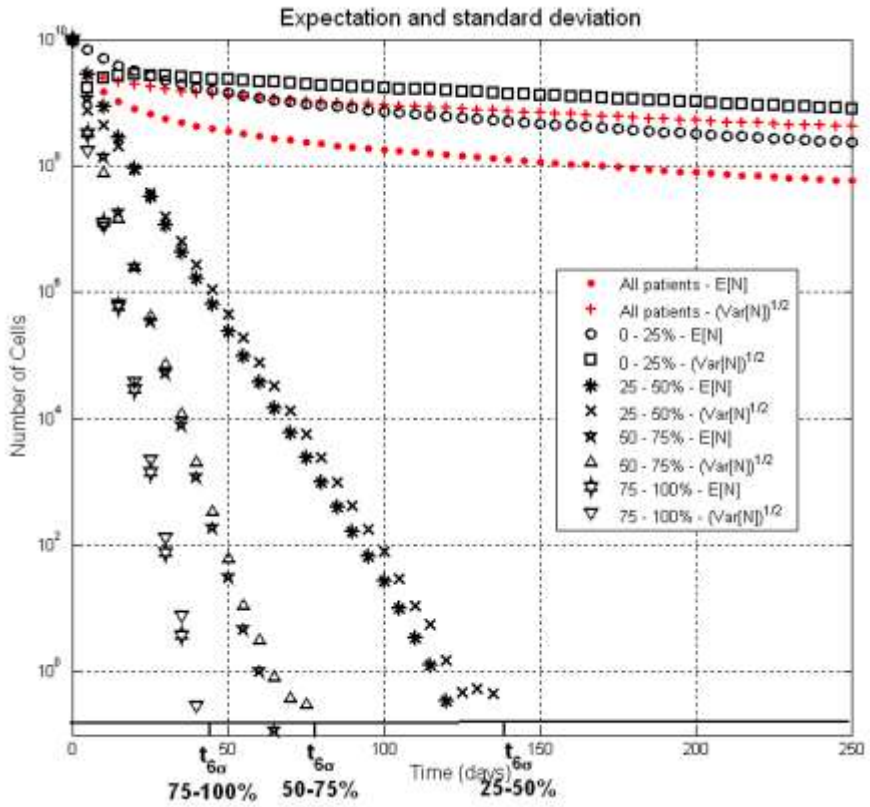

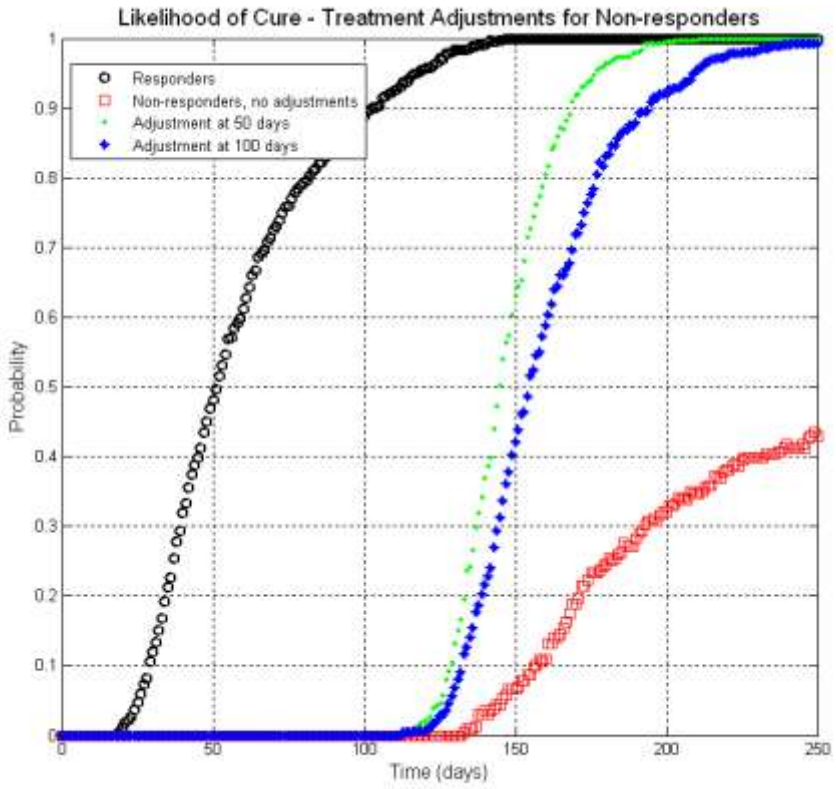

Quiescence – importance of structure of transition rates